SUBSECTION 2.5.4:
STABILITY OF SUBSURFACE MATERIALS AND FOUNDATIONS
TABLE OF CONTENTS

SUBSECTION 2.5.4 LIST OF TABLES

SUBSECTION 2.5.4 LIST OF TABLES (CONT.)

SUBSECTION 2.5.4 LIST OF FIGURES

SUBSECTION 2.5.4 LIST OF FIGURES (CONT.)

SUBSECTION 2.5.4 LIST OF FIGURES (CONT.)

SUBSECTION 2.5.4 LIST OF FIGURES (CONT.)

2.5.4 STABILITY OF SUBSURFACE MATERIALS AND FOUNDATIONS

PTN COL 2.5-1
PTN COL 2.5-5

This subsection presents information on the properties and stability of soils and rocks that may affect the safety of the Seismic Category I facilities (nuclear islands), under both static and dynamic conditions including the vibratory ground motions associated with the ground motion response spectrum (GMRS). An evaluation of the site conditions and geologic features that may affect the nuclear islands or their foundations is also provided.

This subsection is organized into the following subsections:

- Geologic Features (Subsection 2.5.4.1)
- Properties of Subsurface Materials (Subsection 2.5.4.2)
- Foundation Interfaces (Subsection 2.5.4.3)
- Geophysical Surveys (Subsection 2.5.4.4)
- Excavations and Backfill (Subsection 2.5.4.5)
- Groundwater Conditions (Subsection 2.5.4.6)
- Response of Soil and Rock to Dynamic Loading (Subsection 2.5.4.7)
- Liquefaction Potential (Subsection 2.5.4.8)
- Earthquake Site Characteristics (Subsection 2.5.4.9)
- Static Stability (Subsection 2.5.4.10)
- Design Criteria (Subsection 2.5.4.11)
- Techniques to Improve Subsurface Conditions (Subsection 2.5.4.12)

Subsection headings and heading numbers follow RG 1.206 for Subsection 2.5.4.

2.5.4.1 Geologic Features

This subsection presents a summary of the non-tectonic processes and geologic features that could relate, if present, to permanent ground deformations or foundation instability at the Units 6 & 7 safety-related facilities. A summary of the

subsurface conditions based on the Units 6 & 7 subsurface investigation results is presented first, followed by descriptions of the foundation soil and rock properties and the stability of these materials. Processes and features evaluated include: areas of actual or potential subsurface subsidence, solution activity, uplift, or collapse; zones of alteration, irregular weathering, or structural weakness; unrelieved stresses in bedrock; rocks or soils that may become unstable; and a history of deposition and erosion.

The following description is based on the site geology presented in Subsection 2.5.1, surface faulting described in Subsection 2.5.3, and results of the site-specific subsurface investigation activities presented in Subsection 2.5.4.2.

The Units 6 & 7 nuclear island locations are shown on Figure 2.5.4-201. To evaluate the subsurface conditions at these locations, two subsurface investigation programs are executed. During the initial investigation, 88 geotechnical borings and 2 additional geophysical borings are drilled and sampled. During the supplemental investigation, 9 borings are drilled, with geophysical testing performed in 2 borings, pressuremeter testing performed in 3 borings, and cone penetration testing (CPT) performed in 2 borings. During the supplemental investigation, 3 of the borings are inclined towards surface depressions to study potential fractures. In addition, surficial muck samples are collected at 9 locations. Drilling locations are shown on Figure 2.5.4-202. Soil boring and rock coring logs are presented in Appendix B of Reference 257 and Appendix A of Reference 290.

2.5.4.1.1 Summary of Subsurface Conditions

Figures 2.5.4-203 through 2.5.4-205 present geologic cross sections through Unit 6 based on these boreholes, and Figures 2.5.4-206 through 2.5.4-208 present geologic cross sections through Unit 7. The cross section locations are shown on Figure 2.5.4-209.

The depth of sediments and the estimated top of rock are indicated on the cross sections (Figures 2.5.4-203 through 2.5.4-208). Table 2.5.4-201 summarizes the thickness of each stratum encountered and its respective base elevation. Geophysical methods used to identify top of rock are presented in Subsection 2.5.4.4.

2.5.4.1.1.1 Description of Surficial Soil and Rock

The original site was covered by organic muck and the Miami Limestone (Figure 2.5.1-332). The organic muck was the dominant surface cover, whereas the Miami Limestone was at the ground surface in the northwestern portion of the site. The Miami Limestone is a marine carbonate rock, as presented in Subsection 2.5.4.2.

The original site was at or near sea level with a natural relief of approximately 3 feet from its northern-to-southern boundary and approximately 0.5 feet of relief from its western-to-eastern boundary, except where the ground surface was raised to create berms adjacent to the canals. Other than the berms, the site is flat and uniform throughout with the exception of the vegetative depressions as seen in Figure 2.5.1-333. The vegetative depressions are reported to be dissolution features within the Miami Limestone.

2.5.4.1.1.1.1 Correlation with Site Geologic Setting

As presented in Subsection 2.5.1.1.1.1.1.1, the site is within the Southern Slope subprovince of the Atlantic Coastal Plain. The geologic setting is characterized by broad bands of swamps and marshes that are flooded by tides or by freshwater runoff (Figure 2.5.1-217).

The boring logs presented in Reference 257 indicate that the site subsurface is consistent with the Southern Slope subprovince. The results of petrographic examinations of rock core samples, as described in Subsection 2.5.4.2.1, are also consistent with rock of this geomorphic province.

2.5.4.1.2 Subsidence, Dissolution Activity, Uplift, or Collapse

As described in Subsections 2.5.1.2.4 and 2.5.1.2.5.2, no geologic hazards have been identified within the site or site area (5-mile radius). No unusual zones of alteration, weathering profiles, or structural weakness are encountered at the location of the site investigation. As described in Subsection 2.5.1.2.5.3, no geomorphic disturbances or fault-related features are observed by the field reconnaissance. As a result of the reconnaissance investigation, no geomorphic, stratigraphic, or other evidence suggesting the presence of active or recent tectonic deformation within the site vicinity (25-mile radius) is observed.

As described in Subsection 2.5.1.2.5.4, anthropogenic effects in southeastern Florida of urban development, water mining, limestone mining, agriculture, and construction of drainage canals impact the regional groundwater table and

associated saltwater intrusion. Subsection 2.4.12 contains a more detailed description of the Units 6 & 7 groundwater conditions.

The potential for subsidence or collapse pertaining to future subsurface solution activity below Units 6 & 7 is described in Subsection 2.5.4.1.2.1. The potential for uplift is described in Subsection 2.5.4.1.2.2.

2.5.4.1.2.1 Dissolution Activity

The majority of the near-surface geologic units are composed of limestone rock. Based on Florida Geological Survey records, sinkholes in the limestone of southeastern Florida are few in number, shallow, broad, and develop gradually. The Florida Geological Survey has stated that “there is not a great degree of dissolution activity; what does occur is numerous small cavities in rock cores and is considered micro-karst. The Florida Geological Survey does not expect any large cavities or collapse in the site area.”

Florida Geological Survey publications have no documentation of significant karst development in this region of Florida (References 202 and 203). However, according to Renken et al. (Reference 204), there is evidence of karst development in Miami-Dade County along the Atlantic Coastal ridge extending southward from South Miami to the Everglades National Park. Vanlier et al. (Reference 205) state that most of Miami-Dade County is underlain by limestone having solution cavities. Vanlier et al. further indicate that a few localities in the Homestead and Turkey Point area are underlain by exceptionally large cavities between depths of approximately 18 to 31 feet. Parker (Reference 206) states that the Miami Limestone and Fort Thompson Formation have significant permeability and solution features that have created turbulent flow conditions in some wells. According to Cunningham et al. (Reference 207), paleokarst is well-documented in the Lake Belt area of north central Miami-Dade County.

Small dissolution features are present in limestone drill core samples collected during the subsurface investigations at the site and described in Appendix B of Reference 257 and Appendix A of Reference 290. They occur in the form of vugs and moldic secondary porosity, particularly in the Miami and Key Largo limestones. The evaluation of all data (Appendix B of Reference 257 and Appendix A of Reference 290) indicates that outside the vegetated depressions and drainages (in vertical borings), 20.1 feet of interpreted tool drops (due to voids and/or voids filled with soft sediments) are observed in a total of 7918.4 feet cored, for a 0.3 percent of the total cored length in 93 borings. Individual drops in the vertical borings range from 0.4 to 4 feet (1.5 feet maximum within the Units

6 & 7 building footprints). Results from the site investigations (Appendix B of Reference 257 and Appendix A of Reference 290), show that interpreted tool drops are observed more often under the vegetated depressions and drainages. In the 3 inclined borings, 15.2 feet of tool drops are observed in 356.4 feet cored, for a 4.3 percent of the total cored length. Individual drops in the inclined borings range from 0.3 to 2.5 feet. Boring locations with interpreted tool drops, among all sampling locations, are shown in Figure 2.5.1-378. The maximum length of interpreted tool drop (due to voids and/or voids filled with soft sediments) is limited to 1.5 feet within the Unit 6 & 7 building footprints, and the frequency of encountering an interpreted tool drop is less than 0.5 percent site-wide. These statistics are based on the drilling conducted during the initial and supplemental site investigations (Appendix B of Reference 257 and Appendix A of Reference 290). While caliper and acoustic logs from boreholes where downhole geophysical data were obtained do not indicate the presence of large voids, they do support the interpretation of two preferential secondary porosity flow zones. A more detailed discussion of the site geologic hazards is presented in Subsection 2.5.1.2.4. A description of the results of a geophysical survey using microgravity, seismic refraction, and multichannel analysis of surface waves methods to investigate the potential for solution features beneath the site is provided in Subsection 2.5.4.4.5.

2.5.4.1.2.2 Uplift or Collapse

Units 6 & 7 are located on the east coast of the Florida platform. As described in Subsection 2.5.1.1.1.3.2.1, the Florida platform represents a flat, slowly subsiding region dominated by carbonate deposition from northern Cuba to Georgia and between the Florida escarpment in the eastern Gulf of Mexico and the Bahama platform in the east. As presented in Subsection 2.5.3.2, no evidence of tectonic surface deformation is observed within the site vicinity. The absence of karst-related collapse is also described in Subsection 2.5.3.2. Therefore, no uplift due to natural forces or human development is anticipated.

2.5.4.1.2.3 History of Deposition and Erosion

As described in Subsection 2.5.1.2, the site area is characterized by flat, planar bedding in late Pleistocene and older units. The site vicinity geology (Figure 2.5.1-331) was influenced by sea level fluctuations, processes of carbonate and clastic deposition, and erosion. The Paleogene (early Cenozoic) is dominated by the deposition of carbonate rocks, while the Neogene (late Cenozoic) is influenced more by the deposition of quartzitic sands, silts, and clays (Reference 208). Within the site area, the dominant subsurface material types are limestones of the Miami

Limestone, Key Largo Limestone, Fort Thompson Formation, and Arcadia Formation and sands and silts of the Tamiami and Peace River Formations (Figure 2.5.1-332). Minor units of alluvial soils, organic muck, and silt cover the site surface. During the Pleistocene, worldwide glaciation and fluctuating sea levels influenced the geology in the site vicinity. Drops in sea level caused by growth of glaciers increased Florida's land area significantly, which led to increased erosion and clastic deposition. Warm interglacial periods resulted in a rise in sea level and an increase in nutrient-rich waters leading to an increase in carbonate buildup (Reference 208).

2.5.4.2 Properties of Subsurface Materials

PTN COL 2.5-6

This subsection addresses the properties of subsurface materials and the methods of determining these properties. Subsection 2.5.4.2.1 addresses the properties of subsurface materials encountered at the site, while Subsections 2.5.4.2.2 and 2.5.4.2.3 describe the subsurface investigation and laboratory testing program conducted to obtain these properties.

2.5.4.2.1 Description of Subsurface Materials

This subsection addresses the properties of subsurface materials, as follows:

- Subsection 2.5.4.2.1.1 provides an introduction to the soil and rock strata encountered at the site.
- Subsection 2.5.4.2.1.2 describes each soil and rock stratum encountered.
- Subsection 2.5.4.2.1.2.10 describes the subsurface materials below a depth of 600 feet bgs (i.e., below the maximum depth of this subsurface investigation).
- Subsection 2.5.4.2.1.3 describes the evaluation of in situ properties of soil strata investigated (i.e., soils extending to a depth of approximately 600 feet bgs) and presents tables and figures of these properties.
- Subsection 2.5.4.2.1.4 describes the chemical properties of the soil and rock.
- Subsection 2.5.4.2.1.5 describes the field testing program.
- Subsection 2.5.4.2.1.6 describes the laboratory testing program.

2.5.4.2.1.1 Summary of Soil and Rock Strata

Subsurface materials at the site consist of coastal marine sediments underlain by Paleozoic- and Mesozoic-age igneous and metamorphic bedrock (basement rock), which is estimated to be at a depth of at least 15,000 feet bgs (Reference 209). The uppermost 600 feet of site soils, consisting of limestones attributed to the Miami Limestone, Key Largo Limestone, and Fort Thompson Formation, and soils and soil-rock mixtures attributed to the Tamiami Formation and the Hawthorn Group, are the subject of this subsurface investigation. These subsurface materials are divided into eight individual strata, consisting of four predominantly rock strata (Strata 2, 3, 4, and 8), three predominantly soil strata (Strata 5, 6, and 7), and surficial muck (Stratum 1). The final site design includes an additional stratum of compacted limerock fill. The soil and rock strata are described in Subsection 2.5.4.2.1.2.

Subsurface conditions deeper than 600 feet are characterized using information from the geologic literature, most notably References 210 and 211, and from deeper borings drilled in the area for oil and gas exploration (Reference 212). While the depth to competent bedrock (“basement rock”) is significant at the site, layers and lenses of limestone, dolostone, sand, and silt are present intermittently to this depth.

Identification and characterization of the investigated soil and rock strata are based on physical and engineering characteristics. Methods used in identification and characterization are described in detail in Subsections 2.5.4.2.2 and 2.5.4.4 and include:

- Standard penetration testing (SPT) and rock coring in borings
- Cone penetration testing (CPT)
- Test pit (TP) excavations
- Surficial muck sampling using a McCauley Sampler
- Geophysical downhole and P-S suspension logging to measure compression (P, V_p) and shear (S, V_s) wave velocities and other geophysical indices
- Pressuremeter testing
- Groundwater observation well (OW) installations and related field testing

- Extensive laboratory testing of disturbed and intact soil samples and rock cores collected

The natural ground surface at and around the power block at the time of this subsurface investigation was generally level, ranging from approximately El. –2 feet to +1 foot, with an average of El. –1 foot. Note that all references to elevations given in this subsection are to the North American Vertical Datum of 1988 (NAVD 88). The power block finish grade elevation is +25.5 feet.

The natural ground surface at the makeup water reservoir at the time of this subsurface investigation was generally level at approximately El. –0.5 feet. A concrete retaining wall extends to El. +24 feet.

Fracture Density and Characteristics

Shear strength parameters and rock mass modulus are derived for two separate rock masses at the Turkey Point site: the fracture density (FD)—FD1 zone (very slightly fractured) and the FD4 zone (slightly to moderately fractured) (Reference 216).

Other zones of fracturing between FD1 and FD4 are possible in areas where there is no evident sign of permanent vegetation and drainage; however, only healed vertical fractures (R-6-1b, R-7-1, B-620), one healed near horizontal fracture (R-6-2), and one area with an open horizontal fracture and a 60-degree fracture (R-7-2) are described at the site outside of the vegetated areas. The estimated locations of likely fractured zones are indicated in Figure 2.5.4-254.

Three inclined borings intersect the interpreted FD4 zone, which covers significantly less area, and exists beneath the vegetated depressions and drainages (Figures 2.5.4-254 and 2.5.4-255). Not all core runs under vegetated depressions and drainages are characterized as fracture density FD4, but this is considered as the worst-case fracture density under the investigated depression and drainage footprints.

As part of the supplemental investigation, three inclined borings (R-6-1a, R-6-1a-A, and R-7-4) are drilled in areas anticipated to be slightly to moderately fractured (in vegetated depressions and across drainages). The borings are inclined to increase the lateral extent of the investigation and to evaluate fracture density beneath depressions and drainages. Of the 48 observed fractures with measured dips in the inclined borings, only two fractures have a relative dip greater than 65 degrees, which is near vertical (80 to 90 degrees) in the corrected orientation. Fractures with this orientation would be difficult to capture in the vertical borings.

However, it is worth noting that these are the least frequent fractures. The predominant fracture dip is between 30 and 60 degrees, thus, most fractures would also be observable in vertical borings. Outside of depressions and drainages, fractures in general are less frequent and almost all are described as totally healed.

Beneath the vegetated depression to the west of Unit 7, core samples from boring R-7-4 show evidence of fracturing throughout the Key Largo Limestone and the Fort Thompson Formation. In the Miami and Key Largo Limestone, from ground surface to 44 feet (MD), staining observed on fracture walls is dark brown. Below 44 feet (MD), what is observed on the walls of the discontinuities is calcite recrystallization with the rock maintaining similar fracture density. The change in the characteristics of the coating of joints is interpreted as possible evidence of a transition between surface water infiltration inhibiting calcite recrystallization above 44 feet (MD) and groundwater flow promoting calcite recrystallization below. However, because there is no change in fracture density, it is assumed that the interpreted FD4 zones extend from the Miami Limestone through the Fort Thompson Formation.

2.5.4.2.1.2 Description of Soil and Rock Strata

The following is a description of each soil stratum encountered in the subsurface investigation to the maximum investigated depth of 616 feet bgs in the power block and 150 feet bgs in the makeup water reservoir and perimeter areas. The stratum thickness indicated in each description for the power block is the calculated average within the two power block units (Unit 6 and Unit 7) because the subsurface conditions encountered in the subsurface boring program are relatively uniform. Note that the stratum thickness at a particular boring or CPT is only included in the average calculation when the stratum is encountered and fully penetrated by the boring or CPT probe. The Unified Soil Classification System (USCS) (References 213 and 214) classifications included in each of the descriptions are based mainly on the results of grain size analyses and Atterberg limit tests. Most of the strata are present in each boring and CPT within the depth investigated, except as noted.

2.5.4.2.1.2.1 Stratum 1 (Muck/Peat)

Stratum 1 is removed from the plant area at the initiation of construction. Therefore, this stratum is not characterized to the same extent as the underlying strata. The following is a summary of the characterization of this stratum from the site investigation and previous data.

Stratum 1 (muck/peat) is encountered at the ground surface in all borings in the Units 6 & 7 power block and within the entire site, except for boring B-814, which has fill covering Stratum 1. Stratum 1 consists primarily of elastic silt, organic-rich elastic silt, or peat sediments. Where present, the elastic silts represent the uppermost surficial sediments. Organic-rich elastic silt is found widespread on site, but not within vegetated depressions. Peat is found primarily within the vegetated depressions at the site, in main water drainages, and as basal deposits elsewhere on the site (directly above the Miami Limestone). Boreholes fully penetrated this stratum within the Units 6 & 7 power block and the entire site. Muck/peat was sampled via two test pits in the initial investigation (Reference 257) and nine muck/peat borings in the supplemental investigation (using a McCauley Sampler) (Reference 291). This stratum has a very soft to medium stiff consistency. The thickness of Stratum 1 ranges from 2 to 11 feet, with an average of 3.6 feet. The top of this layer is typically at El. -1.1 feet. The average base elevation of this stratum is El. -4.7 feet.

2.5.4.2.1.2.2 Stratum 2 (Miami Limestone)

The Miami Limestone (or the Miami Oolite, as it is referred to in some publications) is a soft rock unit that is generally sampled in South Florida using SPT equipment rather than rock coring. The top of this unit is encountered at elevations ranging from –3.3 to –12.2 feet. The range of thickness for the Miami Limestone varies from 13 to 30 feet with an average of 22.3 feet.

Boreholes fully penetrated this stratum at all of the boring locations. Two exploratory test pits partially penetrated this stratum at two locations, TP-601 and TP-701. This stratum consists of pale yellow, light brownish gray, and white limestone. Based on the logs included in Appendix B of Reference 257 and Appendix A of Reference 290, it has a porous, sometimes fossiliferous texture, comprising oolite grains with varying carbonate cementation. Observed fossils include mollusks, bryozoans, and corals. Stratum 2 is characterized as a boundstone using the Dunham carbonate classification scheme (Reference 215) included in Appendix B of Reference 257. This stratum has a soft to very hard consistency depending on the degree of cementation. Because this stratum is primarily sampled with SPT rather than rock core equipment, this hardness description is the one used in the “Geotechnical Exploration and Testing Report” found in Appendix B of Reference 257 for rocks, which differs from both the standard hardness description for rocks (Reference 216) and the consistency descriptions for fine-grained soils.

Miami Limestone is expected to be more densely fractured beneath vegetated depressions and drainages as described in Subsection 2.5.4.2.1.1 and presented in Figures 2.5.4-254 and 2.5.4-255.

2.5.4.2.1.2.3 Stratum 3 (Key Largo Limestone)

The top of Key Largo Limestone is encountered between El. –23.1 and El. –35.3 feet, at an average of El. –26.9 feet. The thickness varies between 14.6 and 26.9 feet in the borings, with an average thickness of 22.5 feet.

The Key Largo Limestone, or upper Fort Thompson Formation as it is referred to in Reference 257, is a coralline, porous formation with recrystallized calcite infill visible in core samples. The color varies between white, pale yellow, light brownish gray, and gray. The properties of this stratum indicate a rock of medium hardness and strength based on Reference 216.

Key Largo Limestone is expected to be more densely fractured beneath vegetated depressions and drainages as described in Subsection 2.5.4.2.1.1 and presented in Figures 2.5.4-254 and 2.5.4-255.

2.5.4.2.1.2.4 Stratum 4 (Fort Thompson Formation)

The Fort Thompson Formation underlies the Key Largo Limestone across the entire site, except in boring B-802 where the Miami Limestone is directly above the Fort Thompson Formation. The Fort Thompson Formation is fully penetrated in the majority of boring locations. Borings B-622, B-623, B-624, B-626, B-627, B-629, B-631, B-632, B-633, B-639, B-722, B-723, B-724, B-727, B-729, B-730, B-731, B-732, B-733, B-738, B-739, R-6-1a, and R-6-1a-A are terminated in the Fort Thompson Formation.

The top of this unit is encountered at elevations ranging from –44.1 to –54.3 feet. The range of thickness varies from 51.3 to 77.0 feet, with an average of 65.9 feet.

The Fort Thompson Formation consists of white limestone with varying amounts of vugs, shells, and some sand. It is medium hard to hard above approximately El. –60 feet and is medium hard to soft (based on Reference 216) below approximately El. –60 feet.

The Fort Thompson Formation is expected to be more densely fractured beneath vegetated depressions and drainages as described in Subsection 2.5.4.2.1.1 and presented in Figures 2.5.4-254 and 2.5.4-255.

2.5.4.2.1.2.5 Stratum 5 (Upper Tamiami Formation)

The upper Tamiami Formation underlies the Fort Thompson Formation across the entire site. This stratum is fully penetrated in borings B-601(DH), B-602, B-604(DH), B-605, B-608(DH), B-630, B-701(DH), B-702, B-704(DH), B-705, R-6-1b, R-6-2, R-7-2, and R-7-1 and at each of the six CPT locations. The top of the upper Tamiami Formation is encountered between El. –101.6 and –124.7 feet with an average top elevation of El. –115.4 feet. The base of this unit grades into the lower Tamiami Formation.

The bottom of the unit is estimated at El. –167.6 feet. The upper Tamiami Formation consists of light gray to greenish gray silty sands, with varying amounts of gravel. This stratum is generally dense to very dense.

2.5.4.2.1.2.6 Stratum 6 (Lower Tamiami Formation)

The lower Tamiami Formation is encountered below the upper Tamiami Formation in the Units 6 & 7 power block and is present in 13 of the 15 boring logs (included in Appendix B of Reference 257 and Appendix A of Reference 290) that extend below El. –160 feet. This stratum is fully penetrated in boring locations B-601(DH), B-608(DH), B-610, B-630, B-701(DH), B-710(DH), R-6-1b, R-6-2, R-7-2, R-7-1, and CPT locations C-601, C-701, C-702, R-6-3, and R-7-3. The lower Tamiami Formation starts at approximately El. –167.6 feet.

The lower Tamiami Formation consists of light gray to greenish gray sandy silt with minor amounts of silty clay. It generally has a very stiff to hard consistency.

2.5.4.2.1.2.7 Stratum 7 (Peace River Formation)

The Peace River Formation of the Hawthorn Group is encountered in borings that extend to depths of approximately 220 feet or greater. The top of this stratum is encountered at elevations between El. -206.1 feet and -223.4 feet, at an average elevation of -217.8 feet. This unit is fully penetrated in borings B-701(DH), R-6-1b, and R-7-1. The average stratum thickness is 241.7 feet.

The Peace River Formation is a very dense light gray to olive gray silty sand.

2.5.4.2.1.2.8 Stratum 8 (Arcadia Formation)

The Arcadia Formation of the Hawthorn Group is encountered in borings B-701(DH), R-6-1b, and R-7-1. The top of the Arcadia Formation is encountered at approximately El. -454.8 feet. This stratum is not fully penetrated in borings

B-701(DH), R-6-1b, and R-7-1, with the bottom of boring at El. -617 feet, -464.1 feet, and -459.4 feet, respectively.

The Arcadia Formation consists of several different types of limestone (wackestone, packstone, and mudstone), with occasional dolostone and thin silty sand layers near the top of the unit. The color ranges between pale yellow, white, and light greenish gray. This stratum ranges in hardness from soft to hard using Reference 216 criteria. The induration ranges from friable to indurated. Shell molds are observed in some parts of this stratum.

2.5.4.2.1.2.9 Compacted Limerock Fill

Soil laboratory testing conducted on two bulk samples from test pits excavated into Miami Limestone during the subsurface investigation is performed to evaluate this material as a fill source. This excavated and re-compacted limestone is referred to as compacted limerock fill.

The muck layer underneath the power block area is removed and replaced with compacted limerock fill from onsite excavated Miami Limestone, Key Largo, and offsite sources, with fill placement starting from approximately El. –5 feet and building up to El. +25.5 feet. Excavations and fill on other areas of the site as described in Subsections 2.5.4.3 and 2.5.4.5 are completed. All other non-Category I structures are supported on compacted limerock fill.

2.5.4.2.1.2.10 Properties of Subsurface Materials Below 600 Feet

Evaluation of properties of materials deeper than 600 feet is performed through use of published data from the Florida Geological Survey (FGS) Oil and Gas Division and the U.S. Geological Survey (USGS) (References 211 and 212). Both sources contain logs of borings within approximately 115 miles of the site (see Figure 2.5.4-210). The FGS logs contain sonic data from which compression wave velocity can be calculated extending from as shallow as approximately El. –3550 feet to as deep as approximately El. –11,900 feet. The USGS logs, which include both lithology and sonic data, start out shallower than 600 feet and extend to as deep as approximately El. –2350 feet.

Two gaps in the data where compression wave velocity data are unavailable are identified. The shallower gap is between approximately El. –1800 and El. –2200 feet, and the deeper gap is between approximately El. –2350 and El. –3550 feet depth. Compression wave velocity values to fill the upper approximately 362-foot gap are assumed by estimating compression wave velocities from neutron porosity and porosity density logs obtained from the USGS

publication (Reference 211) and by comparing the lithology and stratigraphy in the logged sections with the lithology of these upper data. Compression wave velocity values to fill the lower approximately 1200-foot gap are estimated by comparing the lithology in these lower data to the compression wave velocity values in logged sections with similar lithology.

Compression wave velocities (V_p) from the sonic logs are converted to shear wave velocities (V_s) using the following equation (Reference 218):

$$V_s = V_p / [2(1 - \mu)/(1 - 2\mu)]^{1/2} \qquad \text{Equation 2.5.4-1}$$

Poisson's ratio (μ) computed from P-S suspension shear and compression wave velocities measured in the semi-consolidated calcareous materials in the upper 600 feet was approximately 0.36. Typical values in South Florida reported in the literature below approximately El. –1100 feet are closer to 0.3. Thus, Poisson's ratio was assumed to reduce from 0.35 just below El. –600 feet. Published values for Poisson's ratio in southern Florida are typified by a value of 0.3 at El. –1100 feet (Reference 218). Thus, a Poisson's ratio of 0.3 is assumed for the calculation of shear wave velocity at and below El. –1100 feet.

As shown in Figure 2.5.4-211, the average V_s from the sonic logs initially increases fairly steadily starting at approximately 4000 feet/second at a depth of 600 feet beneath finished site grade until approximately 4500 feet beneath finished site grade, where an average V_s of approximately 10,000 feet/second is attained, which may coincide with the base of the thick anhydrite unit of the middle Cedar Keys formation. V_s then begins a trend of gradual decrease, which continues until a depth of approximately 6750 feet beneath finished site grade and velocities of around 7000 feet/second are attained, which may coincide with the base of the chalky limestones and dolomites of the Pine Key Formation. At this point, the average V_s from the logs begins a gradual increase to approximately 10,000 feet/second, which is estimated to occur at a depth of around 10,000 feet below finished site grade. Thereafter, the average V_s continues to fluctuate, generally in the range of 8500 feet/second to 10,000 feet/second.

The lithology and sonic data for the Class V exploratory well EW-1 at the Turkey Point Units 6 & 7 site (Figure 2.5.4-242) are provided in Reference 287. The sonic data, from which shear wave velocity is calculated, extends from approximately Elevation -1078 feet to Elevation -3226 feet (NAVD 88).

Compression wave velocities (V_p) from the EW-1 log are converted to shear wave velocities (V_s) using Equation 2.5.4-1. A Poisson's ratio value of 0.31 is assumed

for the calculation of V_s down to Elevation -1100 feet and a value of 0.3 is assumed at and below Elevation -1100 feet (Reference 218). As shown in Figure 2.5.4-243, the average V_s from EW-1 is between 5000 and 6000 fps until a depth of approximately 1500 feet beneath finished site grade. Below this depth, the average V_s increases to between 6000 and 8000 to over 8000 fps at a depth of approximately 2000 feet. V_s then remains between 6000 and 8000 fps until a depth of approximately 2800 feet where, again, an average V_s of over 8000 fps is attained. At this point, the average V_s begins to decrease and below a depth of approximately 3100 feet, the average V_s falls to between 4000 and 6000 fps.

The converted sonic data exhibit some V_s values greater than 9000 fps. Such high values generally indicate the presence of hard rock, such as the granitic rock at the V.C. Summer Units 2 & 3 site (Reference 288) and well-indurated Cambro-Ordovician marine carbonates such as those at the proposed Bellefonte Units 3 & 4 site (Reference 289). The detailed lithologic logs in Reference 287 document the absence of such lithologies at the Turkey Point site. Therefore, the V_s values greater than 9000 fps are not included in the average V_s shown in Figure 2.5.4-243. The V_s values that were less than 9000 fps were retained since, in general, they reflect the lithologies noted on the detailed boring log and average values appear to be similar to, although higher than, the previously obtained data.

2.5.4.2.1.3 Evaluation of Properties of In Situ Materials

Properties of in situ materials are evaluated using the results of field and laboratory testing for Units 6 & 7 and outside the power blocks. These results, in the form of boring logs, CPT records, test pit logs, laboratory test results, etc., are contained in References 257 and 290 and are summarized in tables and figures presented in the following subsections. Generally, the results from within Units 6 & 7 and outside the power blocks are similar. The majority of the average property values for each stratum presented in the following subsections are given in Table 2.5.4-209.

2.5.4.2.1.3.1 Stratum Thickness

The thickness of each stratum is estimated from borings that penetrate the particular stratum. Shear wave velocities and CPTs also provide an estimate of thickness for the shallower strata. The thickness and base elevation of each stratum from all the borings and CPTs are averaged and presented in Table 2.5.4-201. Note that the thicknesses and base elevations given in Table 2.5.4-201 are for all areas of the investigated site.

2.5.4.2.1.3.2 SPT N-Values

As noted in Subsection 2.5.4.2.2.3, 88 geotechnical borings are performed for the initial subsurface investigation: 77 borings in the power block and 11 borings outside the power block. SPT samples are taken at approximately 2.5-foot intervals to 15 feet depth, at 5-foot intervals from 15 to 100 feet depth, at 10-foot intervals from greater than 100 feet to the maximum depth sampled using SPT equipment. Intact soil samples are obtained in selected borings.

Where rock is encountered, continuous coring is employed to obtain samples as presented in Subsection 2.5.4.2.2.3.

In addition, SPT and sampling are performed in two of the geotechnical borings in the supplemental subsurface investigation. SPT samples are taken from approximately 0 to 15 feet and 120 to 460 feet depths.

2.5.4.2.1.3.2.1 Uncorrected N-Values

A summary of all N-values (inside and outside of the power block) measured in the field (uncorrected) during the initial and supplemental investigations is presented in Figure 2.5.4-212 and Table 2.5.4-202. Some very low N-values in the upper and lower Tamiami and Peace River Formations are questionable as described in Subsection 2.5.4.8.2. The SPT N-values obtained from the supplemental investigation at R-6-1b and R-7-1 are consistently higher than those obtained during the initial investigation at B-601(DH) and B-701(DH) for both testing/sampling (Figure 2.5.4-270). Furthermore, the summations of 3rd and 4th blow counts obtained at R-6-1b and R-7-1 are consistently higher than the summation of 2nd and 3rd blow counts (SPT N). This is a consistent trend throughout the SPTs, and is attributed to overwashing as defined in Table 13 of NAVFAC DM 7.1 (Reference 301). Overwashing is considered to be the cause of the lower N-values and is described in more detailed in the subsection on disturbance effects below. Engineering analyses or parameter developments are based only on the summation of the 2nd and 3rd blow counts per ASTM D 1586 (Reference 302). The 3rd and 4th blow counts are included for the purpose of investigating potential overwashing. In a conservative approach, the overall pool of “SPT N” values from the initial and supplemental investigations are used in development of engineering parameters (friction angle and modulus of deformation).

2.5.4.2.1.3.2.1.1 Disturbance Effects

Prior to conducting the supplemental field investigation, it was considered that the SPT blow counts, or SPT N-values (Reference 257) associated with the soil formations, were lower than the expected values based on their significant depth (>100 feet) and a high shear wave velocity above 1500 feet/second (Table 2.5.4-209).

Equivalences between shear wave velocities and blow counts are given in the site classification procedure for seismic design in ASCE/SEI 7-10 (Reference 322). From ASCE/SEI 7-10, the equivalent blow count number (average SPT N value) is higher than 50 for the shear wave velocity (V_s) range of between 1200 and 2500 feet/second. Thus, the blow counts at the site would be expected to be higher than the values determined in the initial field investigation (Reference 257). Shear wave velocity measurements are used as the reference engineering parameter as they are not impacted by the disturbance effects.

In advance of SPT sampling/testing, the borehole bottom is typically cleaned by means of mud circulation. To avoid disturbance of the underlying soils to be tested, ASTM D 1586-11 (Reference 302) includes a provision to enforce the requirement of side discharge at the drill bit. However, the erodible nature of the silty sands at the site suggests that even with side discharge of circulating mud, exposure to the effects of overwashing is inevitable. In addition, the soil formations are deep, ranging from approximately 115 to 460 feet depth. For such depths, disturbance due to stress relief effects is compounding with the effects of erosion from overwashing.

Having recognized these challenges, a targeted approach was taken during the supplemental investigation where a 24-inch-long split barrel sampler was used with special attention paid to the overwashing effect (i.e., avoiding prolonged overwashing). It was expected that the soil for the 3rd and 4th intervals would be better protected against the negative impacts of mud circulation, i.e., overwashing, and would therefore be more representative of actual in situ conditions. In addition to using the longer split barrel, the bentonite-water mix was controlled to provide a heavy mud to reduce the effect of stress relief.

From the results, it is recognized that the blow counts obtained with the use of the longer split barrel (3rd and 4th intervals as opposed to 2nd and 3rd) are less impacted by the effects of overwashing as shown on Figure 2.5.4-269.

Disturbance of the soils to be tested can be mitigated to various degrees depending on drilling/sampling requirements and approach. While it is clear that the blow counts based on 3rd and 4th SPT intervals are higher due to the lessened impacts of overwashing at the deeper location of these intervals, specific drilling/sampling conditions are also found to have an influence on the blow counts as obtained from the 2nd and 3rd intervals. The continuous or discontinuous nature of soil sampling has a direct correlation with the degree of exposure of soil to the effects of borehole preparation. Figure 2.5.4-271 is included to graphically show that the volume of material to be washed out of a borehole is higher when a discontinuous sampling method is used as compared to a continuous sampling method. A larger volume of soil to be removed is directly correlated with a longer exposure to the effects of overwashing.

2.5.4.2.1.3.2.2 N-Value Correction

Field SPT N-values are adjusted for SPT hammer energy, borehole diameter (C_B), sampler (C_S) and rod length (C_R). This adjusted N-value, N_{60}, is determined using the following equation (References 219 and 225):

$$N_{60} = N\ C\varepsilon\ C_B\ C_S\ C_R \qquad \text{Equation 2.5.4-2}$$

Where,

N = field measured SPT blow count
$C\varepsilon$ = hammer energy correction factor
C_B = borehole diameter correction factor
C_S = sampler correction factor
C_R = rod length correction factor

The SPT N-value used in correlations with engineering properties is a value traditionally based on 60 percent hammer efficiency. SPT hammer energy measurements are made for each drilling rig/hammer employed, in accordance with ASTM D 6066 (Reference 220), and the hammer energy measurements (expressed as energy transfer ratios, or ETRs) are obtained. As shown in Table 2.5.4-203, average ETRs range from 62.1 percent to 88.0 percent. The resulting energy correction factor, C_ε (expressed as ETR/60%), ranges from 1.04 to 1.47, also as shown in Table 2.5.4-203. N_{60}-values (from Equation 2.5.4-2) from each boring are corrected using the appropriate C_ε value. The resulting SPT N-values are termed N_{60}. For the liquefaction analysis, additional correction factors for overburden pressure are applied.

A summary of all N_{60} values with depth is shown on Figure 2.5.4-213 and in Table 2.5.4-204.

A comparison of corrected N-values, N_{60}, at Unit 6 [B-601(DH) vs. R-6-1b] and Unit 7 [B-701(DH) vs. R-7-1] boreholes shows the same trend discussed in Subsection 2.5.4.2.1.3.2.1, i.e., values from the supplemental investigation are higher than those from the initial investigation (Figure 2.5.4-272). The differences range from slight to more pronounced. A description of the source of these differences is given below in relation to the sampling approach taken during the supplemental investigation at Units 6 and 7.

For R-7-1 and B-701(DH), where a discontinuous sampling method was performed, results are only slightly different. The slight improvement in the results of the supplemental investigation over the initial investigation is likely due to a pre-established target during the supplemental investigation to reduce disturbance effects by avoiding unnecessary delays between sample locations, as well as a tight control on the consistency of circulating mud, with a resulting mitigation in the exposure of soils to the effects of overwashing.

Alternatively, there is a more pronounced difference within Unit 6 boreholes and this is attributed to the continuous sampling approach taken at borehole R-6-1b, as opposed to the discontinuous sampling at B-601(DH). This pronounced difference is attributed to the reduced time exposure of soils in borehole R-6-1b to the effects of borehole cleaning prior to testing.

In summary, the difference between the initial and supplemental field investigation results can be attributed to:

- Drilling/sampling requirements and approach, specifically the time exposure of soils to the effects of borehole cleaning prior to testing, i.e., continuous vs. discontinuous sampling, and

- The fact that the supplemental investigation's target was to reduce disturbance effects by avoiding unnecessary delays between sample locations, and to adopt a tight control on the consistency of circulating mud.

2.5.4.2.1.3.3 CPT Values

As noted in Subsection 2.5.4.2.2.4, four CPTs are performed for the initial subsurface investigation and two CPTs are performed for the supplemental subsurface investigation with three in each of the two power block areas. The CPTs are initiated at a depth of approximately 120–130 feet in a hole cored

through the overlying rock. The CPTs are advanced through the upper and lower Tamiami Formation and into the Peace River Formation. One CPT extends as deep as 290 feet.

CPT corrected (q_t) and normalized (q_{c1n}) tip resistance values are significant factors in liquefaction evaluation (refer to Subsection 2.5.4.8.3). Note that the terms “corrected” and “normalized” used here are as described in Subsection 2.5.4.8.3. Summaries of all of the CPT tip resistance (q_t) values based on elevation, as well as the sleeve friction (f_s) and friction ratio (R_f) values, are shown in Figure 2.5.4-214.

2.5.4.2.1.3.4 Rock Recovery and RQD

Rock is sampled using HQ3 and PQ3 core barrel equipment. The rock quality designation (RQD) is calculated based on the core runs sampled. In addition to recovery, the RQD provides an index of rock strength for general characterization of a rock mass. As shown on Figure 2.5.4-215, the rock RQD is very inconsistent. In general, rock quality appears to be at its maximum in the Key Largo Limestone. A summary of recovery and RQD for the three rock strata cored is presented in Table 2.5.4-206.

2.5.4.2.1.3.5 Natural Moisture Content and Atterberg Limits

The results of natural moisture content and Atterberg limits laboratory tests on samples from all of the soil strata tested are shown in Table 2.5.4-205.

2.5.4.2.1.3.6 Grain Size Distribution

The results of grain size distribution tests performed on all of the samples tested are shown in Table 2.5.4-205. This table shows the percentage (by dry weight) of gravel, sand, silt, and clay, and also the percentage fines, (i.e., the percentage passing the standard number 200 sieve). Specific gravity measurements are also included in this table. Average fines contents are summarized for each soil stratum graphically in Figure 2.5.4-216. This figure clearly shows the marked difference in fines content between the upper Tamiami Formation (silty sand) and the lower Tamiami Formation (sandy silt).

2.5.4.2.1.3.7 Unit Weight

Unit weights of rock and soil samples are recorded by index properties testing, resonant column/torsional shear (RCTS) testing, unconfined compressive

strength (UCS) testing, and triaxial shear strength testing. The results for all samples tested are included in Table 2.5.4-205.

Total unit weights recommended for use in each stratum are summarized in Table 2.5.4-209.

2.5.4.2.1.3.8 Angle of Internal Friction and Soil Cohesion

Triaxial testing was performed on a total of five samples from the lower Tamiami Formation (including the sample from borehole B-630 of the initial investigation). One sample from the upper Tamiami Formation was tested and 15 from the Peace River Formation were tested.

The only sample tested from the upper Tamiami Formation was taken from Borehole R-6-1b from the supplemental investigation, from El. –147.7 to El. –149.8 feet.

Triaxial testing is summarized in Table 2.5.4-208.

The quantity of triaxial samples tested for the lower Tamiami and the Peace River formations is considered to be sufficient to characterize the shear strength parameters of these soils. For the upper Tamiami Formation, the shear strength parameters are established by the analysis and corroborating data described below.

Cohesion of the Upper Tamiami Formation

The only triaxial test result for the upper Tamiami Formation gives a cohesion value of zero. Atterberg testing on samples from the upper Tamiami Formation indicates that the plasticity index (PI) of this material is lower than the PI for the lower Tamiami (1.44 versus 3.53). Since the cohesion of the lower Tamiami is relatively low (0.75 ksf), and considering the lower fines content of the upper Tamiami, the effective cohesion of the upper Tamiami is considered to be zero.

Friction Angle of the Upper Tamiami Formation

Correlated values established from SPT and CPT results are used to determine the effective friction angle φ’ for this formation.

SPT Correlation for Friction Angle of the Upper Tamiami Formation

Average effective friction angle is determined using three correlations for the upper Tamiami Formation.

SPT Correlation for Friction Angle - Method 1

The effective friction angle can be approximated using the following equation from Kulhawy and Mayne (1990) (Reference 292):

$$\varphi'_{tc} = \tan^{-1} \{[N / (12.2 + 20.3\ \sigma'_{vo}/p_a)]^{0.34}\}$$ Equation 2.5.4-3a

Where,

φ'_{tc}: Triaxial compression effective friction angle

σ'_{vo}: Vertical effective stress (same units as p_a)

p_a: Atmospheric pressure (i.e., 1 atm = 101.3 kPa or 2.1 ksf)

N: Uncorrected SPT-N value

SPT Correlation for Friction Angle - Methods 2 and 3

The effective friction angle is approximated from the SPT N-values and relative densities using the correlation table below, obtained from Kulhawy and Mayne (Reference 292):

SPT N-value	Relative Density	Approximate φ' (°)	
		Peck, Hansen and Thornburn Approximation Method 2	Meyerhof Approximation (Method 3)
0–4	very loose	<28	<30
4–10	loose	28–30	30–35
10–30	medium	30–36	35–40
30–50	dense	36–41	40–45
>50	very dense	>41	>45

CPT Correlation for Friction Angle

The effective friction angle is approximated from the CPT data using the correlation below from Mayne (Reference 293):

$$\varphi' = 29.5° B_q^{0.121} [0.256 + 0.336 B_q + \log Q]$$ Equation 2.5.4-3b

Where,

$$Q = \frac{q_t - \sigma_{v0}}{\sigma'_{v0}}$$ Equation 2.5.4-3c

$$B_q = \frac{u_2 - u}{q_t - \sigma_{v0}}$$ Equation 2.5.4-3d

The expression of φ' above is valid for values of $0.1<B_q<1.0$ and the results acceptable when they are within 20 and 45 degrees. If $B_q<0.1$, the following expression can be used, which is appropriate for clean sands:

$$\varphi' = 17.6° + 11.0° \log q_{t1}$$ Equation 2.5.4-3e

Where,

$$q_{t1} = \frac{q_t/\sigma_{atm}}{(\sigma'_{v0}/\sigma_{atm})^{0.5}}$$ Equation 2.5.4-3f

Summary for Upper Tamiami Formation

The table below presents the friction angle values for the upper Tamiami Formation based on triaxial testing, CPT, and SPT. The average effective friction angle, 34 degrees, obtained from correlations (SPT and CPT based) is in agreement with the result of one triaxial test.

Stratum	Triaxial	Effective Friction Angle: φ' (°)			CPT Correlation
		SPT Correlation			
		Method 1	Method 2	Method 3	
Upper Tamiami Formation	35[(a)]	28	33	37	38

(a) Based on one test result.

Therefore, the friction angle of the upper Tamiami Formation is recommended as 34 degrees.

Recommended values of φ' for each stratum are shown in Table 2.5.4-209.

2.5.4.2.1.3.9 Undrained Shear Strength

Only one primarily fine-grained stratum is encountered in the subsurface investigation. The undrained shear strength (s_u) of this one soil stratum (Stratum 6, the lower Tamiami Formation) is estimated from corrected SPT N_{60}-values.

The empirical correlation used to obtain s_u from the N_{60}-value (Reference 223) is:

$s_u = N_{60}/8$ (in kips per square foot [ksf]) Equation 2.5.4-4

2.5.4.2.1.3.10 Rock Unconfined Strength

Rock core samples from three of the rock strata cored (the Key Largo Limestone, Fort Thompson Formation, and Arcadia Formation) are tested for unconfined compressive strength. Although the Miami Limestone is a rock, its texture does not lend itself to typical rock coring and the use of SPT to sample this formation is common in South Florida.

Results of the unconfined strength tests performed on 31 samples from the Key Largo Limestone, 50 samples from the Fort Thompson Formation, and three samples from the Arcadia Formation are summarized on Table 2.5.4-207 and shown on Figure 2.5.4-217.

2.5.4.2.1.3.11 Elastic Modulus and Shear Modulus (High Strain) for Soils

To determine the high strain stiffness of the soil formations, several different methods are used to address the natural variability, measurement variability, and the variability involved in the conversion of measured parameter to stiffness. The methods use data from pressuremeter tests, SPTs, CPTs, P-S suspension logging, and triaxial tests.

Pressuremeter Tests

Initial and unload/reload shear moduli are directly measured during pressuremeter testing and are readily available from the data. The shear modulus, G, of the tested materials corresponds to one-half of the slope of the curve of corrected pressure versus corrected pressuremeter cavity strain. Two shear moduli are of interest in the stiffness characterization of the material, namely the initial modulus and the unload/reload modulus.

The initial shear modulus, G_i, is a modulus obtained from the straight (initial) portion of the curve of corrected pressure versus corrected cavity strain. This initial shear modulus may be converted into a Young's modulus with a Poisson's ratio value using Equation 2.5.4-5a. Poisson's ratios used are provided in Table 2.5.4-209 for all layers.

The pressuremeter derived Young's moduli (initial and unload/reload) are estimated using Equation 2.5.4-5a:

$$E = 2G(1 + \nu')$$ Equation 2.5.4-5a

Where,

E = Young's modulus, or stiffness
G = Shear modulus
ν' = Poisson's ratio

Standard Penetration Tests

Young's modulus is obtained using different SPT N-value correlations from Reference 217 for different types of soils.

The predominant soil type is SM for the upper Tamiami and Peace River formations and ML for the lower Tamiami formations. Therefore, the Young's modulus, stiffness for the upper Tamiami and Peace River formations is determined using Equation 2.5.4-5b based on blow counts. The Young's modulus, stiffness for the lower Tamiami Formation, is obtained from Equation 2.5.4-5c based on blow counts.

$E = (2600 \text{ to } 2900)\ N_{55}$ Equation 2.5.4-5b

$E = 300\ (N_{55}+6)$ Equation 2.5.4-5c

Where,

E = Young's modulus in kPa
N_{55} = the corrected SPT N-values corresponding to an energy ratio of 55 percent and can be obtained from N_{60} as in Equation 2.5.4-5d.

$N_{55} = N_{60} * 60/55$ Equation 2.5.4-5d

Cone Penetration Tests

Young's modulus or stiffness is obtained from CPT data as given in Equation 2.5.4-6 (Reference 310).

$$E = 0.047\ [1 - (q/q_{ult})^{0.3}][10^{0.55I_c+1.68}](q_t - \sigma_{v0})$$ Equation 2.5.4-6

Where,

$q/_{q_{ult}}$ is conservatively assumed to be 0.5
$I_c = [(3.47 - \log Q_{tl})^2 + (\log F_r + 1.22)^2]^{1/2}$
$F_r = [f_s/(q_t - \sigma_{v0})]100\%$
$Q_{tl} = (q_t - \sigma_{v0})/\sigma'_{v0}$
q_t = cone tip resistance
f_s = cone sleeve resistance
σ_{v0} = total overburden stress
σ'_{v0} = effective overburden stress

P-S Suspension Loggings

The Young's modulus or stiffness is obtained using the shear wave velocity and Poisson's ratio as given in Equation 2.5.4-7.

$$E = 0.1\frac{\gamma}{g}V_s^2 2(1+\nu_s)$$

Equation 2.5.4-7

Where,

$\nu_s = \frac{V_p^2 - 2V_s^2}{2(V_p^2 - V_s^2)}$ = Poisson's ratio as obtained from P-S suspension tests, saturated conditions

V_p= compression wave velocity and 0.1 is the reduction factor (Reference 282).

Triaxial Tests (Consolidated-Undrained)

Using the stress-strain curves obtained from triaxial tests, the secant modulus corresponding to the 50 percent of the maximum stress ratio $(\frac{\sigma'_1}{\sigma'_3})$ from the stress-strain curves is used to determine the stiffness.

Design Stiffness for Soils

The stiffness values obtained from P-S suspension logs, triaxial tests, and SPTs are considered as undrained stiffness, whereas the stiffness obtained from pressuremeter tests and CPTs (except for lower Tamiami) is considered as drained stiffness. For the lower Tamiami Formation, the stiffness obtained from CPT results is considered as the undrained stiffness based on the observed pore

pressure behavior. The pore pressure variation in the upper Tamiami and Peace River formations is close to hydrostatic, whereas excess pore pressures are observed throughout the cone penetration in the lower Tamiami Formation. As a final step, all the stiffness values obtained from each methodology are converted to the drained modulus, if required.

The conversion of the undrained stiffness E_u to drained stiffness E_d is performed using Equation 2.5.4-8 (Reference 311).

$$E_d = \frac{2(1+\nu')}{3} E_u \qquad \text{Equation 2.5.4-8}$$

The maximum, minimum, mean, and median values and standard deviation of E_d (drained) associated with five different previously mentioned methodologies for the three different soil layers are calculated. The moduli obtained from the five methodologies are combined using the geometric mean for each layer. The geometric mean is considered to be a better representation than the arithmetic mean given the wide range of stiffness values obtained from different methodologies.

The design E is provided in Table 2.5.4-209 for each of the upper and lower Tamiami and Peace River formations. The SPT based stiffness is exceptionally low for the lower Tamiami Formation compared to the stiffness obtained from other methods, thus, this value is disregarded while determining the design stiffness.

Shear Modulus and Poisson's Ratio

Shear modulus, G, is related to elastic modulus, E, as follows (Reference 225):

$$G = E/(2\,[1 + \mu]) \qquad \text{Equation 2.5.4-9}$$

with the terms as defined before.

Values of G for each stratum are calculated from the E values recommended for use in Table 2.5.4-209. Poisson's ratio values of 0.37, 0.31, and 0.34 are used for rock strata (Strata 2, 3, and 4, respectively), and a Poisson's ratio of 0.35 is used for soil strata (Strata 5, 6, and 7). However, the saturated sand strata will have a higher Poisson's ratio (approaching 0.5) as indicated by the geophysical testing. A Poisson's ratio of 0.36 is recommended for Stratum 8. The resulting high strain G values are given in Table 2.5.4-209 for the power block areas.

Typically, sound rock and even moderately weathered rock exhibit an elastic response to loading with little change, if any, in stiffness properties. For rocks, the elastic and shear modulus values generally remain constant at both low and high strains. Using Equations 2.5.4-6 and 2.5.4-5, E and G (same for high and low strain) can be computed from the shear wave velocities for the Key Largo Limestone and Fort Thompson and Arcadia Formations, see Table 2.5.4-209.

However, at some stage of weathering, rock becomes sufficiently decomposed to exhibit modulus reduction. The Miami Limestone layer is considered to fall into a sufficiently weathered state for its modulus values to become strain dependent.

Note that the results of laboratory elastic modulus testing performed on one sample of the Key Largo Limestone and one sample of the Fort Thompson Formation are compared to the E and G values derived based on the average shear wave velocities measured, and they indicate E = 2700 kips per square inch (ksi) for the Key Largo Limestone and E = 2900 ksi for the Fort Thompson sample. The shear and elastic modulus values based on shear wave velocity are considered more representative because the laboratory results are derived from samples with higher than average RQD.

2.5.4.2.1.3.12 Static Earth Pressure Coefficients

Active, passive, and at-rest static earth pressure coefficients, K_a, K_p, and K_0, are estimated assuming frictionless vertical walls and horizontal backfill using Rankine's theory, and are based on the following relationships (Reference 225):

$$K_a = \tan^2 (45 - \varphi'/2) \qquad \text{Equation 2.5.4-10}$$

$$K_p = \tan^2 (45 + \varphi'/2) \qquad \text{Equation 2.5.4-11}$$

$$K_0 = 1 - \sin (\varphi') \qquad \text{Equation 2.5.4-12}$$

Where,

φ' = drained/effective friction angle of the soil

Calculated static earth pressure coefficients are given in Table 2.5.4-209. Foundations are not constructed at depths below the Fort Thompson Formation (Stratum 4). Thus, earth pressure coefficients are not calculated below this stratum.

Coefficients used for seismic lateral earth pressure calculations are described in Subsection 2.5.4.10.4.2.

2.5.4.2.1.3.13 Coefficient of Sliding

The coefficient of sliding is equal to tangent δ, where δ is the friction angle between the soil and the foundation material bearing against it, in this case concrete.

Based on Reference 223, tangent δ = 0.6 is selected for the Miami Limestone (Stratum 2), and tangent δ = 0.7 is selected for the Key Largo Limestone and Fort Thompson Formation, Strata 3 and 4, respectively. Foundations are not constructed on materials deeper than the Fort Thompson Formation, Stratum 4.

2.5.4.2.1.3.14 Shear and Compression Wave Velocity

The measurement and interpretation of shear wave velocities are addressed in Subsections 2.5.4.4 and 2.5.4.7, respectively, and are briefly summarized here. At both Unit 6 and 7, shear and compression wave velocities are measured with P-S suspension logging in six borings (five initial and one supplemental) for each unit (Subsection 2.5.4.4.2.1) and with downhole velocity logging at one location for each unit (Subsection 2.5.4.4.2.2). Figure 2.5.4-218 is a plot of all of the measured shear wave velocities to depths of 450 and 600 feet at Unit 6 & Unit 7, respectively. Figure 2.5.4-219 is a plot of all the measured compression wave velocities to the same depths. A summary of the measurements with their calculated averages is presented in Table 2.5.4-215. This table summarizes the measured shear and compressive wave velocities using P-S suspension logging with the average and standard deviation for each 10-foot interval investigated to a maximum depth of 610 feet. (El. –611 feet). The recommended values of shear wave velocity are shown versus depth in Figure 2.5.4-220. A description of the data in these plots is given in Subsection 2.5.4.7.

Table 2.5.4-209 provides recommended shear wave velocity values for each stratum investigated.

2.5.4.2.1.3.15 Elastic Modulus and Shear Modulus (Low Strain)

The low strain shear modulus (G_L, normally assumed to be the shear modulus at 1.0E-04 percent shear strain) is derived directly from the shear wave velocity using Equation 2.5.4-7. The value of low strain shear modulus for each stratum shown for the power block in Table 2.5.4-209 is derived from the recommended shear wave velocity value (shown in Table 2.5.4-209). The low strain elastic modulus (E_L) is obtained from the low strain shear modulus (G_L) value using Equation 2.5.4-6 and applying the value of Poisson's ratio given in Table 2.5.4-209.

2.5.4.2.1.3.16 Shear Modulus Degradation and Damping Ratio

Fourteen RCTS tests are performed on intact samples from Stratum 3 (Key Largo Limestone), Stratum 4 (Fort Thompson Formation), Stratum 5 (upper Tamiami Formation) and Stratum 6 (lower Tamiami Formation).

In each RCTS test, values of shear modulus (G) measured at increasing shear strain levels are obtained. These are compared to the value of G_{max}, the shear modulus measured at 1.0E-04 percent shear strain, and shown as the shear modulus degradation (ratio of G/G_{max}) plotted against shear strain. A curve of G/G_{max} from the literature that best fits the test data is selected. This is described further in Subsection 2.5.4.7.3.1.

Table 2.5.4-216 summarizes the selected values of G/G_{max} versus shear strain for each stratum investigated. Each RCTS test also provides measured values of damping ratio (D) at increasing shear strain levels. The same procedure used for G/G_{max} is employed to obtain a best-fit D versus shear strain curve from the literature. Table 2.5.4-216 shows the selected values of D versus shear strain for each test. This is described further in Subsection 2.5.4.7.3.2. RCTS test results are tabulated in Appendix F of Reference 257 and Appendix B of Reference 290.

2.5.4.2.1.3.17 High Strain Rock Stiffness

High strains are associated with the static settlement type of deformation. Rock stiffness associated with high strains may be determined based on in situ and laboratory tests. The design stiffness can be interpreted on the basis of several methods to address natural soil variability, measurement variability, or the variability involved in correlation of the measured parameter to stiffness.

In situ tests conducted at Turkey Point Units 6 & 7 for the rock stiffness include P-S suspension soundings and pressuremeter tests. P-S suspension tests produce the shear high wave velocity profile, which can be converted to low strain stiffness (E_{max}), and high strain stiffness (E).

P-S Suspension Soundings

Shear wave velocity, V_s, can be converted to G_{max} as given in Equation 2.5.4-9a.

$$G_{max} = \rho V_s^2 \qquad \text{Equation 2.5.4-9a}$$

Using theory of elasticity, the maximum shear modulus, G_{max}, is then converted to maximum modulus of elasticity, or stiffness, corresponding to low strains as given in Equation 2.5.4-9b,

$$E_{max} = 2\,G_{max}(1 + \nu_s)$$ Equation 2.5.4-9b

Where,

ν_s= Poisson's ratio.

Poisson's ratio is expressed as given in Equation 2.5.4-9c.

$\nu_s = \frac{(V_p^2 - 2V_s^2)}{2(V_p^2 - V_s^2)}$ = Poisson's ratio as obtained from P-S suspension tests, saturated conditions Equation 2.5.4-9c

Where,

V_p= compression wave velocity.

To obtain the high strain stiffness, E, E_{max} is typically reduced by a factor. This factor is provided in Reference 309 as a function of RQD. Reference 303 also reports that the shear wave velocity based stiffness without reduction may be too high. A more accurate reduction factor can be obtained using the G/G_{max} curves. However, the large stiffness of rocks prevents obtaining strains as large as 0.02 percent during RCTS testing. Therefore, the laboratory data for the G/G_{max} data is limited for high strain assessment. To obtain the high strain modulus, the dynamic low strain modulus is multiplied by 0.25 for the Key Largo Formation (average RQD = 67 percent), 0.15 for the Fort Thompson Formation (average RQD = 39 percent), and by 0.15 for the Miami Formation (average RQD = 37 percent).

Shear strains as obtained from the settlement analysis will not exceed 0.1 percent within rock formations, thus, the assigned reduction factors are conservative.

For the Arcadia Formation, no reduction factor is applied. Since it is more than 450 feet deep, no shear strain is anticipated to be induced due to structural loads. Only shear wave velocity measurements are available due to the depth of the Arcadia Formation, and the design stiffness is established only based on the shear wave velocity measurements.

Pressuremeter Tests

Pressuremeter modulus produces two types of stiffness: initial modulus and the unload/reload modulus. The unload/reload shear modulus, G_{ur}, is obtained from the unload/reload loops performed during pressuremeter testing. During pressuremeter tests, the vuggy nature of the limestone formations caused challenges in obtaining a good quality of test pocket. Therefore, many of the test

attempts were disregarded due to low quality (too large) test pockets. For the successful tests, it was observed that the unload/reload modulus increases substantially with increasing pressure. This trend is not as strong in the underlying soil layers (upper Tamiami, lower Tamiami, and Peace River formations). This indicated that at low strains there may be disturbance on the rock medium. The initial modulus, E_i, was observed to be significantly lower than the first unload/reload modulus, E_u, (the average ratio E_u/E_i = 1.9 for the Key Largo Formation, and the average ratio E_u/E_i = 2.4 for the Fort Thompson Formation). Reference 312 recommends using the unload/reload modulus if disturbance is evident at low strains, which is manifested as a much higher unload/reload modulus than the initial modulus. Therefore, the first unload/reload modulus is considered as the design value. Since the unload/reload modulus also increases with pressure, the selection of the first unload/reload modulus is conservative.

Unconfined Compressive Strength

UCS tests yield the compressive strength and the stiffness. The stiffness is determined as the secant slope to the stress-strain curve at approximately 40 to 60 percent of the compressive strength. The secant stiffness is reduced to account for the rock mass. The reduction factor is obtained from Reference 308. Reference 303 reports that the stiffness obtained from the UCS test (without reduction) may be considered as the upper bound, which is in agreement with the proposed reduction by Reference 308. The reduction factor from the laboratory unconfined compression stiffness to in situ stiffness is considered as 20 percent for the Key Largo Formation and 10 percent for the Fort Thompson Formation.

Rock Mass Rating

In addition to the laboratory and in situ tests, the rock mass stiffness is obtained using the rock mass rating (RMR) and geologic strength index (GSI) classifications. Three different correlations from Reference 307 (Equation 2.5.4-9d), Reference 308 (Equation 2.5.4-9e), and Reference 304 (Equation 2.5.4-9f), are used to obtain rock stiffness.

$$E_{rm}=E_i*10^{\frac{(RMR-100)(100-RMR)}{4000e^{(-RMR/100)}}}$$ Equation 2.5.4-9d

$$E_{rm}=E_i\left(0.0028*RMR^2+0.9e^{\left(\frac{RMR}{22.82}\right)}\right)/100$$ Equation 2.5.4-9e

$$E_{rm}=E_i\left(0.02+\frac{1-D/2}{1+e^{\left(\frac{60+15D-GSI}{11}\right)}}\right)$$ Equation 2.5.4-9f

Where,

E_{rm} = rock mass modulus,
E_i = intact elastic modulus, UCS * modulus ratio, MR (Reference 304),
D = the disturbance factor as used in calculation of φ' and c' ,
RMR = the rock mass rating, and
GSI = the geologic strength index.

Design Rock Stiffness

The stiffness for the limited moderately fractured zone is calculated only through the RMR. However, the stiffness of the slightly fractured zone is calculated based on RMR, P-S suspension, UCS, and pressuremeter calculations.

To obtain the design stiffness for the slightly fractured rocks, first, the mean and median stiffnesses are obtained for each method. Then, the means of all the means and medians (for all four methods) are determined. The lower value is assigned as the design stiffness. This value is considered conservative since the stiffness obtained from each method corresponds to strain levels that would be higher than expected under foundation loads, particularly on the Fort Thompson Formation. The design stiffness of the Fort Thompson Formation is higher than the stiffness obtained from pressuremeter tests. The difference is more pronounced for the Key Largo Formation. This is attributed to the effect of vugs on the stiffness as well as the disturbance at low strains. The vugs are more frequent in the Key Largo Formation, thus, the pressuremeter test results indicate lower stiffnesses for the Key Largo Formation. Also, the second cycle unload/reload stiffness is closer to the design stiffness, which shows the effect of disturbance at lower strains.

For the moderately fractured zone, only the rock mass evaluation-based stiffness values are available. From the slightly fractured zone data pool, the rock mass-based stiffness values are observed to be higher than all other methods. Therefore, it would be unconservative to assign rock mass-based stiffness for the moderately fractured zone. A reduction is applied on the rock mass-based stiffness to obtain the design stiffness. The reduction factor is calculated as the

ratio of the design value for the slightly fractured zone to the rock mass-based slightly fractured zone stiffness.

The design stiffness of the Arcadia Formation is determined using the shear wave velocity measurements without any reduction factor.

The design stiffnesses are provided in Table 2.5.4-209. Reference 309 reports sound limestone stiffness of 200,000 to 400,000 ksf. The design stiffnesses shown in Table 2.5.4-209 are conservative with respect to the typical values reported in Reference 309.

2.5.4.2.1.3.18 Low Strain Rock Stiffness for the Key Largo and Fort Thompson Formations

Low strains represent the levels corresponding to the site response analysis or seismic soil-structure interaction (SSI) analysis. For the low strain range (less than 0.005 percent), the behavior as obtained from RCTS tests is essentially linear for both the Key Largo and Fort Thompson formations. The median strain profile obtained from the site response analysis indicates that the maximum strains are less than 0.005 percent shear strain for both the Key Largo and Fort Thompson formations. For this strain range, stiffness degradation is negligible.

2.5.4.2.1.3.19 Lower-Bound Soil/Rock Parameters

For sensitivity cases regarding settlement, bearing capacity, and bearing pressure uniformity sensitivity analyses, lower-bound parameters for soil and rock formations are developed using two methodologies depending on the available data. If there are too few measurements, the lower bound is considered to be 16th percentile. Usually, a goodness-of-fit test is not performed for a sample with size less than 5 (Reference 318), and this number (5) is adopted hereby as the quantitative criterion for determining the sufficiency of the sample size. If there are sufficient measurements, the following four descriptors are considered to establish the lower bound. Lower-bound parameters are provided in Table 2.5.4-221.

1. $\mu - \sigma$ where μ is sample mean and σ is sample standard deviation

2. 16th percentile

3. BE/(1+COV) where BE is the best estimate or design value, the lower one of mean and median, as given in Table 2.5.4-209, and COV is coefficient of variation

4. $\exp(\ln(\text{Median}) - \sqrt{\ln(1+\text{COV}^2)})$, which is analogous to the equation on Page 18 of the Standard Review Plan (SRP) 3.7.2

2.5.4.2.1.3.20 Rock Mass Classification

Rock mass classification systems are specifically developed to estimate properties of the bearing strata as a whole from characteristics of individual rock cores, core samples, and boring logs. The RMR system accounts for five categories that describe a rock mass and outline ratings for each parameter (Reference 303). The five parameters are:

1. Strength of intact rock

2. RQD

3. Spacing of discontinuities

4. Condition of discontinuities

5. Groundwater condition

An additional rating adjustment for orientation of discontinuities is applied after calculating the sum of the five main ratings. This adjustment is subtracted according to the potential disadvantage of joint set strike and dip to the specific application, such as tunnels, foundations, or slopes (Reference 303).

The first two of the five main ratings are directly determined from laboratory and field data. Strength of intact rock is measured in the laboratory from UCS tests on core samples, and RQD is measured in the field according to lengths of intact rock in a given core run. Discontinuity characterization and groundwater condition are interpreted using boring logs from the initial and supplemental site investigations (Appendix B of Reference 257 and Appendix A of Reference 290).

Laboratory measurements of UCS are summarized in Table 2.5.4-207 and Figure 2.5.4-217.

Field measurements of RQD and recovery lengths are summarized in Table 2.5.4-206. Recovery and RQD values by core run range from 0 to 100 percent in all rock layers except the Arcadia Formation, where the minimum measured recovery is 18 percent. Average recovery by layer ranges from 67 to 86 percent and average RQD by layer ranges from 37 to 67 percent. Figure 2.5.4-215 (Sheet 1) presents

the scatter of RQD values in all rock layers. Figure 2.5.4-215 (Sheet 2) presents the scatter of RQD values in rock layers above El. −150 feet. On Sheet 2, RQD values appear more consistent within layers and a distinction is observed at approximate El. -55 feet between the generally higher RQD values of the Key Largo Limestone and the generally lower RQD values of the Fort Thompson Formation.

The variability of RQD is accounted for in RMR classification by rating each core run separately then statistically summarizing the core run RMR ratings by layer. This allows every RQD value to be included in the RMR classification. The other four RMR parameters are rated according to layer instead of core run.

The boring logs (Appendix B of Reference 257 and Appendix A of Reference 290) present information used for discontinuity characterization (spacing, condition, and orientation) and groundwater condition. Descriptions of joints and fractures include openness, infill thickness, infill strength, wall roughness, and wall weathering. The discontinuity spacing is assumed to be the worst case for evaluation of RMR since the lateral spacing cannot be determined from a limited number of borings. The groundwater condition is determined by water level measurement and drilling notes, indicated on the boring logs, and verified through laboratory moisture content values.

Another method for classifying a rock mass is graphically using the GSI system and the discontinuity characterization from the boring logs. GSI specifically accounts for the structure of the rock mass (spacing of discontinuities) on one axis and the joint surface conditions (condition of discontinuities) on the other.

2.5.4.2.1.3.21 Shear Strength of Rock

Mohr-Coulomb failure parameters, φ' and c′, define the shear strength of a rock mass and are calculated using laboratory UCS test results, overburden stress characterization, and material parameters. This is achieved using the Generalized Hoek-Brown criterion (Reference 305).

2.5.4.2.1.4 Chemical Properties of Soil and Rock

An evaluation of the chemistry of the soil and rock strata is performed to consider possible corrosive effects on buried steel and aggressiveness towards buried concrete. For this evaluation, selected SPT samples are tested.

2.5.4.2.1.4.1 Laboratory Chemical Testing and Evaluation

Twenty-three sets of chemical analysis, consisting of pH, chloride content, and sulfate content, are performed on samples from the power block areas. Depths range from ground surface to approximately 155 feet. Samples tested are from the muck/peat, Miami Limestone, Key Largo Limestone, Fort Thompson Formation, and upper Tamiami Formation. Test results are summarized in Table 4.6 of Reference 257 and Table 4 of Reference 290. As noted in Subsection 2.5.4.5.1, the nuclear island is supported on concrete fill and surrounded by limerock structural fill. Buried piping, duct banks, etc. are founded in limerock structural fill placed from about El. –5 feet (bottom of excavated muck) to El. +25.5 feet (final plant grade).

Measured pH values range from 7.4 to 9.0, with an average of 8.5. The analytical results are indicative of mildly corrosive soils as indicated in the guidelines given in Table 2.5.4-211. This table is a summary of guidelines presented in References 227, 228, 229, and 230.

Measured chloride contents for the same soils are analyzed. The range for the chloride contents is from 1833 to 70,400 parts per million (ppm). These results indicate the soil is very corrosive based on the Table 2.5.4-211 guidelines. However, only one sample contains greater than 8830 ppm and it is a muck sample. Because this stratum is removed, the environment is considered very corrosive but not as severely corrosive as indicated by the maximum measurement.

Measured sulfate contents for the same soils are analyzed. The range for the sulfate content is from 198 ppm to 7590 ppm (equivalent to 0.02 to 0.76 percent). Only one sample contains greater than 1190 ppm (0.119 percent). The sample with the highest sulfate is from the muck stratum (which is removed during construction). Thus, one sample from the muck stratum tested indicates severe aggression towards exposed concrete, but as noted above this stratum is removed. The sulfate content results from the Miami Limestone, Key Largo Limestone, Fort Thompson Formation, and upper Tamiami Formation indicate mild to moderate aggression toward concrete. Based on the guidance from applicable references summarized in Table 2.5.4-211, Type II cement is considered acceptable for nonsafety-related structures that are in contact with these in situ materials. DCD Tier 1, Table 3.3-6 provides an ITAAC to ensure that the exterior walls and the basemat of the nuclear island have a water barrier up to site grade. Since the water barrier will eliminate contact between the fill and the

nuclear island exterior walls and basemat, any potential sulfate or chloride attack on the concrete will be minimized.

In addition to testing soil and rock samples for potential harmful behavior toward buried concrete and steel, selected samples are tested for calcium carbonate content to determine the degree to which the strata are primarily carbonate materials. Table 2.5.4-210 summarizes the results in terms of Calcite Equivalent. The results indicate that the rock strata (Strata 2, 3, 4, and 8) generally have a higher Calcite Equivalent than the soil strata (Strata 5, 6, and 7). The differences in calcite content provide an indication that the soil strata (Strata 5, 6, and 7) underlying the upper rock strata (Strata 2, 3, and 4) are not merely decomposed rock but represent a distinctly different depositional environment. Additionally, the lower calcite composition of the soil strata indicates that the soil strata consist primarily of quartz and as such, no correction of N-values on the basis of calcium carbonate grains is warranted.

2.5.4.2.1.5 Field Testing Program

Initial field subsurface investigation activities were performed at the site from February 2008 through June 2008. Supplemental field subsurface investigation activities were performed at the site from July 2013 to October 2013. The field testing programs are addressed in Subsection 2.5.4.2.2.

2.5.4.2.1.6 Laboratory Testing Program

Laboratory tests are conducted on samples recovered during the field investigations following the retrieval of soil and rock samples.

The laboratory testing program is addressed in Subsection 2.5.4.2.3.

2.5.4.2.2 Subsurface Investigation/Exploration

RG 1.132 provides guidance on conducting site investigations for nuclear power plants, and addresses the objectives of subsurface investigation with respect to the design of foundations and associated critical structures. Because subsurface investigations need to be site-specific, there is recognition in RG 1.132 that flexibility and adjustments to the overall program, applying sound engineering judgment, are necessary to tailor to site-specific conditions. Consequently, adjustments are made to the subsurface investigation (including adjustments to field testing locations and to the types, depths, and frequencies of sampling) during field operations, resulting in a more comprehensive subsurface investigation.

None of the adjustments made to the field testing locations, test methods, testing frequencies, and test depths vary from the recommendations in RG 1.132. The exploration program met the intent of RG 1.132 and met the guidelines of the regulatory guide except that only one boring instead of two (one per unit) was continuously sampled in the deeper soils, and only the borings used for borehole geophysical logging and the inclined borings were surveyed for deviation. This variation in field testing is considered to be acceptable because the soil and rock strata are found to be uniform in depth and thickness across the site.

Subsurface investigation work at the site is performed under an approved quality assurance program with site-specific work procedures, including subsurface investigation work plans and a detailed technical specification. Figure 2.5.4-202 shows the locations of field tests made for this subsurface investigation. The investigation activities at and near the site are conducted to develop a comprehensive characterization of subsurface conditions that influence the performance of safety-related structures, including the static and dynamic engineering properties of soil and rock in the site area. This subsection presents detailed descriptions of the type, quantity, extent, purpose, and results of the investigation activities at Units 6 & 7. Type, quantity, and depth of boreholes and in situ tests are selected to follow the guidance in the RG 1.132, and laboratory tests are performed to follow the guidance in RG 1.138.

Eighty-eight geotechnical borings, 22 groundwater wells, 4 CPTs, and 2 test pits comprise part of the initial subsurface investigation. The supplemental site investigation was conducted to:

- Drill two additional borings at the center of Units 6 & 7, obtain additional undisturbed soil samples, and conduct further laboratory testing (triaxial, consolidation and RCTS tests)
- Drill two inclined borings towards the center of vegetated surface depressions to study potential fractures or potential karstic features
- Perform pressuremeter tests in the power block areas of both units to obtain in situ deformation characteristics of both rock and soil formations
- Perform P-S suspension logging to supplement existing shear and compression wave velocity data and high-resolution televiewer imaging to study potential fractures
- Perform two additional CPTs in the footprint of safety-related structures

- Collect surficial muck deposits to provide additional information related to the recent geologic history at the site

During the supplemental investigation, nine borings are drilled (six vertical and three inclined), with geophysical testing performed in two borings, pressuremeter testing performed in three borings, and CPT performed in two borings. A third inclined boring is drilled due to low core recovery in one of the inclined borings. In addition, nine borings were collected using a McCauley Sampler. The coordinates and elevations associated with each of the boring and CPT locations are shown in Table 2.5.4-212. The coordinates and elevations of the exploratory test pits are presented in Table 2.5.4-213. Profile plots from site explorations are provided in Figures 2.5.4-203 through 2.5.4-208. Figure 2.5.4-209 show the locations of these profiles. Properties of soils and rocks used in evaluations are summarized in Table 2.5.4-209. The results of these subsurface investigations are presented in References 257, 290, and 291.

In the initial site investigation, 11 drill rigs and one CPT rig are used on the site. Ten drill rigs are used for SPT sampling. The types of drilling and CPT equipment used during the subsurface exploration investigation include:

- CME 45, tracked rig (1)
- CME 55, ATV and marsh buggy (2)
- CME 75, truck-mounted rig (1)
- CME 550, ATV and marsh buggy (5)
- CME 750, ATV (1)
- Gus Pech Sonic rig (not used for SPT)
- Fugro CPT rig (not used for SPT)

In the supplemental site investigation, three drill rigs and one CPT truck are used on the site.

Due to the soft surface soil conditions, a geotextile reinforced, crushed limestone gravel roadway along the centerline of the power block provides access to the exploration locations for the site drilling equipment and support vehicles. Timber mats provide access to exploration locations away from the gravel road.

An onsite storage facility for soil sample and rock core retention is established before the start of each subsurface investigation. Each sample is logged into an inventory system, and samples removed from the facility are noted in an inventory logbook. A chain-of-custody form is also completed for all samples removed from the facility. Material storage and handling is in accordance with ASTM D 4220 (Reference 234). Results of these subsurface investigations are presented in References 257, 290, and 291. A summary of field test activities follows.

2.5.4.2.2.1 Planning the Field Testing Program

RG 1.132 provides guidance on spacing and depth of borings, sampling procedures, in situ testing procedures, and geophysical investigation methods. This guidance is employed in preparing the technical specification for the project and addressing the bases for the site-specific subsurface investigation.

For the power block, the quantities of borings and CPTs for major structures (including Seismic Category I structures) are based on a minimum of one boring or one CPT per structure and one boring or one CPT per 10,000 square feet of structure plan area. RG 1.132 also includes a recommendation that borings for Seismic Category I structures extend to a depth approximately equal to the width of the structure below the planned foundation level. The sampling intervals employed in borings made for this subsurface investigation vary slightly from RG 1.132, but are in accordance with the technical specification, and are reasonable for characterizing site subsurface conditions.

Information from the previous Turkey Point subsurface investigation program for Units 3 & 4 (Reference 231) indicates that the site is underlain by the Miami Limestone and the Fort Thompson Formation to a depth of approximately 70 feet. Below this is the Tamiami Formation, a clayey and calcareous marl locally indurated to limestone. Based on this information, borings that extend to a depth of 125 feet are placed beneath each building. In the initial investigation, borings beneath the reactor and other key structures are extended up to approximately 250 feet, and one boring beneath each reactor extends to at least 400 feet. The deepest boring, B-701(DH), extends to a maximum depth of 616 feet. The supplemental investigation provides an additional boring beneath each reactor that extends to at least 450 feet.

2.5.4.2.2.2 Planning the Laboratory Testing Program

The laboratory testing for this site subsurface investigation is planned according to guidance provided in RG 1.138. Laboratory testing details and results are

contained in Appendices E and F of Reference 257, Appendices B and C of Reference 290, and Appendix 3 of Reference 291.

Soil samples assigned for laboratory testing are transported under chain-of-custody from the onsite storage area to the testing laboratories. Geotechnical laboratory testing for this site subsurface investigation is performed at multiple laboratories including:

- MACTEC Engineering and Consulting, Inc. (MACTEC) (Atlanta, Georgia)
- MACTEC (Raleigh, North Carolina)
- Severn Trent Laboratories (STL) (part of Test America, St. Louis, Missouri)
- Fugro Consultants, Inc. (Houston, Texas)
- Geotechnics (Pittsburgh, Pennsylvania)
- Kleinfelder Laboratory (Albuquerque, New Mexico)

The Fugro and Kleinfelder laboratories perform specialty RCTS testing. RCTS test results from Fugro are reviewed by Dr. Kenneth Stokoe of University of Texas at Austin. Fugro also performs a consolidated undrained triaxial test. STL performs chemical testing (pH, chloride, and sulfate). MACTEC performs index property, carbonate content, and compressive strength testing. Geotechnics performs index property, one-dimensional consolidation, consolidated undrained triaxial, chemical, and loss on ignition testing.

2.5.4.2.2.3 Boring and Sampling

The rock core descriptions on the boring logs in Reference 257 are based on the classification system commonly used in Florida. The carbonate rock encountered at the site is classified according to Dunham (Reference 215). The geologic formations encountered in the geotechnical exploration are identified in the field. This preliminary classification is later confirmed or modified by senior geologists based on examination of samples and cores, and the results of laboratory testing.

Of the 88 geotechnical borings drilled and sampled as part of the initial site investigations, one (B-701 DH) has a depth of 616 feet in the Unit 7 power block and one (B-601 DH) has a depth of 420 feet in the Unit 6 power block. The remaining 86 borings range in depth from 100 to 290 feet, with a median depth of approximately 125 feet.

Borings drilled as part of the initial investigation are advanced from the ground surface using mud rotary drilling techniques until encountering SPT refusal (defined as 50 blows for 0.5 feet or less of penetration) or to an approximate depth of 35 feet, whichever occurs first. SPT soil samples at these upper depths from the geotechnical borings are obtained at approximate 2.5-foot and 5-foot intervals depending on sample depth.

Once SPT refusal is encountered or an approximate depth of 35 feet is reached, a steel casing is set, and holes are advanced using triple tube wire-line rock coring equipment and procedures described in ASTM D 2113 (Reference 232). Rock coring is accomplished utilizing HQ3- or PQ3-sized core barrels with split inner-barrel liners. Three-, four-, and/or six-inch diameter casings are used to stabilize the upper portions of borings as necessary. Multiple-sized casings are typically set in borings advanced to more than 100 feet depth. Borings are advanced to a predetermined termination depth. In many of the borings, rock coring is terminated in favor of drilling and SPT sampling (at 10-foot intervals) as the subsurface materials change from the Fort Thompson Formation limestone to the upper Tamiami Formation sand. The sampling method changes at a greater depth as the stratum changes from the Peace River Formation to the Arcadia Formation, where rock coring recommences in B-701 (DH).

Nine borings were drilled and sampled as part of the supplemental investigation. For boring R-6-1b, PQ-coring was conducted in the shallow limestone layers to a depth of 120.5 feet, and SPT and sampling was conducted in the Tamiami and Peace River formations to a depth of 464.1 feet. For boring R-7-1, PQ-coring was performed in shallow limestone layers to a depth of 118.7 feet, and SPT and sampling was conducted in the Tamiami and Peace River formations to a depth of 459.4 feet. For borings R-6-1a, R-6-1a-A, and R-7-4, inclined PQ-coring was performed in the shallow limestone layers to a depth of approximately 115 feet. For borings R-6-2 and R-7-2, destructive drilling (rock and soil) and NWD4-coring (rock) were conducted to allow for subsequent pressuremeter testing. For borings R-6-3 and R-7-3, destructive drilling was used to a depth of 125 feet to allow for CPT in the Tamiami and Peace River formations.

These subsurface investigations are used to obtain detailed information about the near-surface geologic characteristics and composition of sediments underlying the site.

To collect intact samples for testing, thin-walled tube samples are collected at various depths in three borings (B-630, R-6-1b, and R-7-1) in general accordance with ASTM D 1587 (Reference 233). Specifically, samples are

collected with Shelby tubes, Osterberg sampler, and Pitcher barrel sampler equipment. The samples are handled and transported in accordance with ASTM D 4220 (Reference 234).

Rigs used during the initial investigation for the collection of SPT soil samples use automatic hammers. The SPT rig used during the supplemental investigation uses a cathead-rope, safety-type hammer. Energy measurements, in accordance with ASTM D 4633 (Reference 235), are made on the SPT hammer-rod systems on each of the drilling rigs, as presented in Subsection 2.5.4.2.1.3.2. A summary of rig information is presented in Table 2.5.4-203.

Geotechnical field data including boring logs, core photographs, and test pit logs are included in Appendix B of Reference 257 and Appendix A of Reference 290.

The groundwater levels in the borings monitored during drilling operations are generally near or above the existing ground surface. Due to the use of drilling fluid additives, the groundwater conditions observed in the geotechnical borings do not truly reflect the groundwater conditions at the project site. Reliance for determining groundwater level is placed on measurements from the observation wells, as described in Subsection 2.5.4.2.2.7.

Circulation of drilling fluids is typically first lost at, or about, the contact between the Miami Limestone and the Key Largo formations. During the following coring operations, the drilling fluid circulation is regained and lost due to the secondary porosity and connectivity/lack of the vugs encountered in the limestone formations drilled at the site. As a result, demand for water used to complete the borings varies with depth. In borings that terminate at depths below the limestone units, circulation of drill fluids is typically regained by advancing steel casing through the limestone formations. Standard bentonite based drilling additives are used in borings not associated with clusters of observation wells.

At selected locations and following review of the adjacent geotechnical borings, groundwater observation wells are installed by rotary wash drilling methods, rotosonic drilling methods, or in previously drilled PQ3 size core holes as described in Subsection 2.5.4.2.2.7. The borings not used for observation wells are filled using a cement-bentonite grout prior to demobilizing from the site.

2.5.4.2.2.4 Cone Penetration Testing

Six CPTs are conducted in the unconsolidated Tamiami and Peace River formations at the site, four CPTs are performed during the initial investigation, and two CPTs are performed during the supplemental investigation. Three CPTs are

performed in the Unit 6 power block, and three are performed in the Unit 7 power block. A purpose-built approximately 20-ton capacity track-mounted cone penetration unit is used to perform the work. Each probe is advanced beginning at a depth of approximately 120–130 feet to the assigned termination depth or to cone refusal, which marks the limit of the pushing capacity of the rig. CPT soundings are initially advanced through HQ3-size core holes predrilled through the upper limestone layers to about 120-foot depth as described in Appendix B of Reference 257 and in Appendix A of Reference 290. At three locations, a drill rig is used to advance casing through hard zones (El. -120 to El.-130 feet, El. -230 to El. -250 feet, and El. -270 to El. -280 feet), allowing the CPT to be performed to a depth of approximately 290 feet. Selected CPTs are also used for conducting 24 pore pressure dissipation tests in the initial investigation and 5 pore pressure dissipation tests in the supplemental investigation. In the initial investigation, the tests are performed at varying depth intervals ranging from approximately 5 to 50 feet based on encountered stratum. In the supplemental investigation, the tests are performed at varying depth intervals ranging from approximately 135–290 feet.

Seismic shear wave testing is attempted during the first CPT sounding at C-702. However, due to the soft surficial muck layer, it is not possible to generate a shear wave to the depth of the cone tip. CPT locations are filled using a cement-bentonite grout prior to demobilizing from the site.

Results for all CPT are included in Appendix C of Reference 257 and in Appendix E of Reference 290.

2.5.4.2.2.5 Test Pits

Exploratory test pits are excavated at two locations using a rubber-tired backhoe. After removing 3 to 5 feet of muck, the test pits are excavated 2 feet into rock (Miami Limestone). The field representative selects the materials to be sampled, and a rig geologist collects the bulk samples. These bulk samples are placed in new 5-gallon plastic buckets with handles for carrying. Selected portions of the samples are tested in the laboratory for laboratory compaction, California Bearing Ratio (CBR), and Limerock Bearing Ratio (LBR) tests. The rig geologist prepares a Geotechnical Test Pit Log based on visual description of the excavated materials according to ASTM D 2488 (Reference 214). The surveyed locations of the test pits and the Geotechnical Test Pit Logs are included in Appendix B of Reference 257.

2.5.4.2.2.6 Groundwater Observation Wells and Field Testing

A detailed description of groundwater well installation, observations, and testing is contained in Subsection 2.4.12. A summary is given below.

2.5.4.2.2.6.1 Well Installation

Ten observation well pairs are installed within the power block and surrounding areas of the site as part of this project. With two additional deeper wells installed near well clusters 606 and 706, a total of 22 observation wells are installed during this project. The well-construction details are shown in “Observation Well Installation Records” in Appendix G of Reference 257.

The observation well depths and screen intervals are specified by a hydrogeologist after review of borehole records and geophysical logs where appropriate. Borings for the observation wells are advanced through soil using mud rotary drilling techniques with a nominal 6 inch outside diameter, and through rock using PQ3 wire-line coring techniques with a nominal 5-inch outside diameter. Borehole depths shown on the borehole logs indicate the total depth drilled and sampled. Due to small amounts of drill spoil at the base of the drill bit or due to the sampler advancing beyond the drilled depth, the total depth shown on the borehole log may be slightly greater than the well depth reported on the companion well installation record.

Upon reaching the designated depth for a well, machine-slotted PVC casing connected to solid walled PVC casing is set, and a 12/20 silica sand pack and bentonite seal placed in the wells. A cement/bentonite grout mixture is placed from the top of the bentonite seal to the ground surface in each borehole by the tremie method.

2.5.4.2.2.6.2 Water-Level Measurements

The depth to the water table in each well is measured at various times related to development, in situ testing, and water quality sampling using an electric water-level meter. Depth measurements are referenced to the marked top of the PVC casing. These measurements and initial water levels are shown on the various field forms in Appendix G of Reference 257. Water levels are measured for the two deep wells, 606D and 706D, separately. Additionally, data loggers and telemetry units are installed at each of the observation well locations. Water level measurements are included in Subsection 2.4.12.

2.5.4.2.2.6.3 Well Development

After well installation is complete, each well is developed using a submersible pump. A minimum of 10 saturated borehole volumes is removed from each well during the development process. During this process, the pump is cycled off and on to create a surge effect in the well. The wells are considered developed when the pumped water is relatively clear and free of suspended sediment. Field indicator parameters are measured during well development and noted on well development records. Copies of the well development records are included in Appendix G of Reference 257.

2.5.4.2.2.6.4 Well Purging and Sampling

Observation wells OW-606L, OW-606U, OW-62IL, OW-62IU, OW-706L, OW-706U, OW-72IL, OW-72IU, OW-735U, OW-802U, OW-805U, and OW-809U are purged and sampled using a submersible pump. The final field-indicator parameter readings are summarized in Table 5.2 in Volume 1 of Reference 257. Well sampling record sheets are included in Appendix G of Reference 257.

The laboratory-provided sample containers are filled with groundwater directly from the tubing attached to the pump. The containers are placed in a cooler with ice, and the cooler is delivered by overnight courier to the Test America Laboratories, Inc., in Earth City, Missouri, under chain-of-custody. Selected samples are tested for a variety of cations and anions as shown in Table 5.3 of Reference 257.

2.5.4.2.2.6.5 In Situ Hydraulic Conductivity Testing

In situ hydraulic conductivity testing is described in Subsection 2.4.12.

2.5.4.2.2.7 Muck/Peat Sampling

During the supplemental investigation, muck/peat deposits (soft, surficial soil, and sediment layers) are collected at the locations shown in Figure 2.5.4-202. Data from these Holocene-age muck deposits are used to provide additional information related to the recent geologic history at the site. Results of the muck/peat sampling are presented in Reference 291. Information related to the recent geologic history at the site is provided in Subsection 2.5.1.2.2.

2.5.4.2.3 Laboratory Testing

In the initial investigation, soil laboratory testing is conducted on approximately 178 disturbed (split-spoon), 7 intact (tube), and 2 bulk samples (from test pits). In

addition, 88 selected rock core samples are tested for UCS, unit weight, and moisture content, and two of these are tested with stress-strain measurements. Only 80 core samples returned successful UCS results. In the supplemental investigation, laboratory testing is conducted on approximately 4 special care rock samples (3 from the initial investigation), 14 muck (12 McCauley Sampler and 2 Shelby tube) samples, and 48 Shelby tube samples. A summary of the testing performed in the initial investigation is provided in Table 4.3 of Reference 257. A summary of the testing performed in the supplemental investigation is provided in Table 4 of Reference 290 and Table 3-2 of Reference 291. The testing is performed in accordance with the current respective ASTM standards, other standards, or documented test procedures where applicable. Sampling, handling, and transportation of samples are further described in Reference 257.

If the quantity of material is insufficient to perform the assigned testing, either a replacement sample is assigned or the testing is cancelled.

Because of the generally weak character of the rock, preparation of the rock cores for unconfined compressive strength testing requires special considerations. Based on initial experience with sample handling, it is observed that attempting to trim the ends and sides to meet the dimensional tolerance requirements of ASTM D 4543 (Reference 236) has a high potential risk of sample damage. The rock cores are trimmed close to the required length and then capped for testing. The actual dimensions are recorded on laboratory test forms.

Due to the fragility of the rock and the porosity of the limestone, attaching strain gages for determination of stress-strain characteristics is not possible for most samples. Of the 88 rock samples tested for compressive strength in the initial investigation, strain gages could be attached to only two samples. Strength test results for rock cores are presented in Appendix E2 of Reference 257.

In the initial investigation, soil index tests are conducted by MACTEC in the Raleigh, North Carolina laboratory, carbonate content tests are performed by MACTEC in the Atlanta, Georgia laboratory, and rock strength tests are conducted by MACTEC in the Charlotte, North Carolina laboratory.

In the initial investigation, chemical testing for pH, sulfates, and chlorides on selected soil samples is performed by Severn Trent (Test America) in Earth City, Missouri. In all, 15 soil samples are identified for soil chemical testing, and a portion of each jar sample is divided and submitted to Test America for the appropriate testing.

In the initial investigation, RCTS testing of seven selected intact soil samples from B-630 is conducted by Fugro Consultants, Inc., in Houston, Texas, under the technical direction of Dr. K.H. Stokoe of the University of Texas. Intact sample tubes are X-rayed prior to testing to evaluate sample integrity.

In the initial investigation, consolidated undrained (CU) triaxial shear testing of an intact soil sample from Boring B-630 is also performed by Fugro Consultants, Inc., in Houston, Texas.

In the initial investigation, particle size distribution tests are performed on samples of the Miami Limestone (Stratum 2) as obtained from the test pit excavations for TP-601 and TP-701. The results of the particle size distribution tests are presented in Appendix E1 of Reference 257.

In the supplemental investigation, soil index testing, CU triaxial testing, one-dimensional consolidation testing, organic matter content testing, and chemical testing are performed by Geotechnics, Inc., in Pittsburgh, Pennsylvania. RCTS testing is performed by Kleinfelder Laboratory, in Albuquerque, New Mexico.

The assigned tests are performed in accordance with the following ASTM standard or other procedure:

Identification Tests

- Laboratory Determination of Water (Moisture) Content of Soil and Rock by Mass — ASTM D 2216 (Reference 237)
- Specific Gravity of Soil Solids by Water Pycnometer — ASTM D 854 (Reference 238)
- Particle-Size Analysis of Soils — ASTM D 422 (for analysis including hydrometer) (Reference 239)
- Particle-Size Distribution (Gradation) of Soils Using Sieve Analysis — ASTM D 6913 (for analysis not including hydrometer) (Reference 240)
- Liquid Limit, Plastic Limit, and Plasticity Index of Soils — ASTM D 4318 (Reference 241)
- Moisture, Ash, and Organic Matter of Peat and Other Organic Soils — ASTM D 2974 (Reference 242)

- Unit Weight (Sections 5.7-5.9, and 8.1, and Subsection 11.3.2 of ASTM D 5084) (Reference 243), ASTM D 2937 (Reference 300), and ASTM D 7263 (Reference 296)

- Classification of Soils for Engineering Purposes (Unified Soil Classification System) — ASTM D 2487 (Reference 213)

- Description and Identification of Soils (Visual-Manual Procedure) — ASTM D 2488 (Reference 214)

- Rapid Determination of Carbonate Content of Soils — ASTM D 4373 (Reference 244)

- One-Dimensional Consolidation — ASTM D 2435 (Reference 295)

Compaction Tests

- Laboratory Compaction Characteristics of Soil Using Modified Effort — ASTM D 1557 (Reference 245)

- CBR (California Bearing Ratio) of Laboratory-Compacted Soils — ASTM D 1883 (Reference 246)

- LBR (Florida Lime Rock Bearing Ratio) of Laboratory-Compacted Soils — Florida Method FM-5-515 (Reference 247)

Shear Strength Tests

- Unconfined Compressive Strength Testing of Intact Rock Core Samples — ASTM D 7012 (Reference 248)

- Consolidated Undrained Triaxial Shear Testing of Undisturbed Soil Samples — ASTM D 4767 (Reference 249)

Modulus and Damping Tests (RCTS)

- Test Procedures and Calibration Documentation Associated with the RCTS Tests at the University of Texas at Austin, and at the Fugro Laboratory: UTSD RCTS GR06-4, April 25, 2006, Geotechnical Engineering Center, University of Texas, Austin, Texas.

- Test Procedures and Calibration Documentation Associated with the RCTS Tests at Kleinfelder Laboratory: KNS-TP-8.10, Revision 2, May 30, 2012.

Chemical Testing of Soil

- pH — EPA Standard SW 846 9045C (Reference 250) and ASTM D 4972 (Reference 297)
- Chloride — EPA Standard Method MCAWW 300.0A (Reference 251) and AASHTO T 291-94 (Reference 299)
- Sulfate — EPA Standard Method MCAWW 300.0A (Reference 251) and AASHTO T 290-95 (Reference 298)

Reporting of Laboratory Test Data

Except for the RCTS tests, the geotechnical laboratory test reports from the initial investigation, consisting of individual test data as required by the testing standard, are contained in Appendix E of Reference 257. Summaries of the test results are shown in Tables 4.1 through 4.3 of Appendix E of Reference 257.

Geotechnical laboratory test reports from the supplemental investigation are contained in Appendix C of Reference 290 and Appendix 3 of Reference 291.

2.5.4.3 Foundation Interfaces

PTN COL 2.5-5
PTN COL 2.5-6

Subsurface profiles depicting inferred stratigraphy at each power block are presented in Figures 2.5.4-203 through 2.5.4-208. A plan showing the subsurface profile locations is provided in Figure 2.5.4-209. Note that subsurface profiles shown on Figures 2.5.4-203 through 2.5.4-205 illustrate typical conditions at Unit 6, and subsurface profiles shown on Figures 2.5.4-206 through 2.5.4-208 illustrate typical conditions at Unit 7.

The final plant grade is shown in Figure 2.5.4-201. The grade in profile is shown in Figure 2.5.4-221. Seismic Category I structures bear on sub-basemat concrete placed on this stratum as described in Subsection 2.5.4.5. A plan and profiles illustrating power block foundation excavation geometries and the locations and depths of Units 6 & 7 Seismic Category I structures are shown on Figure 2.5.4-222, as well as the relationship of structure foundations to the various subsurface strata. These are addressed further in Subsection 2.5.4.5.

2.5.4.4 Geophysical Surveys

PTN COL 2.5-6

This subsection provides a summary of the geophysical survey methods and analysis undertaken for these subsurface investigations. Refer to Subsection 2.5.4.7 for a description of selected results. Detailed descriptions of methods and results are presented in Appendix D of Reference 257 and in Appendix G of Reference 290.

The geophysical investigation to detect possible solution features is presented in Subsection 2.5.4.4.5.

In the initial investigation, downhole geophysical testing and logging is performed in 12 borings in the power block areas: B-601(DH), B-604(DH), B-608(DH), B-610(DH), B-620(DH), B-640DHT, B-701(DH), B-704G(DH), B-708(DH), B-710G(DH), B-720G(DH), and B-740DHT. Borings designated as “G” on the boring location plan (Figure 2.5.4-202), for example “B-704G(DH),” are offset borings drilled adjacent to the original staked geotechnical boring for geophysical testing. The suite of tests listed below is performed in each boring in accordance with the procedures listed below.

Borings B-640DHT and B-740DHT are used only for downhole velocity testing. (The location designated B-640DHT is the same location that was previously used for the CPT designated as C-602A.) A downhole seismic velocity logging system is used in the two PVC cased borings to validate the suspension velocity data collected at this site. This method is described in Subsection 2.5.4.4.2.2.

In the supplemental investigation, geophysical testing (P-S suspension and acoustic televiewer) is performed in two borings in the power block areas (R-6-1b and R-7-1).

The collected data are presented in Appendix D of Reference 257 and Appendix G of Reference 290.

2.5.4.4.1 Geophysical Borehole Logging

2.5.4.4.1.1 Natural Gamma

Gamma logs record the amount of natural gamma radiation emitted by the soil and rocks surrounding the boring. Natural gamma is recorded using two probes, one combined with the three-arm caliper and one combined with the electrical logging tool. The dual measurements provide a quality check. The natural gamma data are qualitative and provide assistance in identifying strata changes. Natural

gamma testing is performed in accordance with ASTM D 6274 (Reference 252). Natural gamma data are collected using a Model 3ACS three-leg caliper probe, serial number 5368, manufactured by Robertson Geologging, Ltd. With this tool, caliper measurements are collected concurrent with measurement of natural gamma emission from the boring walls. Natural gamma data are also collected using a Model ELXG electric log probe, *SIN* 5490, manufactured by Robertson Geologging, Ltd. This probe measures natural gamma along with Single Point Resistance (SPR), short-normal (16-inch) resistivity, long normal (64-inch) resistivity, and spontaneous potential (SP).

Natural gamma measurements rely upon trace amounts of uranium and thorium that are present in potassium-bearing minerals such as feldspar, mica, and clays that contain a radioactive isotope of potassium. The measurement is useful because the radioactive elements are concentrated in certain soil and rock types (e.g., clay or shale) and depleted in others (e.g., sandstone or coal).

Measurements follow ASTM D 6167 (Reference 253). No analysis is required with the natural gamma logs; however, depths to identifiable boring features are compared to verify compatible depth readings on all logs. Natural gamma data are collected using both the caliper probe system as well as with the ELOG probe. A comparison between the two data sets provides an almost exact match, verifying the performance of the natural gamma measuring systems.

2.5.4.4.1.2 Long and Short Normal Resistivity/Spontaneous Potential

Normal-resistivity logs record the electrical resistivity of the borehole environment and surrounding soil and water as measured by variably spaced potential electrodes on the logging probe. Spacing for potential electrodes is 16 inches for short-normal resistivity and 64 inches for long normal resistivity. Normal resistivity logs are affected by bed thickness, borehole diameter, and borehole fluid, and can only be collected in water or mud filled open holes. Long and short-normal resistivity/spontaneous potential testing are performed in accordance with ASTM D 5753 (Reference 254).

No analysis is required with the resistivity or spontaneous potential data; however, depths to identifiable boring features are compared to verify compatible depth readings in all logs. Using Robertson Geologging Winlogger software version 1.5, build 4011, these data are combined with the caliper and natural gamma logs and converted to LAS 2.0 and PDF formats.

These electrical methods provide poor demarcation of different lithologic units at this site due to the influence of saltwater intrusion. Several of the borings exhibit artesian flow, and the composition of the boring fluid changed significantly during the collection of field data, with the drilling mud being displaced by clear water. The electrical data are not valid above a depth of 40 feet because the upper yoke electrode moves out of the boring fluid at that depth. There may also be differences in the electrical data at the same depth from different logging runs due to changes in the salinity of the boring fluid. In addition, the upper 40 feet of many of the deeper logs are affected by the movement of the yoke electrode into the steel surface casing.

2.5.4.4.1.3 Three-Arm Caliper

Caliper logs record borehole diameter with depth. Changes in borehole diameter are related to boring construction, such as casing or drilling bit size, and to fracturing or caving along the borehole wall. Because borehole diameter commonly affects log response, the caliper log can be useful in the analysis of other geophysical logs. Caliper with gamma logging is used to assist in the identification of strata changes. Three-Arm Caliper testing is performed in accordance with ASTM D 6167 (Reference 253).

Caliper data are collected using a Model 3ACS three-leg caliper probe, serial number 5368, manufactured by Robertson Geologging, Ltd. With the short arm configuration used in these surveys, the probe permits measurement of boring diameters between 1.6 and 16 inches. With this tool, caliper measurements are collected concurrently with measurements of natural gamma emissions from the boring walls.

No analysis is required with the caliper; however, depths to identifiable boring features are compared to verify compatible depth readings on all logs. Using Robertson Geologging Winlogger software version 1.5, build 4011, these data are combined with the resistivity, natural gamma, and spontaneous potential (SP) logs and converted to LAS 2.0 and PDF formats.

The caliper logs for these borings generally show diameters of less than 6 inches below 30 feet. There may be differences in the boring diameters at the same depth from different logging runs due to reaming of the boring, or erosion by the drilling fluid between logging runs.

2.5.4.4.2 Shear Wave Velocity Measurements

2.5.4.4.2.1 Suspension P-S Velocity Logging

Suspension P-S velocity logging is conducted in accordance with GEOVision procedure for OYO P-S Suspension Seismic Velocity Logging, Rev. 1.31. Measurements of compression (P) and shear (S_H) wave velocity are made at 1.6-foot intervals.

Suspension velocity measurements are performed in 10 borings in the initial investigation, and 2 borings in the supplemental investigation. P-S suspension is performed in uncased nominal 3.88- to 5.0-inch diameter borings using the suspension P-S logging system, manufactured by OYO Corporation, and their subsidiary, Robertson Geologging. Components used for these measurements are listed in Appendix D of Reference 257. This system directly determines the average velocity of a 3.3-foot-high segment of the soil column surrounding the boring of interest by measuring the elapsed time between arrivals of a wave propagating upward through the soil column. The receivers that detect the wave, and the source that generates the wave, are moved as a unit in the boring producing relatively constant amplitude signals at all depths.

An ASTM standard is not available for the suspension P-S velocity logging method; therefore, measurements follow the “GEO*Vision* Procedure for P-S Suspension Seismic Velocity Logging,” as presented in Appendix D of Reference 257 and summarized below.

Twelve borings are filled with bentonite or polymer-based drilling mud. Four- or six-inch diameter steel surface casing is used to maintain an open hole through loose soils, necessitating multiple logging runs to access different portions of the borings. Using the proprietary OYO program PSLOG.EXE version 1.0, the recorded digital waveforms are analyzed to locate the most prominent first minima, first maxima, or first break on the vertical axis records, indicating the arrival of P-wave energy. The difference in travel time between receiver 1 and receiver 2 arrivals is used to calculate the P-wave velocity for the 3-foot segment of the soil column. The recorded digital waveforms are analyzed to locate clear S_H-wave (horizontal shear wave) pulses.

The P-wave and S_H-wave velocities are also calculated and plotted from the travel time over the 6.3-foot interval from source to receiver.

The borings at this site are well suited for collection of suspension P-S velocity data, although there are some regions prone to squeezing and washouts,

particularly just below the upper limestone layer, between depths of approximately 115 and 120 feet. All of these data show excellent correlation between source and receiver data, as well as excellent correlation between P-wave and S_H-wave velocities. P-wave and S_H-wave onsets are very clear, and later oscillations are well damped. There is variation between the profiles from all these borings above 115 feet depth, due to different degrees of degradation of the limestone, but the general velocity trends are similar. Below 115 feet, the profiles are very similar, with slight variation of the harder layers between 120 to 150 feet and 210 to 260 feet depth.

Figure 2.5.4-218 shows the measured shear wave velocity profile (receiver to receiver), and Figure 2.5.4-219 shows the corresponding compression wave velocity profile. Subsection 2.5.4.7 contains a description of results.

2.5.4.4.2.2 Downhole Velocity Logging

Downhole velocity logging to measure shear wave velocity is performed in B-640(DHT) and B-740(DHT) using methods described in "Geo*Vision* Procedure for Downhole Seismic Velocity Logging," as presented in Appendix D of Reference 257. (An ASTM standard is not available for the downhole velocity logging method.) The tests are performed to provide a second method of shear wave velocity measurement to compare to the P-S suspension logging results. Downhole velocity testing is conducted in a borehole that has PVC casing installed with a grouted annulus. Logging was planned to be conducted to 150 feet bgs; however, in B-640DHT, curvature of the installed casing prevented passage of the probe beyond approximately 125 feet. The lesser depth is determined acceptable.

There are consistent waveforms between adjacent depth stations, and good consistency in the relationship between P- and S_H-waves. Also there is good consistency between profiles of adjacent borings. P-wave velocities in the fast layer are slower than measured by the suspension method. In order to properly image this fast layer, higher frequency waves are needed from the source. However, these are filtered out by the fill layer at the top of the borehole. Except for the layers near the surface, comparison with suspension velocities is within 10 percent.

Subsection 2.5.4.7 contains a description of results.

2.5.4.4.3 Borehole Acoustic Televiewer Logging

In the initial and supplemental investigations, acoustic image and boring deviation data are collected using a High Resolution Acoustic Televiewer probe (HiRAT), manufactured by Robertson Geologging, Ltd.

This system produces images of the boring wall based upon the amplitude and travel time of an ultrasonic beam reflected from the formation wall.

The acoustic televiewer data quality in all 12 borings (10 from the initial investigation and 2 from the supplemental investigation) are very good, providing clear images of a number of vugs and eroded zones. Many of the borings exhibit diagonal banding (zebra striping) caused by rapid reaming down the boring with new core bits. This alters the characteristic smooth surface of diamond cored borings. This wear pattern can have a significant impact on acoustic televiewer image quality, and in these borings may conceal small dikes, but does not conceal fractures. No large vugs or cavities are observed in the logs. Location of vuggy and weathered zones on the televiewer logs correspond with increases in caliper log diameter and suspension P-S velocity drops.

2.5.4.4.4 S-Wave and P-Wave Velocity Profile Selection

Suspension P-S velocity logging results summarized in Table 2.5.4-215 are used to develop the recommended V_s velocity profiles shown in Figure 2.5.4-220. The data collected at individual suspension P-S velocity logging borings and at individual seismic CPTs are sorted by stratum and averaged, and presented in Table 2.5.4-209. The average thickness and elevation of each stratum is also determined at each of the boring test locations, and averaged. The V_s profiles given in Figure 2.5.4-218 plot measured shear wave versus depth. Figure 2.5.4-220 illustrates the design V_s profile (average) for materials at the site from ground surface to approximately 450 feet deep from data measured at Units 6 and 7. Figure 2.5.4-220 includes the V_s data of one reading from 450−600 feet measured at Unit 7.

2.5.4.4.5 Geophysical Exploration for Possible Dissolution Features

An integrated geophysical survey that focused on the Units 6 & 7 power block area was conducted to evaluate the potential for carbonate dissolution features, including sinkholes, at the site (see Subsections 2.5.1.1.1.1.1.1 and 2.5.1.2.4 for a discussion of the types of sinkholes occurring in Florida). The geophysical survey encompasses an approximately 39-acre area of the site. The survey consists of 11 survey lines that covered over 12,000 linear feet (Figure 2.5.4-223). Lines 1

through 7 extend through and beyond the locations of Category 1 structures associated with Units 6 & 7. Lines 8 through 11 were added during the investigation to further characterize geophysical anomalies located near surface depressions that were filled with water and/or vegetation. Each survey line is composed of stations spaced 20 feet apart. Each station is located horizontally using a Trimble Ag-132 differential GPS with an accuracy of three feet and referenced in feet from the southernmost or westernmost end of the corresponding survey line. The horizontal coordinates are in Florida State Plane East using the North American Datum of 1983 (NAD 83). Elevations for each station were subsequently obtained using a Topcon DL-102 digital level, and tied to an existing benchmark. The elevations are relative to the North American Vertical Datum of 1988 (NAVD 88) and have a loop closure accuracy within 0.06 feet per linear mile.

The investigation consists of three non-invasive geophysical techniques:

- Microgravity to develop profiles that identify lateral variation in subsurface density caused by paleosinkholes, variations in the top of rock, and/or weak zones that may contain cavities.

- Seismic refraction to develop compression wave velocity cross sections that aid in delineating stratigraphic variations in the subsurface and soft zones conducive to the development of karst features.

- Multi-channel analysis of surface waves (MASW) to develop shear-wave velocity cross sections that delineate the top of rock and identify weak zones within the rock.

2.5.4.4.5.1 Microgravity Survey

At least one microgravity measurement is taken at each station along the 11 survey lines using a gravimeter (excluding stations between 500 and 640 along Line 2 where a data gap exists due to localized flooding). Measurements are made at a base station at the start and end of each day to allow corrections related to instrument drift to be made to the survey data. After corrections for other factors (e.g., tide, latitude, free air, and gravimeter height) are applied to the measured gravity data, a planar trend representing the background gravity at the site is subtracted from the Bouguer values to obtain the residual gravity value for each station.

The magnitude of gravity anomalies at the site is dependent on the depth, size, and density contrast of a subsurface feature. Subsurface density variations must be large enough or shallow enough to produce an anomaly above the noise threshold. With repeated measurements at 22 percent (135) of the stations at the site showing an average deviation of approximately ±3 microgals (µGals), anomalies ≥10 µGals should be routinely detectable. Figure 2.5.4-224 shows the magnitude of a low gravity anomaly as a function of depth for the case of various size water-filled spherical cavities in limestone. Figure 2.5.4-224 also illustrates what the measured gravity anomaly would look like for selected diameters and depths. As the figure shows, an isolated spherical void 25 feet in diameter or larger would theoretically be detectable if centered within the Key Largo Limestone at a depth of 40 feet. In general, subsurface structures approximated as spherical in shape can be detected at a depth to their center of approximately two times their effective diameter at the 10 µGal detection threshold. However, if a spherical void were to develop due to dissolution in limestone, it would need to have at least one input and one output tunnel. Thus, it is appropriate to use a more geologically plausible water-filled horizontal conduit scenario, such as the one shown in Figure 2.5.4-225, to guide interpretation when characterizing low density karst features at the site. Figure 2.5.4-225 indicates that a water-filled horizontal conduit 10 feet in diameter would theoretically be near the conservatively chosen detection threshold of –10 µGals if centered within the Key Largo Limestone at a depth of 40 feet. The magnitude of such a low gravity anomaly would in reality likely be larger for a given diameter due to the dissolution of fracture zones and bedding planes above such a conduit. Therefore, low-density features with a large lateral extent should be detectable at depths of up to 5 to 10 times their thickness at the site. Both Figure 2.5.4-224 and Figure 2.5.4-225 illustrate that for a gravity anomaly of a particular size and density contrast, as the depth to the center of the anomaly increases, the overall magnitude measured at the ground surface will decrease and the width of the anomaly when shown in profile view will increase (Reference 257).

The microgravity profiles for Line 5 and Line 9 are included in Figures 2.5.4-226 and 2.5.4-227, respectively. For the overall residual gravity dataset, the median value is 0 µGals with individual measurements ranging from –108 µGals to +37 µGals. Those segments of each profile that are 10 µGals or more below the median value are shaded blue and delineate low-density zones in the subsurface that have the potential to correlate with karst features. Figure 2.5.4-228 depicts the microgravity data contoured across the survey area to assess spatial trends in the data. Comparison of Figure 2.5.4-223 to Figure 2.5.4-228 illustrates that the

three largest (both in magnitude and lateral extent) low gravity anomalies at the site are centered on the surface depressions containing vegetation.

2.5.4.4.5.2 Seismic Refraction Survey

For the seismic refraction survey conducted at the site, compression waves (P-waves) are produced at the ground surface by striking an aluminum plate with a sledgehammer. The P-waves transmitted through the soil and rock are recorded by 24 geophones pushed down into the ground surface at known distances from where the waves were generated. A seismograph is used to record the travel-times of the first arriving energy, from which P-wave velocities were derived.

The maximum depth to which a seismic refraction survey is effective is controlled by a number of factors, including the geophone spread length, the shot offset distance, the P-wave velocity contrast between geologic layers, the thickness of individual layers, and the assumption that velocity increases with depth. Spacing between geophones in each seismic array is 10 feet, resulting in a total spread length of 230 feet. In general, P-waves are generated at five locations for each spread, consisting of shots located in the center, at 20 feet from each end, and at 100 feet from each end of the spreads. The seismic arrays are moved down the survey lines at 200-foot increments, thus providing 30 feet of overlap between spreads. For this survey, the overriding limiting factor on the depth of the investigation is a velocity inversion occurring at an elevation of approximately –50 feet at the interface between the Key Largo Limestone and the Fort Thompson Formation.

Two-dimensional cross sections are developed by processing the seismic refraction data that model P-wave velocity along each survey line. The P-wave models for Line 5 and Line 9 are included in Figures 2.5.4-226 and 2.5.4-227, respectively. Each cross section contains the modeled average P-wave velocity contour for the contact between the muck and Miami Limestone (4280 feet/second) and for the contact between the Miami Limestone and Key Largo Limestone (9570 feet/second). Existing borings located on or near each survey line along with the elevation of subsurface contacts derived from the corresponding boring logs are shown on each P-wave velocity model for comparison. Because seismic P-wave velocities are affected by the presence of the water table, which is close to ground surface at the site, the estimated elevation of the muck/Miami Limestone contact is likely better estimated from the average shear wave (S-wave) velocity contour derived from MASW data collected at the site (Subsection 2.5.4.4.5.3). Vertical resolution of seismic refraction data is a complex function of the geophone spacing, the depth to subsurface refractors,

the seismic velocity contrasts, and site-specific near surface conditions (Reference 255). For this survey, vertical resolution is approximately 20 percent. Thus, if a subsurface feature such as a void existed at a depth of 30 feet at the site, it would be averaged over a thickness of about six feet in the P-wave velocity models. Lateral resolution of a seismic refraction survey is dependent upon geophone spacing and shot-point spacing. For this survey, lateral resolution falls in the range of one to two geophone spacings (10 to 20 feet), with a conservative estimate being 20 feet.

2.5.4.4.5.3 MASW Survey

This technique utilizes seismic noise generated at the ground surface by striking an aluminum plate with a sledgehammer. This action produces Raleigh surface waves, along with other types of seismic waves. Raleigh waves have velocities that depend on their wavelength, with short wavelengths (high frequencies) sampling shallow depths and long wavelengths (low frequencies) sampling to greater depths. Data are collected along each of the 11 survey lines, with a data gap existing along Line 2 between stations 460 and 640 due to localized flooding. Data are recorded using a seismograph and 24 geophones with an inter-geophone spacing of four feet, resulting in a total length of 92 feet for each geophone spread. The 24 geophones are mounted in a land-streamer configuration that allows the 92-foot spread to be pulled from one measurement location to another using a tracked vehicle. Measurements are made at intervals of 20 feet along each of the survey lines. A constant 12-foot distance is maintained between the sledgehammer shot point and the first geophone in each spread during testing.

As Raleigh waves propagate outward along the ground surface at the site, they undergo dispersion due to heterogeneous conditions within the subsurface. After the data are collected, dispersion curves showing the velocity of the surface waves as a function of frequency are calculated from the data. By applying the ratio of Raleigh wave velocity to S-wave velocity (approximately 0.9 to 1) to these calculated dispersion curves, S-wave velocity is estimated. Dispersion curves are manually selected for input into an inversion program by analyzing the phase-velocity power spectra of the surface waves. Shot point records that do not yield coherent dispersion curves are discarded. The resulting one-dimensional models from multiple locations along a survey line are combined and contoured to produce two-dimensional cross sections of S-wave velocity along the 11 survey lines. The S-wave model for Line 5 and Line 9 are included in Figures 2.5.4-226 and 2.5.4-227, respectively. Each cross section contains the modeled average S-wave velocity contour for the contact between the muck and Miami Limestone

(440 feet/second) and for the contact between the Miami Limestone and Key Largo Limestone (3660 feet/second). Existing borings located on or near each survey line along with the elevation of subsurface contacts shown on the corresponding boring logs are provided on the cross sections for comparison. For sites with high S-wave velocity disparities in the subsurface at shallow depths, such as that which exists between the muck and underlying limestone, MASW surveys may not succeed in accurately capturing the absolute S-wave velocity of the rock. While S-wave velocities for limestone in the models are likely underestimated, the modeled depths to limestone as well as the relative changes in velocity within the limestone are considered to be valid.

As indicated above, the depth of investigation for a MASW survey is primarily controlled by the frequency of the surface waves. Because the amplitude of surface waves decreases exponentially with depth, heavier (lower frequency) sources are necessary to penetrate deeper. Due to the relatively high frequencies produced in the soft muck by sledgehammer impacts during the site survey, interpretation of subsurface conditions using the resulting S-wave velocity models should be restricted to shallow depths. While the velocity models show S-wave velocity data down to El. –50 feet at the site, the models should be constrained to the uppermost 35 feet. Vertical resolution of the MASW data is around 20 percent of the depth. Thus, if a subsurface feature such as a void exists at a depth of 30 feet at the site, it would be averaged over a thickness of about six feet in the S-wave velocity models. Because lateral resolution for MASW is approximately 25 percent of the total seismic array length, lateral variations in the subsurface are averaged over a length of approximately 23 feet for this survey. Studies comparing MASW measurements to borehole measurements indicate that MASW velocity models are typically accurate to within 15 percent of actual values.

2.5.4.4.5.4 Results

A comparison of Figures 2.5.4-223 to 2.5.4-228 (References 286 and 320) indicates that the three largest low gravity anomalies, both in magnitude and lateral extent, are centered on the surface depressions containing vegetation located outside the Units 6 & 7 power block areas. The gravitational response to subsurface density variations was modeled along Line 9 (Reference 320) to assess the potential subsurface causes for the microgravity lows associated with the vegetation filled surface depressions (Figure 2.5.4-229). This model is calculated based on the estimated wet density values for the subsurface strata shown in the table below combined with stratigraphic boundaries estimated from the corresponding S-wave and P-wave velocity models (Figure 2.5.4-227).

Material	Wet Density (g/cc)	Reference
Water	1.0	Telford et al. (Reference 278)
Peat	1.08	Measured from onsite samples (Reference 291)
Muck	1.1–1.3	Measured from onsite samples (References 257 and 291)
Miami Limestone	2.0	Telford et al. (Reference 278)
Key Largo Formation	2.2	Geotechnical Exploration and Testing in Reference 257

Results of the muck sampling (Reference 291) were used to remodel the original microgravity survey resulting profiles, for only the lines intersecting the vegetated depression areas (Reference 320). This was done considering the newly described material densities, which correlate with the presence of only peat, with lower densities, inside the vegetated depressions (Reference 291). In these re-modeled microgravity profiles, densities were assigned and held fixed as follows: a density of 1.08 g/cc was used for the peat layer, and a density of 1.32 g/cc was used for the muck (elastic silt) layer (Reference 291); a density of 2.0 g/cc was used for the Miami Limestone, and a density of 2.2 g/cc was used for the Key Largo Limestone (Reference 286). These new models do not include the softer pockets of Miami Limestone presented in the original microgravity survey models (Reference 286) so that the modeled gravity response of the muck and peat thickness could be assessed independently of deeper density variations within the limestone (Reference 320).

Results from this new model (Reference 320) indicate that the microgravity results are in good agreement with the evidence derived from the sampling of the surficial deposits as outlined in the following paragraphs. The MASW models presented in Reference 320 are the same as those presented in the Technos report (Reference 286). In Reference 320, the MASW models have been recontoured with a color scheme that enhances the low end of the shear-wave velocity range. Therefore, the results presented (Reference 320), based on the updated microgravity model and MASW recountering results, do not indicate the presence of the potential cavities originally described (Reference 286).

The evaluated data within the vegetated surface depressions includes: the existing boring data (Appendix B of Reference 257 and Appendix A of

Reference 290), the surficial deposit sampling (Appendix 1 of Reference 291), and the updated microgravity models and recontouring of MASW results (Reference 320). All of these data indicate that the low density measurements are associated with the presence of peat in shallower depressions and density variations within more weathered Miami Limestone (Reference 320), rather than large deep cavities. Significantly lower density of the peat deposits (Reference 291) explains the anomalies encountered during the original microgravity survey (References 286 and 320).

Significantly smaller magnitude microgravity lows are present at a number of locations outside the surface depressions containing vegetation at the site, such as the –20 µGal anomaly found between stations 400 and 500 along survey Line 5 (Figures 2.5.4-226 and 2.5.4-228). A model of the gravitational response to subsurface density variations is produced for this anomaly using the same methodology discussed above (Figure 2.5.4-230). The model indicates that this small magnitude low-gravity anomaly is caused by a wedge of soft Miami Limestone with a bulk density 0.2 to 0.3 grams per cubic centimeter (g/cc) lower than the surrounding Miami Limestone. This model correlates well with data collected from boring B-728, where SPT sample refusal occurred at El. –28.7 feet as compared to El. –18.1 feet for nearby boring B-710.

The gravitational effects due to thickness variations of the muck across the site are stripped from the residual gravity dataset using the following approximation from Telford et al. (Reference 278):

$$\Delta g = (12.77)\ \Delta \rho\ D \qquad \text{Equation 2.5.4-13}$$

Where,

Δg = gravity anomaly in µGals
$\Delta \rho$ = density contrast (–0.7 g/cc) between the muck and underlying limestone
D = thickness of the muck (estimated from MASW data)

Figure 2.5.4-231 shows a contour map of microgravity at the site with residual gravity values corrected for muck thickness variations using the relationship defined above. Once this muck thickness correction is applied to the microgravity dataset for the site, all low gravity anomalies can be explained by softer zones within the Miami Limestone having a density 0.2 to 0.3 g/cc lower than 2.0 g/cc. This statement is supported by an evaluation of the magnitude and width of low gravity anomalies (excluding those found on and around the surface depressions filled with vegetation) at the site, which are conducive to soft zones in the Miami

Limestone. It is also supported by SPT N-values obtained within the Miami Limestone across the site, which indicate the presence of very soft to hard soils. Existing borings associated with low gravity anomalies generally have lower SPT N-values when compared to SPT N-values from borings associated with relatively higher microgravity values.

2.5.4.4.5.5 Summary and Commitment

Based on geophysical site characterization data (References 286 and 320), and drilling observations as outlined in Subsection 2.5.4.1.2.1, there is no apparent indication that sinkhole hazards exist at the site. There is also no apparent evidence for the presence of underground openings within the survey area that could result in surface collapse. Large low gravity anomalies with magnitudes less than –30 µGals are only detected outside the power block areas, primarily in areas associated with surface depressions containing vegetation. Once the effects of variations in muck thickness are removed from the residual gravity data, all the remaining low gravity anomalies can be explained by density variations within the Miami Limestone. The results of the drilling program and borehole geophysical data (Subsections 2.5.1.2.4 and 2.5.4.1.2.1) indicate the existence of two preferential secondary porosity flow zones. The extent of rod drops integrated with the field geophysical data supports the interpretation that large voids are absent beneath the footprints of the Units 6 & 7 nuclear islands.

However, considering the uncertainties related to resolution in the geophysical data at depth and away from survey lines, the subsurface grouting program will be considered in the determination of constrained void sizes. The zone between El. –35 feet and El. –60 feet within the diaphragm walls will be grouted according to the closure criteria that will be developed as part of the grout test program (determined from the results of water pressure tests, evaluation of available boring data, and the target residual permeability of the grouted zone). This grouting will ensure that potential voids in this zone are filled. In addition, for the zone between El. –60 feet and El. –110 feet within the diaphragm walls, grouting will be performed in every primary grout borehole. Primary grout holes will be spaced less than or equal to 20 feet on center (Figure 2CC-239). This configuration is expected to constrain the maximum undetected void size to approximately 20 feet.

2.5.4.4.6 Pressuremeter Testing

In the supplemental investigation, pressuremeter testing is performed in three boreholes at the site: R-6-2, R-6-1b, and R-7-2. The main objective of the

pressuremeter testing program is to obtain high strain shear modulus for the subsurface materials of the Key Largo, Fort Thompson, upper Tamiami, lower Tamiami, and Peace River formations.

The instrument used for this investigation is a Cambridge style pre-bored high-pressure pressuremeter. The pressuremeter is of the monocell type, with a testing range of 2000 psi and 18 percent strain. It has 3 electronic displacement sensors spaced 120 degrees apart and located at the center of a flexible membrane, and a pressure cell. The flexible membrane is placed over the sensors, clamped at each end. The membrane is covered by a protective sheet of stainless steel strips. The unit is pressurized using compressed air to expand the membrane and deform the adjacent material. The electronic signals from displacement sensors and the pressure sensor are transmitted by cable to the surface.

In the pressuremeter test, the membrane is expanded by controlling the flow of compressed gas into the pressuremeter, increasing the pressure smoothly until the membrane starts to expand against the borehole wall. During the test, the average expansion versus pressure is displayed on a computer screen. Once the instrument has deformed the borehole sidewall and the response curve appears to be deforming intact material, the pressure is reduced to no more than 40 percent of the highest applied pressure, and then increased again to form an unload/reload loop. The resulting unload/reload loop can be used to evaluate the elastic behavior of the material.

A total of 96 pressuremeter tests were attempted in the investigation: 48 tests were conducted in borehole R-6-2, 6 tests were conducted in borehole R-6-1b, and 42 tests were conducted in borehole R-7-2. Approximately two-thirds of the test attempts were successful and produced useful data for stiffness characterization. The remaining tests resulted in oversized test pockets due to the combination of drilling conditions and the deformation limit of the apparatus, which has a 6.35 millimeter radial displacement range.

Pressuremeter results, in the form of initial shear modulus and unload/reload shear modulus, are presented in Table 2.5.4-220 and Figures 2.5.4-244 and 2.5.4-245.

PTN COL 2.5-7

2.5.4.5 Excavations and Backfill

PTN COL 2.5-13

2.5.4.5.1 Source and Quantity of Backfill and Borrow

Significant earthwork is required to establish finish grades at the Units 6 & 7 project area, especially to raise the power block to finish grade (as high as El. +25.5 feet at the center of the power block area) and to provide for backfilling around the embedded major power block structures including Seismic Category I structures. The grade change is achieved by constructing a mechanically stabilized earth (MSE) retaining wall around the perimeter of the plant area. The MSE wall will be constructed around the perimeter of the Units 6 & 7 plant area, excluding the south side of the plant area where the makeup water reservoir would provide the plant area exterior wall. The construction of the MSE wall will be standard for this type of retaining wall, with successive lifts of compacted, controlled fill reinforced with either strip- or grid-type reinforcement between lifts. The finished height of the MSE wall will range from 20 to 21.5 feet. From the MSE wall, the finished grade would slope upward for some distance towards Units 6 & 7 to an elevation approximately 5 feet higher than the top of the retaining wall. Modular facing panels will form the outside face of the MSE wall. The MSE wall will be designed to retain the soil mass and resist loading resulting from the probable maximum hurricane.

The MSE wall is not required to maintain the function of any Seismic Category I structures. As described in Subsection 2.5.5.5, the distance from the retaining wall to any Seismic Category I structures of Units 6 & 7 is greater than 500 feet (Figure 2.5.4-201) which is very large compared to the height of the wall, and thus a failure of the wall could not affect the Seismic Category I structures.

The deepest excavation is to approximately El. –35 feet. Structural fill is placed around but not below the power block structures extending to as deep as El. –16 feet. Lean concrete fill is placed between the bottom of the mudmat at El. –16 feet and the bottom of excavation. Lean concrete is unreinforced concrete with a lower ratio of cement to aggregate than structural concrete. The final grade is shown on Figure 2.5.4-201. The grade in profile is shown in Figure 2.5.4-221.

2.5.4.5.1.1 Replacement of Stratum 1 with Compacted Limerock Fill

Due to the poor soil properties of Stratum 1 (muck/peat), Stratum 1 is removed in its entirety prior to commencing the major earthwork and grading operations. After removing the muck/peat, the grade is raised to approximately El. +0 feet through placement and compaction of Miami Limestone and Key Largo fill materials and limerock material from other sources.

The evaluation of the Miami Limestone (Stratum 2) for construction purposes involves the excavation of two exploratory test pits at the power block, located as shown on Figure 2.5.4-202. The maximum depth of each test pit is 5 feet bgs. The results of laboratory testing on bulk samples collected from the test pits for moisture-density (modified Proctor compaction), CBR, and LBR are summarized in Table 2.5.4-214. These tests show that, when excavated with construction equipment and not crushed, Miami Limestone-derived materials are gravel-sand mixtures with fines contents of 12 percent to 17 percent. The grain size distribution of actual fill material is expected to vary based on the degree of cementation of the native material in excavated areas and the methods of excavation, handling, and crushing (if performed).

The most likely offsite structural fill sources are identified, as follows:

- SDI Quarry (Florida City, Florida)
- CEMEX/Florida Rock (Card Sound Road, Homestead, Florida)
- White Rock South (Miami, Florida)

Each of these sources, as well as onsite material excavated from the power block excavations, offers Miami Limestone (Stratum 2) material and other limestone-derived materials in granular form. This material is locally known as limerock. Limerock can be graded into a variety of grain size distributions ranging from gravel to sand-sized particles.

The results of laboratory index tests (natural moisture content, gradation), chemical tests (pH, sulphate content, chloride content), moisture-density relationship tests (modified Proctor compaction), and strength tests (LBR and CBR) for these materials are contained in Appendix E.1 of Reference 257. Once the final backfill source(s) for structural fill is determined, additional material testing is required to verify the design properties.

2.5.4.5.1.2 Power Block and Site Grade Raising

Approximately 10 million cubic yards of structural fill are required to fill the site to finish grade. The fill material is from identified offsite sources as well as the power block excavation for each unit.

Power block area materials excavated during site grading consist of fill material derived from onsite and local limerock sources with the proposed sources identified in Subsection 2.5.4.5.1.1.

Structural fill consisting of excavated fill material is placed around but not below any nuclear island structure. Replacement material below the nuclear islands consists of concrete fill. The selection of concrete fill mix design is made at project detailed design. A mix is selected that achieves the mechanical properties used for the design analyses. The compressive strength of 1.5 ksi is estimated for concrete fill. To ensure that the compressive strength is equal to or greater than this value, concrete test cylinders are made in the field and tested according to ACI 311.5 (Reference 324). The selection of the mix considers the strength requirements as well as the durability requirements to prevent potential sulfate attack.

The concrete fill exposure to sulfate attack from groundwater is classified as Class 2 exposure according to Reference 323. Recommendations for improving sulfate resistance are provided in the ACI Guide to Durable Concrete, ACI 201.2R-08 (Reference 323). For the first lift of concrete (bottom lift), the requirements in Table 6.3 of Reference 323 for water-cementitious material ratio and type of cementitious materials are followed in order to provide resistance to sulfate attack. The minimum thickness of the first lift of concrete fill is 2.5 feet. The concrete mix for the first lift contains a maximum water-cementitious material ratio by mass of 0.45, and a sulfate resisting Type V cement or equivalent as defined in Sections 6.2.5, 6.2.7, and 6.2.9 of the ACI Guide to Durable Concrete, ACI 201.2R-08 (Reference 323). In addition, Type V cement or equivalent according to ACI 201.2R-08 (Reference 323) is used for all the lifts for additional protection. Delivery tickets are prepared according to ACI 311.5 (Reference 324) and inspected to ensure that the water-cementitious material ratio and the type of cementitious materials for the first lift meet durability requirements in Reference 323 for Class 2 sulfate exposure.

The approximately 19-foot-thick layer of lean concrete fill qualifies as mass concrete. As such, a thermal control plan will be developed during detailed design to minimize thermal cracking of the lean concrete fill.

The thermal control plan will include the following elements as outlined in ACI 207 (Reference 281) and detailed below:

- Controls on cementitious material content

  Choosing the type and amount of cementitious material can lessen the heat-generating potential during concrete curing. Since the strength of the lean concrete fill, and therefore the amount of cementitious materials, is relatively low, the heat of hydration is less than that found in higher strength mixes.

Furthermore, the use of pozzolans (such as fly ash) reduces the heat generated during the curing process.

- Precooling

  The precooling of aggregates and mixing water can enable a lower placement temperature, thereby reducing the risk of cracking during the curing process. This can be achieved by shading the aggregate, sand chillers, water chillers, and ice.

- Construction management

  Construction scheduling and procedures can be optimized for concrete placement to reduce the risk of cracking. These methods include the placement of concrete at night and placement of the concrete in properly sized lift thicknesses and blocks determined in advance with thermal analysis.

DCD Subsection 2.5.4.1.3 requires that the compressive strength of the mudmat (located beneath the nuclear island foundation) have a minimum compressive strength of 2500 psi. The mudmat used at this site consists of approximately 1-foot-thick upper and lower concrete layers with waterproofing membrane sandwiched between them. The mudmat will be approximately 2 feet thick from EI. –16 to EI. –14 NAVD 88. The 1500 psi lean concrete fill is placed directly beneath the mudmat from EI. –35 to EI. –16 and is used for filling purposes to replace in situ limestone material with best estimate unconfined compressive strengths of 200 and 2689 psi, as noted in Table 2.5.4-209. It provides a uniform base with well-defined material properties.

The lower strength of 1500 psi for the concrete fill will require less cement and thus reduce the heat of hydration found in stronger mixes. Uncontrolled heat of hydration is the cause of thermal cracking and thus minimizing the heat of hydration for this mass concrete will reduce the possibility of such cracking. ACI 207 (Reference 281) will be used for guidance in developing a thermal control plan to reduce thermal cracking of the lean concrete as noted in Subsection 2.5.4.12.

Construction of the lean concrete fill follows the guidance in ACI 207 (Reference 281). Although the lean concrete fill is not safety-related, the construction and associated testing described below follow requirements equivalent to NQA-1.

Testing of materials and lean concrete fill during construction verifies that the as-placed concrete properties are consistent with the properties established during the mix design. At a minimum, the construction verification and testing includes:

- Verification of manufacturer's certifications for cementitious materials
- Aggregate testing for gradation, moisture content, and specific gravity
- Fresh concrete testing of slump and placement temperature
- Hardened concrete testing of compressive strength

The lean concrete is batched on site and placed in a series of successive layers and lifts. One lift consists of several layers.

Within each lift, concrete is placed in successive layers. Layer thickness is determined prior to construction based on the maximum aggregate size of the concrete mix.

Concrete consolidation is achieved for each layer by internal vibration from pneumatically driven vibrators. The vibrator size and dynamic characteristics are selected such that it is suitable for the mixture, layer thickness, and placement rate. Vibration of the lean concrete is systematic and thoroughly covers and deeply penetrates each layer. To ensure proper consolidation, the vibrators penetrate the lower layer for approximately 2 to 4 inches and are maintained in a nearly vertical position at each penetration during vibration.

The lift thickness and placement schedule is determined prior to construction based on the requirements in the thermal control plan.

Horizontal lift joint surfaces are prepared between lifts to ensure bond between joints, as described in Reference 281. As late as is feasible, but before placement of the next lift, surface film and contamination is removed to expose a fresh, clean mortar and aggregate surface. This is accomplished by means of sandblasting or high-pressure water jet. Green cutting, which is the early removal of the surface mortar with an air-water jet at about the time the concrete approaches final set, may also be used. The clean concrete surface approaches dryness and is free from surface moisture at the time new concrete is placed on it.

The lean concrete fill is water-cured between lift placements and curing continues for at least 14 days after placement of the final lift. If pozzolan is used as a cementitious material, curing continues up to 28 days after placement of the final

lift. Surfaces of horizontal construction joints are kept moist until the wetting no longer provides beneficial cooling. Curing is stopped long enough to ensure that the joint surface is free of water but still damp and clean before new concrete is placed.

By selecting an appropriate mix design, performing verification testing during construction, and following industry guidance for construction and placement methods, the mechanical properties of the lean concrete fill are consistent with the properties used for the design analyses.

2.5.4.5.1.3 Makeup Water Reservoir

The base of the makeup water reservoir is set at El. –2 feet. To construct the subgrade and mat for the base of the reservoir, the excavation bottom is approximately El. –4 feet. The exact final subgrade elevation is determined during final design.

2.5.4.5.2 Extent of Excavations, Fills, and Slopes

The plan arrangement of the power block, including major structure footprints, is shown on Figure 2.5.4-201. The existing natural ground surface elevation at the power block is generally level at approximately El. –0.5 feet. The power block finish grade elevation is raised approximately 26 feet to El. +25.5 feet using compacted structural fill as shown on Figure 2.5.4-221. Structural fill is used to backfill against the nuclear island, and nonsafety-related (Category II) structural fill (also termed general fill) is used below shallower nonsafety-related structures as shown in Figure 2.5.4-222. Structural fill is further described below in this subsection.

The approximate foundation dimensions, foundation elevation, and predominant soil strata at the foundation elevation of the nuclear island buildings are as follows:

Structure	Approximate Foundation Dimensions (feet)	Approximate Foundation El. (feet)[(a)]	Predominant Soil Stratum at Foundation
Reactor & auxiliary building (nuclear island)	88 to 159 by 254	–14 (–35)	Lean concrete fill over Key Largo Limestone

(a) The foundation elevation shown in "( )" symbols denotes the elevation and soil stratum at the base of significant over-excavation (to reach a suitable bearing stratum) at the particular structure (e.g., at the nuclear island buildings). Strata 1, 2, and 3 are over-excavated to approximately El. –35 feet or suitable subgrade of Stratum 3. The over-excavation is replaced by lean concrete fill.

To achieve the anticipated excavation level for each nuclear island, foundation excavations require removing approximately 100,000 cubic yards of soil and rock at each location. The extent of excavation, filling, and the approximate limits of temporary ground support for major structures are shown in plan and profile on Figure 2.5.4-222. This figure shows that the excavations for foundations result in the nuclear islands being founded directly onto lean concrete above the competent rock of Stratum 3 (Key Largo Limestone).

The deepest excavation at the power block (i.e., the bottom of over-excavation for the nuclear island foundations) is approximately 35 feet below existing ground surface and 60 feet below finish grade (El. –35 feet) as shown on Figure 2.5.4-222. The profiles from the power block subsurface investigation (refer to Figures 2.5.4-203 through 2.5.4-208) show that the subsurface strata to support foundations are relatively horizontal. However, it should be noted that the extent of excavation to final subgrade and/or to final over-excavation level is determined during construction. This determination is based on observation of actual subsurface conditions encountered, and their suitability for foundation support. Once subgrade suitability at the proposed bearing stratum is confirmed, nuclear island excavations are backfilled with lean concrete fill up to the foundation level of the structures. Structural fill used as backfill against the nuclear island is controlled and placed in accordance with a quality program per Appendix B of 10 CFR Part 50. General fill is compacted in accordance with standard construction practices, including applicable standards of the Florida Department of Transportation. Nonsafety-related power block structures are founded on general fill above the Miami Limestone. Compaction and quality control/quality assurance programs for filling are addressed in Subsection 2.5.4.5.3.

There is no permanent or temporary safety-related excavation or fill slopes created by power block site grading as described in Subsection 2.5.5.

2.5.4.5.3 Compaction of Backfill

Prior to earthwork operations, borrow sources for various required fill materials (i.e., power block structural fill and general fill) are qualified by testing for index properties, chemical properties, and engineering properties, especially: grain size and plasticity characteristics; soil pH, sulfate content, chloride content characteristics; and moisture-density relationships. The following compaction criteria apply:

- Structural fill used as backfill around the nuclear island structures and beneath nonsafety-related power block structures is compacted to a minimum of 95 percent of modified Proctor (Reference 245) maximum dry density.

- At power block non-structure areas, general fill is compacted to a minimum of 92 percent of modified Proctor (Reference 245) maximum dry density.

Fill placement and compaction control procedures are addressed in a technical specification prepared at project detailed design. The specification includes requirements for suitability of the various required fill materials, sufficient testing to address potential material variations, and in-place density and moisture content testing frequency (e.g., typically a minimum of one test per 10,000 square feet of fill placed per lift). The specification also includes requirements for an onsite testing firm for quality control, especially to ensure specified material gradation and plasticity characteristics, the achievement of specified moisture-density criteria, earthwork equipment, maximum lift thickness, and other requirements to ensure that fill operations conform to a high standard of practice. The onsite testing firm is required to be independent of the earthwork contractor and to have an approved quality assurance/quality control program. A sufficient number of laboratory tests are required to ensure that any variations in the various required fill materials are accounted for. A materials-testing laboratory is established onsite to exclusively serve the project site work.

2.5.4.5.4 Dewatering and Excavation Methods

Groundwater control in major power block structure excavations is required during construction. With the deepest excavation level at approximately El. –35 feet, i.e., extending approximately 35 feet below the groundwater level, a complete construction dewatering system is required. Power block groundwater conditions and construction dewatering requirements are addressed in more detail in Subsection 2.5.4.6.

Power block excavations are primarily open cuts, with temporary ground support provided by a reinforced concrete diaphragm wall surrounding each power block excavation area. Excavation is performed with standard excavation equipment, but may be supplemented with other methods. The reinforced diaphragm walls resist lateral earth and hydrostatic pressures while providing a barrier to groundwater flow. The reinforced diaphragm walls are seated at approximately El. –60 feet, just below the most competent portion of the Fort Thompson Formation. Tiebacks to provide resistance to the lateral earth and hydraulic pressures are installed based on the final design that includes embedment, spacing and other

details, as applicable. The completed reinforced diaphragm walls effectively impede any overturning or sliding from the lean concrete fill, provided as a sub-basemat for Category I seismic structures, confined within the walls.

The excavation limits for the nuclear island are defined laterally by the boundary created by the reinforced concrete diaphragm walls (as shown on Figure 2.5.4-201) and vertically by the target elevation for the bottom of excavation (El. –35 feet NAVD 88), which is selected by careful evaluation of geologic data and consideration of design details of the plant.

The excavation limits are maintained through visual inspection and survey measurements as excavation proceeds. As the excavation proceeds, geologic mapping is conducted on the exposed rock surfaces.

Excavation of materials above El. –35 feet (the bottom of excavation) is not classified as safety-related. Geologic mapping, inspection, and survey measurements are conducted to meet 10 CFR 50 Appendix B and ASME NQA-1 quality requirements.

Excavation for the nuclear island consists of excavation of the top layer of surficial sediments or “muck” and the underlying Miami Limestone down to approximately El. –35 feet to expose the Key Largo Limestone. Excavation of the muck is accomplished with common excavation equipment such as bulldozers, loaders, track mounted excavators, etc. Excavation of the limestone rock is accomplished using similar equipment for more weathered or poorly cemented rock (generally the Miami Limestone) and a variety of commercially available rock excavation tools such as ripping teeth, rock excavation buckets, and/or road header attachments for more intact rock (generally the Key Largo Limestone). Drilling and blasting has been eliminated as a possible construction method.

The location of the diaphragm wall and the corresponding horizontal extent of the excavation have established coordinates based on survey measurements. The bottom of the excavation is monitored by geologic mapping and survey. In addition, excavator mounted tools such as rippers and road headers allow for precise control of the extents of the excavation because the operator, with the assistance of spotters as necessary, is able to maintain visual contact with the area being excavated. These methods ensure that the integrity of the diaphragm wall and grout plug is maintained throughout the excavation process. Measurement of the elevation of the excavation floor is the primary means of preventing over-excavation into the grout plug zone.

Inspection, geologic mapping, and surveying are performed during excavation to ensure the complete removal of the Miami Limestone and that the required depth is reached.

A detailed excavation and foundation preparation plan is developed prior to construction. While the excavation activities are not classified as safety-related, these plans are treated as NQA-1 deliverables. The program includes similar items to the following list:

- Specification of excavation methods. As discussed above, excavation methods include mass excavation of soils (muck) and highly weathered or soft rock with conventional excavation equipment and ripping of moderately weathered rock with rock excavation tools.

- Quality control and quality assurance programs.

- Methods for dewatering and protection from degradation at the bottom of excavation during excavation and dewatering. Construction dewatering requirements are discussed in Subsection 2.5.4.6.2. It is not expected that the sound rock at the bottom of excavation will significantly degrade due to excavation, dewatering, or exposure to the elements during construction. Observable degraded or raveling rock at the bottom of excavation is removed prior to placement of dental concrete or the mudmat.

- Specification of methods for construction dewatering, disposal of water, and management of seepage and piping.

- As the excavation proceeds, geologic mapping of the exposed rock is performed by an appropriately qualified geologist. This activity is in accordance with NQA-1 requirements. Geologic mapping of the intermediate stages of the excavation is focused on major features such as prevailing fracture sets and bedding features in addition to general description of the exposed rock.

- The inspection and mapping of the completed excavations is performed by appropriately qualified and trained project inspection personnel. Soundings, test holes, and similar measures are used to augment visual identification of areas needing repairs and to document acceptance of corrective measures, as appropriate.

- The rock surface at the target excavation elevation (El. –35 feet) is expected to be undulatory and to require a variable amount of foundation preparation across the footprint, which may include additional excavation, supplemental grouting, placement of dental concrete or slush grout backfill, or other methods.

Predicted pumping rates to enable the required dewatering for each unit are given in Subsection 2.5.4.6.2. That subsection also describes how these rates can be reduced significantly by installing a grout plug between approximately El. -35 feet and the bottom of the diaphragm wall at approximately El. -60 feet. With the grout plug installed, the seepage can be controlled during excavation using sumps and discharge pumps.

Final subgrades are inspected and approved prior to placement of lean concrete. Safety-related concrete placement is conducted under a quality program in accordance with Appendix B of 10 CFR 50. Inspection and approval procedures are addressed in the foundation and earthwork technical specifications developed at project detailed design. These specifications include, among other things, measures such as over-excavation and replacement of unsuitable rock (if encountered) and protection of surfaces from deterioration. Unsuitable rock includes soft, highly fractured, and highly porous materials. Excavations additionally comply with applicable OSHA regulations (Reference 256).

Foundation subgrade rebound (or heave) is monitored in excavations for each nuclear island. Subgrade rebound is not anticipated at the site based on the competency of the Key Largo Limestone at the base of the excavation and the underlying Fort Thompson Formation. The nuclear island is monitored during construction for:

- Groundwater levels, both interior and exterior to temporary excavations
- Horizontal and vertical movement of temporary slopes
- Loads in temporary ground support anchorages and/or struts
- Earth pressures acting on underground structures
- Foundation settlements

An instrumentation and monitoring technical specification is developed during project detailed design. The specification addresses issues such as the proper

installation of a sufficient number of instruments to measure the parameters of interest, monitoring and recording frequency, and reporting requirements.

PTN COL 2.5-6
PTN COL 2.5-8

2.5.4.6 Groundwater Conditions

Groundwater conditions for the site are established by periodic measurements of groundwater levels following observation well installation in 2008, as discussed in Subsection 2.4.12.1.4. Evaluation of these measurements provide a basis for engineering design and for the conceptual construction dewatering discussion provided in Subsection 2.5.4.6.2.

2.5.4.6.1 Site-Specific Data Collection and Monitoring

Groundwater conditions at the site are summarized in Subsection 2.5.4.2.2.6. In order to more accurately define aquifer parameters, four pumping wells and 50 observation wells were installed for the performance of aquifer pumping tests. Two pumping wells were installed at each reactor site. One well was open from depths of 22 to 45 feet to test the Key Largo Limestone and the second well was open from depths of 66 to 105 feet to test the Fort Thompson Formation. In addition to the pumping wells, each reactor site included 5 well clusters of 5 observation wells each, installed in the following zones:

— Upper aquitard (Miami Limestone)

— Upper Biscayne aquifer test zone (Key Largo Limestone)

— Middle aquitard (freshwater limestone unit)

— Lower Biscayne aquifer test zone (Fort Thompson Formation)

— Lower aquitard (Upper Tamiami Formation)

Descriptions and locations of the aquifer pumping test wells and observation wells are presented in Subsection 2.4.12.2.4.1 and Appendix 2BB, along with the results of the aquifer pumping tests.

2.5.4.6.1.1 Groundwater Elevations

Site groundwater elevations are discussed in Subsection 2.4.12.2.2.

2.5.4.6.1.2 Hydraulic Conductivity Tests

Twenty groundwater observation wells are installed at the site to monitor seasonal fluctuations in groundwater elevations and to evaluate the hydraulic conductivity of the soil and rock strata. Further investigation in the form of aquifer pumping tests was conducted to better define site-specific aquifer parameters. The results of these investigations are described in Subsection 2.4.12. The locations of the observation wells are shown on Figure 2.4.12-209. The groundwater elevations, gradients, and hydraulic conductivity results are discussed in Subsection 2.4.12.2.

2.5.4.6.2 Construction Dewatering

The excavation for each new unit will be surrounded by a reinforced concrete diaphragm wall that will act as a cut-off for horizontal groundwater flow into the excavation. Conceptual plans indicate each excavation will have dimensions of approximately 210 feet by 310 feet. The planned bottom of the wall is at El. –60 feet, i.e., just below a layer of limestone situated between the Key Largo Limestone (Subsection 2.5.4.2.1.3) and the Fort Thompson Formation (Subsection 2.5.4.2.1.2.4) that is considerably less permeable than either of these strata. This is referred to as the Freshwater Limestone in Appendix 2BB and Appendix 2CC. The layer has a lower permeability and thus reduces the amount of vertical inflow into the bottom of the excavation during dewatering.

The existing groundwater elevation in the power block areas is dependent on tidal variations, but averages close to El. 0 feet. The base of the excavation for the nuclear island is approximately El. –35 feet. Thus, temporary construction dewatering is needed down to at least El. –35 feet. The pumping test program described in Subsection 2.4.12.1.4 resulted in the development of estimates of the hydraulic conductivity of the Freshwater Limestone and the underlying Fort Thompson Formation. Freshwater Limestone used in the groundwater model described in Appendix 2CC is assumed to have a vertical hydraulic conductivity of approximately 2.3E-06 cm/sec, compared to approximately 1.7E-01 cm/sec for the Fort Thompson Formation. In the groundwater model, the Freshwater Limestone is assumed to be absent if the available information (from borings, etc.) indicates a thickness of less than 1.5 feet.

Various geologic features can provide potential pathways for water flow such as: zones of secondary porosity, fractures, bedding planes, and voids. As discussed in Appendix 2.5AA, zones of secondary porosity contain vugs on the order of centimeter scale. Fracturing and jointing at the site is widely spaced except under the vegetated depressions and drainages, where the Miami Limestone, Key Largo

Limestone, and Fort Thompson formations are slightly to moderately fractured as observed within the inclined borings of the supplemental investigation (Reference 290).

Within the slightly to moderately fractured zones, openness of discontinuities varies from tight (no visible separation) to moderately wide (0.03 to 0.1 feet), averaging slightly open (less than 0.003 feet). As discussed in Subsection 2.5.4.1.2.1, the largest potential voids or sediment infills that were found are limited in size and extent. As discussed in Subsection 2.5.4.4.5.5, potential voids in the grouted zone will be grouted and the maximum equivalent spherical diameter of potential voids between El. –60 feet and El. –110 feet will be constrained to 20 feet by the grout program. The elevation range from El. –60 feet to El. –100 feet is called “the extended zone.” Based on the field data described above, a void size is defined as equal to or greater than 0.5 feet.

For construction-related groundwater control, a grouted zone or “plug” will be constructed via grout injections into the rock mass between the bottom of the excavation at approximately El. –35 feet and the bottom of the diaphragm wall at approximately El. –60 feet. In general, grouting will be performed in a series of split spaced borings starting with primary order grout boreholes, and continuing through secondary order grout boreholes at a minimum. In the primary grout boreholes, individual grout stages will initially be grouted to “absolute refusal” closure criteria. Absolute refusal will be defined as zero (no measureable) flow of grout into the rock formation while the injection pressure is maintained equal to the target pressure for the stage for a duration of five minutes.

After enough (not more than eight adjacent) of the primary grout boreholes have been grouted using these criteria, the closure criteria may be adjusted based on grout takes, the results of water pressure tests, evaluation of available boring data, and the target residual permeability of the grouted zone. Upon completion of the grout stages in the primary grout boreholes, secondary grout boreholes will be drilled and grouted to the adjusted closure criteria. The water pressure test results and grout takes from the primary and secondary grout boreholes will be evaluated to determine the need for tertiary and higher order grout boreholes. Tertiary grout boreholes are likely to be required in some areas. Quarternary grout boreholes are anticipated to be minimal but may be needed at some locations where excessive grout take occurs in higher order grout boreholes. Grouting parameters will be measured in real-time including injection pressures, rate of injection, Apparent Lugeon value (hydraulic conductivity), and total volume of grout. When the grout takes have been reduced, the residual hydraulic conductivity of the grout

mass will be determined via water pressure tests performed in cored verification borings in the area.

An area of the grouted zone will be accepted as complete when the results of verification borings indicate that the residual hydraulic conductivity of the rock mass is equal to or below the target residual hydraulic conductivity.

As discussed in Subsection 2.5.4.4.5.5, primary grout boreholes will be extended to El. –110 feet (i.e., just above the interface between the Fort Thompson and Upper Tamiami formations) in order to constrain the maximum undetected spherical void size to approximately 20 feet.

The groundwater model simulation (Appendix 2CC) assumes hydraulic conductivity of the grout plug is 1.0E-04 cm/sec. The corresponding predicted groundwater extraction rate is 96 gpm per unit. In addition to using this value of hydraulic conductivity, a series of sensitivity analyses using a range of hydraulic conductivities (1.0E-03, 1.0E-05 and 1.0E-06 cm/sec) is conducted to determine the feasible range of dewatering discharge rates, which range from approximately 1000 to 1 gpm per unit. These values demonstrate that grouting can significantly reduce the quantity of discharge water generated during excavation dewatering activities.

2.5.4.6.2.1 Grout Test Program

A grout test program will be performed to validate the grout design and grouting techniques, and to determine the approximate grout takes for the Key Largo Limestone and Fort Thompson formations.

Grouting will be performed to facilitate construction dewatering and is not classified as safety-related. Mix design, material control, laboratory testing, grout placement, and field testing will be performed under a quality program.

The layout for the grout test program will be selected to resemble the planned construction grouting configuration. Grout borehole spacing will be set with regard to the spacing of the dominant geologic features and the construction grouting configuration. Grout borehole orientations and inclinations will be selected to promote intersections with the dominant fractures and bedding features in the area of the work. Since the fractures in the Key Largo Limestone and Fort Thompson formations range from vertical and subvertical to around 40 degree dip, it is anticipated that the inclination of the grout boreholes will be adjusted to best intercept the dominant features in the treatment area.

It is anticipated that on the order of 10 primary grout boreholes will be drilled for the grout test program, with a spacing of approximately 20 feet. It is anticipated that on the order of five secondary grout boreholes will be drilled for the grout test program, and will be offset from primary grout boreholes such that a secondary grout borehole is at the center of the square formed by four adjacent primary grout boreholes. Verification borings will be drilled at various locations within the grouted area to measure residual hydraulic conductivity of the rock mass and to physically and visually assess the suitability of grouting parameters. It is anticipated that five verification borings will be drilled for the grout test program.

The grout test program will be used to optimize and finalize the grouting and dewatering specifications, including:

- Spacing for primary and secondary grout boreholes. Primary grout boreholes will be spaced less than or equal to 20 feet on center. Spacing of primary and secondary grout boreholes may be reduced based on results from the grout test program.

- Suitability of the formation for grouting via downstages, upstages, or a combination of upstages and downstages. Upstage grouting is a method whereby packers or expansion plugs block off preselected portions of the grout boreholes in ascending stages while those portions are being grouted. In this method, grout boreholes are drilled to their full depth, pressure tested, and grouted in successive stages from the bottom up. Alternatively, downstage grouting is the grouting of progressively deeper zones in stages, with the deeper zones accessed by drilling through previously injected grout. Effectiveness of the staging method will be determined by borehole conditions during drilling including borehole instability during or after drilling, loss of circulation of drill fluid, difficulties setting packers in boreholes during water pressure testing and grouting, and by the level of improvement of borehole conditions after grouting has been performed in an area.

- Inclination of grout boreholes (vertical or inclined). As described above, boring orientations and inclinations will be selected to promote intersections with the dominant fractures and bedding features in the area of the work. It is anticipated that the inclination of the grout boreholes will be adjusted during the grout test program to best intercept the dominant features.

- Effective grout mixes using locally available materials and water sources. Multiple grout mixes will be identified for high and low mobility grout. Grout mixes will be tested to assess their mobility, stability, and durability. Different

grout mixes will be considered for the grouted zone and the extended zone. As shown in Table 2.4.12-211, the sulfate values measured from 24 water samples range from 2280 to 4400 ppm, resulting in a median value of about 3800 ppm, or close to 0.4 percent by weight. The grout within potential voids is not expected to be a uniform material in terms of strength-stiffness properties. Therefore, potential cracking within the grout material due to sulfate attack will not significantly alter the mechanical response of the grout-rock mass. In addition, stability analyses do not consider any increase in strength or stiffness due to the presence of the grout.

- Drilling and flushing of grout boreholes. The grout boreholes will be advanced using water flushed, rotary, or rotary percussive drilling. The primary grout boreholes in an area will be drilled, water pressure tested, and grouted before the drilling proceeds on the secondary grout boreholes. Primary and secondary grout borehole rock drilling will be monitored for penetration rate, down thrust pressure, rod torque, drilling fluid pressure and flow. Rock mass data will be collected using a drilling parameter recorder.

- Injection rates and pressure. Grouting pressures will be selected using a combination of best practices (e.g., Reference 327 uses 0.5 psi per foot of overburden and 1.0 psi per foot of rock) and experience from similar projects. Injection rates will be dictated by the ability to reach and maintain the target pressure. Injection volume limits will be optimized in the test program by evaluating the grout travel distance. Additionally, a rock pressure capacity test can be performed to determine the peak allowable grouting pressure for the site.

- Grouting conditions will be evaluated by using computer controlled real time monitoring of grout injected volumes, injection pressures, injection flow rates, Apparent Lugeon values, grout mix changes, and automatic recording of data.

- Initially, closure criteria for individual grout stages will be based on absolute refusal, or a time interval (approximately 5 minutes) where the grout is maintained at the target pressure and no measurable flow is occurring. Closure criteria will be modified for efficiency as the grout test program progresses. If the grout take for a stage is significant, closure will be achieved by using progressively thicker mixes that have reduced mobility. If necessary to reach closure, grouting may be stopped temporarily to allow grout to set and then resumed.

- Verification borings will be drilled and cored for the performance of water pressure tests to measure the residual hydraulic conductivity of the rock mass and to physically and visually assess the suitability of grout borehole spacing and inclination. Acceptance criteria for a completed area of the grouted zone will be based on water pressure testing performed in verification boreholes. A target area residual hydraulic conductivity of 10 Lugeons or less is reasonable. The acceptance criteria will be confirmed to be adequate for the site based on the results from the grout test program. The extended zone will not have a residual hydraulic conductivity requirement, as the purpose of grouting this zone is to constrain maximum undetected void size.

2.5.4.6.3 Seepage or Potential Piping Conditions During Construction

No earthwork structures are used during construction of Units 6 & 7 to retain water. Therefore, no adverse conditions due to seepage or piping through such structures are anticipated.

2.5.4.6.4 Permeability Testing

Permeability (or hydraulic conductivity) testing is described in Subsection 2.5.4.6.1.2.

2.5.4.7 Response of Soil and Rock to Dynamic Loading

PTN COL 2.5-2
PTN COL 2.5-6

The site subsurface profile is characterized with respect to the properties of strata pertinent for dynamic loading. Detailed descriptions of the development of the GMRS and the associated probabilistic seismic hazard assessment (PSHA), as well as the geologic characteristics of the site, are addressed in Subsection 2.5.2. Refer also to Subsection 2.5.4.4 for additional description on site-specific geophysical methods and results.

2.5.4.7.1 Site Seismic History

The seismic history of the area and of the site, including any prior history of seismicity and any historical evidence of liquefaction or boiling, is addressed in Subsection 2.5.2.

2.5.4.7.2 P- and S-Wave Velocity Profiles

Because of the significant depth of unconsolidated sediments at the site (refer to Subsection 2.5.4.1) compared to the depth of compression and shear wave

velocity measurements made during this subsurface investigation (i.e., to approximately 600 feet depth), additional information is required to complete the velocity profile for the site for use in seismic ground response analyses. Velocities in the upper 600 feet are measured at the site, and velocities deeper than 600 feet are obtained from available references as described in Subsection 2.5.4.7.2.2.

2.5.4.7.2.1 Seismic Velocities in the Upper 600 Feet

Geophysical measurements in the upper 600 feet of site soils are obtained by suspension P-S velocity logging methods and by downhole geophysical methods, as presented in Subsections 2.5.4.4.2.1 and 2.5.4.4.2.2, respectively. Recommended shear wave velocity profiles for the upper 600 feet of site soils at the power block are shown on Figure 2.5.4-220. Average shear wave velocities (V_s) are summarized in Table 2.5.4-215.

A significant range of shear and compression wave velocities within Strata 2, 3, and 4 with a peak near the top of Stratum 4 is observed. This variation is due to the different degrees of degradation of these materials. The velocities measured in soil Strata 5, 6, and 7 are observed to be appreciably more consistent.

P-S suspension velocity logging is performed in 12 dedicated borings (six borings in each of the two power blocks), with depths ranging from 150 feet to 600 feet, and at the locations shown on Figure 2.5.4-202. Downhole geophysical testing including gamma, caliper, resistivity, spontaneous potential, and caliper measurements extend as deep as 400 feet bgs. The suspension P-S logging data and the downhole geophysical data are contained in Appendix D of Reference 257 and in Appendix G of Reference 290.

Comparison of measured V_s results between the two power block areas indicates similar velocities.

The design/average V_s is summarized in Subsection 2.5.4.4.4.

2.5.4.7.2.2 Seismic Velocities Deeper than 600 Feet

Refer to Subsection 2.5.4.2.1.1 for a brief description of geologic conditions at depths greater than 600 feet. Cenozoic bedrock (“basement rock”) occurs at a depth of at least 15,000 feet (Reference 209). Additional subsurface data, in the form of sonic logs performed for oil field exploration borings and installation of exploratory well EW-1 supplement the site data to characterize conditions below 615.5 feet depth explored in the present investigation. Eight sonic logs, taken at borings drilled within the site region, (Figure 2.5.4-210) have sonic data ranging in

elevation from approximately –500 feet to approximately –11,900 feet (References 209 and 211). Sonic data obtained from EW-1 (Figure 2.5.4-243) ranges in elevation from approximately –1078 feet to approximately –3226 feet NAVD 88 (Reference 287).

Shear wave velocities are derived from the sonic log data using the relationship given in Subsection 2.5.4.2.1.2.10 (Equation 2.5.4-1). Average shear wave velocities are calculated for all eight sonic logs. These average shear wave velocity values are presented on Figures 2.5.4-211 and 2.5.4-243.

These figures also include profiles of average V_s values plus or minus one standard deviation. Note that sonic data from the eight sonic logs show shear wave velocities of strata deeper than 600 feet below finished site grade to increase from approximately 4000 feet/second at 600 feet to approximately 8500 to 10,000 feet/second below 10,000 feet.

2.5.4.7.3 Static and Dynamic Laboratory Testing

Static laboratory testing of representative soil samples obtained from this subsurface investigation are conducted, with results summarized on Table 2.5.4-209 and in Subsection 2.5.4.2.1.3.

Dynamic laboratory RCTS tests obtain data on shear modulus degradation and damping characteristics of site soils and rocks over a wide range of strains and are performed on 14 samples recovered in this subsurface investigation. Samples tested for RCTS ranged in depth from 29.6 to 294 feet. The samples are all from the Key Largo, Fort Thompson, upper and lower Tamiami, and Peace River formations (Strata 3, 4, 5, 6, and 7). The results of these tests are described briefly below in Subsections 2.5.4.7.3.1 and 2.5.4.7.3.2.

2.5.4.7.3.1 Selected Shear Modulus Degradation Curves for Site Strata

As described in Subsection 2.5.4.2.1.3.16, 14 RCTS tests are performed on Strata 3, 4, 5, 6, and 7 intact samples collected. Each of these intact samples is from the power block area. In each RCTS test, values of shear modulus (G) measured at increasing strain levels are obtained. These values are compared to the value of G_{max}, the shear modulus measured at 1.0E-04 percent shear strain. The shear modulus degradation (ratio of G/G_{max}) is plotted against shear strain, and a curve of G/G_{max} from the literature that best fits the test data is selected. Literature curves are used rather than an actual best-fit curve through the test data because the literature curves typically extend over a greater range of shear

strain than the test data. Curves recommended by the Electric Power Research Institute (EPRI) for non-cohesive soils are employed (Reference 258).

The modulus degradation curves (plots of G/G_{max} versus shear strain) from actual RCTS tests are presented on Figure 2.5.4-232 for the Key Largo Formation, Figure 2.5.4-246 for the Fort Thompson Formation, Figure 2.5.4-247 for natural soils less than 150 feet deep, and Figure 2.5.4-248 for natural soils greater than 150 feet deep. Figure 2.5.4-233 shows the selected values of G/G_{max} versus shear strain for the five strata tested in the power block in addition to the other site strata addressed in this evaluation. The selected G/G_{max} versus strain values for each stratum are also presented in Table 2.5.4-216.

Stratum 1 is removed from the site so the shear modulus degradation properties of that stratum are not relevant.

Stratum 2 is a weak rock stratum described in Subsection 2.5.4.7.3.3.

Due to the similarity of the grain size distribution and the materials, the recommended shear modulus degradation for Stratum 7 is the same as for Stratum 6, i.e., natural soil deeper than 150 feet depth in Figure 2.5.4-233. This modulus degradation curve is also selected for Stratum 8 which consists of very weak rock and is part of the same geological formation (Hawthorn Group) as Stratum 7.

Rock Strata 3 and 4 are considered not to be subject to modulus degradation in the shear strain range of 1.0E-04 percent to 5E-03 percent, as described in Subsection 2.5.4.7.3.3. The recommended shear modulus degradation curves for rock Strata 3 and 4 are provided on Figure 2.5.4-233.

Dynamic properties of compacted structural fill are described in Subsection 2.5.4.7.3.4.

For soil/rock beneath 600 feet, strain levels are so small that it can be reasonably assumed that there is no shear modulus degradation.

2.5.4.7.3.2 Selected Damping Curves for Soils

Each RCTS test also provides measured values of damping ratio (D) at increasing shear strain levels. The damping data for tests performed on natural soils are shown on Figure 2.5.4-249. The same procedure used for shear modulus degradation (G/G_{max} versus shear strain) is employed to obtain a D versus shear strain best-fit curve from the literature. Figure 2.5.4-235 shows the selected

values of D versus shear strain for tested Strata 3, 4, 5, 6, and 7, i.e., the rock curve for Strata 3 and 4 and the natural soil curve used for the remaining soil strata. The natural soil D versus shear strain curve is also selected for Stratum 8.

2.5.4.7.3.3 Shear Modulus and Damping for Rock

Rock strata are encountered at several depths at the site. For Strata 3 and 4, RCTS test results were used to find best-fit shear modulus degradation and damping curves. The modulus degradation curves (plots of G/G_{max} versus shear strain) from actual RCTS tests are presented on Figure 2.5.4-232 for the Key Largo Formation and Figure 2.5.4-246 for the Fort Thompson Formation. Recommended shear modulus degradation curves are presented on Figure 2.5.4-233. Based on these results, for Strata 3 and 4 (Key Largo and Fort Thompson formations), the shear modulus is considered non-strain-dependent based on the competency of the rock. The damping data for tests performed on the Key Largo and Fort Thompson formations are shown on Figure 2.5.4-234. The recommended damping curve for the Key Largo and Fort Thompson formations is shown on Figure 2.5.4-235. Below a shear strain of 0.01 percent, the damping ratio varies between 0.8 percent and 1.2 percent. Considering the small variation in damping in the shear strain range of interest, the damping ratio is considered as constant at 1 percent. For the Miami Limestone (Stratum 2), the limestone is considered sufficiently weak as to have a strain-dependent shear modulus. A recommended shear modulus degradation for this stratum based on literature (Reference 259) for mudstones/shales is provided in Figure 2.5.4-233. Similarly, a recommended damping curve for Stratum 2 is provided in Figure 2.5.4-235.

See Subsection 2.5.4.1 for a brief description of geologic conditions at depths greater than 600 feet based upon regional data. See Subsection 2.5.4.7.2.2 for a description of deep shear wave velocity profiles pertinent to the site derived from sonic logging data.

2.5.4.7.3.4 Dynamic Properties of Structural Fill

The muck layer underneath the power block area at Units 6 & 7 is removed and replaced with compacted limerock fill from onsite excavated Miami Limestone, Key Largo, and offsite sources, with fill placement starting from El. –5 feet and building up to El. +25.5 feet. Non-Category I structures are supported on compacted structural limerock fill.

Estimated shear wave velocity for structural limerock fill with upper and lower boundary estimates using a coefficient of variation (COV) of 1.5 applied to the shear modulus is shown on Figure 2.5.4-236. This relatively large COV is selected because of uncertainty about the degree of cementation of the limerock fill that could occur after placement. There is evidence of such cementation in the shear wave velocity measurements made at two locations within the existing Unit 5 at Turkey Point during a non-safety related investigation of the compacted limerock fill. Measured shear wave velocity values in the top 12 feet or so of the fill average between 1450 and 1500 feet/second, close to the upper boundary value shown in Figure 2.5.4-236 between 10 and 15 feet depth. It is noted that increase in shear wave velocity due to cementation of the fill is more pronounced close to the surface. The confining pressure increase with increasing depth in the fill results in higher shear wave velocities with depth, as shown in Figure 2.5.4-236, while the cementation effects with depth remain relatively constant.

The large particle sizes of the gravel/sand structural fill preclude RCTS testing of this material. Therefore, modulus degradation and damping ratio versus strain are estimated based on applicable literature (Reference 260). The adopted shear modulus degradation and damping ratio curves for compacted structural fill are presented in Figures 2.5.4-233 and 2.5.4-235, respectively, and Table 2.5.4-216. Refer to Subsection 2.5.4.5.1 for structural fill and general fill requirements.

2.5.4.7.4 Low Strain Shear Modulus Estimation

With shear wave velocity and other parameters established, low strain shear modulus values can be calculated from Equation 2.5.4-7. Note that shear wave velocity and unit weight values for use in the equation are given in Table 2.5.4-209. Refer to Subsection 2.5.4.2 for a stratum-by-stratum description of the derivation of shear modulus (G) and other geotechnical engineering parameters for use in design.

2.5.4.7.5 Seismic Parameters for Liquefaction Evaluation

The site-specific soil column extending to the proposed ground surface is developed for evaluation of liquefaction potential. The Cyclic Stress Ratio (CSR) is calculated following the methodology given in Reference 219. The stress reduction factor, r_d, used in the calculation of CSR is based on Reference 313. A constant value equal to 0.5 is used for depths equal to and larger than 98.4 feet (30 meters). The CSR is used to evaluate liquefaction potential as described in Subsection 2.5.4.8.

2.5.4.8 Liquefaction Potential

PTN COL 2.5-9

The potential for soil liquefaction at the site is evaluated following guidance given in RG 1.198. Current state-of-the-art deterministic methods, outlined in Reference 219, are followed. The subsurface conditions and soil properties considered are those described in Subsection 2.5.4.2.1.

Liquefaction can only occur where the stratum is saturated. The shallowest saturated stratum is the proposed compacted limerock fill layer that is only saturated for the lowest approximately 5 feet of section. This material (exact composition to be determined at final design phase) consists of a granular mixture including fines compacted to at least 95 percent maximum dry density in accordance with structural fill requirements. Typically, a compacted fill of similar material under the approximately 20 feet of overburden has a sufficiently high shear wave velocity and strength, as determined from the corrected N-values, to provide more than adequate resistance to liquefaction. As such, it is not prone to liquefaction and the factor of safety for liquefaction resistance of this stratum is not calculated.

As described in Subsection 2.5.1, the site rock strata (Strata 2, 3, 4, and 8) have sufficiently high shear wave velocities and cementation to avoid liquefaction. Thus, only the soil strata of the upper and lower Tamiami and Peace River Formations (Strata 5, 6, and 7) are considered for liquefaction potential analysis.

The Tamiami and Peace River Formations are attributed to the Pliocene and Miocene ages, respectively. Conventionally, only younger deposits, especially Holocene age and, to a lesser extent, Pleistocene age deposits, are considered potentially liquefiable. Accepted practice for the investigation and mapping of areas with seismic liquefaction potential is limited to soils younger than middle Pleistocene (700,000 years ago). Publications on liquefaction cite the assessments presented by Reference 261 that relate liquefaction susceptibility to the age of the soil deposit. These publications cover liquefaction studies from the east coast as well as the central and western United States (i.e., References 262, 263, 264, 265, and 266). An analysis of paleoliquefaction features along the Atlantic seaboard in Reference 267 for the Nuclear Regulatory Commission states that “no liquefaction sites were found in materials older than about 700,000 years.” RG 1.198 also notes the low probability of liquefaction of sediments older than late Pleistocene.

Unconsolidated soil deposits at the site are Pliocene (at least 1.6 million years old) or older. Additionally, the overburden of rock from Strata 2, 3, and 4 should preclude development of liquefaction-induced features, such as lateral spreading and settlement, from propagation to the ground surface. To be complete and conservative, a comprehensive liquefaction analysis for all CPT, shear wave velocity, and SPT data is made.

2.5.4.8.1 Liquefaction Evaluation Methodology

Liquefaction is the transformation of a granular soil material from a solid to a liquefied state as a consequence of increased pore water pressure and reduced effective stress. Soil liquefaction occurrence (or lack thereof) depends on geologic age, state of soil saturation, density, gradation, plasticity, and earthquake intensity and duration. The liquefaction analysis presented here employs state-of-the-art deterministic methods (Reference 219).

As noted in Subsection 2.5.4.6.1, groundwater levels selected as representative of the conditions at the time of the site-specific subsurface investigation (i.e., prior to the conditions expected during operation) are assumed at El. 0.

The natural soil at the power block is found mainly in muck, the upper and lower Tamiami Formation (Strata 5 and 6), and the Peace River Formation (Stratum 7).

There are several key aspects of liquefaction potential of Strata 5, 6, and 7 that should be considered prior to numerical evaluation. These aspects are age, depth, and rock overburden.

As addressed above, only the soil strata of the upper and lower Tamiami Formation and Peace River Formation (Strata 5, 6, and 7) are considered for liquefaction potential analysis. As noted above, the Tamiami and Peace River Formations are attributed to the Pliocene and Miocene ages, respectively. Conventionally, only younger deposits, especially Holocene age and, to a lesser extent, Pleistocene age deposits, are considered potentially liquefiable. As the unconsolidated soil deposits at the site below rock are Pliocene (at least 1.6 million years old) or older, the probability of liquefaction is considered extremely low. Reference 269 proposes an age correction factor, C_A, that accounts for the low probability of liquefaction of older deposits. Although this factor is not applied in this calculation, it would be approximately 2 to 2.5; therefore, use of this factor would increase the calculated factors of safety against liquefaction by a factor of 2 to 2.5.

The depth of the unconsolidated deposits of Strata 5, 6, and 7 makes liquefaction very unlikely. Although liquefaction has reportedly been observed in soils greater than 50 feet deep, a maximum depth of 50 feet may be adequate for evaluation of liquefaction potential in most cases (Reference 270). Because data on liquefaction are very sparse for depths greater than approximately 50 feet, calculation results for greater depths have a lower degree of certainty (Reference 219).

Liquefaction potential and the potential damage associated with liquefaction of loose sands under a stiff “crust” is considered in Reference 270. The overlying rock of Strata 2, 3, and 4 and the proposed limerock fill at the ground surface can be considered such a crust. Ishihara (Reference 271) considers thickness of a crust layer as deep as 26 feet and predicts that for a similar thickness of liquefiable strata, a maximum ground acceleration of greater than approximately 0.5 g is required to induce ground damage. The estimated peak ground acceleration at the proposed Units 6 & 7 is approximately 0.1g. For liquefaction to develop ground damage, the crust has to shear. This is extremely unlikely in the case of Strata 2, 3, and 4, which are approximately 100 feet thick in total and have reasonable shear strength (using rock criteria). Therefore, even if liquefaction occurs at depth, no effects at or near the ground surface are experienced.

For completeness, calculations to evaluate the factor of safety (FOS) against liquefaction are performed. The measured CPT values, the shear wave velocity, V_S, and SPT data are used for liquefaction analysis. These evaluations are performed separately, using the state-of-art approaches summarized in Reference 219. SPT results from Reference 257 are not used in the liquefaction calculations; the liquefaction assessment based on SPT data considers only the data obtained from Appendix A of Reference 290, as explained in the following subsection.

2.5.4.8.2 Liquefaction Resistance Based on SPT Data

As discussed in Subsection 2.5.4.2.1.3.2.1, the blow counts obtained from the initial site investigation (Reference 257) are lower than anticipated. The blow counts from the initial investigation are based on the second and third (2+3) 6-inch increments in penetration of an 18-inch-long sampler. The lower blow counts are further examined during the supplemental field investigation (Appendix A of Reference 290). For this purpose, the sampler type used is the 24-inch-long type rather than the 18-inch-long sampler. With a longer sampler, an additional blow count can be obtained (last 6 inches of the 24-inch-long sampler), allowing the observation of both blow counts, namely, the blow counts for the second and third

(2+3) 6-inch increments in penetration, and the blow counts for the third and fourth (3+4) 6-inch increments in penetration.

The summations of 3+4 blow counts are consistently and substantially higher than the summations of 2+3, as discussed in Subsection 2.5.4.2.1.3.2.1. The low value of the 2nd blow count directly impacts the “SPT N” value, since the “SPT N” is based on 2+3 blow counts in accordance with Reference 302. The 3+4 blow counts are at least 1 foot away from the last drilled location (bottom of borehole) before the initiation of the SPT. The soil zone penetrated by 3+4 blow counts is considered to be less influenced by overwashing as defined in Table 13 of NAVFAC DM 7.1 (Reference 301) associated with the upper half of the sampler length (as evidenced by the low 1st and 2nd blow count readings) and drilling conditions that affect the first two 6-inch increments.

Due to the effect of overwashing as discussed in Subsection 2.5.4.2.1.3.2.1, the original SPT-N values are too low and not representative of the actual soil conditions at the Turkey Point Units 6 & 7 site. The liquefaction analysis based on SPT considers only the results of the supplemental investigation (Appendix A of Reference 290), which are believed to best represent the actual soil conditions at the Turkey Point Units 6 & 7 site.

The equivalent clean-sand $CRR_{7.5}$ value based on SPT measurements is calculated following recommendations provided in Reference 219, based on corrected SPT N-values $(N_1)_{60}$, including corrections based on hammer-rod combination energy measurements at the site and corrections based on average fines content.

The SPT-based liquefaction analysis considers both blow counts 2+3 and 3+4 of the supplemental investigation (Appendix A of Reference 290). It is noted that for the more representative conditions of the soil in situ, represented by the blow counts 3+4, 70 points out of 79 points are directly classified as non-liquefiable given that the parameter $(N_1)_{60}$ results in values equal to or higher than 30. The nine remaining points have factors of safety ranging between 1.06 and 3.21. The value of 1.06 (at El. −119.78 feet in borehole R-7-1) is the only value under 1.4 and corresponds to the transition between the Fort Thompson and upper Tamiami formations. The graphical results of FOS are given in Figure 2.5.4-250. Based on SPT data, there is no potential for liquefaction for the Turkey Point Units 6 & 7 power block area.

2.5.4.8.3 FOS Against Liquefaction Based on CPT Data

CPT at the Turkey Point Units 6 & 7 site includes the measurement of commonly measured cone parameters (tip resistance and sleeve friction). The evaluation of liquefaction based on commonly measured parameters is discussed herein. The equivalent clean-sand $CRR_{7.5}$ value, based on CPT measurements, is calculated following recommendations found in Reference 219, based on normalized clean sand cone penetration resistance (q_{c1Ncs}) and other parameters such as the soil behavior type index, I_c. Cone tip resistance values from CPT soundings are shown in Figure 2.5.4-214 for the power block area. The deepest CPT soundings (C-701, R-6-3, and R-7-3) penetrate 289 feet below the ground surface, encountering refusal at that depth. Tip resistance measurements are made at 2-centimeter intervals (0.79 inches) during the initial investigation (Reference 257) and at 5-centimeter intervals (2 inches) during the supplemental investigation (Appendix E of Reference 290). The results showing FOS against liquefaction using the CPT data are provided in Figure 2.5.4-238 for the power block area. The value of FOS is consistently higher than 1.1 across the full depth of testing at the site. Based on CPT data, there is no potential for liquefaction for the Turkey Point Unit 6 & 7 power block area.

2.5.4.8.4 FOS Against Liquefaction Based on V_s Data

Similar to the FOS calculations for the SPT and CPT values, equivalent clean-sand $CRR_{7.5}$ values based on V_s measurements are calculated following recommendations provided in Reference 219. The curve proposed by Andrus and Stokoe (Reference 219) relating V_s to $CRR_{7.5}$ is used. Shear wave velocity data from P-S logging and downhole measurements are used for the FOS calculations. The collected raw (uncorrected) V_s data are shown in Figure 2.5.4-218 for the power block area. Suspension P-S velocity logging measurements were made at 1.64-feet intervals (0.5 meter). The deepest measurements (B-701) extend to approximately 600 feet below the ground surface. A total 1247 V_s data points from the upper Tamiami, lower Tamiami, and Peace River formations are used for the FOS calculations. The results showing FOS against liquefaction using the shear wave velocity data are provided in Figure 2.5.4-251. The limiting upper value of V_{s1} for liquefaction resistance is referred to as V_{s1}*; a conservative value for fines content of 20 percent is used resulting in a V_{s1}* equal to 680.6 fps (207.5 m/s). A cutoff value of 647.5 fps (197.4 m/s) for V_{s1} is used such that the maximum $CRR_{7.5}$ is set equal to 0.35. Almost all (99.8 percent) of the FOS calculated among the 1247 measurement points (1244 out of 1247) are above 1.4. Of the three remaining values, two values fall in the intermediate zone between 1.1 and 1.4, namely 1.22 at El.−124.47 feet and 1.30 at El. −127.75 feet at borehole R-7-1

(Unit 7), and one FOS is equal to 1.07 at El. −152.32 feet at CPT B-601 (Unit 6). This value of 1.07 corresponds to a tributary thickness to its measurement point equal to 1.64 feet. If the FOS is calculated as an average over adjacent measured points, it is equal to 2.40 (among the central point and 1 adjacent point on each side [top and bottom] for a total of 3 points), 2.93 (5 points), and 3.16 (7 points); this shows that the low value of 1.07 of the single point at El. −152.32 feet is a localized exception and does not represent a weak zone. Based on shear wave velocity data, there is no potential for liquefaction for the Turkey Point Unit 6 & 7 power block area.

2.5.4.8.5 Conclusions for Liquefaction Analysis

From the collective results obtained following the methodology outlined in Reference 219, it is concluded that soils at the Turkey Point Units 6 & 7 site are not likely to liquefy given the ground motion level for the site.

A negligible portion of the data at isolated locations indicates potentially liquefiable soils. The state-of-the-art methodology used for the liquefaction evaluation is intended to be conservative, not necessarily to encompass every data point; therefore, the presence of a few data points beyond the CRR base curve is acceptable (Reference 219). Additionally, in the liquefaction evaluation, the effects of age, overconsolidation, and cementation are ignored. These factors tend to increase resistance to liquefaction. Finally, the earthquake acceleration and magnitude levels adopted for the liquefaction analysis are conservative (M_w=7.3 and PGA = 0.1g). The earthquake magnitude of 7.3 selected is the highest earthquake magnitude among the controlling magnitudes from deaggregation (Table 2.5.2-225). The PGA associated with the GMRS is less than 0.1g (Figure 2.5.2-253) and has to be scaled up in accordance with RG 1.208 so that the PGA is 0.1g. Therefore, it is concluded that liquefaction is not a concern for the Turkey Point Units 6 & 7 site.

2.5.4.9 Earthquake Site Characteristics

PTN COL 2.5-2

The consideration of possible earthquake site characteristics is described in Subsection 2.5.2.

2.5.4.10 Static Stability

PTN COL 2.5-10

As noted earlier, finish grade at the power block is approximately El. +25.5 feet. Also as noted, the reactor and auxiliary buildings (nuclear island) are Seismic Category I structures. This subsection addresses the stability of foundation soils for these structures, the locations of which are shown on Figure 2.5.4-201. Other major structures, including the turbine buildings, the radwaste buildings, and the annex buildings, although not Seismic Category I structures, are considered in the settlement analysis.

2.5.4.10.1 Units 6 & 7 Foundations and Subsurface Conditions

Approximate foundation dimensions, foundation elevations, and required foundation-bearing capacities for the site Seismic Category I structures are indicated in the following table.

Structure	Approximate Foundation Dimensions (feet)	Approximate Foundation El. (feet)	Average Required Bearing Capacity (Static) (ksf)[a]	Maximum Required Dynamic Bearing Capacity (ksf)[b]
Reactor and auxiliary buildings (Units 6 & 7)	88 to 159 by 254 (irregular)	–14.0	8.9	35

(a) This pressure is the required design pressure required per the DCD.
(b) This pressure is the total pressure considering all static and short-term loads required per the DCD.

Power block subsurface conditions are described in detail in Subsection 2.5.4.2. Geotechnical engineering parameters selected for design for each of the various soil strata occurring at the site are also described in Subsection 2.5.4.2 and are summarized in Table 2.5.4-209. The parameters contained in this table are used as the basis for foundation analyses presented here.

For foundation analysis purposes, the specific subsurface conditions/profiles associated with each of the Seismic Category I structures at both Unit 6 and Unit 7 are developed as shown on Figures 2.5.4-203 through 2.5.4-208. Associated strata depths and elevations for each of these structure-specific conditions/profiles are shown in Table 2.5.4-201. As described in Subsection 2.5.4.10.7, the subsurface conditions in the upper 120 feet can be considered uniform in accordance with RG 1.132, therefore, there is no extreme lateral variability in the subgrade stiffness.

As noted in Subsection 2.5.4.6.1, based on groundwater observation well measurements, the current (preconstruction) groundwater level at the power block is El. 0 feet, very close to the existing ground surface. The estimated post-construction depth to groundwater at the power block is 25.5 feet. The actual groundwater level fluctuates due to changes in the tidal and cooling water canal levels. The groundwater level (El. 0 feet) used in foundation analyses is considered conservative but representative based on groundwater measurements presented in Subsection 2.4.12.2.2. Due to positive surface gradients away from the nuclear islands, the potential for infiltration of groundwater to raise the ground water level to within 2 feet of the finished grade is considered negligible.

2.5.4.10.2 Units 6 & 7 Bearing Capacity Evaluation

Application of classical bearing capacity hand calculations, such as Vesic's methodology (Reference 225) or methods outlined in Reference 272, to obtain the bearing capacity of the foundation media underlying the nuclear island is not straightforward due to the strength difference between rock and soil formations as seen in Table 2.5.4-209. Therefore, simplified configurations are assumed to calculate bearing capacity on:

1. Rock only, using Hoek-Brown's methodology (Reference 314), local shear failure for rock (References 272 and 316), and punching failure (Reference 272)

2. Rock and soil together, using local shear failure for rock (Reference 272)

3. Soil only, using local shear failure from Vesic's methodology (Reference 225), as if the nuclear island basemat was founded on the upper Tamiami layer

Due to the predominantly massive nature of rock layers at Units 6 & 7, as well as the rough condition of observed discontinuities, jointed rock failure modes are not considered in this bearing capacity analysis. Without open joints, stress is permitted to transmit continuously through the foundation media promoting a general shear failure mode.

The ultimate bearing capacity, q_{ult}, of a foundation on soil is calculated using Vesic's methodology for general shear failure from Reference 225:

$$q_{ult} = c\, N_c\, \zeta_c + q\, N_q\, \zeta_q + 0.5\, \gamma'\, B\, N\gamma\, \zeta_\gamma \qquad \text{Equation 2.5.4-14}$$

For foundations bearing on rock, References 272 and 316 equations calculate bearing capacity from general shear failure.

Using Reference 272, the ultimate bearing capacity (qult) formula for a footing on weak rocks with little fracturing is calculated as:

$$q_{ult} = c\, N_c\, C_{f1} + \gamma\, D_f\, N_q + 0.5\gamma\, B\, N_\gamma C_{f2} \qquad \text{Equation 2.5.4-15}$$

Where,

c = rock mass cohesion

γD_f = effective overburden pressure at base of foundation

γ = effective unit weight of rock

D_f = depth from ground surface to base of foundation

B = width of foundation

N_c, N_q, and N_γ are bearing capacity factors for rock

C_{f1} and C_{f2} are shape factors that replace the ζ shape factor in Equation 2.5.4-14.

From Table 5.4 of Reference 272,

$C_{f1} = C_{f2} = 1.0$ for L/B>6 strip foundation — Equation 2.5.4-16a

$C_{f1} = 1.12$, $C_{f2} = 0.9$ for L/B=2 — Equation 2.5.4-16b

$C_{f1} = 1.05$, $C_{f2} = 0.95$ for L/B=5 — Equation 2.5.4-16c

$C_{f1} = 1.25$, $C_{f2} = 0.85$ for square foundation — Equation 2.5.4-16d

$C_{f1} = 1.2$, $C_{f2} = 0.7$ for circular foundation — Equation 2.5.4-16e

Where,

L = length of footing.

From Equation 5.8 of Reference 272,

$$N_\varphi = \tan^2(45+\varphi/2) \qquad \text{Equation 2.5.4-17}$$

$$N_c = 2\ N_\varphi^{0.5}(N_\varphi+1)$$ Equation 2.5.4-18

$$N_\gamma = 0.5\ N_\varphi^{0.5}(N_\varphi^2-1)$$ Equation 2.5.4-19

$$N_q = N_\varphi^2$$ Equation 2.5.4-20

Equations 2.5.4-14 and 2.5.4-15 can be simplified to a local shear failure mode:

$$q_{ult}=c\ N_c\ \zeta_c+0.5\ \gamma\ B\ N_\gamma\ \zeta_\gamma$$ Equation 2.5.4-14a

$$q_{ult} = cN_cC_{f1}+ 0.5\ \gamma\ B\ N_\gamma\ C_{f2}$$ Equation 2.5.4-15a

This simplification is conservative because it neglects the contribution of the second term relating to surcharge resistance. Therefore, local shear failure evaluation is used in bearing capacity analysis instead of the general shear failure assumption.

In addition to Equation 2.5.4-15a for a local shear failure in rock, the Hoek-Brown methodology considers the strength criterion for jointed rock masses to calculate ultimate bearing capacity. The Hoek-Brown methodology assumes a strip footing, but does not take foundation dimensions into account. Instead, the method relies on rock descriptions and UCS, shown in Equation 3-6 of Reference 314:

$$q_{ult}=\left[\sqrt{s}+m\right]\times U$$ Equation 2.5.4-20a

Where,

q_{ult} = ultimate bearing capacity,
U = UCS of a rock mass, and
m and s = empirically determined strength parameters according to rock type, and rock condition, listed in Reference 274.

Punching failure describes a case where the overlying rock layers fail in shear on all sides of the foundation due to the concentrated force on thin rock layers. This failure is also applicable to bearing capacity analysis of Units 6 & 7. Punching failure bearing capacity is defined as the rock layer shear strength multiplied by the shearing surface area. The shearing surface area is equal to the loading perimeter multiplied by the thickness of the rock layer.

$$q_{ult}=\frac{U}{2}*(2B+2L)*H/\ (B*L)$$ Equation 2.5.4-20b

Where,

q_{ult} = ultimate bearing capacity,
U = UCS of a rock mass,
B = width of foundation,
L = length of foundation, and
H = thickness of Key Largo plus Fort Thompson beneath the bearing surface (Table 2.5.4-209).

To adequately consider both rock and soil formations, bearing capacity is additionally obtained using SLOPE/W software (limit-equilibrium method) and justified using PLAXIS 2D. In SLOPE/W the foundation bearing demand is increased until the desired factor of safety is observed (FOS = 3.0). Allowable bearing capacity is obtained at FOS = 3.0. When the load is further increased, the ultimate failure surface is observed at FOS = 1.0. These conditions are presented in Figures 2.5.4-256 and 2.5.4-257. These surfaces are checked with PLAXIS 2D (finite element method) to obtain a unique solution independent of the prescribed failure surfaces in SLOPE/W.

PLAXIS 2D is used to verify the validity of failure surfaces from SLOPE/W using the unique solution found from increasing the bearing demand to failure. As seen in a plot of plastic points (i.e., points reaching Mohr-Coulomb failure), this unique surface becomes evident (Figure 2.5.4-268). This is the same depth reached by the prescribed failure surface from SLOPE/W (Figures 2.5.4-256 and 2.5.4-257).

The PLAXIS 2D model is also used to check for beam tension failure. The tension cutoff for the rock layers (i.e., tensile strength of rock) is determined according to equation 3.20 in Reference 272.

$$\sigma_t=0.5\ \sigma_u\ (m-\sqrt{m^2+4s}) \qquad \text{Equation 2.5.4-20c}$$

In PLAXIS 2D, the beam tension failure is checked for the required bearing demand (8.9 ksf) as well as three times the required bearing demand (26.7 ksf). In Figures 2.5.4-266 and 2.5.4-267, points in tension are shown with black squares. As evident in both cases, there are minimal black squares, i.e., no significant tensile failure, is observed, even for loads three times the required bearing demand.

Bearing capacity is evaluated for two extreme foundation widths (B): the shortest east-west dimension on the south edge of the building (B = 88 feet) and the longest east-west dimension through the shield building and the auxiliary building (B approximately 160 feet). Rock and soil properties (c', φ', γ) are determined by

an arithmetic average weighted by thickness of the underlying strata (Table 2.5.4-209). These properties are determined for the following cases:

1. Rock-only bearing capacity is evaluated using a weighted average with properties of the Key Largo and Fort Thompson formations only

2. Soil and rock together uses weighted averages to a depth of 2B, including soil layers

3. Soil-only bearing capacity is evaluated using weighted averages of the upper Tamiami, lower Tamiami, and Peace River to a depth of 2B

Properties for rock are varied between assumptions of very slightly fractured rock, FD1 (Table 2.5.4-209), slightly to moderately fractured rock, FD4 (Table 2.5.4-209), and lower-bound FD4 rock (Table 2.5.4-221).

Soil properties are varied between best estimate and lower-bound properties. For lower-bound properties in soil, the upper Tamiami properties are reduced to the properties in Table 2.5.4-221 while lower Tamiami and Peace River properties remain as best estimate properties. It is unrealistic to assign lower-bound properties to all layers, so the upper Tamiami properties are reduced as it is the bearing layer in soil-only calculations.

To obtain static bearing capacity according to Hoek-Brown methodology, material properties are estimated from Reference 319. The rock mass at Units 6 & 7 site is tightly interlocking undisturbed carbonate rock, classified as very good quality. These material properties are used in Hoek-Brown bearing capacity and calculation of tensile strength for the beam tension failure check in PLAXIS 2D. The average UCS value of the two rock layers is adopted.

Punching failure also uses the average UCS of the Key Largo and Fort Thompson formations. This failure is determined for the two foundation configurations (88 feet and approximately160 feet).

In SLOPE/W, a case is considered where zones representing open discontinuities are placed beneath and to the side of the nuclear island to represent zones of FD4 material as shown in Figure 2.5.4-254. This case is unrealistic because joints in FD4 rock are only moderately open, but the comparison to no simulated joints is presented in Figures 2.5.4-258 and 2.5.4-259.

Foundation-bearing capacities are calculated using Equations 2.5.4-14a, 2.5.4-15a and 2.5.4-16a through 2.5.4-20c. A summary of the cases evaluated and allowable

bearing capacities (using FOS = 3.0) of Seismic Category I structures (nuclear island) is given in Table 2.5.4-217. Analysis results show that for the Seismic Category I structures (including both units), the minimum allowable static bearing capacity is 39 ksf from the lower-bound SLOPE/W analysis, which greatly exceeds the average required bearing capacity of 8.9 ksf specified in the DCD.

2.5.4.10.2.1 Dynamic Bearing Capacity

Dynamic bearing capacity is determined using Soubra's bearing capacity factors (Reference 315), N_{cE} and $N_{\gamma E}$, in Equations 2.5.4-14a and 2.5.4-15a, replacing N_c and N_γ, respectively. These factors are chosen from Soubra's Tables 6 and 8 based on horizontal acceleration K_H = 0.1g and the friction angle according to the foundation media rounded down to the nearest 5.

The maximum dynamic bearing capacity required is 35 ksf (DCD). This total load includes normal loading plus seismic conditions with a 0.3g peak ground acceleration, which greatly exceeds the seismicity in Florida. Using the calculated allowable bearing capacity of 41 ksf for rock and lean concrete overlying the rock, this condition is satisfied even with the 0.3g peak ground acceleration.

Note that for concrete, no guidance is given in ACI 349-06 (Reference 273) for increasing or decreasing the design bearing strength for dynamic loading.

2.5.4.10.3 Settlement

PTN COL 2.5-12
PTN COL 2.5-16

The settlement analyses consist of a hand calculation that uses stress distributions appropriate for layered systems as well as a three-dimensional finite element model using PLAXIS 3D Foundation (PLAXIS 3D). Settlement analyses use the revised best estimate material properties. These updated material properties are based on laboratory data from both the initial (Appendix E of Reference 257) and supplemental (Appendix C of Reference 290) field investigations.

The containment and auxiliary buildings (nuclear island) share the same mat foundation and are founded on lean concrete placed above rock of the Key Largo Limestone. Therefore, for settlement computations, the bottom of the foundation is taken at El. –14 feet on lean concrete. The best estimate settlement of the rock and soil strata is computed using the elastic modulus values tabulated in Table 2.5.4-209. The elastic modulus for the lean concrete used for settlement estimates is derived as follows:

The thickest part of lean concrete is between El. –14 feet and El. –35 ft, i.e., 21 feet thick (see Figure 2.5.4-222). The elastic modulus of lean concrete with a unit weight of 150 pcf can be calculated using the following equation (Reference 317).

$$E_c = 57{,}000\sqrt{f'_c}\ (\text{psi}) \qquad \text{Equation 2.5.4-21}$$

where,

f'_c = specified compressive strength of concrete (psi)

The lean concrete placed on rock is expected to have a minimum compressive strength of 1500 psi.

$$f'_C = 1.5\ \text{ksi, then } E_C = 57{,}000\sqrt{1500} = 2.21 * 1.0E06\ \text{psi} \approx 318{,}500\ \text{ksf}$$

2.5.4.10.3.1 Hand Calculation of Settlement

In the hand calculation, vertical incremental strains are calculated assuming linear elastic properties. The resulting settlement is obtained by integrating the vertical incremental strains over the soil/rock column using Equations 2.5.4-22a through 2.5.4-22e (Reference 217).

Two cases are considered in the settlement hand calculation. The first is a best estimate case using the design stiffness for each layer. The second case acts as a sensitivity analysis by using the lower-bound stiffness for two layers (the upper Tamiami and Peace River). The lower-bound stiffness is defined as the 16th percentile, indicating a 16 percent probability of that or a lower stiffness occurring. Therefore, the probability of having two layers with lower-bound stiffness is approximately 2.5 percent. The upper Tamiami and Peace River layers are chosen for the lower-bound case because they are the layers that impact settlement the most. Average lower-bound properties are given in Table 2.5.4-221.

The Key Largo Limestone and the Fort Thompson Formation form a stiff upper layer, while the layers below (upper Tamiami, lower Tamiami, and Peace River) are comprised primarily of dense, silty sands. Because of this layering, a typical Boussinesq stress distribution may not provide realistic stress distributions, showing very high settlement in the deep sand layers. Therefore, stress distributions appropriate for layered systems are used.

For the nuclear island, a stress distribution from Milovic (Reference 316) for a two-layered system was used with rock (Key Largo and Fort Thompson) as the first layer and soil (upper Tamiami, lower Tamiami, and Peace River) as the second layer. For the remaining buildings (turbine, first bay, annex, and radwaste), a stress distribution from Poulos and Davis (Reference 275) for a three-layered system was used with the fill as the first layer; rock (Miami Limestone, Key Largo, and Fort Thompson) as the second layer; and soil (upper Tamiami, lower Tamiami, and Peace River) as the third layer. In each case, the stress distribution is dependent on the stiffness and thickness of each layer, the area of the building, and the depth of interest. The stress distributions assume a circular foundation. Based on the layering information, I_z coefficients, defined as the percentage of the building pressure, are found.

$$\Delta\sigma_z = PI_z$$ Equation 2.5.4-22a

Where,

σ_z= the vertical stress,
P= the building pressure,
and I_z = the percentage of building pressure at depth z

$$\Delta\sigma_h = \Delta\sigma_z * K_0$$ Equation 2.5.4-22b

Where,

σ_h= the horizontal stress,
and K_0= the at rest earth pressure coefficient

$$K_0 = 1 - \mathrm{Sin}(\varphi)$$ Equation 2.5.4-22c

Where,

φ= the friction angle

$$\Delta\varepsilon = \frac{1}{E}\left(\Delta\sigma_z - 2v'\Delta\sigma_h\right)$$ Equation 2.5.4-22d

Where,

Δε= the vertical strain,
E= the Young's modulus,
and v'= Poisson's ratio

$$\Delta S = \Delta\varepsilon^* \Delta z$$ Equation 2.5.4-22e

Where,

ΔS= the settlement,
and Δz= the thickness

Heave is considered for the excavation below the nuclear island. Dewatering will occur before the construction process to an elevation of -38 feet under the nuclear island. Up to the construction of the lean concrete layer, pumping rates are assumed to create conditions of zero pressure in the bottom of the foundation (no buoyancy). Conservatively, these conditions are assumed during loading, i.e., the buoyancy forces acting to reduce settlement are neglected. The effects of buoyancy are calculated and reported separately.

Lastly, consolidation settlement is also considered using Equation 2.5.4-23 (Reference 217) for the lower Tamiami layer. Consolidation settlement is found to be negligible, as expected, because the soil types at the site (upper Tamiami, lower Tamiami, and Peace River) are silty sands and are therefore not considered to be prone to consolidation-type settlement. Any secondary consolidation (creep) would be even smaller than consolidation settlement, and is therefore not considered in this analysis.

$$\Delta\varepsilon = \frac{C_r}{1+e_0} * \log \frac{\sigma'_v + \Delta\sigma_z}{\sigma'_v}$$ Equation 2.5.4-23

Where,

$\Delta\varepsilon$= the strain,
C_r = the recompression index,
e_0= the void ratio,
σ'_v= the in situ effective stress,
and $\Delta\sigma_z$= the vertical stress

2.5.4.10.3.2 PLAXIS 3D Settlement Model

In addition to the settlement hand calculation, settlement is determined using PLAXIS 3D, a finite element method (FEM)-based computer code designed for geotechnical analyses. The program calculates displacements with the use of numerical integration methods. In addition to the typical capabilities of a general FEM application for elastic solids, PLAXIS 3D incorporates advanced constitutive

models, (stress vs. strain relationship) that are capable of simulating the response of soils to external loading.

The PLAXIS 3D model includes the following phases:

1. Initial conditions: Initial effective stresses for the soil column are obtained. The structural fill from El. –5 to El. 25.5 feet is already in place in this phase.

2. Dewatering: The water level, initially assumed to be at the ground surface (El. –1 feet) is lowered to El. –38 feet in the footprint of the nuclear island. The vertical effective stresses across the depth of the soil column increase due to dewatering, causing incremental settlement.

3. Excavation and lean concrete placement: Upon dewatering down to El. –38 feet, the material between El. 25.5 and El. –35 feet is removed in the footprint of the nuclear island and a lean concrete backfill is installed from El. –35 feet up to El. –14 feet. In the PLAXIS 3D model, the net effect of the removal of soil/rock and the addition of the lean concrete is an incremental heave due to the drop in effective stresses across the depth. In the excavation phase, the area of the turbine building that is founded on El. 8.25 feet is also excavated.

4. Construction of power block structures (excluding the nuclear island): Loads on the footprints of the turbine, first bay, radwaste, annex, and diesel generator buildings and water tanks are applied. Effective stresses increase causing incremental settlement in this stage.

5. Construction of the nuclear island: Loads are applied on the footprint of the nuclear island. Effective stresses increase causing incremental settlement in this stage. It is important to note that the loads on the footprint of the nuclear island are applied while the pore pressure is assumed to be zero at the bottom of the foundation.

6. Rewatering: The water table is redefined in the PLAXIS model to be back at El. –1 foot for the nuclear island footprint, which has the effect of generating the hydrostatic pressures acting on the bottom of the nuclear island foundation from the stage where pumping for dewatering purposes ceased. The net effect of buoyant forces is to reduce settlements as calculated in the previous phase. However, for conservative purposes, this effect is neglected.

The actual construction sequence may involve simultaneous dewatering and excavation as well as simultaneous building construction and rewatering. The phases modeled in PLAXIS allow for determining settlements/heaves associated with each activity. Furthermore, initial conditions in the model include the backfill in place up to El. 25.5 feet. Therefore, the excavation prediction includes slightly more material removal (larger heave number reported).

RG 1.132 Appendix D states that, "*Where soils are very thick, the maximum required depth for engineering purposes, denoted* d_{max}*, may be taken as the depth at which the change in the vertical stress during or after construction for the combined foundation loadings is less than 10% of the effective in situ overburden stress*." The analysis depth of El.–450 feet, which is greater than 2B (B = the least dimension of the foundation), was assumed to be adequate to meet the aforementioned criterion. In situ initial overburden effective vertical stress at the bottom of the model is 31,037 pounds per square foot (psf). The vertical effective stress at the bottom of the model becomes: 32,057 psf at the end of excavation, 32,475 psf at the end of loading other buildings, 33,039 psf at the end of loading the nuclear island, and 31,709 psf at the end of the rewatering phase. The changes in effective vertical stresses are less than 10 percent of the effective in situ stress for each phase, demonstrating that the model depth is appropriate.

The plan dimensions considered in the model are 1724 feet by 1396 feet. The total displacement at the corner of the model is less than 0.1 inch, confirming that the horizontal extent of the model is appropriate.

The foundations are considered as plate elements with a thickness corresponding to the basemat thickness. The plate elements have no self weight, as the building is assumed to be inclusive of the foundation weight.

The analysis uses 15-node wedge elements. The total number of elements is 70,152 for the design mesh. The boundary conditions for the sides of the model are set to allow for the vertical displacement, and restrain the two horizontal displacement components in the x- and z- directions. The bottom of the model is restrained in the vertical and horizontal directions.

The four following sensitivity analyses are included in the PLAXIS 3D calculation:

1. Mesh Sensitivity:

   Four models with the following numbers of elements are considered:

   - very coarse – 11,514

- moderately coarse – 25,650
- design – 70,152
- finest – 115,810

The change in mesh density for these models is focused on the loaded areas. Both vertical and horizontal meshes are varied. These models have the best estimate material properties (slightly fractured [FD1], for rock). Figure 2.5.4-260 shows the design mesh.

2. Fracture Density:

Two main fracture zones are identified: slightly fractured (FD1) and moderately fractured (FD4). The zone of moderately fractured rock is significantly smaller than the zone of slightly fractured rocks as shown in Figure 2.5.4-254. The stiffness of the FD4 zone is less than the FD1 zone. However, the effect of including FD4 zone in the 3D settlement model is anticipated to be negligible, since the settlement is governed by the lower stiffness of the soil layers. An additional sensitivity run is conducted to check this assumption. FD4 zones are incorporated into the model, assuming FD4 zones for Unit 6, since an FD4 zone extends below the Unit 6 nuclear island, and the fracture density is higher for Unit 6 than for Unit 7 (Figure 2.5.4-254). Best estimate material properties are used for soil, and FD1 properties are used for the remaining rock.

3. Soil Constitutive Behavior:

Soil layers are modeled using an elasto-plastic Mohr-Coulomb model, since the strain levels are expected to be low and within the relatively elastic range. The use of a Mohr-Coulomb model also dictates the use of the constant stiffness throughout soil layers. This assumption is justified based on the insensitivity that the shear wave velocity shows against depth for the soil layers, particularly for the upper and lower Tamiami Formations. To check this assumption, a more comprehensive hardening soil model is adopted for the soil layers.

The hardening soil model is a hyperbolic model developed based on the theory of plasticity. The hardening soil model accounts for the stress-dependency of the soil stiffness by increasing stiffness with increasing pressure. When the soil experiences reloading, such as foundation loading after excavation, the hardening soil model will account for the previous stress history. This is because the reloading stiffness is typically

approximately three to five times higher than the loading stiffness. Unlike the loading portion of the stress-strain curve, the reloading portion of the stress-strain curve is linear. The reloading stiffness is used during the reloading until the stresses induced by the applied load exceed the stresses that the soil has previously experienced. At that point, PLAXIS 3D automatically switches to using the reloading portion of the hyperbolic curve.

To determine the material properties to use in the hardening soil model (triaxial stiffness E_{50}, triaxial unloading stiffness E_u, and the oedometer loading stiffness E_{oed}), a calibration was done varying the material parameters, while keeping the E_u/E_i ratio constant, until the stress-strain plot from PLAXIS 3D matches the stress-strain plots from the triaxial testing results. Figures 2.5.4-261 through 2.5.4-263 show the plots of the hardening soil calibration, where all the triaxial test results from each layer are shown, along with the soil hardening based PLAXIS 3D curves at the mid-depth, top, and bottom of each layer. In addition, Figures 2.5.4-261 through 2.5.4-263 show the Mohr-Coulomb stress-strain curves obtained from the PLAXIS 3D best estimate model.

4. Lower Bound:

For the lower-bound model, soil layers (upper Tamiami, lower Tamiami, and Peace River) are given lower-bound stiffness values, defined as the 16th percentile, indicating a 16 percent probability of that or a lower stiffness occurring. The rock layers are given FD1 stiffness values.

2.5.4.10.3.3 Settlement Results

Table 2.5.4-219 shows the maximum settlement per building predicted by the hand calculation.

The following PLAXIS 3D results do not include the excavation and dewatering phases because the basemat is expected to be placed and leveled before the structural loads are applied, and excess pore pressures generated prior to basemat placement are considered to be dissipated. Therefore, monitored settlements on the basemat will not reflect the effects of dewatering and excavation. In the PLAXIS 3D model, the average heave of the nuclear island due to excavation is estimated to be 1 inch.

Table 2.5.4-222 shows the results of the mesh sensitivity analysis. Maximum settlement predicted for the nuclear island varies from the design mesh by 0.4 percent, 0.0 percent, and 0.4 percent for the coarse, moderately coarse, and finest meshes, respectfully. Based on these results, the design mesh is confirmed to be appropriate for the settlement analysis.

Table 2.5.4-223 shows the results of the fracture density, hardening soil, and lower bound sensitivity analyses for the PLAXIS 3D models. Maximum settlement predicted for the nuclear island varies by 0.8 percent between the model without fractures and the model with FD4 fractures. This confirms that the effect of including FD4 zone in the 3D settlement model is negligible, since the settlement is governed by the lower stiffness of the soil layers. Maximum settlement predicted for the nuclear island does not vary based on the type of model (Mohr-Coulomb or hardening soil), confirming that the Mohr-Coulomb best estimate model is appropriate. The maximum settlement predicted for the nuclear island varies by 35.5 percent between the lower bound and best estimate cases, again confirming that the settlement is governed by the lower stiffness of the soil layers.

Table 2.5.4-224 shows the comparison between the settlement predicted by the hand calculation and the PLAXIS 3D model to the DCD requirements. The lower bound and best estimate cases for the hand calculation and the PLAXIS 3D model are within the acceptable limits provided by the DCD. The reported differential settlements between the nuclear island and other adjacent buildings are calculated in both the hand calculation and the PLAXIS 3D model by subtracting the settlement of adjacent buildings from the settlement of the nuclear island building at center locations of each respective building. The differential settlement between the nuclear island and other adjacent buildings does not account for the influence of the nuclear island loads on the settlement of adjacent buildings, and is therefore conservative. If nuclear island loads are considered in the settlement of adjacent structures, then the differential settlement between the nuclear island and radwaste building is reduced.

The sensitivity analyses presented in Tables 2.5.4-222 and 2.5.4-223 demonstrate that the best estimate model used is appropriate. Figure 2.5.4-264, shows the PLAXIS 3D total displacement output for the best estimate model after the loading of the nuclear island. Figure 2.5.4-265 shows the PLAXIS 3D total displacement output for the best estimate model after rewatering.

2.5.4.10.4 Earth Pressures

PTN COL 2.5-7
PTN COL 2.5-11

The static and seismic active and at-rest lateral earth pressures acting on underground structure below-grade walls are addressed in this subsection. The analysis of seismic earth pressure is addressed generically. Note that active earth pressures apply to yielding walls such as steel sheet pile walls, MSE walls, and, to a lesser extent, more rigid concrete slurry (diaphragm) walls, which are used primarily as temporary ground support in construction. At-rest earth pressures occur in the case of non-yielding walls, such as the rigid, below-grade walls of underground structures (e.g., for the containment/auxiliary buildings, control buildings, etc.).

Increases in lateral earth pressures resulting from compaction close-in to below-grade structures are not considered here. These increases are controlled at the construction stage by limiting the size of compaction equipment and its proximity to below-grade walls. Note that the magnitude of compaction-induced earth pressure increases can only be assessed once a range of allowable equipment sizes and types are selected/specified.

For the seismic active and at-rest earth pressure cases, earthquake-induced horizontal ground accelerations are accounted for by employing the factor $k_h g$. Here, $k_h = 0.1$ is used. Vertical ground accelerations (k_v g) are considered negligible (Reference 276).

2.5.4.10.4.1 Static Lateral Earth Pressures

The static active earth pressure, p_{AS}, is calculated using Reference 225:

$$p_{AS} = K_{AS} \cdot \gamma \cdot z \qquad \text{Equation 2.5.4-24}$$

Where,

K_{AS} = Rankine coefficient of static active lateral earth pressure

γ = unit weight of the structural fill and general fill (γ', effective unit weight when below the groundwater level)

z = depth bgs

The Rankine coefficient, K_{AS}, is calculated from:

$$K_{AS} = \tan^2 (45 - \varphi'/2) \qquad \text{Equation 2.5.4-25}$$

Where,

φ'= effective friction angle of the structural fill and general fill, in degrees

The static at-rest earth pressure, p_{0S}, is calculated using Reference 225:

$$p_{0S} = K_{0S} \cdot \gamma \cdot z \qquad \text{Equation 2.5.4-26}$$

Where,

K_{0S} = coefficient of at-rest static lateral earth pressure

The coefficient, $K_{0S,}$ is calculated from:

$$K_{0S} = 1 - \sin(\varphi') \qquad \text{Equation 2.5.4-27}$$

Hydrostatic groundwater pressure is considered for both the active and the at-rest static conditions, calculated by:

$$p_w = \gamma_w \cdot z_w \qquad \text{Equation 2.5.4-28}$$

Where,

p_w = hydrostatic pressure

z_w = depth below the groundwater level

γ_w = unit weight of water = 62.4 pcf

2.5.4.10.4.2 Seismic Lateral Earth Pressures

The active seismic pressure, p_{AE}, is given by the Mononobe-Okabe equation (Reference 276), represented by:

$$p_{AE} = \Delta K_{AE} \cdot \gamma \cdot (H - z) \qquad \text{Equation 2.5.4-29}$$

Where,

ΔK_{AE} = coefficient of active seismic earth pressure = $K_{AE} - K_{AS}$

K_{AE} = Mononobe-Okabe coefficient of active seismic earth thrust

H = below-grade height of the wall

The coefficient K_{AE} is calculated from:

$K_{AE} = \cos^2 (\varphi' - \theta)/\{\cos^2 \theta \cdot [1 + (\sin \varphi' \sin (\varphi' - \theta)/\cos (\theta))^{0.5}]^2\}$ Equation 2.5.4-30

Where,

$\theta = \tan^{-1} (k_h)$

k_h = horizontal earthquake acceleration, as in Subsection 2.5.4.10.4.

Using the ASCE 4-98 method (Reference 277), the design ground motion is used to calculate a seismic at-rest pressure as a function of depth for below-grade walls.

2.5.4.10.4.3 Lateral Earth Pressures Due to Surcharge

Lateral earth pressure resulting from surcharge applied at the ground surface alongside a below-grade structure wall, p_{sur}, is calculated using:

$p_{sur} = K\ q$ Equation 2.5.4-31

Where,

K = earth pressure coefficient; K_{AS} for active, K_0 for at-rest, ΔK_{AE} or ΔK_{oE} for seismic loading, depending on the nature of the loading (ΔK_{oE} = seismic at-rest coefficient)

q = uniform surcharge pressure

Note that surcharge pressures of 500 psf and 4000 psf are included in the earth pressure calculations summarized here. The validity of these pressures is reviewed during the detailed design phase.

2.5.4.10.4.4 Lateral Earth Pressure Diagrams

Using the relationships outlined above and the compacted limerock fill properties summarized in Table 2.5.4-209, sample earth pressure diagrams are developed. Compacted limerock fill properties (granular soils) used have a unit weight (γ) of 130 pcf and a drained friction angle (φ') of 33 degrees (refer to Table 2.5.4-209). These values apply to both structural and general fill. Uniform surcharge loads of 500 psf and 4000 psf are included.

2.5.4.10.5 Sample Earth Pressure Diagrams

Recommended diagrams for use in calculating lateral earth pressures against walls are developed based on strata thicknesses and lateral earth pressure

coefficients. Figures 2.5.4-239 (500 psf surcharge) and 2.5.4-252 (4000 psf surcharge) show the diagrams for above grade walls where the walls can rotate or deflect away from the soil mass, known as the active case. This case considered walls extending from the highest finish grade (El. +25.5 feet) to a depth of El. –35 feet, and models active earth pressures on the diaphragm wall during the construction period.

Figures 2.5.4-240 (500 psf surcharge) and 2.5.4-253 (4000 psf surcharge) show the pressure diagrams for below grade walls where no rotation is possible (at-rest case). This case considers walls from El. +25.5 to El. –14 feet, the base of the deepest structure wall.

2.5.4.10.6 Selected Design Parameters and Results Overview

The results of the investigation indicate that the site is underlain by rock overlying unconsolidated deposits. The risk of subsidence due to karst is not considered significant. The risk associated with settlement is considered insignificant. A summary of the parameters recommended for geotechnical design is presented in Table 2.5.4-209.

2.5.4.10.7 Lateral Variability

In Table 2-1 of the DCD, the “Lateral Variability” item reads:

> *Soils supporting the nuclear island should not have extreme variations in subgrade stiffness. This may be demonstrated by one of the following:*
>
> *1. Soils supporting the nuclear island are uniform in accordance with Regulatory Guide 1.132 if the geologic and stratigraphic features at depths less than 120 feet below grade can be correlated from one boring or sounding location to the next with relatively smooth variations in thicknesses or properties of the geologic units, or*
>
> *2. Site-specific assessment of subsurface conditions demonstrates that the bearing pressures below the nuclear island do not exceed 120% of those from the generic analyses of the nuclear island at a uniform site, or*
>
> *3. Site-specific analysis of the nuclear island basemat demonstrates that the site-specific demand is within the capacity of the basemat.*

The following is an evaluation in terms of both stratigraphic uniformity and bearing pressure uniformity as defined in the first and second items of Table 2-1 of the DCD.

Following the DCD criterion, the dip angles for all the layers along some predefined sections in Figure 2.5.4-209 are calculated using the layering and boring coordinates information. The calculated dip is less than 5 degrees in 95 percent of layer interfaces between adjacent borings (Figures 2.5.4-203 through 2.5.4-208). In four places, the interfaces dip between 5 and 10 degrees, at the top and bottom of the upper Tamiami layer. In one place, between borings B-718 and B-710, on Section A-A' (Figure 2.5.4-206), the interface between the upper and lower Tamiami formations dips steeper than 20 degrees due to interpretation of the interface in adjacent borings. The termination depth of B-718 is limited to 150.8 feet, and the true interface may not have been reached in this boring. The other adjacent boring B-719 is also shallow boring with a termination depth of 126.7 feet, and does not reach the interface. If B-718 and B-719 are not considered in the interpretation of this interface due to their shallow termination depths, all layer interfaces dip less than 20 degrees and satisfy the DCD dip criteria, with more than 95 percent of the layer interfaces between adjacent borings dipping less than 5 degrees.

As a result, geologic and stratigraphic features at depths less than 120 feet below grade can be correlated from one boring or sounding location to the next with relatively smooth variations in thicknesses.

To evaluate the bearing pressures for site-specific conditions, a two-dimensional plane-strain PLAXIS 2D model is developed. Both a laterally uniform subsurface model and a laterally variable subsurface model are considered in the PLAXIS simulation. For the laterally uniform case, the best estimate stiffness for soil and rock strata are assigned for each stratum. For the laterally variable case, a worst-case scenario (extremely unlikely scenario) is considered in which half of the foundation rests on the softer soil/rock column and half of the foundation rests on stiffer soil/rock column. The softer soil/rock column is assigned the lower-bound parameters (as defined in Subsection 2.5.4.2.1.3.17), whereas the stiffer soil-rock column is assigned the best estimate parameters. To avoid numerical issues with this contrast of stiffness, a transition zone is assigned between the soft and stiff zones. The stiffness of the transition zone is taken as the average of best estimate and lower-bound stiffness for each stratum. The width of the transition zone is taken as one-third, one-fifth, and one-sixteenth of B = 160 feet, where B is the shorter foundation dimension. For all cases considered, the maximum bearing

pressure difference is less than 20 percent. Therefore, the DCD criterion for lateral uniformity as cited earlier is satisfied.

2.5.4.10.8 Stability of Category I Structures Considering Postulated Voids in Subsurface

Although large voids and karst features are not considered likely at the site, as described in Appendix 2.5AA, a sensitivity analysis is performed to consider stability of Category I Structures with postulated voids in the subsurface.

As discussed in Subsection 2.5.4.4.5.5, the grouting program will be utilized to constrain void sizes. The zone between El. –35 feet and El. –60 feet within the diaphragm walls will be grouted using a multi-stage grouting program; this will ensure that potential voids in this zone are grouted. For the zone between El. –60 feet and El. –110 feet within the diaphragm walls, grouting will be conducted in every primary grout borehole, constraining the maximum undetected void size to approximately 20 feet.

The void size (20 feet) constrained by the grouting program is conservatively much larger than the estimated void sizes present on site, and is evaluated in the static (settlement and bearing capacity) and dynamic (pseudo-dynamic) analyses.

A very extreme case of a tunnel-shaped (i.e., cylindrical) void with a 20-foot diameter circular cross-section is considered where the void extends east-west across the nuclear island with the top of the void just below the grout plug (El. –60 feet). This direction is selected since the maximum dynamic bearing demand occurs under the west edge of the shield building and is primarily due to the response to the east-west component of the earthquake (DCD Subsection 2.5.4.2).

The sensitivity analysis considers extremely unlikely and conservative cases that are only assessed to show the safety margin provided by the rock mass; these cases are highly unlikely and are not for design purposes.

For the analysis, the 3D finite element model (as presented in Subsection 2.5.4.10.3.2) is updated for the void case presented above. Best estimate material properties (FD1 properties for rock layers) are used for this analysis, as described in Subsection 2.5.4.10.3.

The postulated void is assumed to be water-filled, and is therefore modeled with the same pore pressures as the surrounding rock.

The model considers a construction sequence that includes the following activities:

- Initial gravity loading (without the void),
- Gravity loading (with the void),
- Dewatering,
- Excavation and fill placement,
- Loading, and
- Rewatering.

The void is not considered in the initial gravity loading phase because it would have developed over time; further, inserting the void in the second phase allows for an evaluation of any points reaching Mohr-Coulomb failure due to the presence of the void independent from the other construction activities.

Figure 2.5.4-273 shows the PLAXIS 3D model. The 3D mesh is refined to the extent possible in the area surrounding the void. The total number of elements is 103,136.

Settlement

Vertical deformation due to loading is evaluated in the PLAXIS 3D finite element models to determine the impact of the potential void on the settlement of the nuclear island. Differential settlements are calculated and the results are compared to the DCD requirements.

Bearing Capacity

To determine the impact of the potential void on the bearing capacity, the model is incrementally loaded up to much higher loads than the actual building loads and a load displacement curve is developed. This curve is used to evaluate the bearing capacity.

Concrete Fill Properties

In order to assess potential tension in the concrete, the concrete is assumed to be a Mohr-Coulomb material in the PLAXIS 3D model with a friction angle of 0 degrees, cohesion of 108,000 psf, and tensile strength of 21,600 psf based on

Equation 2.5.4-32 (Reference 217), Equation 2.5.4-33 (Reference 325), and a compressive strength of 1500 psi. The tensile strength calculated based on Equation 2.5.4-33 is conservative compared to the tensile strength calculated according to ACI 207.1R-05 (Reference 281).

$$Cohesion = \frac{Compressive\ Strength}{2} \qquad \text{Equation 2.5.4-32}$$

$$Tensile\ Strength \approx 0.1 \times Compressive\ Strength \qquad \text{Equation 2.5.4-33}$$

Pseudo-Dynamic

To consider the impact of the potential voids under dynamic conditions, dynamic bearing pressures from the SASSI model are converted to equivalent (approximately) static loads and applied to the PLAXIS 3D model.

The forces from the dynamic bearing pressures are summed up and distributed uniformly over areas of the eastern (maximum uplift) and western (maximum compression) halves of the nuclear island. The maximum uplift bearing pressures as obtained from the upper bound, lower bound, and best estimate cases are applied on the eastern half of the nuclear island, whereas the maximum compressive bearing pressures as obtained from the upper bound, lower bound, and best estimate cases are applied on the western half of the nuclear island, such that the maximum overturning moment is applied on the western edge of the nuclear island.

This approach is very conservative because

- Nodal maximum bearing pressures are used regardless of their time step (note that maximum pressures for each node correspond to different time steps, i.e., they do not happen at the same time)

- Maximum compressive pressures and tensile pressures are applied at the same time to maximize the overturning moment

Additionally, a case is considered where the load combinations are multiplied by a safety factor of 2. Table 2.5.4-225 shows the total loads considered (static and pseudo-dynamic). The sum of the static load and the seismic uplift pressure is negative, if the overall pressure is compressive.

The bearing pressures corresponding to the combination of dead loads and the maximum moment are checked against the bearing capacity of the concrete fill. The ultimate bearing capacity for the concrete fill is estimated to be 1275 psi

(184 ksf) using Equation 2.5.4-34 (Reference 317) and a compressive strength of 1500 psi.

Ultimate Bearing Capacity = 0.85 x f'c Equation 2.5.4-34

Where,

f'c = compressive strength

Results

All model results presented are for the case with a tunnel-shaped (i.e., cylindrical) void with a 20-foot diameter circular cross-section. The tunnel-shaped (i.e., cylindrical) void is considered to be more critical than a smaller 20-foot diameter spherical void, or a distribution of spherical voids.

The static stability check is governed by the following four factors:

1. Accumulation of plastic points indicating a local (e.g., around the void) or global (e.g., bearing capacity) failure.

2. Deformations exceeding DCD limits.

3. Concrete layer experiencing tension failure.

4. Bearing capacity with FOS <3.

Yield at any point is considered to occur if the stress state reaches the Mohr-Coulomb failure envelope. As shown in Figure 2.5.4-274, there are no plastic points or tension cut-off points near the void location, indicating that the rock mass surrounding the void is not experiencing compressive failure according to Mohr-Coulomb failure envelope or points where the tensile load exceeds the tensile capacity. No tension cut-off points are identified within the concrete fill, i.e., the tension in the concrete fill is less than the tensile capacity of the concrete fill.

Another useful parameter to consider is the relative shear stress, which is a measure to define how close the stress state is to the Mohr-Coulomb failure envelope. Relative shear stresses are defined in Equation 2.5.4-35 (Reference 326).

$$\tau_{rel} = \frac{\tau_{mob}}{\tau_{max}}$$ Equation 2.5.4-35

Where,

τ_{rel} = relative shear stress,
τ_{mob} = mobilized shear strength (maximum value of shear stress), and
τ_{max} = maximum value of shear stress for the case where the Mohr's circle is expanded to touch the Coulomb failure envelope while keeping the center of Mohr's circle constant.

Based on Equation 2.5.4-35, relative shear stresses provide a measure of margin compared to Mohr-Coulomb failure. For example, if the relative shear stress is equal to 1, then that location is marked with a plastic point. If the relative shear stress is much less than 1, the point is not close to the Mohr-Coulomb failure envelope. As shown by Figure 2.5.4-275, the rock surrounding the void indicates relative shear stresses much less than 1.

In conclusion, the presence of a 20-foot wide tunnel as modeled here does not present stability concerns, i.e., no subsurface collapse is anticipated.

The total and differential settlements from the PLAXIS 3D model indicate that the presence of the void has no impact on settlement, and that the DCD criteria are still met. The total vertical deformation (loading nuclear island phase) from the PLAXIS 3D model is shown in Figure 2.5.4-276. Therefore the void cases considered are not critical to the settlement of safety-related structures.

To evaluate bearing capacity, the nuclear island load was incrementally increased and a load displacement curve was developed, as shown in Figure 2.5.4-277. Figure 2.5.4-277 also shows ultimate static and dynamic bearing capacities required by the DCD for factors of safety of 3 and 2, respectively. The required ultimate static and dynamic bearing capacities from the DCD are within the linear elastic range of the load displacement curve. Actual bearing capacity as defined by the load-displacement curve shown in Figure 2.5.4-277 is much higher than DCD limits. The load-displacement curve indicates that the significant reduction in stiffness, which can be defined as the ultimate bearing capacity, does not occur for loads up to 250 ksf, i.e., the actual bearing capacity according to Figure 2.5.4-277 is higher than 250 ksf.

As indicated by the results discussed above and shown in Figures 2.5.4-274 through 2.5.4-277,

- No plastic points or tension cut-off points are observed during the loading phase (1x bearing demand),
- The factor of safety for bearing capacity is greater than 3,
- The DCD criteria for settlement are met, and
- The tensile capacity of the concrete fill is not reached.

In summary, the void size constrained by the grouting program has been demonstrated to not be critical to the static stability of safety-related structures.

Response under Dynamic Loads

Under pseudo-dynamic loading (multiplier of 1 and multiplier of 2) there are no plastic points or tension cut-off points near the void location, indicating that the rock mass surrounding the void is not experiencing compressive failure according to Mohr-Coulomb failure envelope or points where the tensile load exceeds the tensile capacity. No tension cut-off points are identified in the concrete fill.

Effective vertical stresses for pseudo-dynamic loading (multiplier of 1) are shown for the concrete fill in Figure 2.5.4-278. Effective vertical stresses for pseudo-dynamic loading (multiplier of 2) are shown for the concrete fill in Figure 2.5.4-279. For both cases, the maximum compressive stresses are provided in Table 2.5.4-226 and are much less than the ultimate bearing capacity of the concrete. The maximum compressive stresses provided in Table 2.5.4-226 conservatively represent local maximums for one element and one node only; these stresses are not averaged over multiple elements to distribute the stresses.

As indicated by the results described above and shown in Figures 2.5.4-278 and 2.5.4-279 and in Table 2.5.4-226:

- No plastic points or tension cut-off points are observed during the pseudo-dynamic loading conditions,
- The effective vertical compressive stresses are smaller than the ultimate bearing capacity of the concrete, and
- The tensile capacity of the concrete fill is not reached.

In summary, the void size constrained by the grouting program has been demonstrated to not be critical to the pseudo-dynamic stability of safety-related structures. In other words, subsurface collapse is not anticipated under the combination of seismic and static nuclear island loads.

2.5.4.11 Design Criteria and References

PTN COL 2.5-3

The design criteria summarized below are geotechnical design criteria and/or geotechnical-related design criteria that pertain to structural design. Refer to the respective subsections above for additional details.

Under “Factor of Safety Against Liquefaction,” RG 1.198 indicates that FOS < 1.10 is generally considered a trigger value. The FOS = 1.25 selected for the analysis of site soils is considered appropriate and conservative, especially when also considering the conservatism employed in ignoring the rock overburden, the depth, and the geologic age of the deposits.

Subsection 2.5.4.10 describes allowable bearing capacities and estimated settlement values for plant structures, and compares them to threshold values published in the DCD.

Table 2.5.4-217 contains calculated allowable bearing capacities, both static and dynamic, for Units 6 & 7 Seismic Category I structures. In the case of static bearing capacity, a minimum FOS = 3.0 is used to evaluate allowable static bearing capacity of a structure. For the Units 6 & 7 Category I structures, the computed allowable bearing capacity (including FOS = 3.0) of 39 ksf exceeds the DCD maximum static loading of 8.9 ksf. In the case of dynamic bearing capacity, an FOS = 2.0 is applied against the calculated ultimate bearing capacity in evaluating the required allowable dynamic bearing capacity of a structure (i.e., the calculated allowable bearing capacity of subsurface materials for normal loads plus the SSE as per the DCD). (Because the SSE in the DCD has a 0.3g peak ground acceleration that is much higher than that anticipated for South Florida, the dynamic bearing capacity in the DCD is substantially higher than the maximum dynamic loading that would be realized at the site). For the Units 6 & 7 Category I structures, the computed allowable bearing capacity (including FOS = 2.0) of 41 ksf exceeds the DCD maximum dynamic loading of 35 ksf.

Table 2.5.4-219 contains estimated settlements of Units 6 & 7 Seismic Category I structures and other structures under design foundation loads. The calculated total settlements are less than the threshold described in Table 2.5-1 of the DCD.

Subsection 2.5.4.10 also addresses criteria for static and seismic earth pressure estimation. The calculated lateral earth pressure diagrams shown on Figures 2.5.4-239, 2.5.4-240, 2.5.4-252, and 2.5.4-253 are best estimates, and thus contain an FOS = 1.0. In the analyses of sliding and overturning due to these lateral loads when the seismic component is included, an FOS = 1.10 is recommended.

PTN COL 2.5-7

2.5.4.12 Techniques to Improve Subsurface Conditions

Given the depths of structure foundations and the subsurface conditions that occur at those depths, as shown in part on Figures 2.5.4-221 and 2.5.4-222, special ground improvement measures are not warranted. Ground treatment is limited to over-excavation of unsuitable materials, such as zones of less competent materials occurring at foundation subgrades, and their replacement with lean concrete fill. Groundwater control is required as part of this over-excavation as described in Subsections 2.5.4.5 and 2.5.4.6.

Over-excavation of approximately 21 feet at the reactor/auxiliary building is designed to replace soils and weak rock that are not adequate to directly support the high foundation loads of these structures, with the required FOS. For all affected structures, compacted limerock fill and lean concrete fill are placed according to engineering specifications and quality control/quality assurance testing procedures established during detailed design phase.

According to ACI 207 (Reference 281), the lean concrete fill under the nuclear island is defined as mass concrete. A thermal control plan considering the geometry of the fill concrete, the proposed 1,500 psi strength, total volume of fill concrete placement, and rate of concrete production, will be prepared to minimize thermal cracking in accordance with ACI 207 guidelines.

Across the entire plant area, the muck of Stratum 1 is removed and replaced with compacted limerock fill as described in Subsection 2.5.4.5.1.1.

2.5.4.13 References

201. Not Used.

202. Sinclair, W., and J. Stewart, *Sinkhole Type, Development, and Distribution in Florida*, U.S. Geological Survey, Map Series No. 110, 1985.

203. Lane, E., *Karst in Florida*, Special Publication 29, Florida Geological Survey, 1986.

204. Renken, R., J. Dixon, J. Koehmstedt, S. Ishman, A. Lietz, R. Marella, P. Telis, J. Rogers, and S. Memberg, *Impact of Anthropogenic Development on Coastal Ground-Water Hydrology in Southeastern Florida, 1900–2000*, U.S. Geological Survey, Circular 1275, 2005.

205. Vanlier, K., J. Armbruster, Z. Altschuler, and H. Mattraw, *Natural Hazards in Resource and Land Information for South Dade County*, U.S. Geological Survey, Florida Geological Survey Investigation I-850, 1973.

206. Parker, G., G. Ferguson, S. Love, et al., *Water Resources of Southeastern Florida,* U.S. Geological Survey, Water Supply Paper 1255, 1955.

207. Cunningham, K., J. Carlson, G. Wingard, E. Robinson, and M. Wacker, *Characterization of Aquifer Heterogeneity Using Cyclostratigraphy and Geophysical Methods in the Upper Part of the Karstic Biscayne Aquifer, Southeastern Florida*, U.S. Geological Survey, Water-Resources Investigations Report 2003-4208, 2004.

208. Lane, E., Florida's *Geological History and Geological Resources*, Florida Geological Survey, Special Publication 35, 1994.

209. Arthur, J., *Petrogenesis of Early Mesozoic Tholeiite in the Florida Basement and an Overview of Florida Basement Geology*, Florida Geological Survey, Report of Investigations 97, 1988.

210. Salvador, A., *Origin and Development of the Gulf of Mexico Basin*, The Geology of North America, Vol. J, The Gulf of Mexico Basin, Geological Society of America, 1991.

211. Reese, R. and E. Richardson, *Synthesis of the Hydrogeologic Framework of the Floridan Aquifer System and Delineation of a Major Avon Park Permeable Zone in Central and Southern Florida*, U.S. Geological Survey, Scientific Investigations Report 2007-5207, 2008.

212. Pollastro, R., *1995 USGS National Oil and Gas Play-Based Assessment of the South Florida Basin, Florida Peninsula Province,* National

Assessment of Oil and Gas Project: Petroleum Systems and Assessment of the South Florida Basin, U.S. Geological Survey, Digital Data Series 69-A, 2001.

213. ASTM International, *Standard Practice for Classification of Soils for Engineering Purposes (Unified Soil Classification System),* ASTM D 2487-06, Conshohocken, Pennsylvania, 2006.

214. ASTM International, *Standard Practice for Description and Identification of Soils (Visual-Manual Procedure),* ASTM D 2488-06 Conshohocken, Pennsylvania, 2006.

215. Dunham, R., *Classification of Carbonate Rocks According to Depositional Texture, Classification of Carbonate Rocks: A Symposium,* American Association of Petroleum Geologists, AAPG Memoir 1, 1962.

216. U.S. Department of the Interior Bureau of Reclamation, *Engineering Geology Field Manual*, 2001.

217. Bowles, J., *Foundation Analysis and Design*, 5th ed., McGraw-Hill Companies Inc., New York, 1996.

218. Schlumberger, *Poisson's Ratio, Oilfield Glossary.* Available at http://www.glossary.oilfield.slb.com/Display.cfm?Term=Poisson%27s%20ratio, accessed July 28, 2008.

219. Youd, T. et al., *Liquefaction Resistance of Soils: Summary Report from the 1996 National Center for Earthquake Engineering Research (NCEER) and 1998 NCEER/National Science Foundation (NSF) Workshops on Evaluation of Liquefaction of Soils,* ASCE Journal of Geotechnical and Environmental Engineering, Vol. 127, No. 10, American Society of Civil Engineers, October 2001.

220. ASTM International, *Standard Practice for Determining the Normalized Penetration Resistance of Sands for Evaluation of Liquefaction Potential*, ASTM D 6066-96, Conshohocken, Pennsylvania, 2004.

221. Winterkorn, H. and H. Fang, *Soil Technology and Engineering Properties of Soils,* Foundation Engineering Handbook, Van Nostrand Reinhold Co., New York, 1975.

222. Robertson, P. and R. Campanella, *Interpretation of Cone Penetration Tests: Part I Sands,* Canadian Geotechnical Journal, Vol. 20(4), pp. 718–733, 1983.

223. Naval Facilities Engineering Command, *Foundations & Earth Structures*, Design Manual 7.02, Alexandria, Virginia, 1986.

224. Not Used.

225. Coduto, D., *Foundation Design Principles and Practices*, 2d ed., Prentice Hall, New Jersey, 2001.

226. Senapathy, H., J. Clemente, and J. Davie, *Estimating Dynamic Shear Modulus in Cohesive Soils*, XVth International Conference on Soil Mechanics and Geotechnical Engineering, Istanbul, Turkey, 2001.

227. American Petroleum Institute, *Cathodic Protection of Aboveground Petroleum Storage Tanks*, API Recommended Practice 651, 3d ed., Washington, D.C., 2007.

228. STS Consultants Inc., *Reinforced Soil Structures*, Vol. 1, Design and Construction Guidelines, FHWA Report No. FHWA-RD-89-043, McLean, Virginia., 1990.

229. Federal Highway Administration, *Corrosion/Degradation of Soil Reinforcements for Mechanically Stabilized Earth Walls and Reinforced Soil Slopes*, FHWA Publication FHWA-NHI-00-044, 2000.

230. American Concrete Institute, *Manual of Concrete Practice, Part 1, Materials and General Properties of Concrete*, Detroit, Michigan, 1994.

231. Florida Power & Light Company, *Updated Final Safety Analysis Report, Turkey Point Nuclear Units 3 & 4,* Miami-Dade County, Florida, Docket Nos. 50-250 and 50-251, 1992.

232. ASTM International, *Standard Practice for Rock Core Drilling and Sampling for Site Investigation*, ASTM D 2113-08, Conshohocken, Pennsylvania, 2005.

233. ASTM International, *Standard Practice for Thin-Walled Tube Sampling of Undisturbed Soils for Geotechnical Purposes*, ASTM D 1587, Conshohocken, Pennsylvania, 2008.

234. ASTM International, *Standard Practices for Preserving and Transporting Soil Samples,* ASTM D 4220-95, Conshohocken, Pennsylvania, 2007.

235. ASTM International, *Standard Test Method for Energy Measurement for Dynamic Penetrometers*, ASTM D 4633-05, Conshohocken, Pennsylvania, 2005.

236. ASTM International, *Standard Practices for Preparing Rock Core as Cylindrical Test Specimens and Verifying Conformance to Dimensional and Shape Tolerances*, ASTM D 4543-08, Conshohocken, Pennsylvania, 2008.

237. ASTM International, *Standard Test Methods Laboratory Determination of Water (Moisture) Content of Soil and Rock by Mass*, ASTM D 2216-05, Conshohocken, Pennsylvania, 2005.

238. ASTM International, *Standard Test Methods Specific Gravity of Soil Solids by Water Pycnometer*, ASTM D 854-06, Conshohocken, Pennsylvania, 2006.

239. ASTM International, *Standard Test Method for Particle-Size Analysis of Soils*, ASTM D 422-63, for Analysis Including Hydrometer, Conshohocken, Pennsylvania, 2007.

240. ASTM International, *Standard Test Methods for Particle-Size Distribution (Gradation) of Soils Using Seive Analysis,* ASTM D 6913-04, for analysis not including hydrometer, Conshohocken, Pennsylvania, 2004.

241. ASTM International, *Standard Test Methods for Liquid Limit, Plastic Limit, and Plasticity Index of Soils,* ASTM D 4318-05, Conshohocken, Pennsylvania, 2005.

242. ASTM International, *Standard Test Methods for Moisture, Ash, and Organic Matter of Peat and Other Organic Soils,* ASTM D 2974-07a, Conshohocken, Pennsylvania, 2007.

243. ASTM International, *Standard Test Methods for Measurement of Hydraulic Conductivity of Saturated Porous Materials Using a Flexible Wall Permeameter,* ASTM D 5084-03, Conshohocken, Pennsylvania, 2003.

244. ASTM International, *Standard Test Method for Rapid Determination of Carbonate Content of Soils*, ASTM D 4373-02, Conshohocken, Pennsylvania, 2007.

245. ASTM International, *Standard Test Methods for Laboratory Compaction Characteristics of Soil Using Modified Effort*, ASTM D 1557-07, Conshohocken, Pennsylvania, 2007.

246. ASTM International, *Standard Test Method for CBR (California Bearing Ratio) of Laboratory-Compacted Soils*, ASTM D 1883-07, Conshohocken, Pennsylvania, 2007.

247. Florida Department of Transportation, *Florida Method of Test for Limerock Bearing Ratio*, FDOT FM-5-515, 2000.

248. ASTM International, *Standard Test Method for Compressive Strength and Elastic Moduli of Intact Rock Core Specimens Under Varying States of Stress and Temperatures*, ASTM D 7012-07, Conshohocken, Pennsylvania, 2007.

249. ASTM International, *Standard Test Method for Consolidated Undrained Triaxial Compression Test for Cohesive Soils*, ASTM D 4767-04, Conshohocken, Pennsylvania, 2004.

250. U.S. Environmental Protection Agency, *Soil and Waste pH,* Method SW 846 9045D, last updated September 17, 2008.

251. U.S. Environmental Protection Agency, *Methods for Chemical Analysis of Water and Wastes,* EPA-600/4-79-020, March 1983 and subsequent revisions.

252. ASTM International, *Standard Guide for Conducting Borehole Geophysical Logging — Gamma*, ASTM D6274-98(04), Conshohocken, Pennsylvania, reapproved 2004.

253. ASTM International, *Standard Guide for Conducting Borehole Geophysical Logging in Mechanical Caliper*, ASTM D 6167-97(04), Conshohocken, Pennsylvania, 2004.

254. ASTM International, *Standard Guide for Planning and Conducting Borehole Geophysical Logging,* ASTM D 5753-05, Conshohocken, Pennsylvania, 2005.

255. ASTM International, Standard Guide for Using the Seismic Refraction Method for Subsurface Investigation, ASTM D 5777-00, Conshohocken, Pennsylvania, 2000.

256. Occupational Safety and Health Administration, *Safety and Health Regulations for Construction*, 29 CFR Part 1926, 2000.

257. MACTEC Engineering and Consulting, Inc., *Final Data Report—Geotechnical Exploration and Testing: Turkey Point COL Project Florida City, Florida,* Rev. 2, included in COL Application Part 11, October 6, 2008.

258. Electric Power Research Institute, *Guidelines for Determining Design Basis Ground Motions*, Vol. 1-5, EPRI Report TR-102293, Palo Alto, California, 1993.

259. Sun, J., R. Golesorkhi, and H. Seed, *Dynamic Moduli and Damping Ratios for Cohesive Soils*, Earthquake Engineering Research Center, Report 88/15, University of California, Berkeley, 1988.

260. Seed, H., R. Wong, I. Idriss, and K. Tokimatsu, *Moduli and Damping Factors for Dynamic Analyses of Cohesionless Soils,* Earthquake Engineering Research Center, Report EERC 84/14, University of California, Berkeley, 1984.

261. Youd, T. and D. Perkins, *Mapping Liquefaction-Induced Ground Failure Potential*, ASCE Journal of the Geotechnical Engineering Division, Vol. 104, No. GT4, 1978.

262. Amick, D., G. Maurath, and R. Gelinas, *Characteristics of Seismically Induced Liquefaction Sites and Features Located in the Vicinity of the 1886 Charleston, South Carolina Earthquake*, Seismological Research Letters, Vol. 61, No. 2, pp. 117–130, 1990.

263. Palmer, S., S. Magsino, E. Bilderback, J. Poelstra, D. Folger, and R. Niggemann, *Liquefaction Susceptibility and Site Class Maps of Washington State, by County,* Open-File Report 2004-20, Washington Division of Geology and Earth Resources, September 2004.

264. Rauch, A., *EPOLLS: An Empirical Method for Predicting Surface Displacements Due to Liquefaction-Induced Lateral Spreading in*

Earthquakes, doctoral dissertation, Virginia Polytechnic Institute and State University, May 5, 1997.

265. California Geological Survey, *Guidelines for Evaluating and Mitigating Seismic Hazards in California*, Special Publication 117, updated 2008.

266. Sykora, D. and D. Yule, *Reassessment of Liquefaction Potential and Estimation of Earthquake-Induced Settlements at Paducah Gaseous Diffusion Plant, Paducah, Kentucky,* U.S. Army Corps of Engineers, April 1996.

267. Amick, D., R. Gelinas, G. Maurath, R. Cannon, D. Moore, E. Billington, and H. Kemppinen, *Paleoliquefaction Features Along the Atlantic Seaboard*, U.S. NRC Report NUREG/CR-5613, 1990.

268. Not Used.

269. Lewis, M. I. Arango, and M. McHood, *Site Characterization Philosophy and Liquefaction Evaluation of Aged Sands — A Savannah River Site and Bechtel Perspective,* J. Laier, D. Crapps, and H. Mohamad (eds.) From Research to Practice in Geotechnical Engineering, ASCE Geotechnical Special Publication 180, 2008.

270. Southern California Earthquake Center of University of Southern California, *Recommended Procedures for Implementation of DMG Special Publication 117,* Guidelines for Analyzing and Mitigating Liquefaction Hazards in California, 1999.

271. Ishihara, K., *Stability of Natural Deposits During Earthquakes,* Proceedings, 11th International Conference on Soil Mechanics and Foundation Engineering, Vol. 1, Balkema, Rotterdam, The Netherlands, pp. 321–376, 1985.

272. Wyllie, D., *Foundations on Rock*, 2d ed., E&FN SPON, New York, 1999.

273. American Concrete Institute, *Code Requirements for Nuclear Safety-Related Concrete Structures* (ACI 349-06) and Commentary, Detroit, Michigan, 2006.

274. American Association of State Highway and Transportation Officials, *LRFD Bridge Design Specification*, 2d ed., Washington, D.C., 1998.

275. Poulos, H. and E. Davis, *Elastic Solutions for Soil and Rock Mechanics*, John Wiley & Sons, New York, 1974.

276. Seed, H. and R. Whitman, *Design of Earth Retaining Structures for Dynamic Loads, Proceeding of the Specialty Conference on Lateral Stresses in the Ground and Design of Earth-Retaining Structures,* American Society of Civil Engineers, New York, 1970.

277. American Society of Civil Engineers, *Seismic Analysis of Safety-Related Nuclear Structures and Commentary*, Standard 4-98, ASCE, Reston, Virginia, 1998.

278. Telford, W. L. Geldart, R. Sheriff, and D. Keys, *Applied Geophysics*, Cambridge University Press, 1976.

279. Not Used.

280. Not Used.

281. American Concrete Institute, *Guide to Mass Concrete* (ACI 207), Detroit, Michigan, 2006.

282. Kulhawy, F. and P. Mayne, *Manual on Estimating Soil Properties for Foundation Design*, Report No. EL-6800, EPRI, August 1990.

283. Not Used.

284. Not Used.

285. Not Used.

286. Technos, Inc., *Geophysical Survey for Karst Characterization at Proposed Units 6 and 7 Turkey Point Nuclear Plant, Miami-Dade County, Florida,* prepared for MACTEC Engineering and Consulting, Inc., Project No. 08-148, March 27, 2009.

287. McNabb Hydrogeologic Consulting, Inc., *Report on the Construction and Testing of Class V Exploratory Well EW-1 at the Florida Power & Light Company Turkey Point Units 6 & 7*, Vol. 1, in Turkey Point Units 6 & 7 Site Certification Application Amendment Rev. 2, September 2012. Available at http://publicfiles.dep.state.fl.us/Siting/Outgoing/FPL_Turkey_

Point/Units_6_7/Amendment_Application_Rev2/08_APPENDIX%2010.2.8.pdf, accessed January 10, 2013.

288. South Carolina Electric & Gas Company, *Final Safety Analysis Report*, V.C. Summer Nuclear Units 2 & 3, Figure 2.5.4-224, Docket Nos. 52-027 and 52-028, South Carolina, August 17, 2011.

289. Tennessee Valley Authority, *Final Safety Analysis Report, Bellefonte Nuclear Units 3 & 4*, Figure 2.5.4-331, Docket Nos. 52-014 and 52-015, Alabama, January 21, 2009.

290. Paul C. Rizzo Associates, Inc., *Supplemental Field Investigation Data Report*, Turkey Point Nuclear Power Plant Units 6 & 7, Rev. 2, Pittsburgh, Pennsylvania, included in COL Application Part 11, April 15, 2014.

291. Paul C. Rizzo Associates, Inc., *Surficial Muck Deposits Field and Laboratory Investigation Data Report*, Turkey Point Nuclear Power Plant Units 6 & 7, Rev. 1, Pittsburgh, Pennsylvania, included in COL Application Part 11, April 3, 2014.

292. Kulhawy, F.H., and P.W. Mayne, *Manual on Estimating Soil Properties for Foundation Design,* Electric Power Research Institute, Palo Alto, California, August 1990.

293. Mayne, P.W., *Cone Penetration Testing,* A Synthesis of Highway Practice, Transportation Research Board, 2007.

294. Not Used.

295. ASTM International, S*tandard Test Methods for One-Dimensional Consolidation Properties of Soils Using Incremental Loading*, ASTM D 2435/ D 2435 M-11, West Conshohocken, Pennsylvania, 2011.

296. ASTM International, *Standard Test Methods for Laboratory Determination of Density (Unit Weight) of Soil Specimens*, ASTM D 7263-09, West Conshohocken, PA, 2009.

297. ASTM International, *Standard Test Method for pH of Soils*, ASTM D 4972-01(2007), West Conshohocken, Pennsylvania, 2007.

298. AASHTO, *Standard Method of Test for Determining Water-Soluble Sulfate Ion Content of Soil*, AASHTO T-290-95, American Association of State Highway and Transportation Officials, Washington, DC, 2003.

299. AASHTO, *Standard Method of Test for Determining Water-Soluble Chloride Ion Content of Soil*, AASHTO T-291-94, American Association of State Highway and Transportation Officials, Washington, DC, 2004.

300. ASTM International, *Standard Test Method for Density of Soil in Place by the Drive-Cylinder Method*, ASTM D2937-10, West Conshohocken, Pennsylvania, 2010.

301. Naval Facilities Engineering Command, *Soil Mechanics*, Design Manual 7.01, Alexandria, Virginia, 1986.

302. ASTM International, *Standard Test Method for Standard Penetration Test (SPT) and Split-Barrel Sampling of Soils*, ASTM Standard D1586-11, DOI: 10.1520/D 1586 11, ASTM International, West Conshohocken, Pennsylvania, 2011.

303. U.S. Army Corps of Engineers, *Rock Foundations*, Engineering Manual EM 1110-1-2908, 1994.

304. Hoek, E. and M.S. Diederichs, *Empirical Estimation of Rock Mass Modulus*, International Journal of Rock Mechanics & Mining Sciences, Vol. 43, pp. 203−215, 2006.

305. Hoek, E., C. Carranza-Torres, and B. Corkum, *Generalized Hoek-Brown Failure Criterion - 2002 Edition*, 5th North American Rock Mechanics, 2002.

306. Nicholson, G.A. and Z.T. Bieniawski, *A Nonlinear Deformation Modulus Based on Rock Mass Classification*, International Journal of Mining and Geological Engineering, Vol. 8, pp. 189−190, 1990.

307. Sonmez H., C Gokceoglu, H.A. Nefeslioglu, and A. Kayabasi, *Estimation of Rock Modulus: For Intact Rocks with an Artificial Neural Network and for Rock Masses with a New Empirical Equation*, International Journal of Rock Mechanics and Mining Science, Vol. 43, p. 231, 2006.

308. Bieniawski, Z.T., *Determining Rock Mass Deformability: Experience from Case Histories*, Int. J. Rock Mech. Min. Sci & Geomech., Vol.15, pp 237-247, 1978.

309. Hunt, R. E., *Geotechnical Engineering Investigation Handbook*, 2nd Edition, Taylor & Francis Group, pp. 234−235, Florida, 2005.

310. Robertson, P.K., *Interpretation of Core Penetration Tests, A Unified Approach*, Canadian Geotechnical Journal, 2009.

311. Wood, D.M., *Geotechnical Modeling*, Ver. 2.2, Spon Press, New York, New York, 2004.

312. Mair, R.J. and D. Wood, *Pressuremeter Testing: Methods and Interpretation*, CIRIA Ground Engineering Report: In-situ Testing, 1987.

313. U.S. Army Corps of Engineers, NUREG/CR-5741, *Technical Bases for Regulatory Guide for Soil Liquefaction,* March 2000.

314. Carter, J.P. and Kulhawy, F.H., *Analysis and Design of Drilled Shaft Foundations Socketed into Rock*, Report EL-5918, Electric Power Research Institute, Palo Alto, California, 1988.

315. Soubra, A. H., *Upper-Bound Solutions for Bearing Capacity of Foundations*, J. Geotechnical and Geoenvironmental Engineering, Vol. 125, No. 1, January 1999.

316. Milovic, D., *Stresses and Displacements for Shallow Foundations*, Elsevier, 1992.

317. American Concrete Institute, *Building Code Requirements for Structural Concrete and Commentary*, ACI 318-11, 2011.

318. Ang, A.H-S., W.H. Tang, *Probability Concepts in Engineering: Emphasis on Applications to Civil and environmental Engineering*, 2d Ed., John Wiley & Sons Inc., New Jersey, 2007.

319. Hoek, E. and E.T. Brown, *The Hoek-Brown Failure Criterion–a 1988 Update*, Proceedings of the 15th Canadian Rock Mechanics Symposium, Toronto, 1988.

320. Spotlight Geophysical Services, *Microgravity Modeling and MASW Re-Contouring in Vegetated Surface Depressions FPL Turkey Point Nuclear Power Plant Units 6 and 7, Miami-Dade County, Florida*, for AMEC Environment & Infrastructure Durham, North Carolina, Supplemental Report, Rev. 0, SGS Project No.: 2014230, AMEC Project No.: 6468-07-1950, 21 p., April 9, 2014.

321. Saxena, S.K., *Geotechnical Properties of Calcareous Rocks of Southern Florida*, K.R. Demars and R.C. Chaney (eds.), Geotechnical Properties, Behavior, and Performance of Calcareous Soils, ASTM STP 777, pp. 340–358, 1982.

322. American Society of Civil Engineers/Structural Engineering Institute, ASCE/SEI 7-10, *Minimum Design Loads for Buildings and Other Structures*, 2010.

323. American Concrete Institute, *Guide to Durable Concrete* (ACI 201.2R-08), 2008.

324. American Concrete Institute, *Guide for Concrete Plant Inspection and Testing of Ready-Mixed Concrete* (ACI 311.5-04), 2004.

325. McCormac, J. and J. Nelson, *Design of Reinforced Concrete*, Seventh Edition, John Wiley & Sons, Inc., 2006.

326. Brinkgreve, R.B.J. and W.M. Swolfs, *PLAXIS 3D Foundation Version 2 Part 2*: *Reference Manual*, PLAXIS bv, 2007.

327. U.S. Army Corps of Engineers, *Grouting Technology*, Engineer Manual 1110-2-3506, January 1984.

PTN COL 2.5-1
PTN COL 2.5-5
PTN COL 2.5-6
PTN COL 2.5-10

Table 2.5.4-201
Summary of Layer Thicknesses

Stratum		Top Elevation (ft)			Layer Thickness (ft)		
		Minimum	Maximum	Average	Minimum	Maximum	Average
1	Muck/Peat	–3.2	0.2	–1.1	2.0	11.0	3.6
2	Miami Limestone	–12.2	–3.3	–4.7	13.0	30.0	22.3
3	Key Largo Limestone	–35.3	–23.1	–26.9	14.6	26.9	22.5
4	Fort Thompson Formation	–54.3	–44.1	–49.4	51.3	77.0	65.9
5	Upper Tamiami Formation	–124.7	–101.6	–115.4	20.0	81.0	51.2
6	Lower Tamiami Formation	–196.3	–136.2	–167.6	27.0	62.3	43.7
7	Peace River Formation	–223.4	–206.1	–217.8	235.5	250.0	241.7
8	Arcadia Formation	–458.0	–450.3	–454.8	—	—	—

Data from References 257, 290, and 291.

PTN COL 2.5-6

Table 2.5.4-202
Summary of Uncorrected N-Values

Stratum	Muck	Miami Limestone	Key Largo Limestone	Fort Thompson Formation	Upper Tamiami Formation	Lower Tamiami Formation	Peace River Formation	Arcadia Formation
Number of Tests	142	587	107	41	268	77	116	3
Minimum N	0	0	1	0	0	2	13	76
Maximum N	29	100	100	100	100	100	100	100
Average N[(a)]	4	27	64	49	18	17	70	92

(a) Averaged to nearest whole number

Data from References 257 and 290.

PTN COL 2.5-6

Table 2.5.4-203
SPT Hammer Efficiency Corrections

Drill Rig	Rods	Number of Measurements	Min. ETR[a] (%)	Max. ETR (%)	Avg. ETR (%)	C_ε (Avg. ETR%/60%)
MACTEC Atlanta CME 55LC (Hammer Serial No. MEC-02)	AW-J	3	81.7	86.6	83.7	1.40
MACTEC Atlanta CME 550 Marsh Buggy (Hammer Serial No. 893)	AW-J	8	84.6	94.0	88.0	1.47
MACTEC Atlanta CME 550 ATV (Hammer Serial No. MEC-03)	AW-J	3	77.1	82.3	79.6	1.33
MACTEC Atlanta CME 550 ATV (Hammer Serial No. MEC-04)	AW-J	4	79.4	83.1	80.4	1.34
MACTEC Atlanta 550 Track Rig (Hammer Serial No. MEC-05)[b]	AW-J NW-J	6	80.0	88.0	83.6	1.39
Miller Drilling CME 550 ATV (Hammer Serial No. M06)	AW-J	4	81.1	84.9	83.6	1.39
Miller Drilling CME 750 ATV (Hammer Serial No. 07)[c]	AW-J NW-J	9	79.7	89.4	83.4	1.45
MACTEC Charlotte CME 75 (Hammer Serial No. MEC-09)	NW-J	3	77.1	84.3	82.8	1.38
MACTEC Atlanta (Raleigh) CME 45C (Hammer Serial No. MEC-12)	AW-J	6	79.4	89.7	83.2	1.39
Failing 1500 (Hammer Serial No. 85133	NW-J	5	59.2	65.4	62.1	1.04

(a) ETR = energy transfer ratio = the percent of measured SPT hammer energy versus the theoretical SPT hammer energy (350 ft-pounds).
(b) Both AW-J and NW-J rods were used with this rig. The average for the AW-J rods was 82.2 percent. The average for the NW-J rods was 86.3 percent.
(c) Both AW-J and NW-J rods were used with this rig. The average for the AW-J rods was 81.8 percent. The average for the NW-J rods was 88.9 percent.

PTN COL 2.5-6

Table 2.5.4-204
Summary of Corrected N-Values (N_{60})

Stratum	Muck	Miami Limestone	Key Largo Limestone	Fort Thompson Formation	Upper Tamiami Formation	Lower Tamiami Formation	Peace River Formation	Arcadia Formation
Number of Tests	142	587	107	41	268	77	116	3
Minimum N	0	0	2	0	0	3	21	94
Maximum N	35	100	100	100	100	100	100	100
Average N[(a)]	4	30	72	58	27	24	79	98

(a) Averaged to nearest whole number

Data from References 257 and 290.

PTN COL 2.5-6

Table 2.5.4-205 (Sheet 1 of 2)
Summary of General Physical and Chemical Properties Test Results

Layer	Statistical Parameters	Sieve Analysis					Atterberg Limits			w (%)	Dry Unit Weight γ (pcf)	Bulk Unit Weight γ (pcf)	Specific Gravity	Ash Content (%)	Organic Matter (%)	Chemical Tests		
		Gravel (%)	Sand (%)	Fines (%)	Silt (%)	Clay (%)	LL	PL	PI							pH	Chloride (mg/kg)	Sulfate Content (mg/kg)
Muck/Peat	minimum	0	3	12	—	—	78	55	0	171	9.4	65.5	1.73	42	3	7.40	8830	1190
	maximum	42	71	97	—	—	93	67	28	592	30.0	81.1	2.73	97	58	8.30	70400	7590
	mean	5	38	58	—	—	87	62	9	381	19.7	73.3	2.21	75	25	7.85	39615	4390
	number of samples	17	17	17	—	—	4	4	11	2	2	2	15	14	14	2	2	2
Miami Limestone	minimum	0	18	1	6	6	—	—	—	—	—	—	2.73	—	—	8.40	3250	334
	maximum	71	92	49	23	26	—	—	—	—	—	—	2.73	—	—	8.90	6790	953
	mean	39	43	18	11	12	—	—	—	—	—	—	2.73	—	—	8.65	5130	655
	number of samples	60	60	60	7	7	—	—	—	—	—	—	2	—	—	4	4	4
Key Largo Limestone	minimum	14	24	9	—	—	—	—	—	3	103.9	114.9	2.65	—	—	8.70	1960	252
	maximum	59	69	40	—	—	—	—	—	21	151.4	156.4	2.65	—	—	8.86	3111	461
	mean	38	44	18	—	—	—	—	—	10	125.1	137.1	2.65	—	—	8.77	2673	319
	number of samples	6	6	6	—	—	—	—	—	34	34	34	1	—	—	5	5	5
Fort Thompson	minimum	0	70	30	—	—	—	—	—	3	94.1	109.7	2.68	—	—	8.24	1833	198
	maximum	0	70	30	—	—	—	—	—	23	148.7	153.2	2.68	—	—	8.98	3404	457
	mean	0	70	30	—	—	—	—	—	11	124.5	137.0	2.68	—	—	8.70	2268	342
	number of samples	1	1	1	—	—	—	—	—	57	57	57	1	—	—	4	4	4
Upper Tamiami Formation	minimum	0	31	8	2	5	18	14	0	20	89.5	116.1	2.63	—	—	8.30	4290	560
	maximum	57	92	64	56	15	26	24	5	33	106.3	127.9	2.67	—	—	8.70	7020	1180
	mean	6	65	29	19	10	23	21	1	29	93.9	119.3	2.65	—	—	8.41	5400	941
	number of samples	75	75	75	38	38	5	5	9	6	5	5	7	—	—	8	8	8
Lower Tamiami Formation	minimum	0	21	53	44	9	21	12	0	20	85.7	114.8	2.62	—	—	—	—	—
	maximum	1	47	79	61	18	34	24	13	34	100.1	119.9	2.66	—	—	—	—	—
	mean	0	36	64	53	12	25	19	4	31	89.9	116.7	2.64	—	—	—	—	—
	number of samples	33	33	33	10	10	12	12	19	19	23	23	6	—	—	—	—	—

PTN COL 2.5-6

Table 2.5.4-205 (Sheet 2 of 2)
Summary of General Physical and Chemical Properties Test Results

Layer	Statistical Parameters	Sieve Analysis					Atterberg Limits			w (%)	Dry Unit Weight γ (pcf)	Bulk Unit Weight γ (pcf)	Specific Gravity	Ash Content (%)	Organic Matter (%)	Chemical Tests		
		Gravel (%)	Sand (%)	Fines (%)	Silt (%)	Clay (%)	LL	PL	PI							pH	Chloride (mg/kg)	Sulfate Content (mg/kg)
Peace River Formation	minimum	0	45	5	6	5	20	4	0	16	84.8	102.3	2.60	—	—	—	—	—
	maximum	6	95	55	48	9	31	25	17	33	121.7	129.8	2.70	—	—	—	—	—
	mean	0	79	21	16	7	25	19	1	25	97.5	120.6	2.64	—	—	—	—	—
	number of samples	51	51	51	7	7	9	9	42	50	68	68	28	—	—	—	—	—
Arcadia Formation	minimum	—	—	—	—	—	—	—	—	18	99.9	124.3	—	—	—	—	—	—
	maximum	—	—	—	—	—	—	—	—	24	113.8	133.9	—	—	—	—	—	—
	mean	—	—	—	—	—	—	—	—	20	107.2	129.0	—	—	—	—	—	—
	number of samples	—	—	—	—	—	—	—	—	5	5	5	—	—	—	—	—	—

Data from References 257, 290, and 291.

Notes:

pcf = pounds per cubic foot
LL = Liquid Limit
PL = Plastic Limit
PI = Plasticity Index
w = water content
mg/kg = milligrams per kilogram (a.k.a. parts per million)

PTN COL 2.5-6

Table 2.5.4-206
Summary of Recovery and RQD Values for Rock Strata

Stratum	Description of Value	Recovery (%)	RQD (%)	No. of Samples	
				Recovery	RQD
Miami	Minimum	0	0	78	78
	Maximum	100	100		
	Average	67	37		
Key Largo	Minimum	0	0	437	437
	Maximum	100	100		
	Average	86	67		
Fort Thompson	Minimum	0	0	1189	1189
	Maximum	100	100		
	Average	67	39		
Arcadia	Minimum	18	0	34	34
	Maximum	100	100		
	Average	82	57		

Data from References 257 and 290.

PTN COL 2.5-6

Table 2.5.4-207
Summary of Unconfined Strength Testing of Rock

Stratum	Number of Tests		Description of Value	Unconfined Compressive Strength (psi)	Unit Weight (pcf)
	For Unconfined Compressive Strength	For Unit Weight			
Key Largo	31	34	Minimum	309	114.9
			Maximum	7800	156.4
			Average	2689	137.1
Fort Thompson	50	57	Minimum	172	109.7
			Maximum	5031	153.2
			Average	2301	137.0
Arcadia	3	5	Minimum	18	124.3
			Maximum	310	133.9
			Average	141	129.0

Data from References 257 and 290.
psi = pounds per square inch
pcf = pounds per cubic foot

PTN COL 2.5-6

Table 2.5.4-208
Summary of Triaxial Testing Results

Borehole	Sample	Elevation (ft)		c' (ksf)	φ' (°)	Conf Press 1 (psi)	Conf Press 2 (psi)	Conf Press 3 (psi)	E_{50} 1 (psi)	E_{50} 2 (psi)	E_{50} 3 (psi)	σ' (psi)(1)	y=mx+b(2)	E_{50} at Effective Mean Stress at Mid Layer (ksf)	Engineering Layer
		From	To												
R-6-1b	ST-3	–147.7	–149.8	0.00	35	26.20	50.70	101.80	1903	6756	17186	41.63	4984	718	Upper Tamiami F.
B-630	UD 12	–180.4	—	1.70	20	34.70	69.40	104.20	2717	7058	20156	54.79	6302	907	Lower Tamiami F.
R-6-1b	ST-5	–162.5	–165.2	0.25	33	28.60	56.20	117.70	12317	14259	28104	50.18	15019	2163	Lower Tamiami F.
R-6-1b	ST-11	–184.7	–187.4	0.46	31	32.70	62.90	127.40	9767	16451	43949	56.98	16946	2440	Lower Tamiami F.
R-6-1b	ST-15	–199.5	–202.2	0.99	29	34.30	69.00	136.90	6815	19485	4458	61.51	11186	1611	Lower Tamiami F.
R-7-1	ST-4	–189.9	–190.4	0.37	31	32.40	66.00	132.00	6778	15034	31813	58.29	13216	1903	Lower Tamiami F.
R-6-1b	ST-22	–224.2	–226.3	0.69	35	37.80	77.40	—	6038	11010	—	66.33	9619	1385	Peace River F.
R-6-1b	ST-31	–250.9	–253.3	0.08	33	45.10	89.00	172.60	6234	10253	20621	74.23	9169	1320	Peace River F.
R-6-1b	ST-40	–279.8	–282.5	0.82	30	50.20	99.00	191.40	11361	21299	50563	82.79	19048	2743	Peace River F.
R-6-1b	ST-46	–299.6	–302.3	0.38	33	51.40	103.10	204.80	6254	17212	34591	88.62	13658	1967	Peace River F.
R-6-1b	ST-55	–325.9	–328.0	3.82	33	56.00	115.10	223.50	7430	10950	42573	96.27	12563	1809	Peace River F.
R-6-1b	ST-66	–355.9	–358.6	1.12	33	62.40	123.10	241.70	6235	11395	22812	105.19	10021	1443	Peace River F.
R-6-1b	ST-82	–401.0	–404.6	0.00	34	68.90	141.90	276.00	16006	22005	37844	118.61	20613	2968	Peace River F.
R-7-1	ST-7	–231.8	–234.5	0.83	32	40.20	81.60	158.70	8509	13547	23277	68.71	12017	1730	Peace River F.
R-7-1	ST-9	–254.8	–257.3	1.11	27	44.20	89.50	180.10	3002	15193	28240	75.45	10239	1474	Peace River F.
R-7-1	ST-10	–265.8	–268.5	3.85	20	48.00	90.30	182.00	7926	15107	39592	78.72	14109	2032	Peace River F.
R-7-1	ST-11	–276.8	–279.5	0.94	31	46.80	94.60	190.10	6924	23224	40022	81.96	17023	2451	Peace River F.
R-7-1	ST-13	–297.8	–300.5	0.82	32	51.10	104.00	203.40	6483	24281	34612	88.15	16327	2351	Peace River F.
R-7-1	ST-16	–319.5	–322.0	8.20	27	55.50	108.40	219.10	13804	16760	45636	94.51	18611	2680	Peace River F.
R-7-1	ST-20	–353.8	–355.8	0.15	35	59.90	124.50	241.80	6759	7387	47221	104.53	11574	1667	Peace River F.
R-7-1	ST-23	–389.8	–392.3	0.00	37	68.70	135.70	266.00	6796	13972	27451	115.21	11725	1688	Peace River F.

(1) Effective mean stress (σ')
(2) m and b are linear correlation factors of Confining Pressure and E_{50} and x is the effective mean stress (σ')

PTN COL 2.5-6
PTN COL 2.5-7
PTN COL 2.5-10
PTN COL 2.5-11
PTN COL 2.5-12
PTN COL 2.5-16

Table 2.5.4-209 (Sheet 1 of 2)
Summary of Recommended Geotechnical Engineering Parameters

Stratum	1	2	3	4	5	6	7	8	Fill
Description	Muck/Peat	Miami	Key Largo	Ft. Thompson	Upper Tamiami	Lower Tamiami	Peace River	Arcadia	—
Elevation of top of layer (ft)	–1.1	–4.7	–26.9	–49.4	–115.4	–167.6	–217.8	–454.8	—
USCS symbol	SM, MH, PT, SP-SM	GM, GP, GP-GM, SP-SM, SM, GW, SC, SW-SM, Limestone	GM, SW-SM, SP-SM, SM, Limestone	SM, Limestone	SM, ML, SC-SM, SP-SM, GM, GW-GM	ML, CL-ML, SM, CL	SM, SP-SM, ML, SC-SM, SC, SW-SM, SP	Limestone	—
Total unit weight, γ (pcf)	73	125[(a)]	137	137	119	117	121	129	130
Natural water content, w, (%)	381	—	10	11	29	31	25	20	33
Fines content (%)	58	18	18	30	29	64	21	—	15
Atterberg limits									
Liquid limit, LL	87	—	—	—	23	25	25	—	—
Plastic limit, PL	62	—	—	—	21	19	19	—	—
Plasticity index, PI	9	—	—	—	1	4	1	—	—
SPT N_{60}-value (blows/ft)	0	20	—	—	27	24	79	—	30
Undrained properties									
Undrained shear strength, s_u (ksf)	—	—	—	—	—	4.0	—	—	—
Internal friction angle, φ, (deg)	—	—	—	—	—	—	—	—	—
Drained properties									
Effective cohesion, c′ (ksf)	—	6.2 (FD1) 2.0 (FD4)	22.5 (FD1) 6.8 (FD4)	22.4 (FD1) 8.8 (FD4)	0	0.75	1.52	—	—
Effective friction angle, φ' (deg)	—	56	55 (FD1) 56 (FD4)	52	34	29	31	—	33
Average Rock core recovery (%)	—	67	86	67	—	—	—	82	—
Average RQD (%)	—	37	67	39	—	—	—	57	—
Unconfined compressive strength, U (psi)	—	200	2,689	2,301	—	—	—	141	—
Elastic modulus for soils (high strain), E_H	—	—	—	—	1,150 ksf	1,950 ksf	2,700 ksf	—	1,100 ksf
Elastic modulus for rock (high strain), general (ksf)	—	32,900 ksf	83,900 ksf	46,600 ksf	—	—	—	145,200 ksf	—
Elastic modulus for rock (high strain), moderately fractured zones (ksf)	—	11,100 ksf	32,200 ksf	26,900 ksf	—	—	—	—	—
Shear wave velocity, V_s, (ft/sec)	850	3,400	6,250	4,450	1,500	1,600	1,600	3,650	860

PTN COL 2.5-6
PTN COL 2.5-7
PTN COL 2.5-10
PTN COL 2.5-11
PTN COL 2.5-12
PTN COL 2.5-16

Table 2.5.4-209 (Sheet 2 of 2)
Summary of Recommended Geotechnical Engineering Parameters

Stratum	1	2	3	4	5	6	7	8	Fill
Description	Muck/Peat	Miami	Key Largo	Ft. Thompson	Upper Tamiami	Lower Tamiami	Peace River	Arcadia	—
Compression wave velocity, V_c, (ft/sec)	4,900	7,450	11,750	9,000	5,650	5,700	5,850	7,950	1,600
Coefficient of sliding	—	0.6	0.7	0.7	0.4	0.3	—	—	0.5
Poisson's ratio, v' for drained or effective conditions	—	0.37	0.30	0.34	0.30	0.35	0.30	0.36	0.3
Poisson's ratio, v_s for saturated conditions[(b)]	—	0.37	0.30	0.34	0.46	0.46	0.46	0.36	—
Static earth pressure coefficients									
Active, K_a	—	0.3	—	—	0.27	0.5	—	—	0.29
At-rest, K_o	—	0.5	—	—	0.5	0.66	—	—	0.46

(a) Unit weight of Stratum 2 (Miami) is assumed to be 125 pcf based on the dry density and porosity data presented in Reference 321 for the Miami Limestone.
(b) Poisson's ratio for saturated conditions, as obtained from P-S Suspension tests. Poisson's ratios for saturated conditions are only used with shear wave velocity data.

The values tabulated for use as design guideline only. Refer to specific boring logs, CPT logs, and laboratory test results for appropriate modifications at specific design locations.
USCS = Unified Soil Classification System (ML = silt; MH = silt of high plasticity; GM = silty gravel; GP = poorly graded gravel; SM = silty sand; SW = well graded sand; SP = poorly graded sand, PT = Peat)
Data from References 257, 290, and 291.
ft = feet
pcf = pounds per cubic foot
ksf = kips per square foot
deg = degrees
psi = pounds per square inch
ft/sec = feet per second

PTN COL 2.5-6

Table 2.5.4-210
Summary of Calcite Content Testing Results

Stratum	Description of Value	Calcite Equivalent (%)
Miami Limestone	Number of Tests	17
	Minimum	86
	Maximum	95
	Average	91
Key Largo Limestone	Number of Tests	4
	Minimum	78
	Maximum	93
	Average	89
Fort Thompson Formation	Number of Tests	4
	Minimum	68
	Maximum	95
	Average	87
Tamiami Formation	Number of Tests	22
	Minimum	11
	Maximum	40
	Average	21
Peace River Formation	Number of Tests	3
	Minimum	20
	Maximum	34
	Average	25
Arcadia Formation	Number of Tests	3
	Minimum	78
	Maximum	93
	Average	86

Data from Reference 257.

PTN COL 2.5-6

Table 2.5.4-211
Guidelines for the Evaluation of Soil Chemistry

Potential for Attack on Buried Steel (Corrosiveness/Chlorides)					
Parameter	Range For Steel Corrosiveness				
	Noncorrosive	Mildly Corrosive	Moderately Corrosive	Corrosive	Very Corrosive
Resistivity (ohm-meters)	>100[a],[b]	20–100[a] 50–100[b] >30[b],[c]	10–20[a] 20–50[b]	5–10[a] 7–20 [b]	<5[a] <7[b]
pH	—	>5 and <10[b]	—	5–6. 5[a]	<5[a]
Chlorides (ppm)	—	<200[b]	—	300–1,000[a]	>1,000[a]

Potential for Attack on Concrete in Contact with the Ground (Aggressiveness/Sulphates)			
Recommendations For Normal Weight Concrete Subject To Sulfate Attack[d]			
Concrete Exposure	Water Soluble Sulfate (SO_4) in Soil, %	Cement Type	Maximum Water/ Cement Ratio
Mild	0.00–0.10	—	—
Moderate	0.10–0.20	II, IP(MS), IS(MS)	0.5
Severe	0.20–2.00	V[e]	0.45
Very Severe	Over 2.00	V with pozzolan	0.45

(a) Reference 226
100 ohm – cm = 1 ohm – m
PPM = parts per million (weight) and is equivalent to milligrams/kilograms

(b) Reference 227
% (percent by weight) is converted to ppm(w) or milligrams/kilograms per kilogram with the equivalence 1% = 10,000 ppm

(c) Reference 228

(d) Reference 229

(e) Alternatively, a blend of Type II cement and a ground granulated blast furnace slag or a pozzolan that gives equivalent sulfate resistance, can be considered

PTN COL 2.5-6

Table 2.5.4-212 (Sheet 1 of 2)
As-built Boring and CPT Probe Information

Depth (ft)	Boring/CPT/TP Number	Northing (U.S. ft) [a]	Easting (U.S. ft) [a]	Ground Surface El. (ft)[b]	Boring/CPT/TP Number	Northing (US ft)[a]	Easting (US ft) [a]	Ground Surface El. (ft)[b]	Depth (ft)
419.2	B-601(DH)	396,967.9	876,642.9	–1.4	B-710(DH)R	397,087.2	875,781.9	–1.3	15.0
204.1	B-602	397,019.6	876,594.1	–1.4	B-710G(DH)	397,075.1	875,792.2	–1.4	273.5
151.2	B-603	397,018.4	876,697.0	–1.4	B-711	397,085.6	875,884.8	–1.1	151.7
165.0	B-604(DH)	396,915.9	876,591.6	–1.5	B-712	397,082.1	876,022.1	–1.1	128.3
201.0	B-605	396,916.8	876,694.1	–1.7	B-713	397,179.3	875,959.0	–1.1	152.5
151.2	B-606	396,958.9	876,738.0	–1.4	B-714	397,258.7	876,020.6	–1.0	125.6
152.5	B-607	396,830.0	876,644.2	–1.5	B-715	397,259.2	875,908.5	–0.9	150.1
265.4	B-608(DH)	396,829.5	876,735.9	–1.5	B-716	397,214.3	875,872.7	–1.1	126.6
150.7	B-609	396,762.5	876,689.0	–1.5	B-717	397,287.0	875,873.1	–1.1	127.2
269.0	B-610(DH)	397,084.2	876,644.4	–1.4	B-718	397,190.9	875,792.6	–1.2	150.8
151.5	B-611	397,086.7	876,735.0	–1.5	B-719	397,293.2	875,791.3	–1.1	126.7
125.1	B-612	397,085.5	876,869.1	–1.5	B-720(DH)	397,396.7	875,791.1	–0.9	204.9
150.2	B-613	397,162.2	876,809.4	–1.4	B-720G(DH)	397,385.2	875,794.0	–1.1	220.8
128.0	B-614	397,204.1	876,870.7	–1.5	B-721	397,338.0	876,120.1	–1.5	127.4
150.6	B-615	397,167.4	876,761.8	–1.5	B-722	397,434.2	875,979.6	–1.0	103.2
125.0	B-616	397,207.9	876,723.7	–1.2	B-723	397,421.2	875,675.4	–1.0	100.6
126.1	B-617	397,288.1	876,721.7	–1.4	B-724	397,325.5	875,663.2	–0.7	100.0
154.7	B-618	397,207.6	876,643.1	–1.4	B-725	397,099.8	876,111.2	–1.0	126.6
128.7	B-619	397,293.9	876,653.7	–1.7	B-726	396,875.6	876,003.9	–1.4	100.5
215.0	B-620(DH)	397,394.9	876,648.3	–1.5	B-727	397,117.7	875,666.1	–1.3	100.9
126.5	B-621	397,367.6	876,949.3	0.2	B–728	397,070.5	875,620.1	-1.4	126.6
100.2	B–622	397,421.2	876,810.7	0.2	B-729	396,970.7	875,493.4	–1.2	100.9
100.2	B-623	397,422.6	876,523.2	–1.3	B-730	396,868.0	875,621.0	–1.0	103.2
103.2	B-624	397,327.1	876,514.1	–1.4	B-731	396,645.6	875,423.1	–1.5	103.2
126.7	B-625	397,106.5	876,960.5	–1.4	B-732	396,412.1	875,682.4	–1.0	104.5
100.6	B-626	396,874.5	876,857.2	–1.6	B-733	396,117.5	875,897.5	–1.0	103.5
102.0	B-627	396,835.2	876,332.9	–1.3	B-734	395,833.2	875,546.3	–0.6	130.0
127.9	B-628	397,072.9	876,473.2	–1.5	B-735	395,824.7	875,689.4	–0.8	128.0
100.3	B-629	396,971.9	876,346.1	–1.1	B-736	395,808.5	876,107.1	–0.5	125.0
294.0	B-630	396,871.5	876,462.1	–1.5	B-737	395,803.7	876,237.8	–0.6	153.3
100.8	B-631	396,655.1	876,514.1	–1.2	B-738	397,728.1	875,607.3	0.1	101.2
100.3	B-632	396,432.4	876,737.0	–1.6	B-739	396,962.9	876,149.6	–1.6	101.0
100.4	B-633	396,113.3	876,993.9	–1.5	B-740(DHT)	397,137.2*	875,841.7*	–0.8	150.0

PTN COL 2.5-6

Table 2.5.4-212 (Sheet 2 of 2)
As-built Boring and CPT Probe Information

Depth (ft)	Boring/CPT/TP Number	Northing (U.S. ft) [a]	Easting (U.S. ft) [a]	Ground Surface El. (ft)[b]	Boring/CPT/TP Number	Northing (US ft)[a]	Easting (US ft) [a]	Ground Surface El. (ft)[b]	Depth (ft)
127.5	B-634	395,758.2	876,677.2	–0.7	B-802	398,817.1	876,265.7	–1.5	128.5
128.5	B-635	395,770.9	876,798.2	–0.9	B-805	396,883.0	877,239.5	–1.6	125.3
126.0	B-636	395,714.8	877,193.2	–1.1	B-806	395,288.3	877,237.4	–0.4	127.4
150.0	B-637	395,693.1	877,310.3	–0.2	B-807	395,277.5	875,987.8	–0.7	128.5
102.6	B-639	396,963.5	876,998.2	–1.4	B-808	396,204.9	875,331.8	–1.0	126.4
150.0	B-640(DHT)	397,116.6	876,528.3	–0.3	B-809	397,028.0	875,151.3	–1.3	124.5
615.5	B-701(DH)	396,976.1	875,792.3	–1.1	B-810	397,806.7	875,012.4	–1.2	127.0
202.5	B-702	397,017.9	875,745.9	–1.2	B-811	398,325.2	874,953.8	–1.4	127.3
15.0	B-703	397,018.1	875,846.1	–1.3	B-812	398,913.2	875,043.1	–1.4	128.7
151.5	B-704(DH)	396,930.7	875,741.7	–1.4	B-813	399,047.6	876,097.3	–1.3	126.5
163.5	B-704G(DH)	396,938.6	875,749.0	–1.3	B-814	399,138.9	877,404.8	9.0	153.2
200.0	B-705	396,919.2	875,846.4	–1.3	C-601	397,129.8	876,361.3	–0.1	120–226.5
151.9	B-706	396,962.5	875,885.3	–1.2	C-602 A	397,116.6	876,528.3	–0.5	120–221.7
152.0	B-707	396,828.8	875,790.8	–1.8	C-701	397,100.2	875,839.3	–1.4	120–289.7
266.5	B-708(DH)	396,829.7	875,885.7	–1.4	C-702	397,149.4	876,042.2	0.3	120–220.8
150.0	B-709	396,760.5	875,840.6	–1.3	R-6-1a[1]	397,115.74	876,594.72	–0.07	121.80
250.9	B-710(DH)	397,086.9	875,792.9	–1.3	R-6-1a-A[1]	397,112.22	876,590.79	–0.09	111.90
459.40	R-7-1	396,976.23	875,797.30	0.22	R-6-1b	396,966.10	876,609.04	–0.03	464.10
370.00	R-7-2	396,966.03	875,788.86	0.06	R-6-2	396,967.24	876,648.22	–0.06	360.00
288.20	R-7-3	396,957.30	875,783.79	0.01	R-6-3	396,967.75	876,633.36	–0.15	289.70
126.00	R-7-4[1]	396,958.51	875,605.22	–0.53	M-6-1a	397,160.96	877,019.73	–1.32	2.85
6.10	M-7-2b	396,928.33	875,636.38	–1.42	M-6-1b	397,117.71	877,034.98	–1.27	3.30
3.70	M-7-2c	396,897.85	875,630.22	–1.15	M-6-2a	396,691.76	876,549.80	–1.30	2.85
2.90	M-7-3a	396,852.38	875,967.82	–1.75	M-7-1a	397,495.08	875,787.83	–1.15	4.30
4.95	M-7-3b	396,903.26	876,137.69	–1.22	M-7-2a	396,951.72	875,656.19	–1.07	6.85

(a) Horizontal northing and easting data are Florida state plane coordinates NAD 83/Adjustment of 1990, Florida East, Zone 0401
(b) Ground surface elevation is with reference to NAVD 88

* Location adjacent to PVC pipe in hole.
(1) Inclined borings, depth in table is measured depth in boring.
Data from References 257, 290, and 291.

PTN COL 2.5-6

Table 2.5.4-213
Summary of Test Pit Location

Boring/CPT/TP Number	Northing (US ft) [a]	Easting (US ft) [a]	Ground Surface Elevation (ft) [b]
TP-601	397,105.6	876,035.8	–1.4
TP-701	396,988.2	875,508.5	–1.4

(a) Horizontal northing and easting data are Florida state plane coordinates NAD 83/ Adjustment of 1990, Florida East, Zone 0401
(b) Ground surface elevation is with reference to NAVD 88
CPT = Cone penetration test
TP = Test pit
Data from Reference 257.

PTN COL 2.5-7

Table 2.5.4-214
Summary of Laboratory Compaction, and CBR Results

Test Pit Number	Sample Depth (ft.)	USCS Symbol	Moisture-Density		LBR (%)	CBR			
			Max. Dry Density (pcf)	Optimum Moisture (%)		Molded Density (pcf)	Molded Moisture (%)	Soaked CBR (0.10")	Soaked CBR (0.20")
TP-601	3.2-5	SP-SM	106.5	16.3	112	103.0	15.9	66.5	63.9
						104.5	16.5	69.1	65.8
						107.5	16.9	67.3	78.9
TP-701	3-4.5	SM	106.9	17.4	129	96.1	16.2	22.2	20.9
						96.8	16.5	24.9	21.2
						105.5	16.4	58.9	61.4

Data from Reference 257.
LBR = Lime rock ratio
CBR = California bearing ratio
USCS = Unified Soil Classification System (SM = Silty sand; SP = Poorly graded sand)

PTN COL 2.5-6

Table 2.5.4-215 (Sheet 1 of 2)
Summary of Measured Shear Wave Velocities and Compressive Wave Velocities

Top Elevation (ft)	Bottom Elevation (ft)	Shear Wave Velocity, V_s (ft/s)			Compressive Wave Velocity, V_p (ft/s)		
		Average	Upper Bound	Lower Bound	Average	Upper Bound	Lower Bound
0	–10	2097	—	—	5566	—	—
–10	–20	3659	4853	1903	7568	9825	4851
–20	–30	4480	6348	1850	9249	12114	6086
–30	–40	5770	7575	4566	11004	14256	9002
–40	–50	6751	8104	4945	12540	15158	9405
–50	–60	5684	7663	3818	10742	13769	7894
–60	–70	4472	7011	2749	9349	12679	6382
–70	–80	4575	6509	2586	9379	12425	6558
–80	–90	4579	6538	3049	9142	12238	7283
–90	–100	4261	5294	2529	8706	10702	6674
–100	–110	4381	5065	2926	8565	9380	7667
–110	–120	2246	4739	725	6553	8882	5074
–120	–130	1271	1610	982	5491	5814	5183
–130	–140	1794	2597	1021	5938	6795	5159
–140	–150	1383	1676	1048	5526	5828	5254
–150	–160	1524	1773	1162	5621	5864	5237
–160	–170	1644	1770	1555	5724	5860	5586
–170	–180	1590	1661	1476	5694	5783	5607
–180	–190	1562	1642	1452	5681	5825	5564
–190	–200	1636	1800	1468	5738	5865	5570
–200	–210	1778	1923	1591	5787	6000	5641
–210	–220	2236	2592	1809	6390	6983	5832
–220	–230	2354	2976	1796	6465	7019	5991
–230	–240	1950	2652	1535	6058	6640	5550
–240	–250	2045	2932	1553	6079	6771	5554
–250	–260	1835	2273	1344	6003	6311	5612
–260	–270	1668	1940	1354	5856	6073	5587
–270	–280	1696	1785	1525	5844	6109	5577
–280	–290	1823	2051	1656	5954	6192	5775
–290	–300	1757	2023	1523	5980	6217	5729
–300	–310	1713	1963	1409	5866	6101	5662
–310	–320	1572	2026	1243	5732	5916	5560
–320	–330	1444	1636	1298	5816	5971	5679
–330	–340	1436	1632	1299	5682	5958	5523
–340	–350	1436	1566	1262	5754	5947	5549
–350	–360	1481	1571	1377	5787	5940	5563
–360	–370	1470	1570	1285	5811	6032	5559
–370	–380	1439	1521	1318	5718	6098	5446
–380	–390	1492	1630	1299	5755	5930	5527
–390	–400	1430	1606	1261	5727	5929	5497
–400	–410	1450	1717	1242	5690	5916	5488
–410	–420	1449	1587	1363	5736	5979	5538

PTN COL 2.5-6

Table 2.5.4-215 (Sheet 2 of 2)
Summary of Measured Shear Wave Velocities and Compressive Wave Velocities

Top Elevation (ft)	Bottom Elevation (ft)	Shear Wave Velocity, V_s (ft/s)			Compressive Wave Velocity, V_p (ft/s)		
		Average	Upper Bound	Lower Bound	Average	Upper Bound	Lower Bound
–420	–430	1469	1566	1338	5786	6025	5514
–430	–440	1449	1657	1273	5716	6031	5479
–440	–450	1460	—	—	5565	—	—
–450	–460	4046	—	—	8842	—	—
–460	–470	4046	—	—	8842	—	—
–470	–480	4171	—	—	8247	—	—
–480	–490	3818	—	—	7739	—	—
–490	–500	3953	—	—	8021	—	—
–500	–510	3917	—	—	8118	—	—
–510	–520	3961	—	—	8256	—	—
–520	–530	3843	—	—	7743	—	—
–530	–540	3860	—	—	8088	—	—
–540	–550	3569	—	—	7873	—	—
–550	–560	3364	—	—	7627	—	—
–560	–570	3083	—	—	7275	—	—
–570	–580	3040	—	—	7398	—	—
–580	–590	3174	—	—	7453	—	—
–590	–600	3741	—	—	8307	—	—
–600	–610	3331	—	—	7847	—	—

Data from References 257 and 290.

PTN COL 2.5-6

Table 2.5.4-216
Summary of Recommended Shear Modulus Degradation and Damping Curves

	Shear Strain, γ (%)	0.0001	0.0003	0.001	0.003	0.01	0.03	0.1	0.3	1
G/G_{max}	**Natural Soil (Depth > 150 ft)**	1.00	1.00	1.00	1.00	0.95	0.87	0.65	0.42	0.19
	Natural Soil (Depth < 150 ft)	1.00	1.00	1.00	0.99	0.93	0.81	0.56	0.33	0.14
	Miami Limestone	1.00	1.00	1.00	1.00	1.00	0.98	0.87	0.63	0.33
	Key Largo[(a)]	1.00	1.00	0.99	0.98	0.95	0.85	0.64	0.37	0.15
	Fort Thompson[(a)]	1.00	1.00	0.99	0.96	0.89	0.73	0.45	0.21	0.07
	Structural Fill	1.00	0.96	0.87	0.74	0.55	0.37	0.21	0.11	0.05
D (%)	**Natural Soil**	0.6	0.6	0.6	0.8	1.3	2.6	5.6	10.4	17.0
	Miami Limestone	0.6	0.6	0.6	0.6	0.6	0.6	2.7	8.2	17.0
	Key Largo & Fort Thompson[(b)]	0.8	0.8	0.8	0.9	1.2	—	—	—	—
	Structural Fill	1.3	1.3	1.6	2.4	4.4	8.2	14.3	20.6	27.9

(a) Up to the strain level of 0.005 percent, the rocks are considered non strain-dependent.
(b) The damping is assumed to be constant at 1 percent.

Data from References 257, 258, 259, 260, and 290.

PTN COL 2.5-3
PTN COL 2.5-10

Table 2.5.4-217
Summary of Bearing Capacity

Evaluation Method	Foundation Width, B (ft)	Properties[a]	Local Shear Failure		Hoek-Brown[b]	Punching[c]
			Static, q_{ALL}	Dynamic, q_{ALL}	Static, q_{ALL}	Static, q_{ALL}
Rock-Only Hand Calculation	88	FD1 Rock	845	1811	543	136
Rock-Only Hand Calculation	160	FD1 Rock	1150	2249		91
Rock-Only Hand Calculation	88	FD4 Rock	565	1006	—	—
Rock-Only Hand Calculation	160	FD4 Rock	869	1422		—
Rock-Only Hand Calculation	88	LB FD4 Rock	322	630	—	—
Rock-Only Hand Calculation	160	LB FD4 Rock	544	1030	—	—
Rock & Soil Hand Calculation	88	FD4 Rock & BE Soil	118	313	—	—
Rock & Soil Hand Calculation	160	FD4 Rock & BE Soil	101	189	—	—
Rock & Soil Hand Calculation	88	LB FD4 Rock & BE Soil	81	214	—	—
Rock & Soil Hand Calculation	160	LB FD4 Rock & BE Soil	84	154	—	—
Soil-Only Hand Calculation	88	BE Soil	49	41	—	—
Soil-Only Hand Calculation	160	BE Soil	76	65	—	—
Soil-Only Hand Calculation	88	LB Soil	40	41	—	—
Soil-Only Hand Calculation	160	LB Soil	68	65	—	—
SLOPE/W	88	FD1 Rock & BE Soil	79	—	—	—
SLOPE/W	160	FD1 Rock & BE Soil	52	—	—	—
SLOPE/W	160	LB FD4 Rock & LB Soil	39	—	—	—
		Minimum:	39	41	543	91

Notes:
(a) LB Soil includes LB properties of Upper Tamiami and BE properties for Lower Tamiami and Peace River
(b) Hoek-Brown methodology is dimension independent
(c) Punching failure is based on lowest average UCS of rock layers
q_{ALL} = allowable bearing capacity (ksf)
BE = Best Estimate LB = Lower Bound

Table 2.5.4-218
Not Used

Table 2.5.4-219
Estimated Foundation Settlements

Structure	Contact Pressure (ksf)	Subsurface	Area (ft^2)	Hand Calculation Best Estimate Maximum Settlement[(b)] (inch)
Reactor & Auxiliary	9.2	Lean Concrete Fill on Rock	31,318	2.4
Turbine	4.2	Compacted Fill	41,925	1.8
First Bay	3.7	Compacted Fill	4,740	0.9
Annex[(a)]	2.4	Compacted Fill	19,888	0.9
Radwaste	1.3	Compacted Fill	13,363	0.4

(a) Excludes annex office building.
(b) Excludes heave due to rewatering.

Table 2.5.4-220
Summary of Average Stiffness Properties Based on Pressuremeter Testing

Formation	Initial Modulus		Unload/Reload Modulus		
	Shear Modulus (psi)	Young's Modulus, E_i (psi)	Shear Modulus (psi)	Young's Modulus, E_u (psi)	E_u/E_i
Key Largo	48,079	125,968	91,918	240,826	1.9
Fort Thompson	40,761	110,055	95,792	258,638	2.4
Upper Tamiami	1,934	5,029	5,747	14,942	3.0
Lower Tamiami	4,362	11,778	17,547	47,378	4.0
Peace River	10,319	26,828	29,992	77,980	2.9

Table 2.5.4-221
Recommended Lower Bound Properties

Strata		Unit Weight (kcf)	Cohesion c' (ksf)	Friction Angle (degrees)	E (ksf)
Unfractured (FD1)	Key Largo	0.125	8.78	55	47,918
	Fort Thompson	0.125	3.02	50	20,407
Fractured (FD4)	Key Largo	0.125	2.32	55	16,723
	Fort Thompson	0.125	1.96	49	14,062
Upper Tamiami		0.116	0.00	29	702
Lower Tamiami		0.115	0.25	24	1,280
Peace River		0.117	0.00	27	1,685
Arcadia		0.125	0.00	27	107,650

Table 2.5.4-222
Comparison of Mesh Sensitivity Results in the Loading Phases

Maximum Settlement (inch)		Nuclear Island	Turbine Building Interior	Turbine Building Exterior	Annex Building	First Bay Building	Radwaste Building	Ancillary Water Tank	Condensate Water Tank	Diesel Generator
Load Other Buildings	Design	—	2.0	2.1	2.1	1.9	1.0	1.9	1.9	0.9
	Coarse	—	2.0	2.0	2.0	1.9	1.0	1.9	1.9	0.8
	Moderately Coarse	—	2.0	2.1	2.0	1.9	1.0	1.9	1.9	0.8
	Finest	—	2.0	2.1	2.1	1.9	1.0	1.8	1.9	0.9
Load Nuclear Island[(a)]	Design	2.5	2.9	3.0	3.0	3.0	2.2	3.1	2.9	1.4
	Coarse	2.5	2.9	3.0	3.0	3.0	2.1	3.2	3.0	1.3
	Moderately Coarse	2.5	2.9	3.0	3.0	3.0	2.2	3.1	2.9	1.3
	Finest	2.5	2.9	3.0	3.0	3.0	2.2	3.1	2.9	1.4

(a) The loading nuclear island phase is inclusive of the previous phase.

Table 2.5.4-223
Fracture Density, Hardening Soil, and Lower Bound Sensitivity Analyses

Maximum Settlement (inch)		Nuclear Island	Turbine Building Interior	Turbine Building Exterior	Annex Building	First Bay Building	Radwaste Building	Ancillary Water Tank	Condensate Water Tank	Diesel Generator
Load Other Buildings	Best Estimate	—	2.0	2.1	2.1	1.9	1.0	1.9	1.9	0.9
	Lower Bound	—	2.5	2.5	2.5	2.4	1.3	2.2	2.3	1.2
	Soil Hardening	—	1.9	2.0	2.0	1.8	0.9	1.7	1.8	0.8
	Fractured Zone	—	2.1	2.1	2.1	1.9	1.0	1.9	1.9	0.9
Load Nuclear Island[(a)]	Best Estimate	2.5	2.9	3.0	3.0	3.0	2.2	3.1	2.9	1.4
	Lower Bound	3.4	3.8	3.9	3.9	3.9	2.9	4.0	3.8	2.0
	Soil Hardening	2.5	3.0	3.1	3.1	3.1	2.2	3.1	3.0	1.5
	Fractured Zone	2.6	2.9	3.1	3.0	3.0	2.2	3.1	3.0	1.4
Rewatering	Best Estimate	2.1	2.6	2.7	2.7	2.7	1.8	2.7	2.6	1.1
	Lower Bound	2.9	3.3	3.4	3.4	3.4	2.4	3.4	3.3	1.6
	Soil Hardening	2.4	2.8	3.0	2.9	2.9	2.0	3.0	2.9	1.4
	Fractured Zone	2.2	2.6	2.7	2.7	2.7	1.8	2.8	2.6	1.1

(a) The loading nuclear island phase is inclusive of the previous phase.

Table 2.5.4-224
Comparison of Limits of Acceptable Settlement without Additional Evaluation

		Differential Across Nuclear Island Foundation Mat (inch per 50 feet)	Total for Nuclear Island Foundation Mat (inch)	Differential Between Nuclear Island and Turbine Building[(a)] (inch)	Differential Between Nuclear Island and Other Buildings[(a)] [(b)] (inch)
DCD Requirement		0.5	6	3	3
Best Estimate[(c)]	PLAXIS 3D	0.20	2.5	0.8	1.6
	Hand Calculation	0.22	2.4	0.6	2.0
Lower Bound[(c)]	PLAXIS 3D	0.23	3.4	1.2	2.2
	Hand Calculation	0.26	3.2	0.9	2.7

(a) Differential settlement is measured at the center of the nuclear island and the center of adjacent structures.
(b) Maximum differential settlement occurs between nuclear island and radwaste buildings.
(c) Settlements presented exclude the rewatering phase.

Table 2.5.4-225
Total Static and Pseudo-Dynamic Loads (ksf) Considered in Sensitivity Model with 20-Foot Diameter Cylindrical Void

Building	Multiplier of 1		Multiplier of 2	
	West Half of NI	East Half of NI	West Half of NI	East Half of NI
Shield Building	-16.2	-8.1	-32.3	-4.3
North Auxiliary Building	-9.5	-1.4	-18.9	2.4
South Auxiliary Building	-12.1	-4.0	-24.1	-0.2

Note: Negative sign indicates compressive loads, positive sign indicates uplift loads.

Table 2.5.4-226
PLAXIS 3D Effective Vertical Stress on Concrete Fill for Sensitivity Model with 20-Foot Diameter Cylindrical Void

Pseudo-Dynamic Loading Condition	Maximum Compressive Stress (ksf)	Ultimate Bearing Capacity of Concrete (ksf)
Multiplier of 1	61	184
Multiplier of 2	77	

PTN COL 2.5-1
PTN COL 2.5-5
PTN COL 2.5-6
PTN COL 2.5-7
PTN COL 2.5-10

Figure 2.5.4-201 Site Plan Showing Structures and Finish Grade

PTN COL 2.5-1
PTN COL 2.5-2
PTN COL 2.5-5
PTN COL 2.5-6
PTN COL 2.5-7

Figure 2.5.4-202 Site Plan Showing Boring Locations

Note:TP = Test pit
CPT = Cone penetration test

PTN COL 2.5-1
PTN COL 2.5-5
PTN COL 2.5-6
PTN COL 2.5-7
PTN COL 2.5-10

Figure 2.5.4-203 Geotechnical Cross Section D-D' Through Unit 6 Power Block

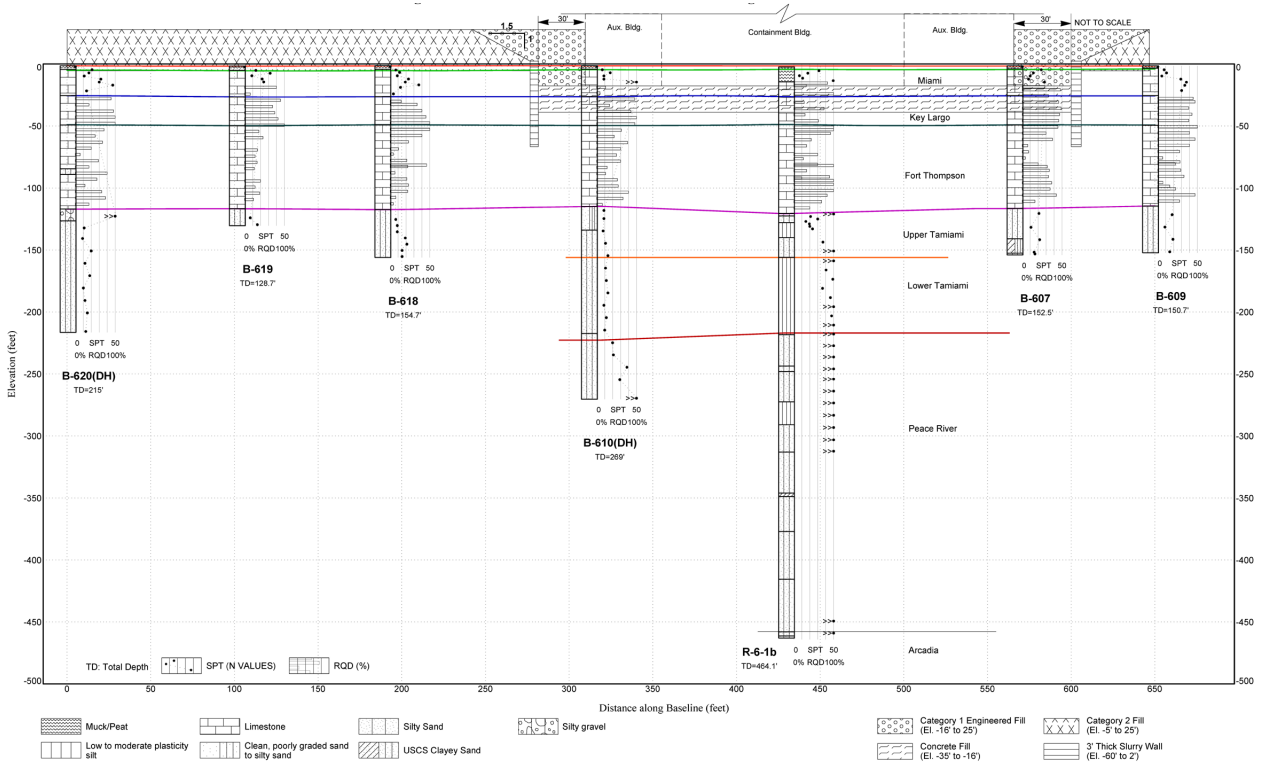

Data from References 257 and 290.
Note: Please see Figure 2.5.4-209 for location of geotechnical profile line D-D'.

PTN COL 2.5-1
PTN COL 2.5-5
PTN COL 2.5-6
PTN COL 2.5-7
PTN COL 2.5-10

Figure 2.5.4-204 Geotechnical Cross Section E-E' Through Unit 6 Power Block

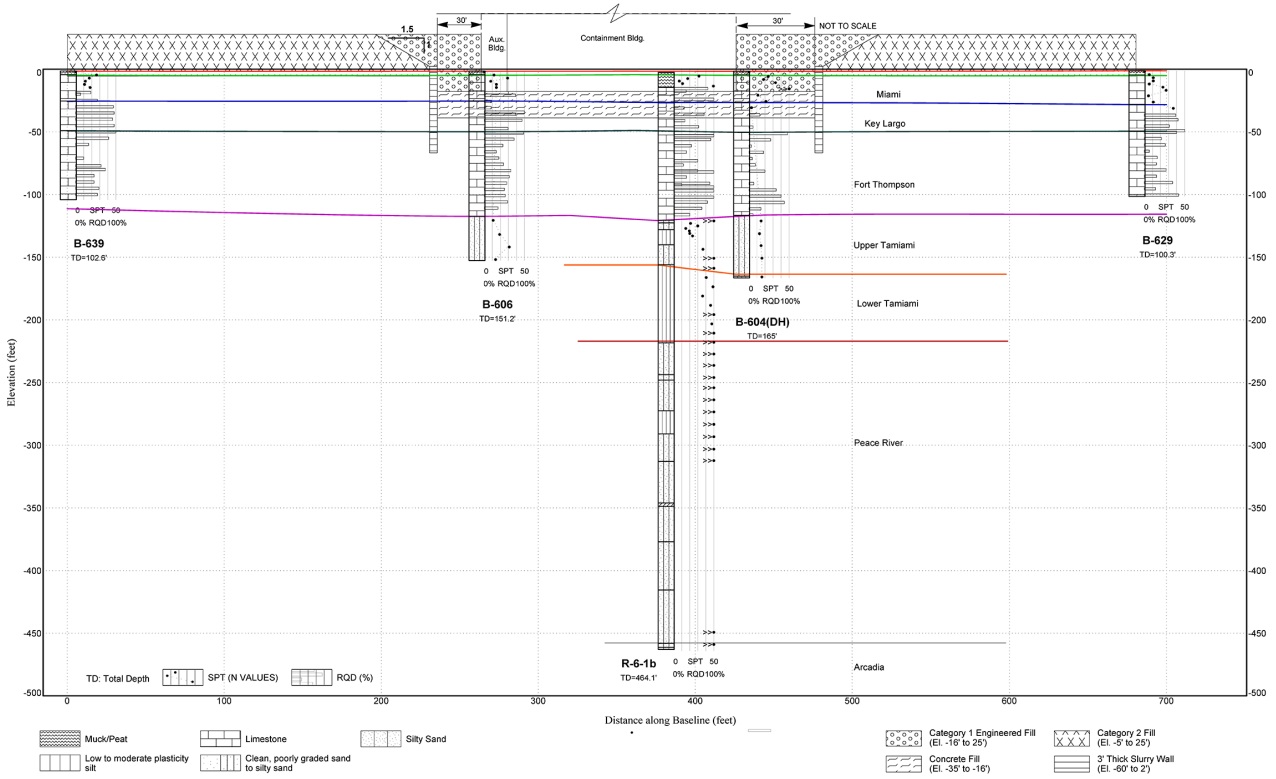

Data from References 257 and 290.
Note: Please see Figure 2.5.4-209 for location of geotechnical profile line E-E'

PTN COL 2.5-1
PTN COL 2.5-5
PTN COL 2.5-6
PTN COL 2.5-7
PTN COL 2.5-10

Figure 2.5.4-205 Geotechnical Cross Section F-F' Through Unit 6 Power Block

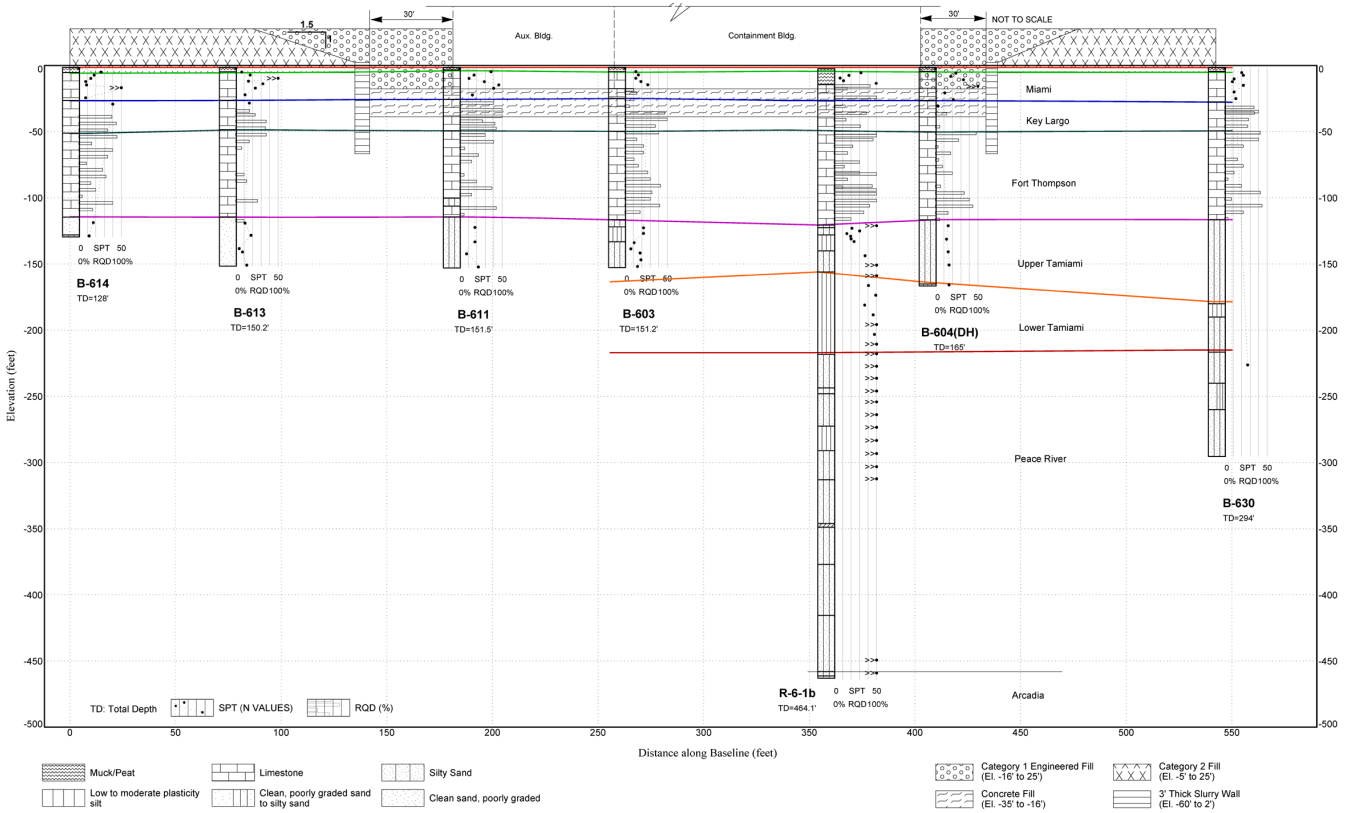

Data from References 257 and 290.
Note: Please see Figure 2.5.4-209 for location of geotechnical profile line F-F'

PTN COL 2.5-1
PTN COL 2.5-5
PTN COL 2.5-6
PTN COL 2.5-7
PTN COL 2.5-10

Figure 2.5.4-206 Geotechnical Cross Section A-A' Through Unit 7 Power Block

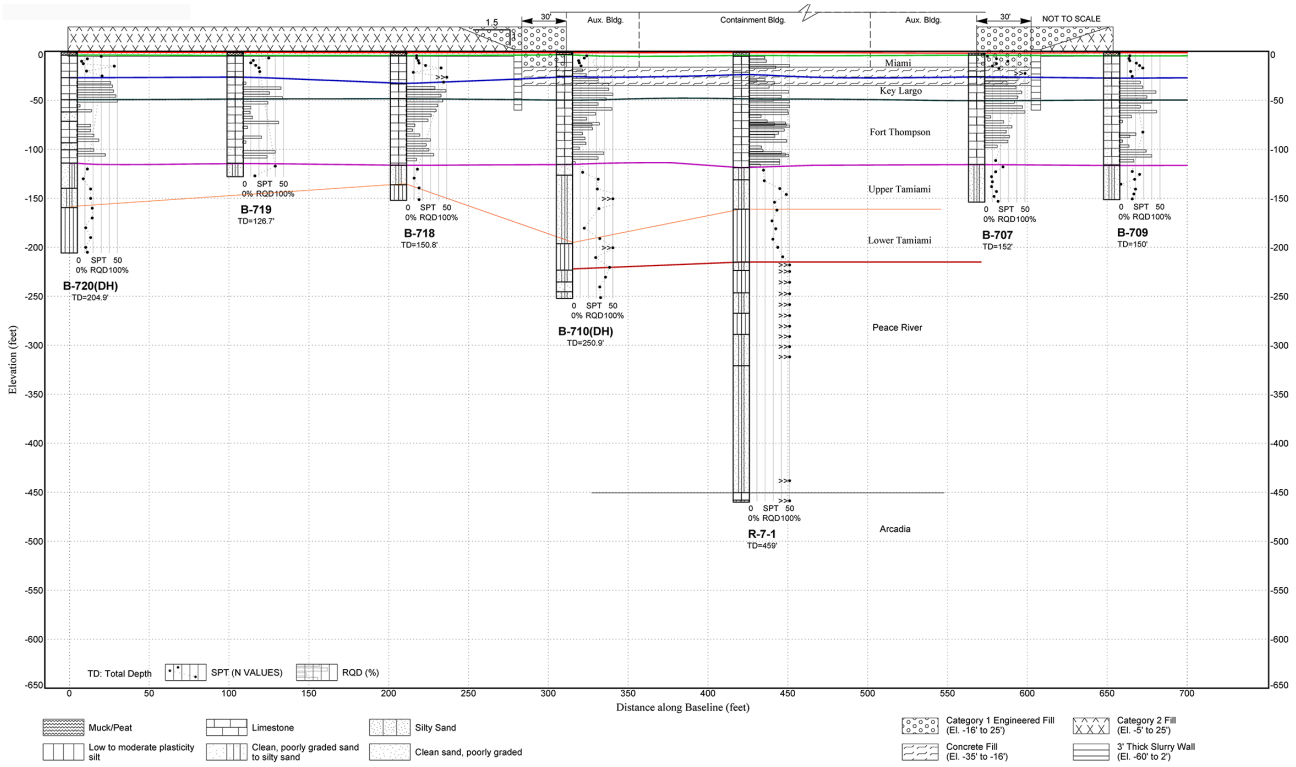

Data from References 257 and 290.
Note: Please see Figure 2.5.4-209 for location of geotechnical profile line A-A'

PTN COL 2.5-1
PTN COL 2.5-5
PTN COL 2.5-6
PTN COL 2.5-7
PTN COL 2.5-10

Figure 2.5.4-207 Geotechnical Cross Section B-B' Through Unit 7 Power Block

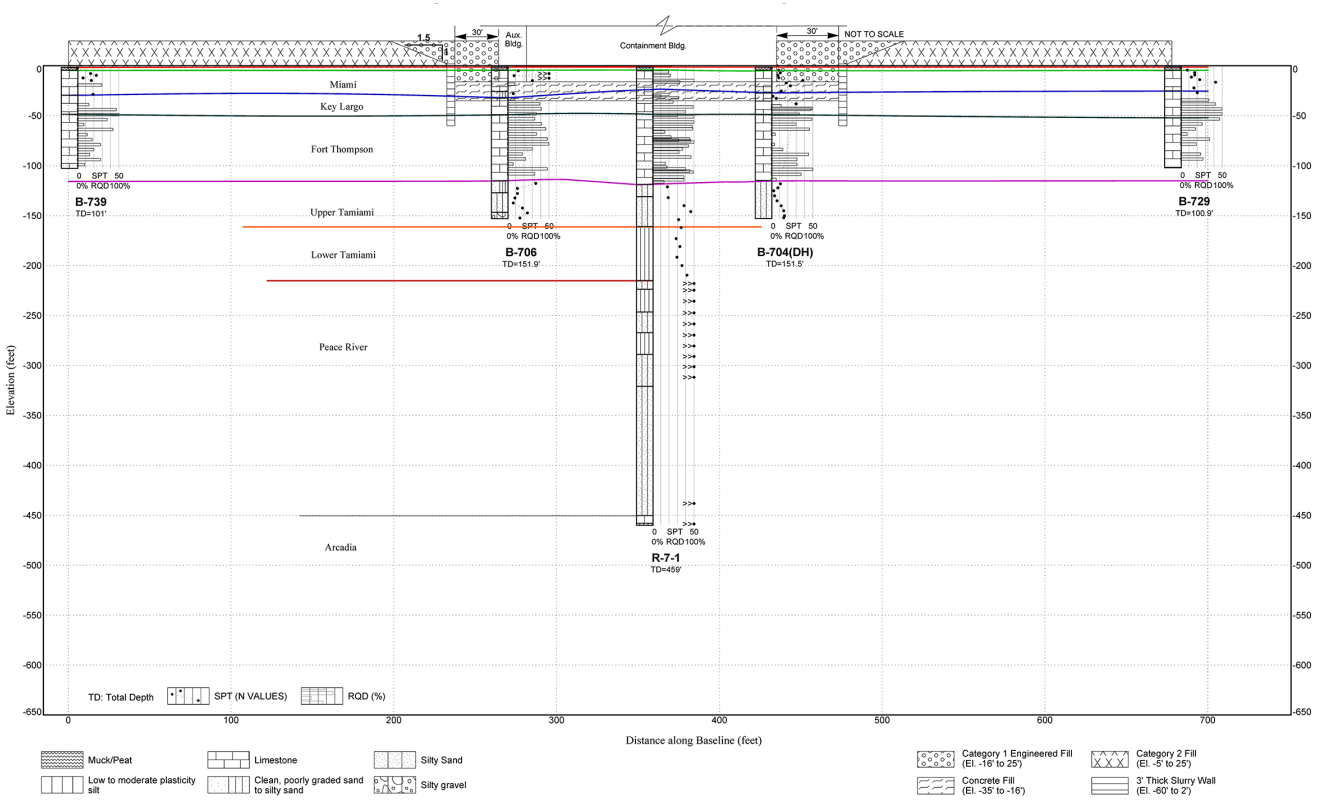

Data from References 257 and 290.
Note: Please see Figure 2.5.4-209 for location of geotechnical profile line B-B'

PTN COL 2.5-1
PTN COL 2.5-5
PTN COL 2.5-6
PTN COL 2.5-7
PTN COL 2.5-10

Figure 2.5.4-208 Geotechnical Cross Section C-C' Through Unit 7 Power Block

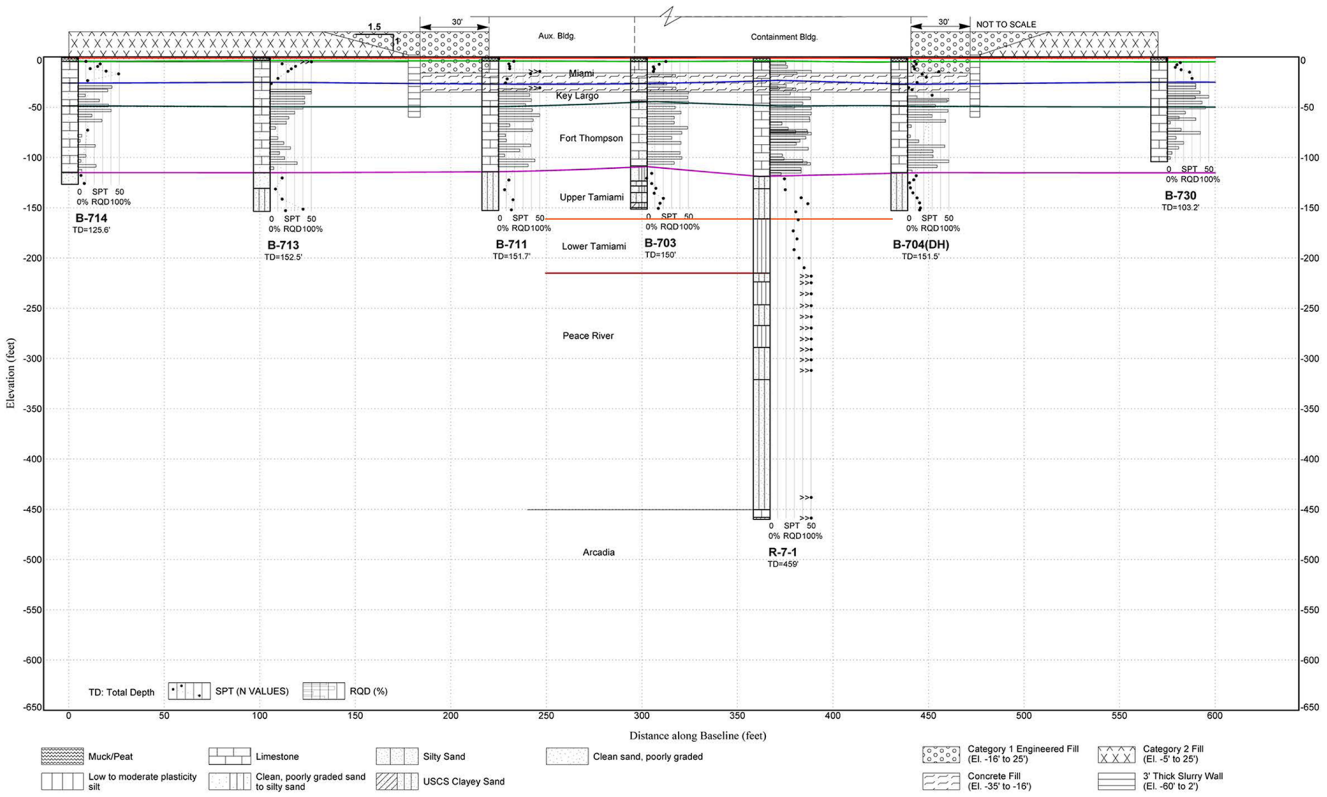

Data from References 257 and 290.
Note: Please see Figure 2.5.4-209 for location of geotechnical profile line C-C'

PTN COL 2.5-1
PTN COL 2.5-5
PTN COL 2.5-6
PTN COL 2.5-8

Figure 2.5.4-209 Plan Showing Geotechnical Cross Section Locations

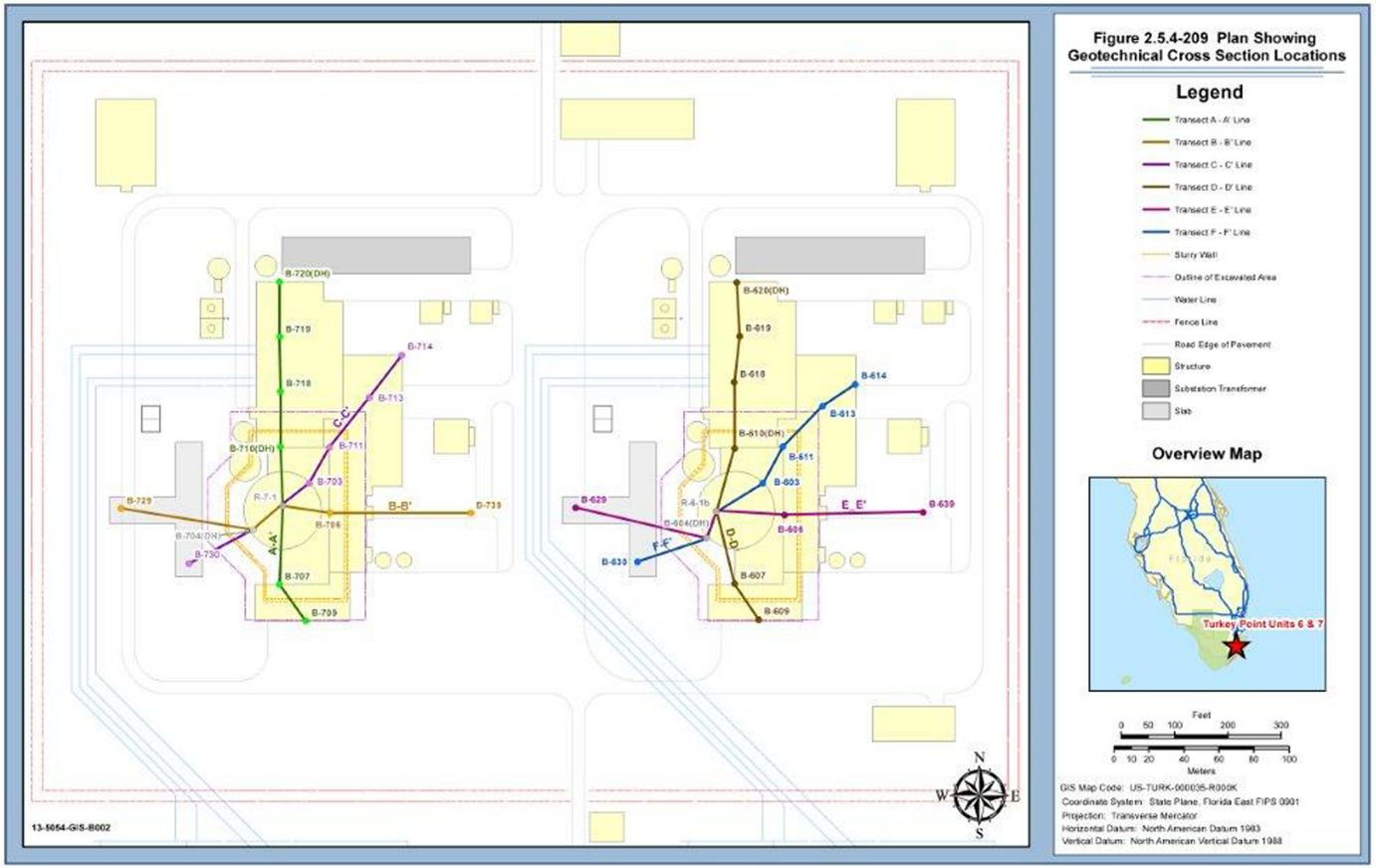

PTN COL 2.5-2
PTN COL 2.5-6

Figure 2.5.4-210 Sonic Log Locations

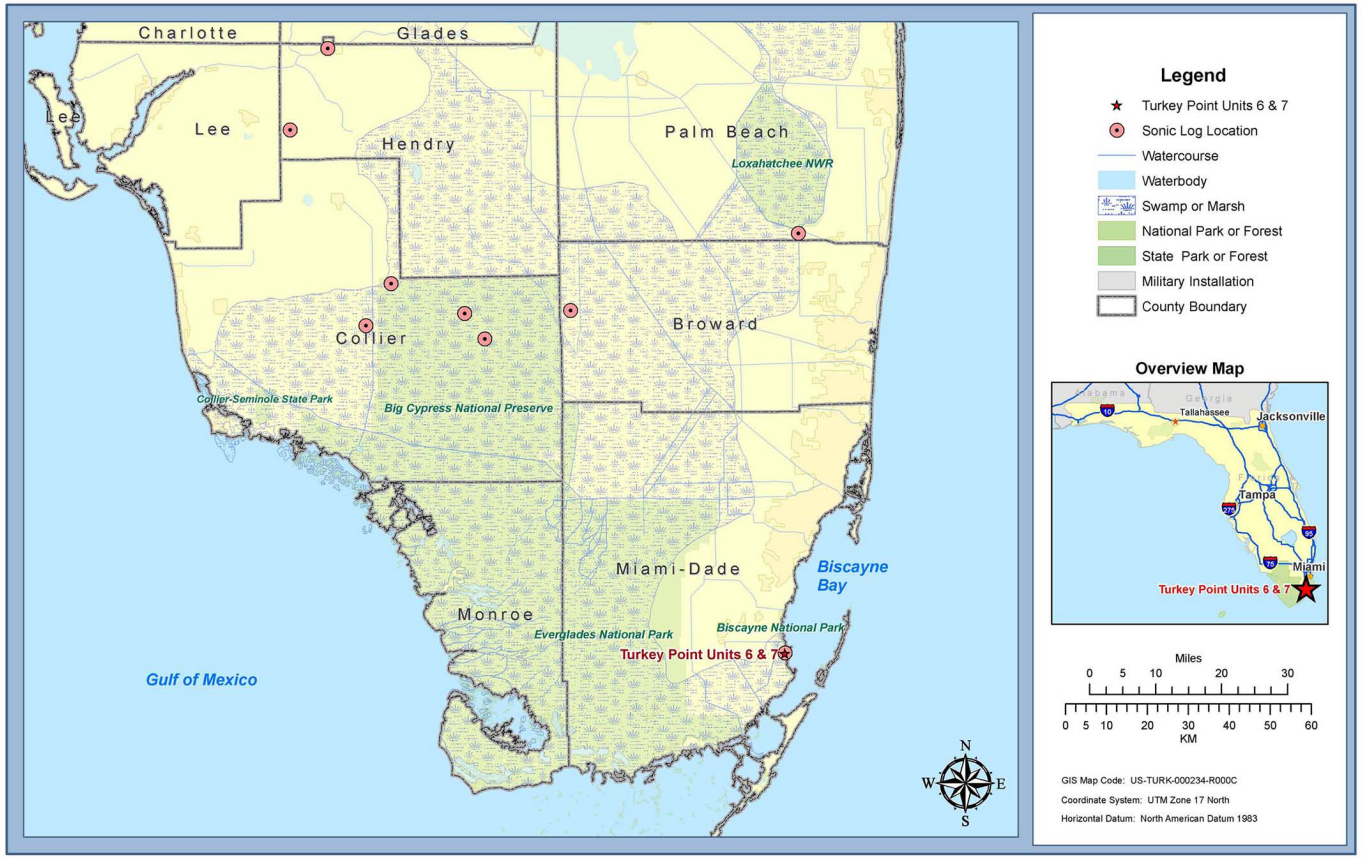

PTN COL 2.5-2
PTN COL 2.5-6

Figure 2.5.4-211 Shear Wave Velocity at Greater Depth

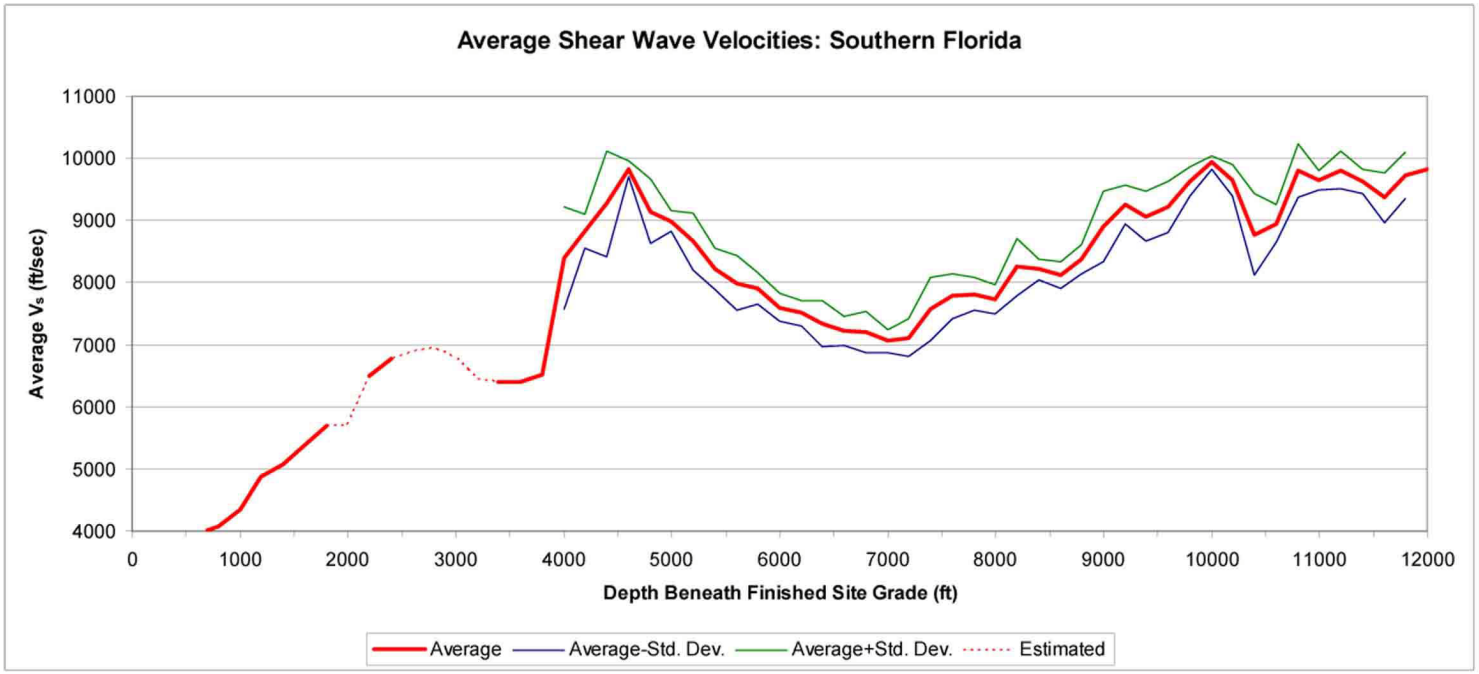

Note: The finished grade is El. 25.5 feet at the nuclear island.

PTN COL 2.5-6

Figure 2.5.4-212 Plot of Uncorrected SPT N-Values with Elevation

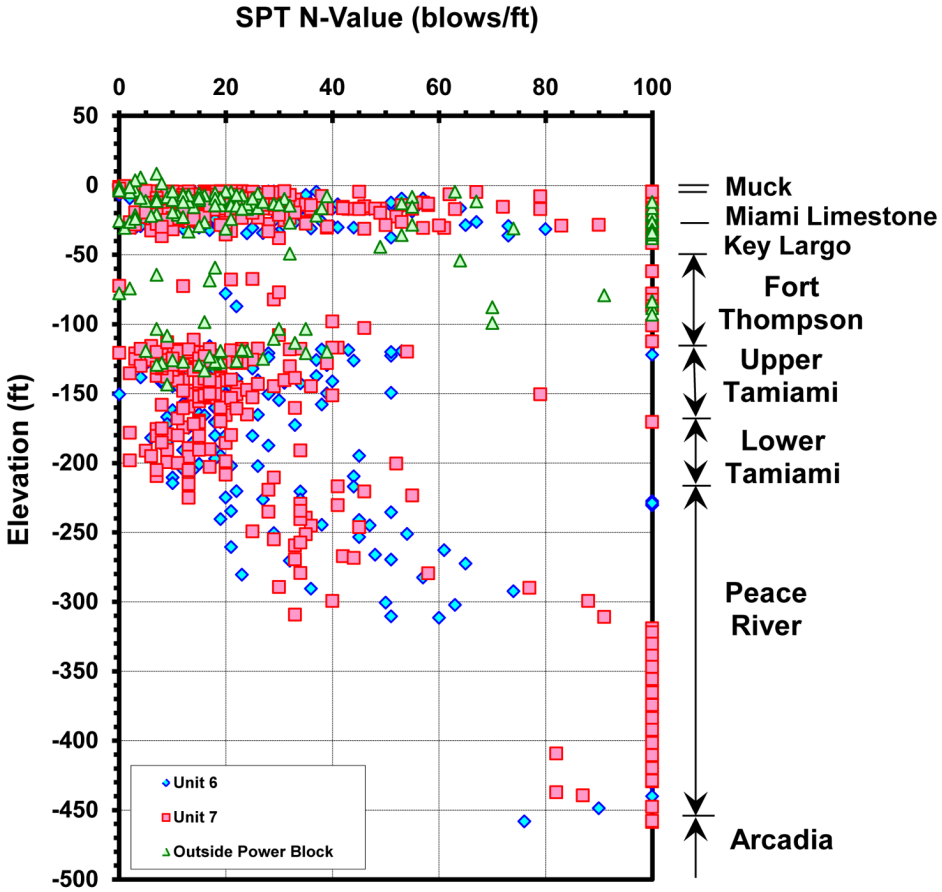

Data from References 257 and 290.
Note: Elevation is NAVD 88

PTN COL 2.5-6

Figure 2.5.4-213 Plot of Corrected SPT-N_{60} Values with Elevation

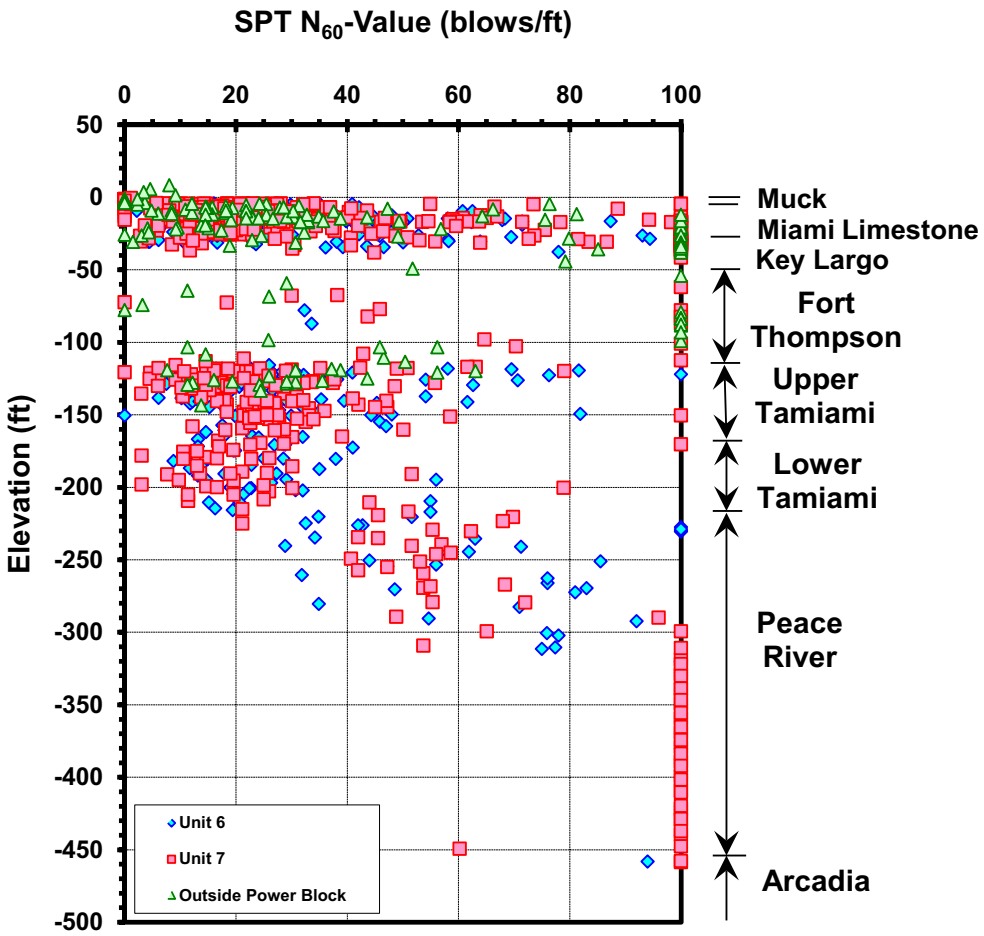

Data from References 257 and 290.
Note: Elevation is NAVD 88

PTN COL 2.5-6

Figure 2.5.4-214 Plot of CPT Data with Elevation

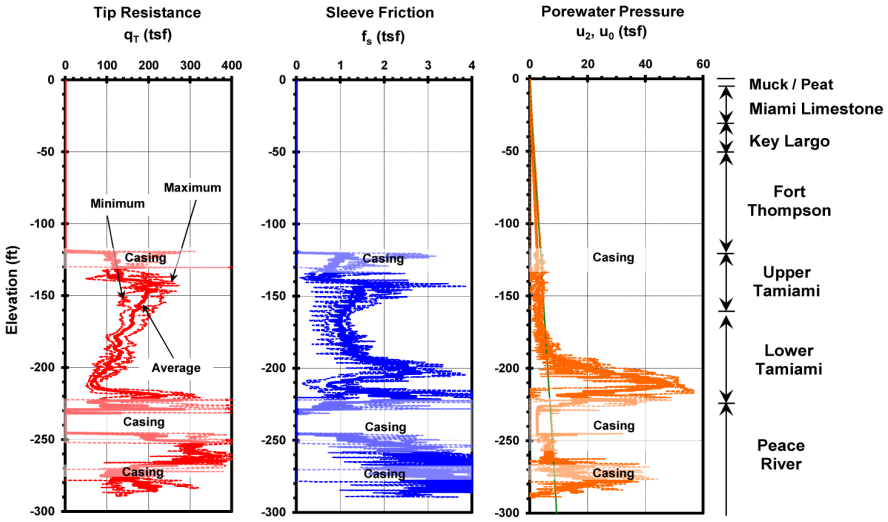

Data from References 257 and 290.

Notes:

CPT started at depth of 120–130 feet in each of the six probes

Rock coring was required to advance some of the CPTs between approximate El. –120 and El. –130 feet, El. –220 and El. –250 feet, and El. –270 and El. –280 feet

u_2 is the porewater pressure measured by CPT

u_0 is the static porewater pressure

PTN COL 2.5-6

Figure 2.5.4-215 Plot of Rock RQD Data with Elevation (Sheet 1 of 2)

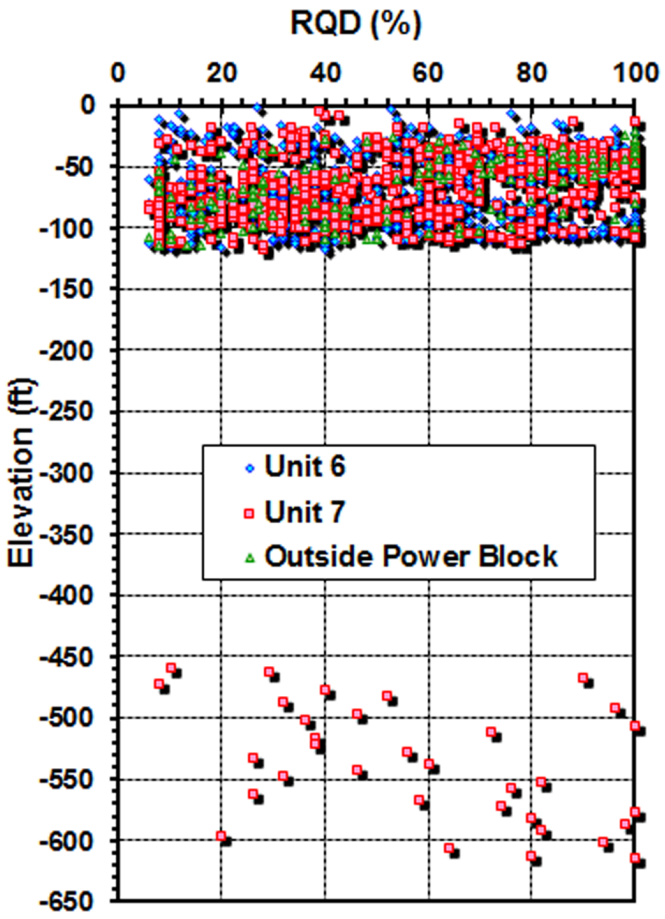

Data from References 257 and 290.

PTN COL 2.5-6

Figure 2.5.4-215 Plot of Rock RQD Data with Elevation (Sheet 2 of 2)

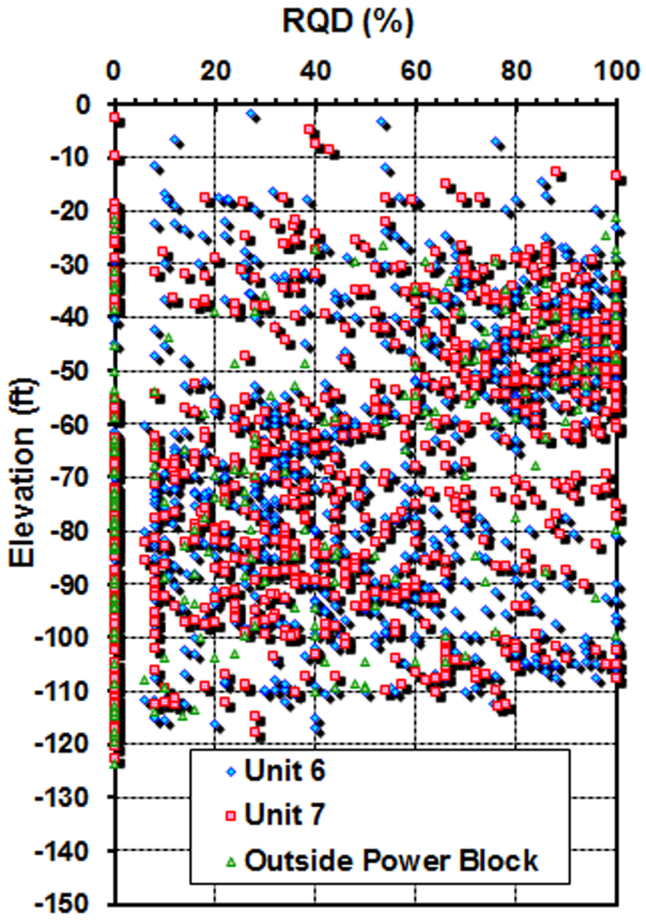

Data from References 257 and 290.

PTN COL 2.5-6

Figure 2.5.4-216 Plot of Fines Content with Elevation

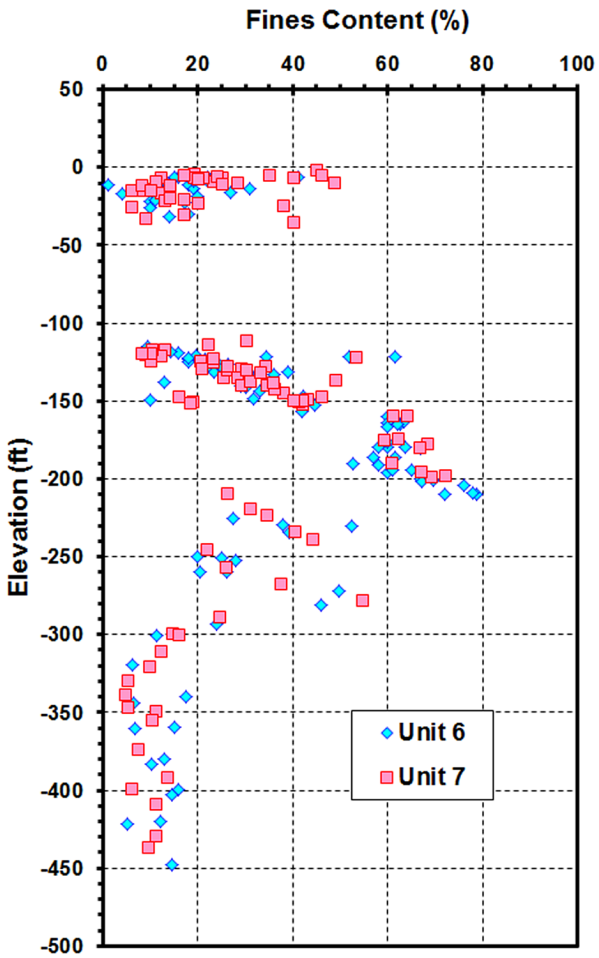

Data from References 257 and 290.

Notes:

Fines contents were tested from samples collected using SPT and thin-walled tube equipment.

Fines content is the percent of the sample passing the standard number 200 sieve.

Excludes fines content data from surficial muck samples collected using a McCauley Sampler in the supplemental investigation.

PTN COL 2.5-6

Figure 2.5.4-217 Plot of Rock Unconfined Compressive Strength with Elevation

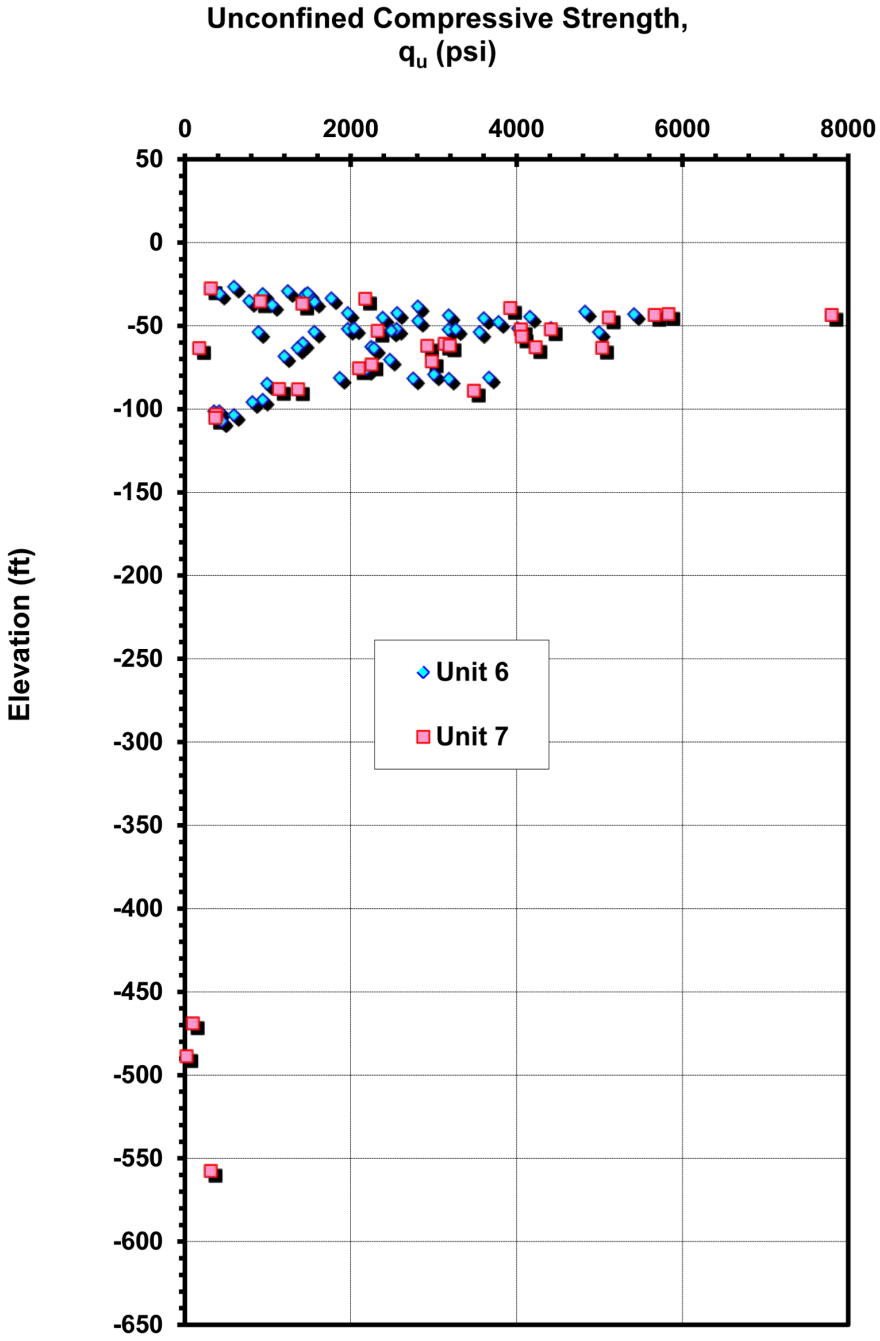

Data from References 257 and 290.

PTN COL 2.5-6

Figure 2.5.4-218 Plot of Shear Wave Velocity Measurements with Elevation

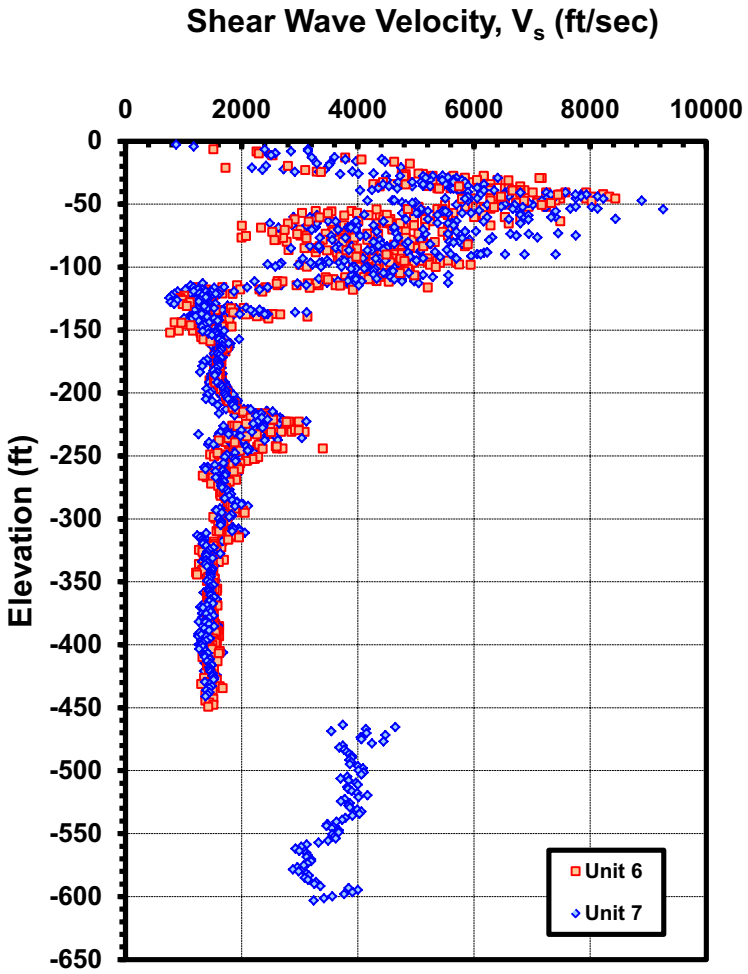

Data from References 257 and 290.

PTN COL 2.5-6

Figure 2.5.4-219 Plot of Compression Wave Velocity with Elevation

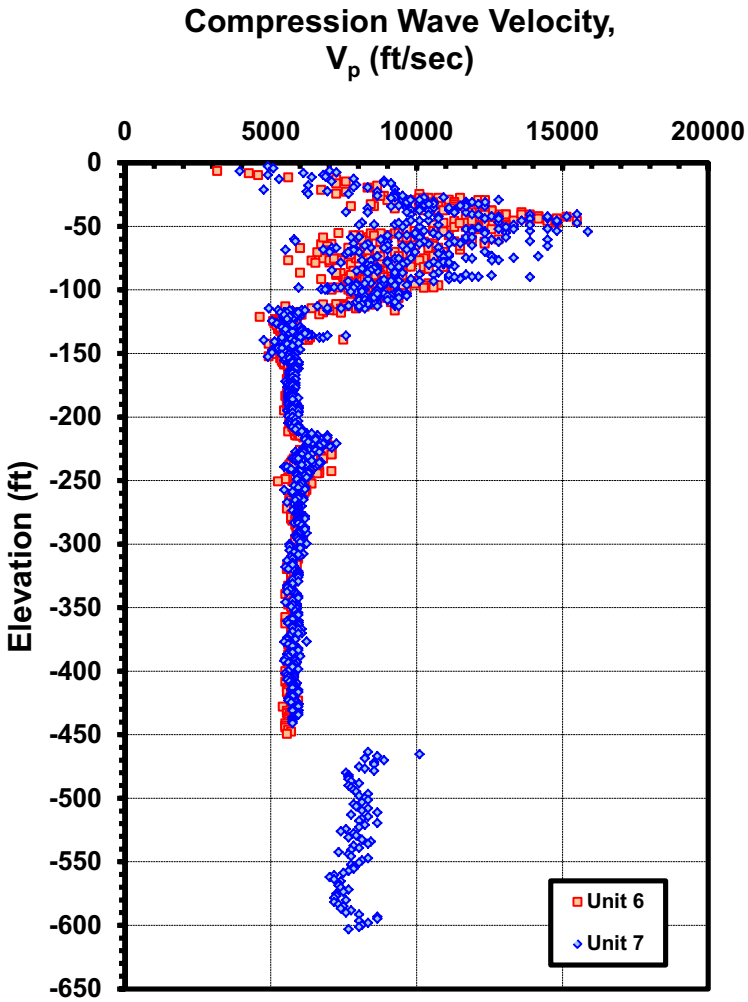

Data from References 257 and 290.

PTN COL 2.5-2
PTN COL 2.5-6

Figure 2.5.4-220 Plot of Recommended Shear Wave Velocity with Elevation

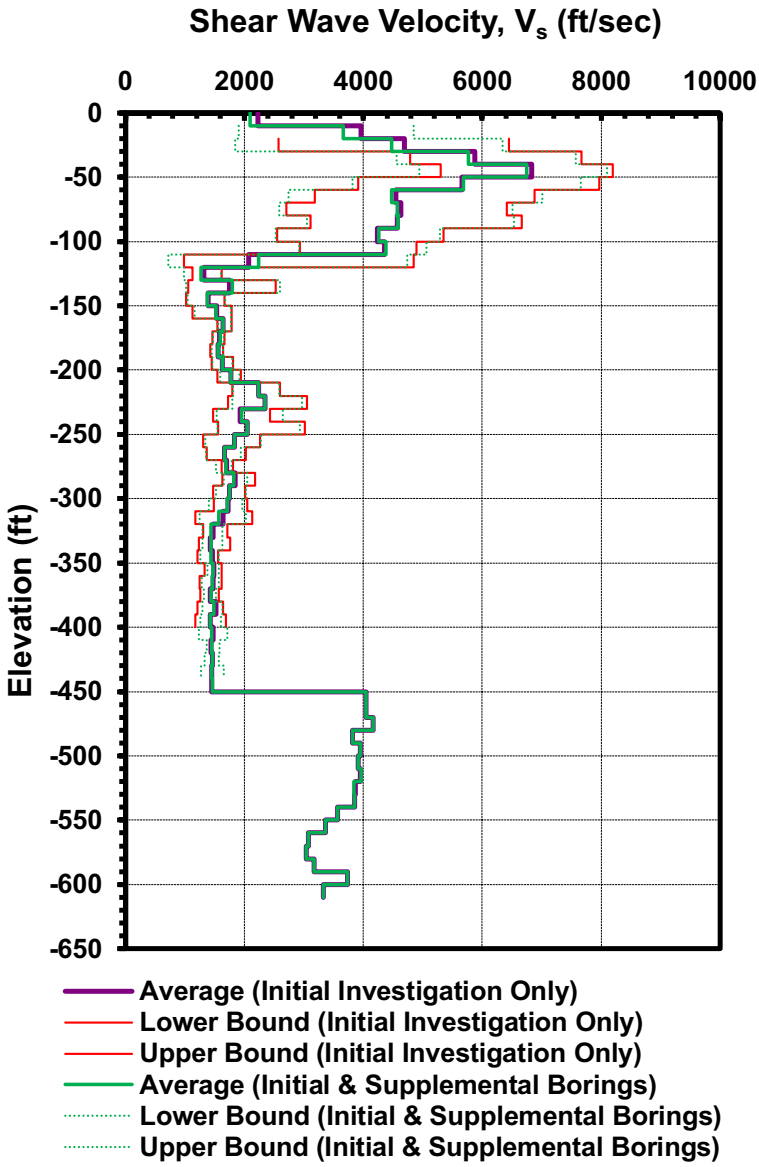

Data from References 257 and 290.
Note: Average and boundary values above contain both Unit 6 and Unit 7 measurements.

PTN COL 2.5-5
PTN COL 2.5-6
PTN COL 2.5-7

Figure 2.5.4-221 Profile of Site Grading

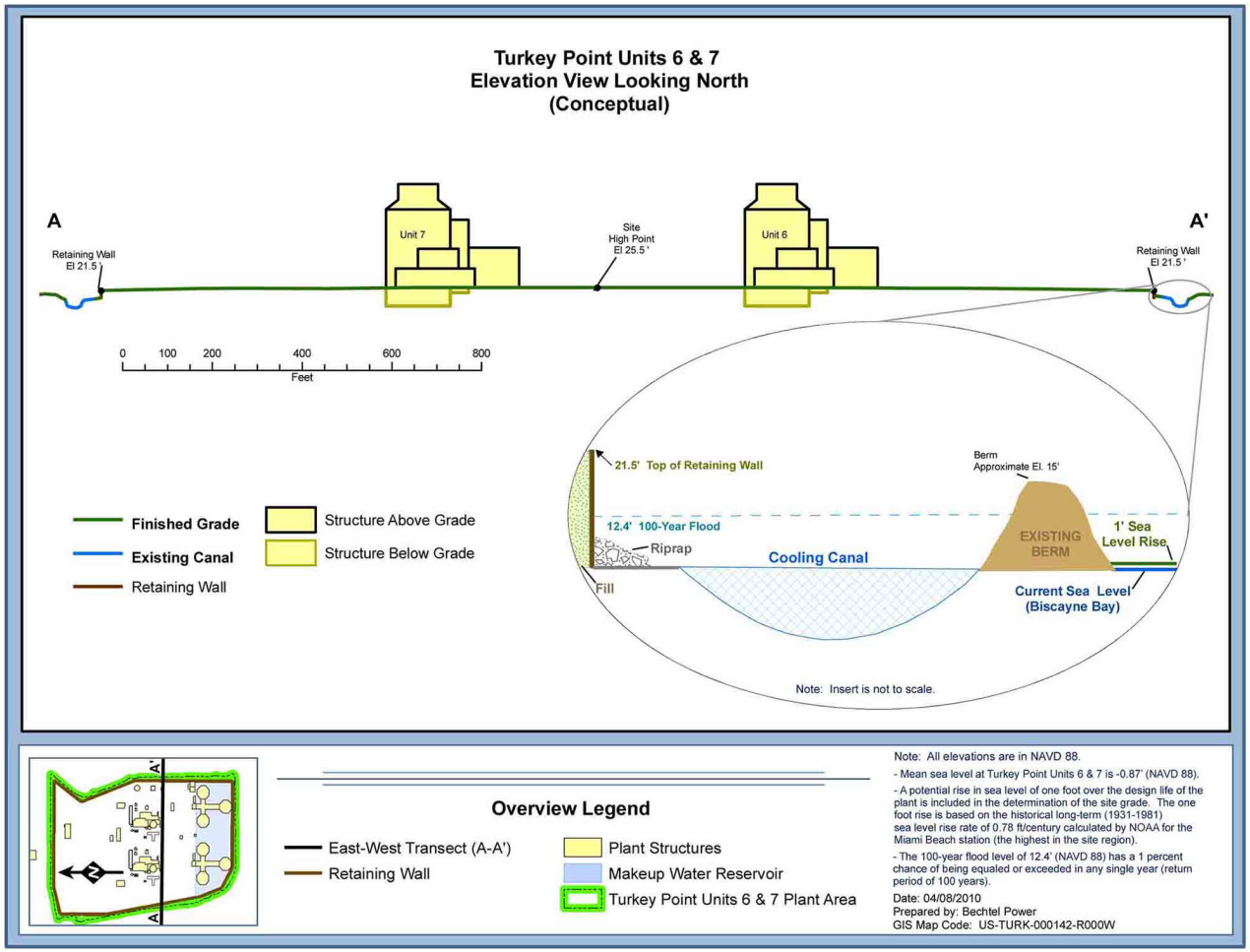

PTN COL 2.5-5
PTN COL 2.5-6
PTN COL 2.5-7
PTN COL 2.5-12
PTN COL 2.5-16

Figure 2.5.4-222 Excavation at Power Block

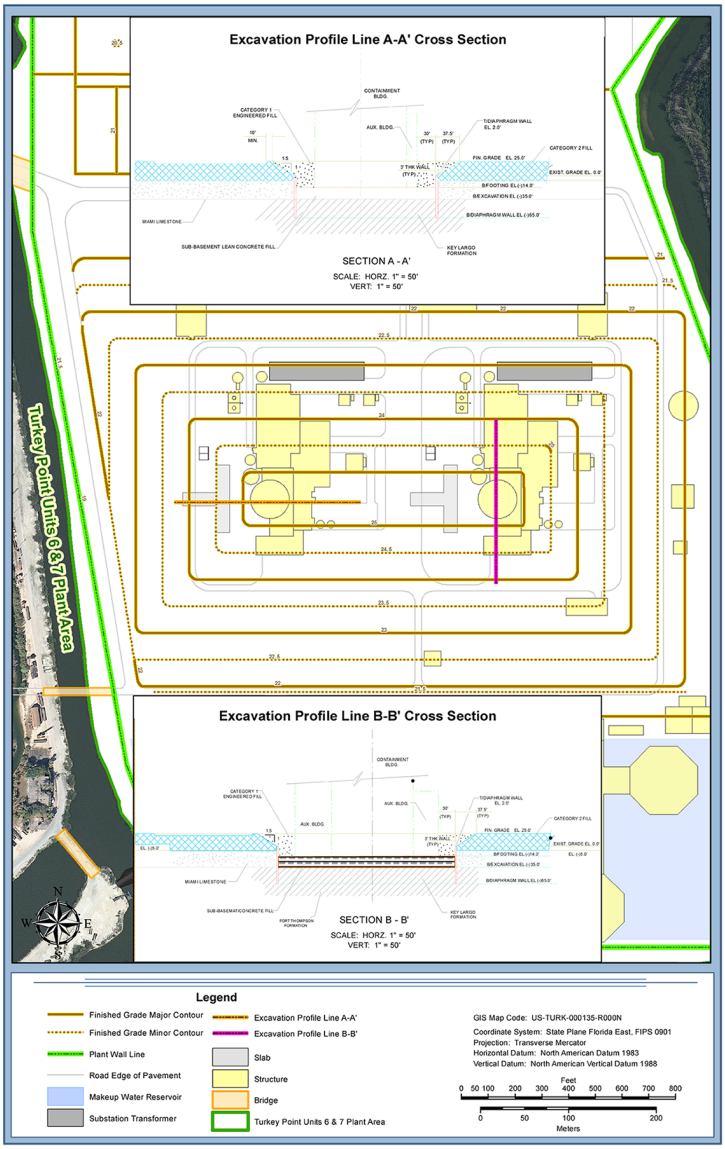

Figure 2.5.4-223 Geophysical Survey Lines

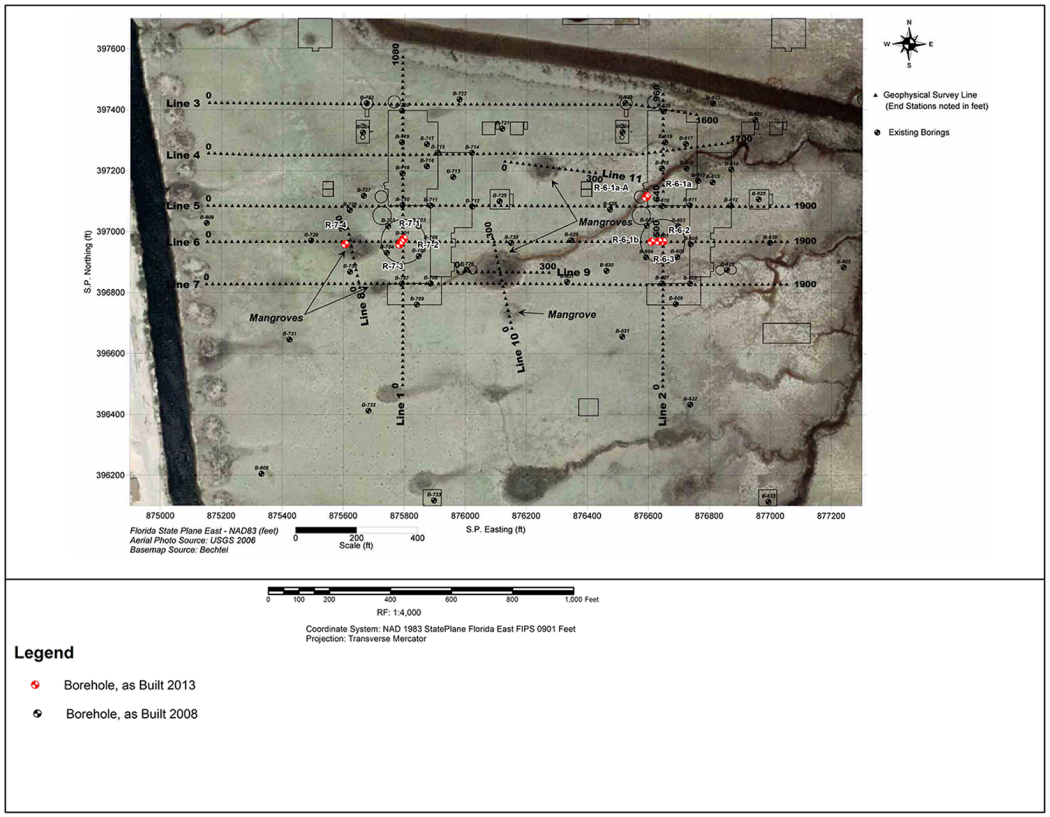

Figure 2.5.4-224 Microgravity Models for Water-Filled Spherical Cavities in Limestone (Sheet 1 of 2)

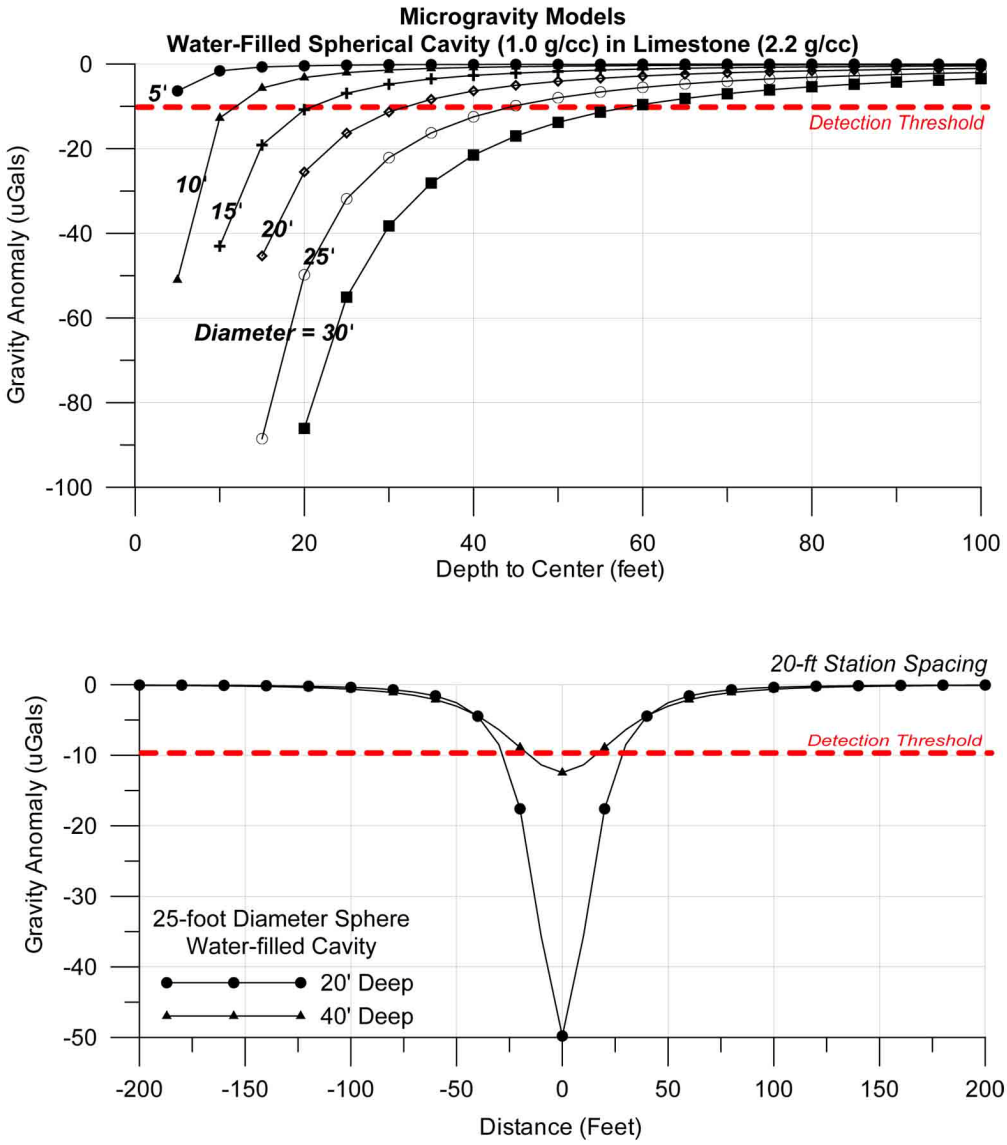

Figure 2.5.4-224 Microgravity Models for Water-Filled Spherical Cavities in Limestone (Sheet 2 of 2)

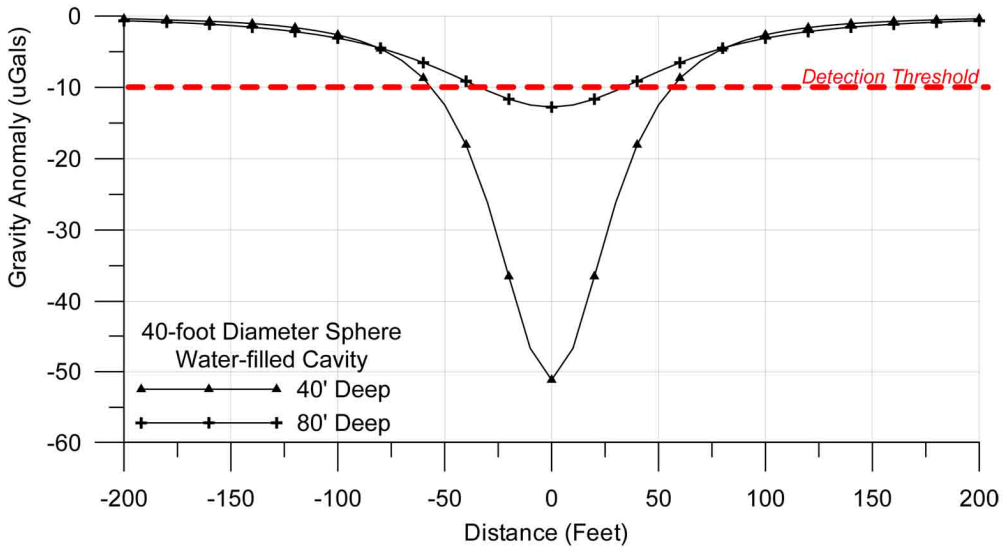

Figure 2.5.4-225 Microgravity Models for Water-Filled Horizontal Conduits in Limestone

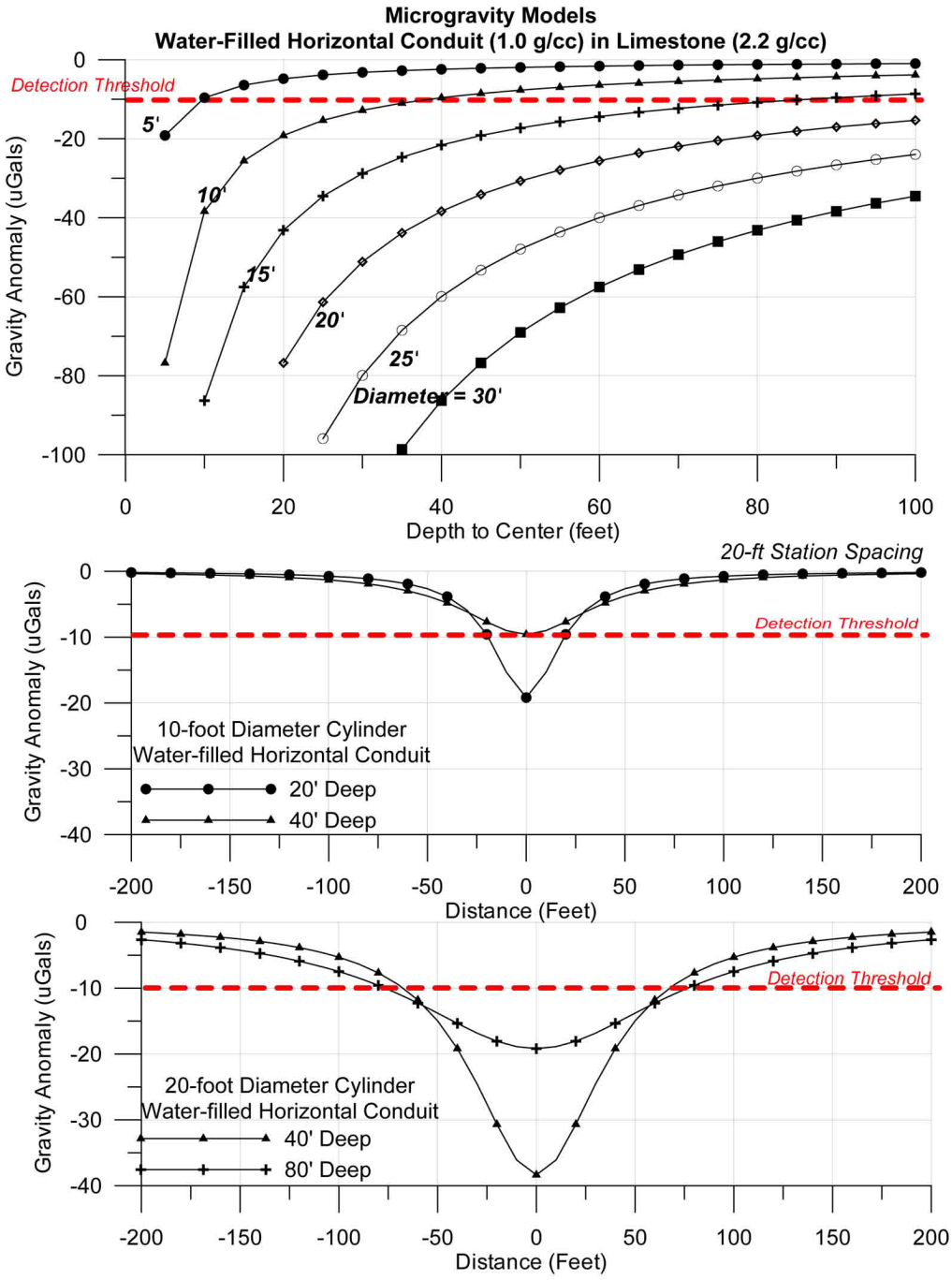

Figure 2.5.4-226 Line 5 Geophysical Data

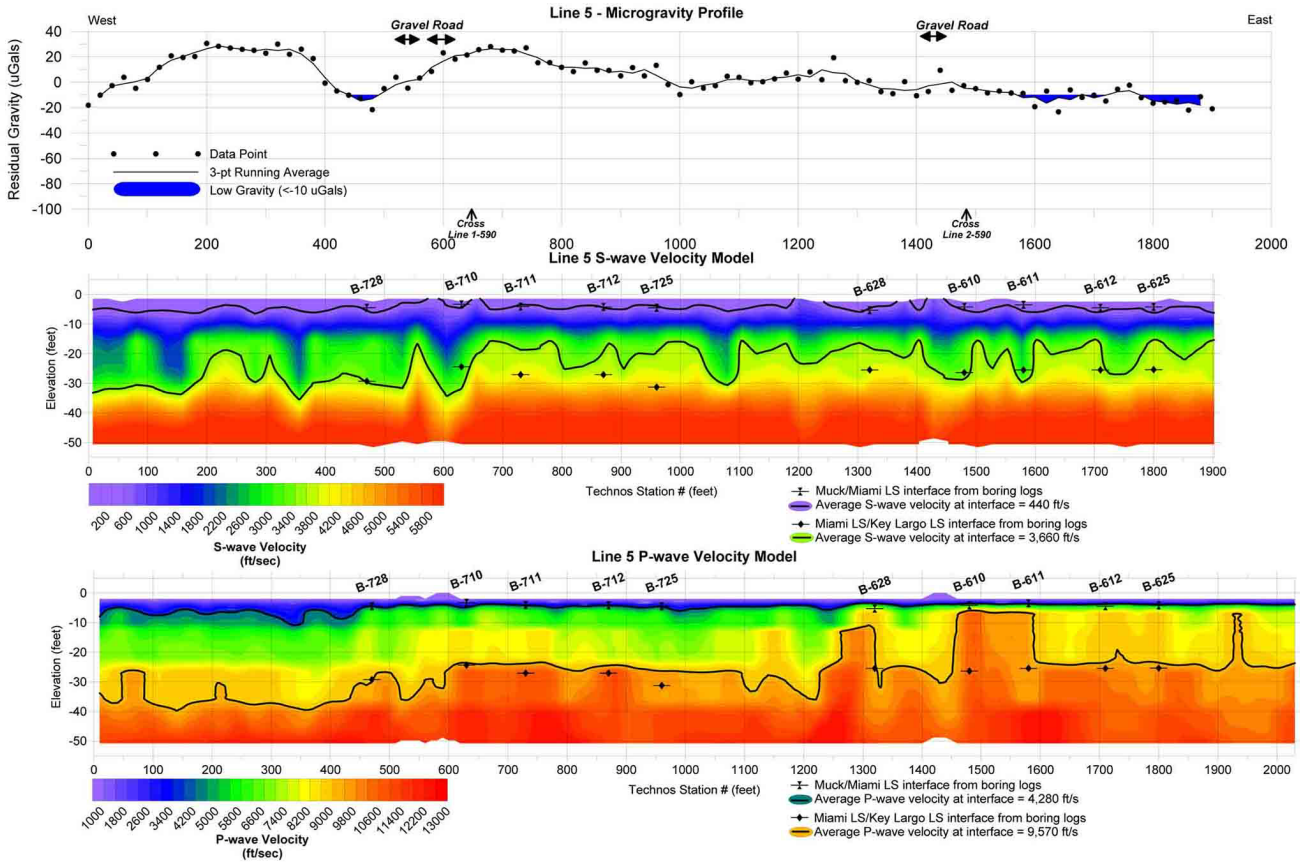

Figure 2.5.4-227 Line 9 Geophysical Data

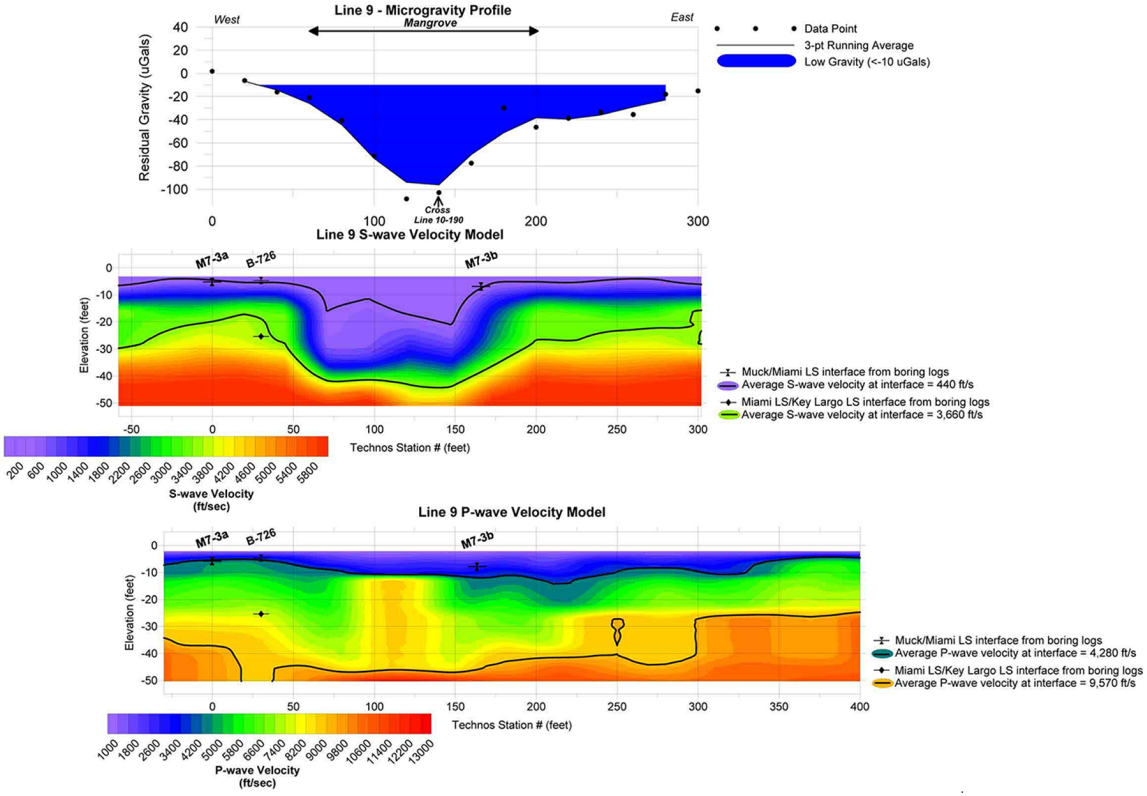

Figure 2.5.4-228 Microgravity Contour Map

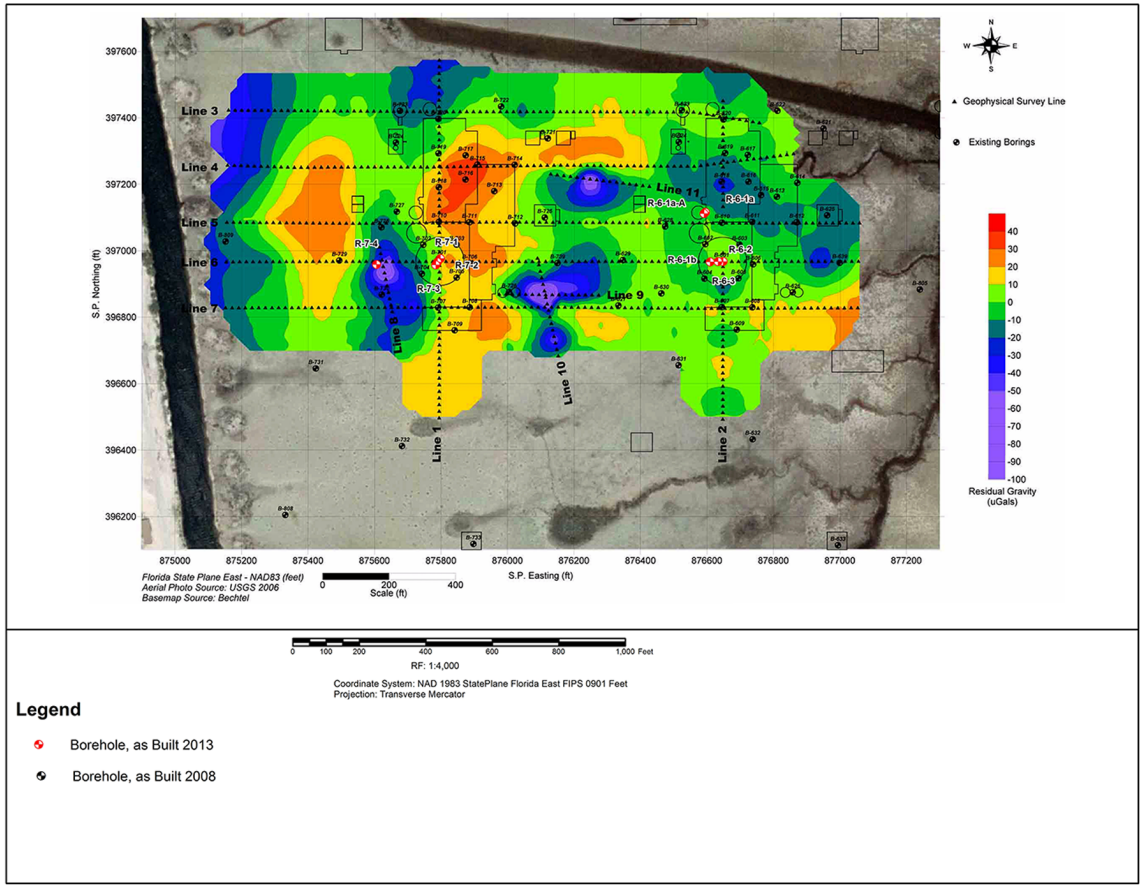

PTN COL 2.5-9

Figure 2.5.4-229 Line 9 Microgravity Model

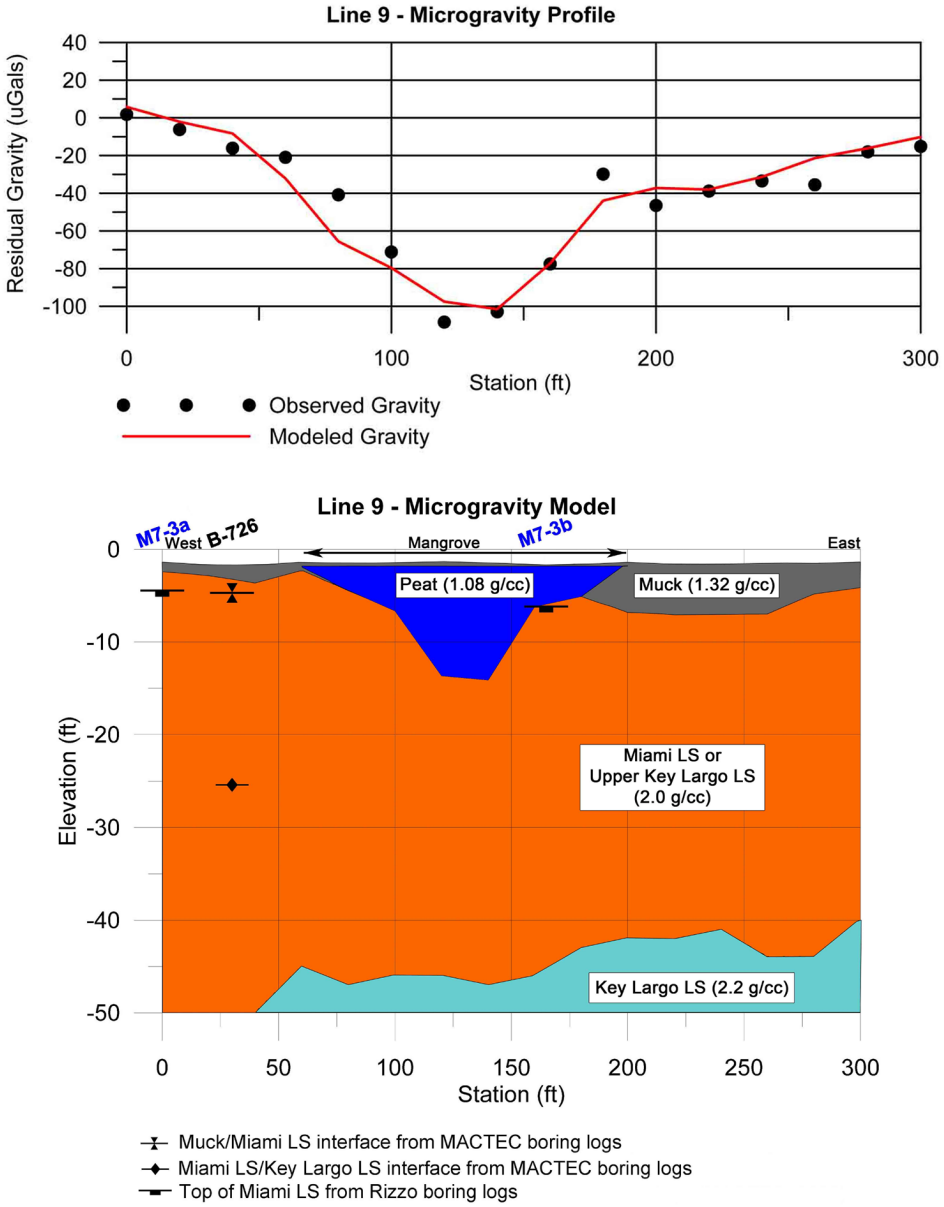

References 257 and 290.

Figure 2.5.4-230 Line 5 Microgravity Model

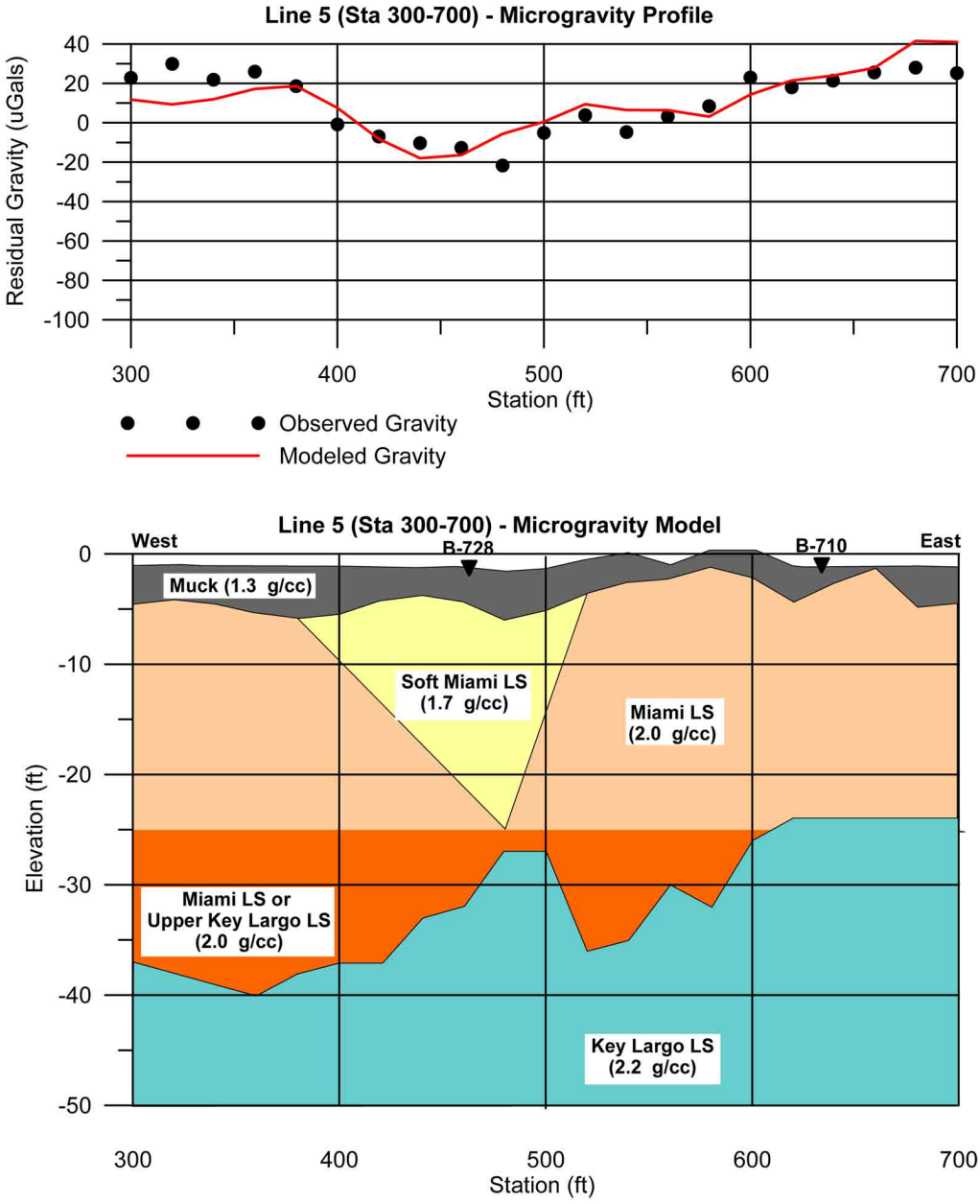

Figure 2.5.4-231 Microgravity Contour Map with Muck Effects Removed

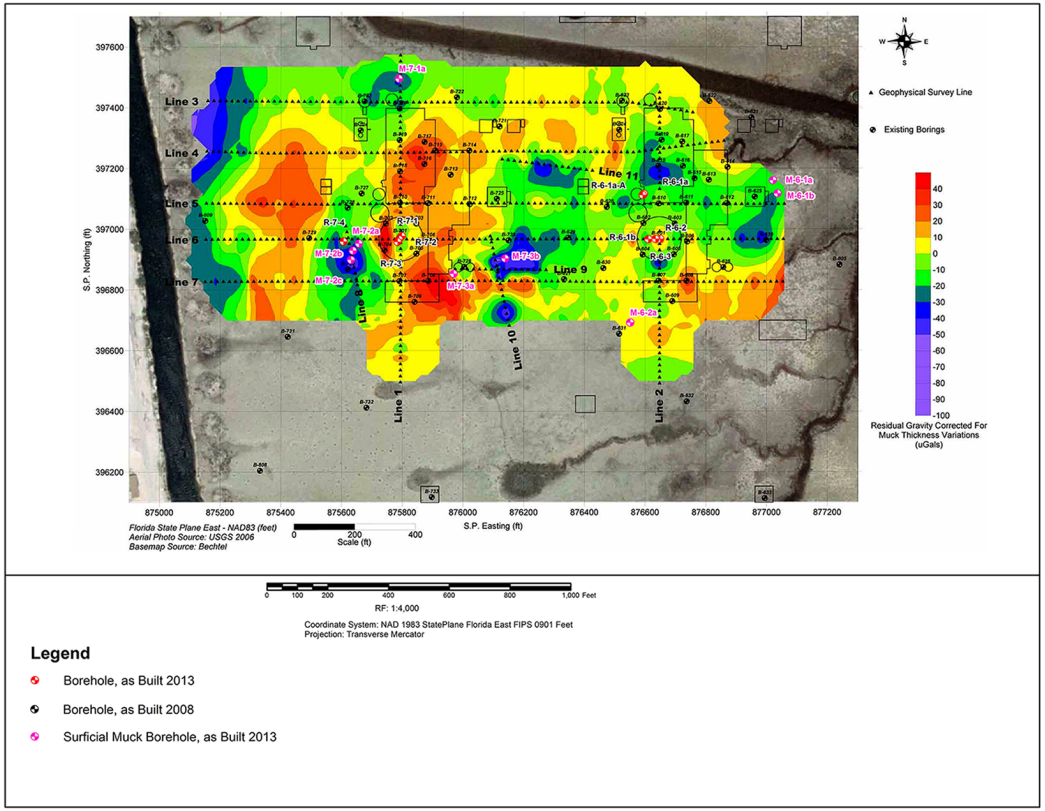

PTN COL 2.5-2
PTN COL 2.5-6

Figure 2.5.4-232 Shear Modulus Degradation for Key Largo Based on RCTS Testing

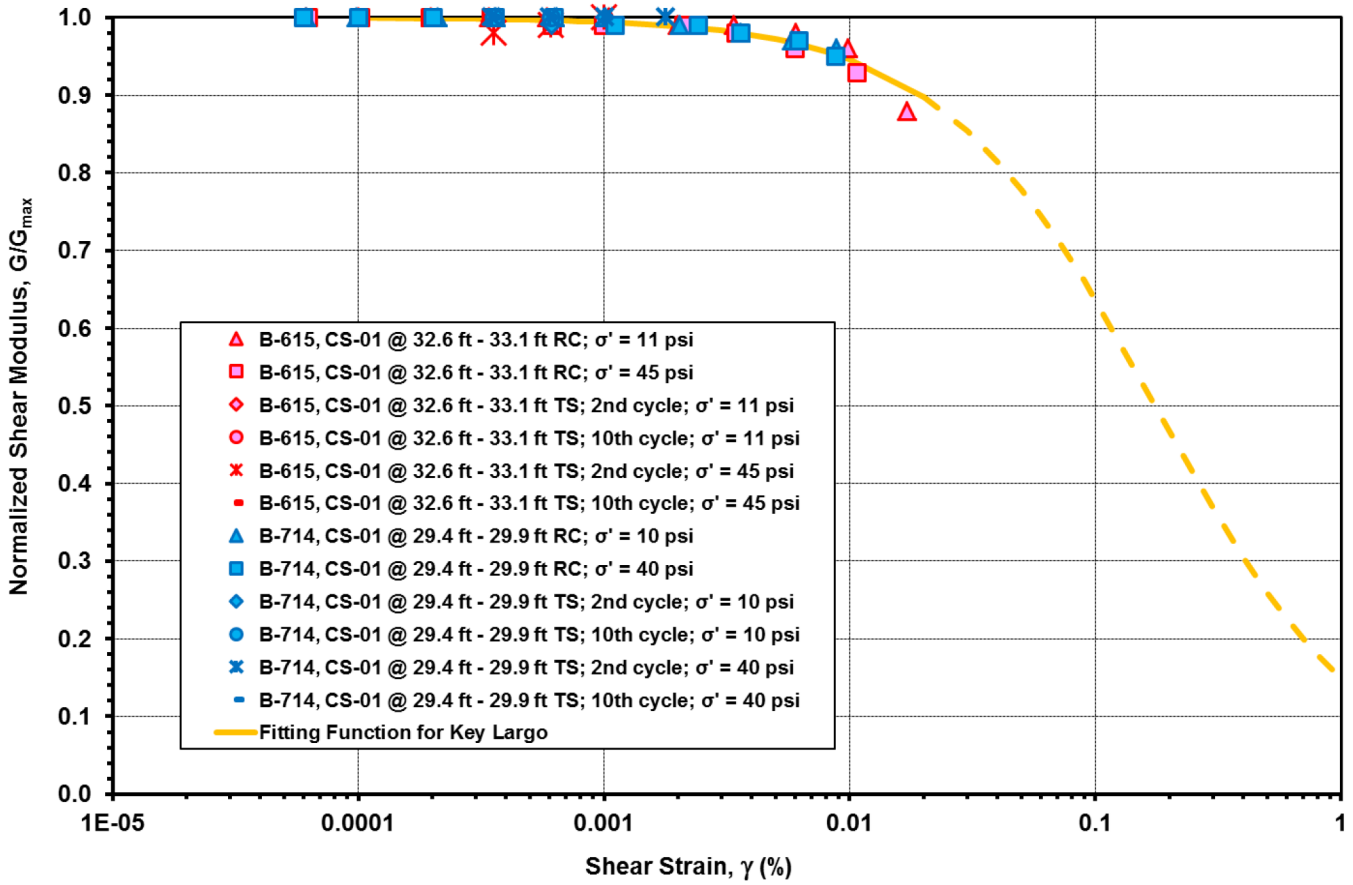

Data from References 257 and 290.

PTN COL 2.5-1
PTN COL 2.5-2
PTN COL 2.5-5
PTN COL 2.5-6
PTN COL 2.5-12
PTN COL 2.5-16

Figure 2.5.4-233 Recommended Shear Modulus Degradation Curves

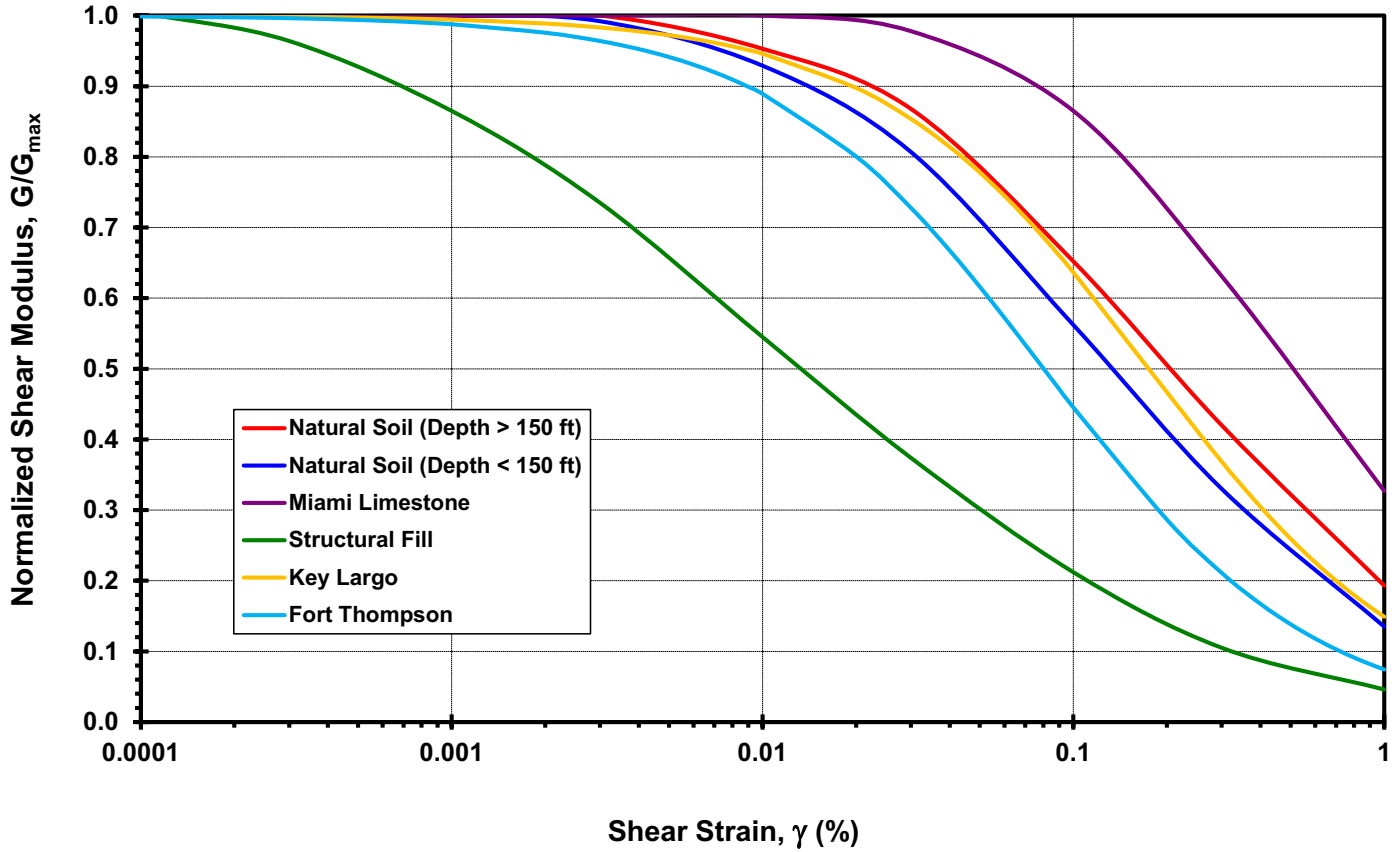

Data from References 257, 258, 259, 260, and 290.

PTN COL 2.5-1
PTN COL 2.5-2
PTN COL 2.5-5
PTN COL 2.5-6

Figure 2.5.4-234 Damping Curve Measurements for Key Largo and Fort Thompson Based on RCTS Testing

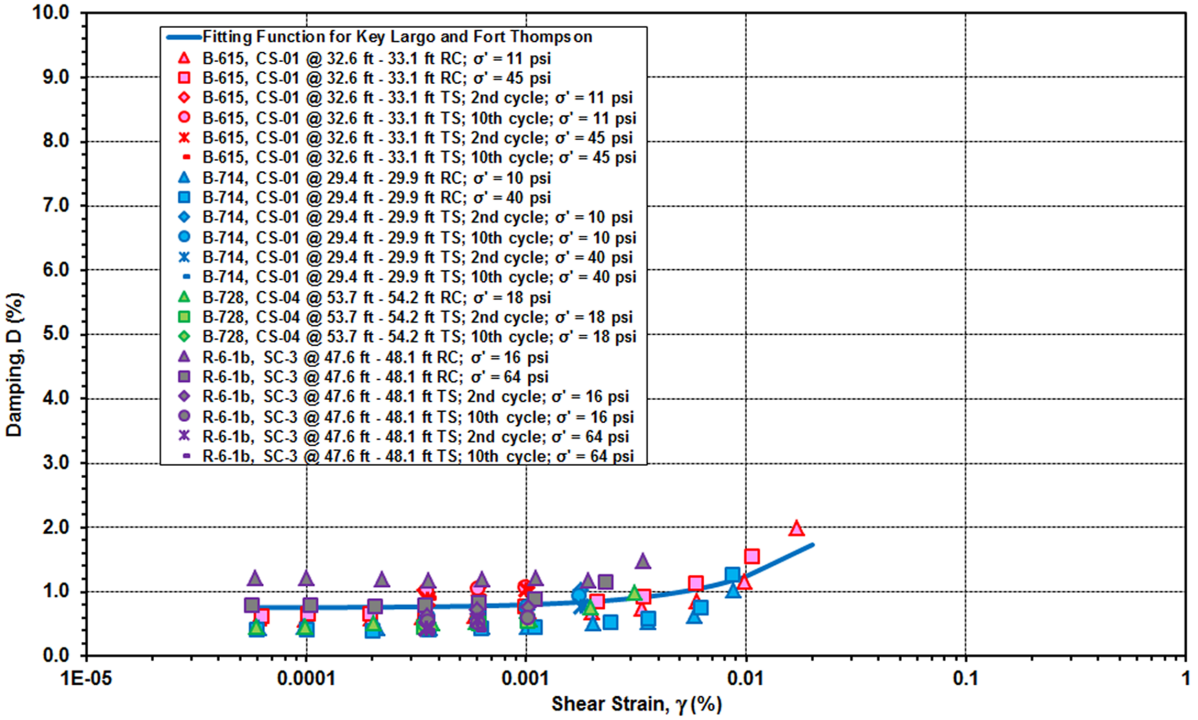

Data from References 257 and 290.

PTN COL 2.5-1
PTN COL 2.5-2
PTN COL 2.5-5
PTN COL 2.5-6

Figure 2.5.4-235 Recommended Damping Curves

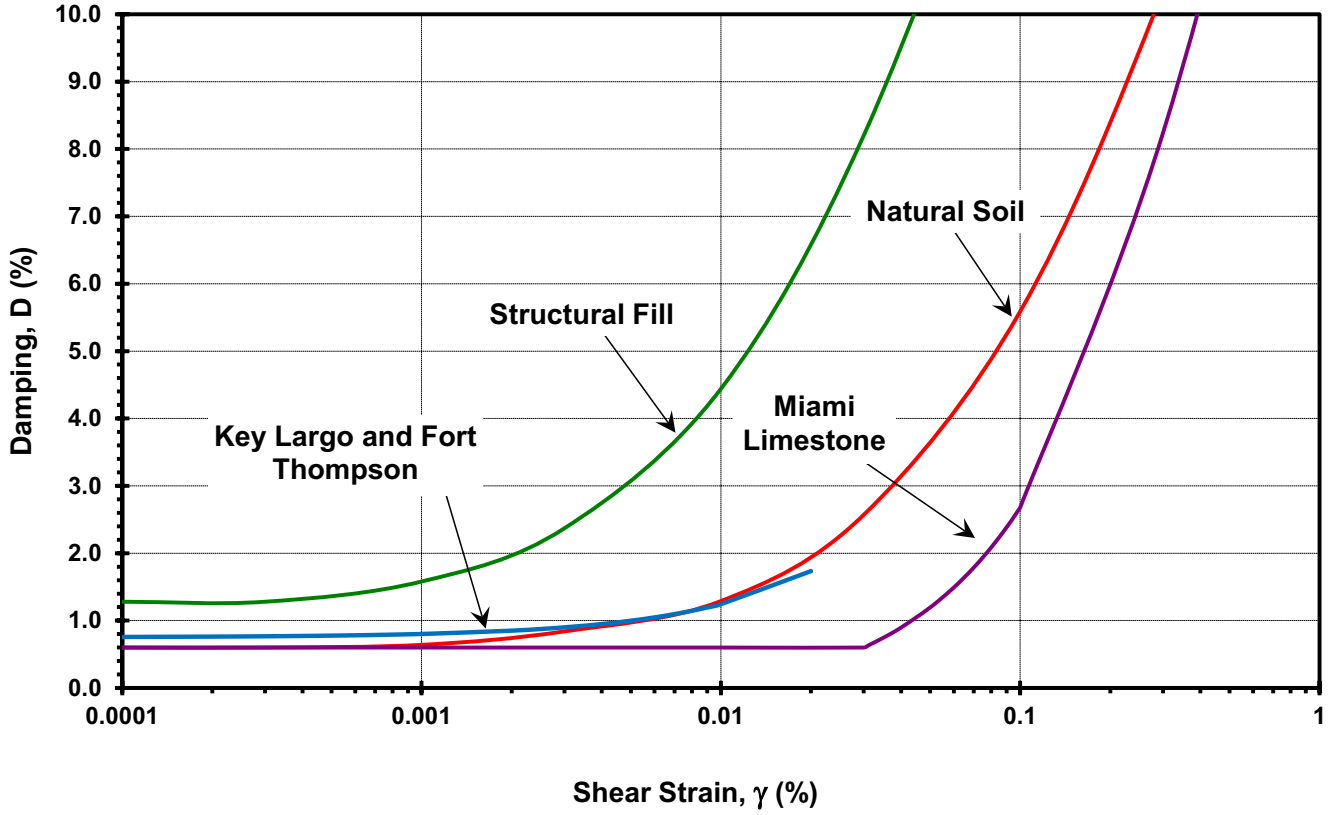

Data from References 257, 258, 259, 260, and 290.

PTN COL 2.5-2
PTN COL 2.5-6

Figure 2.5.4-236 Recommended Shear Wave Velocity and Shear Modulus for Fill

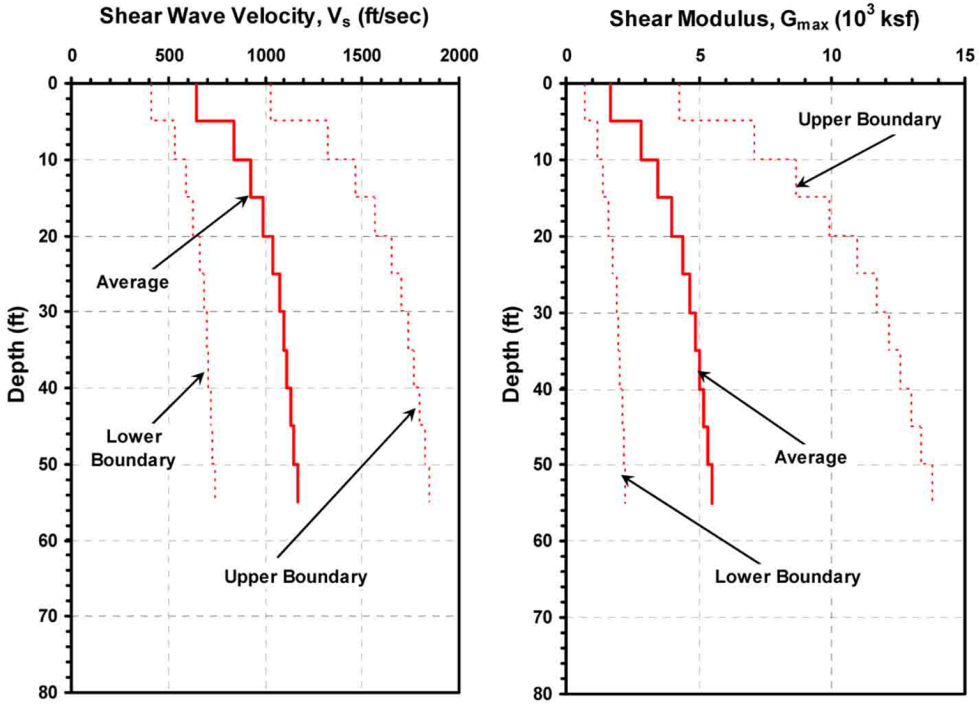

Data from Reference 257.

Figure 2.5.4-237 Not Used

PTN COL 2.5-9

Figure 2.5.4-238 FOS against Liquefaction Based on CPT Values

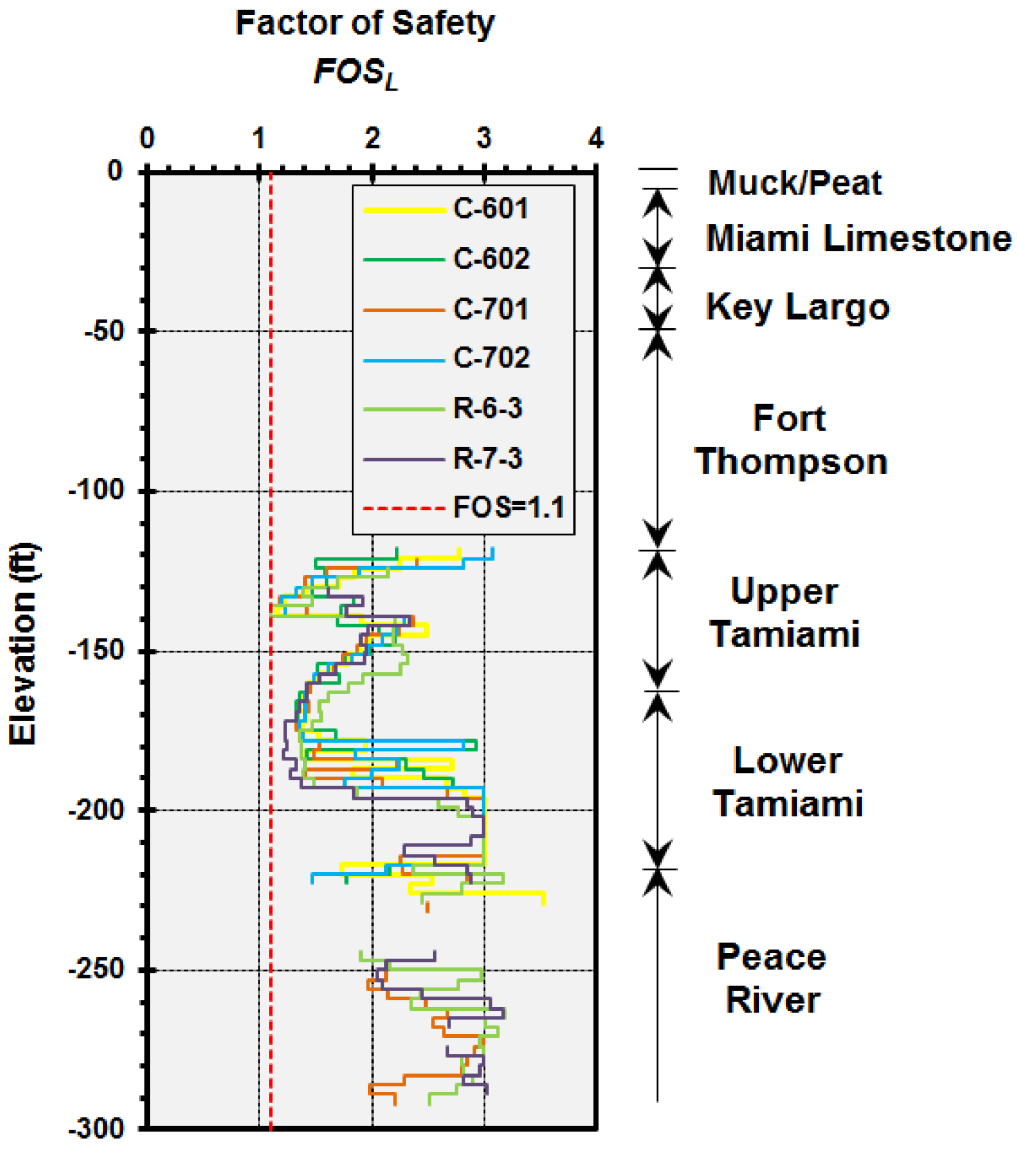

PTN COL 2.5-3
PTN COL 2.5-7
PTN COL 2.5-11

Figure 2.5.4-239 Active Earth Pressure Considering a 500 psf Surcharge on Fill

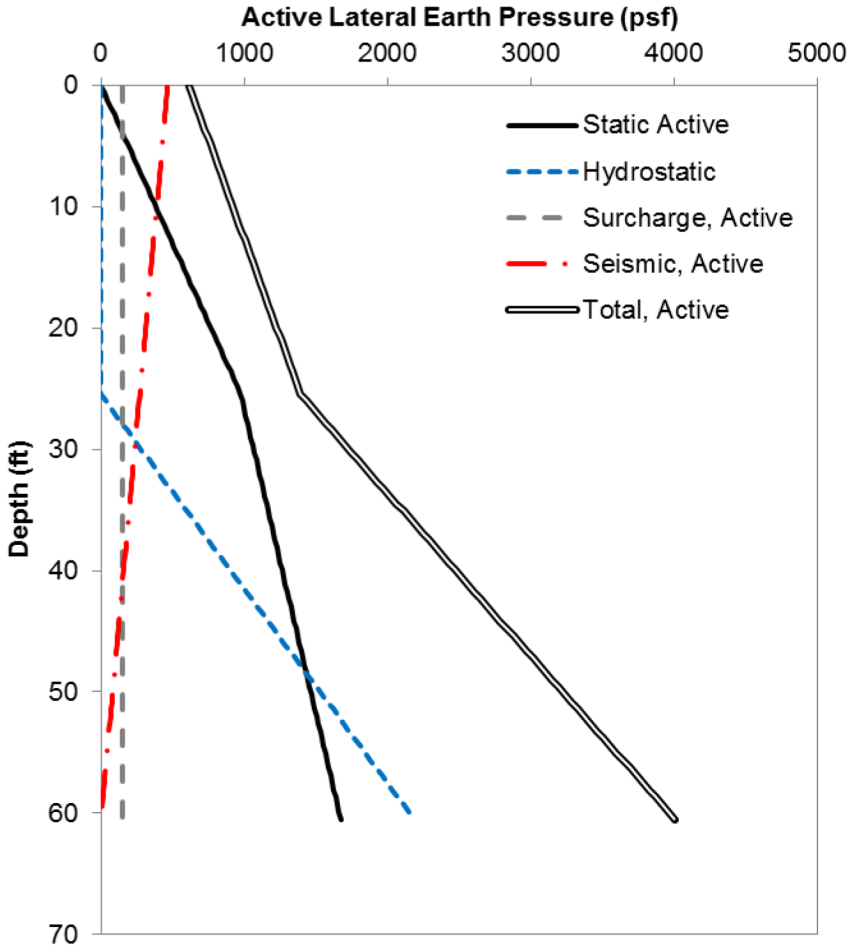

Data from Table 2.5.4-209 for compacted limerock fill.

PTN COL 2.5-3
PTN COL 2.5-7
PTN COL 2.5-11

Figure 2.5.4-240 At-Rest Earth Pressures Considering a 500 psf Surcharge on Fill

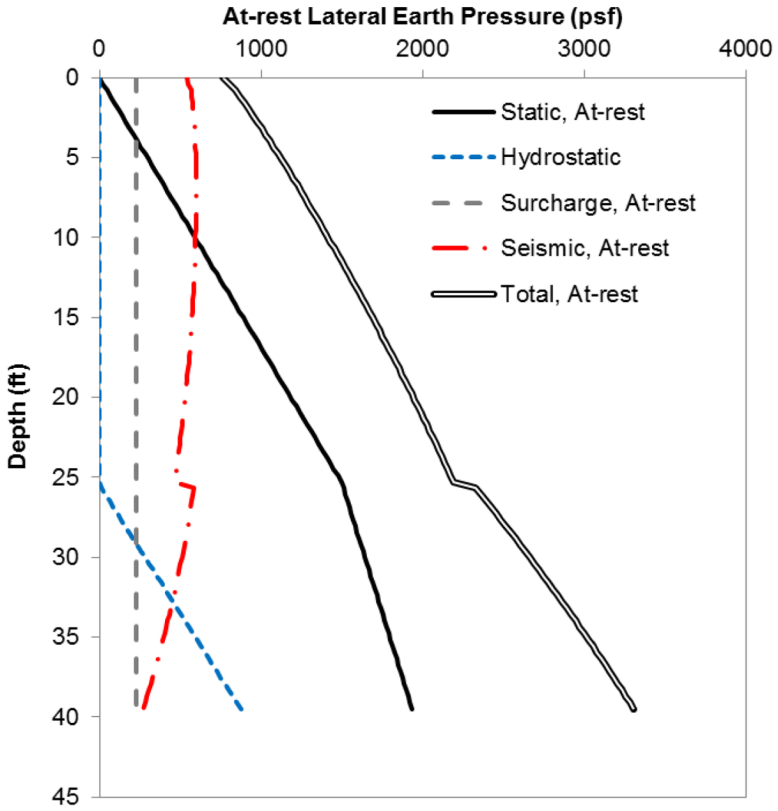

Data from Table 2.5.4-209 for compacted limerock fill.

Figure 2.5.4-241 Line 10 Geophysical Data

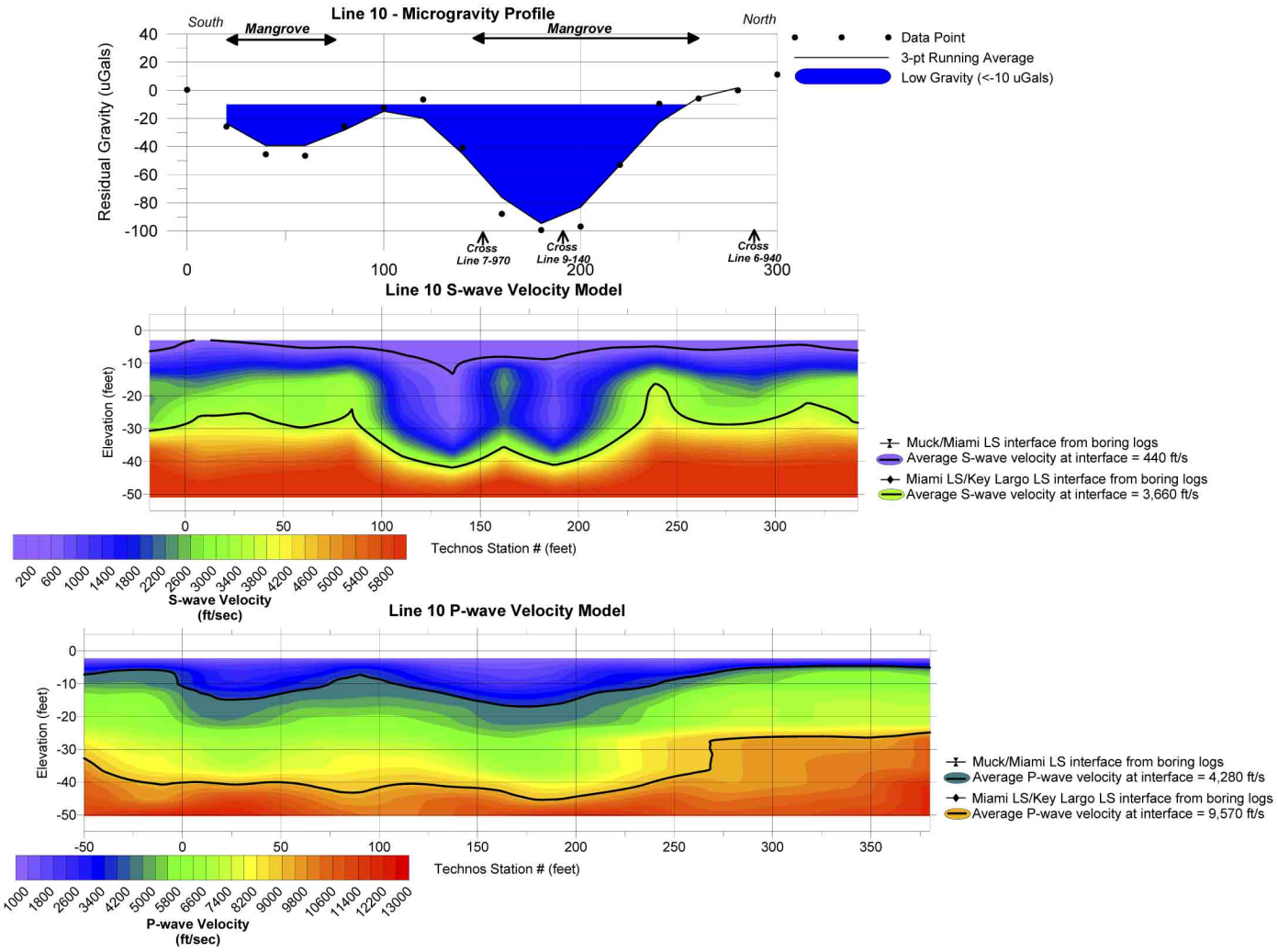

Source: Reference 286

Figure 2.5.4-242 EW-1 Location at the Turkey Point Site

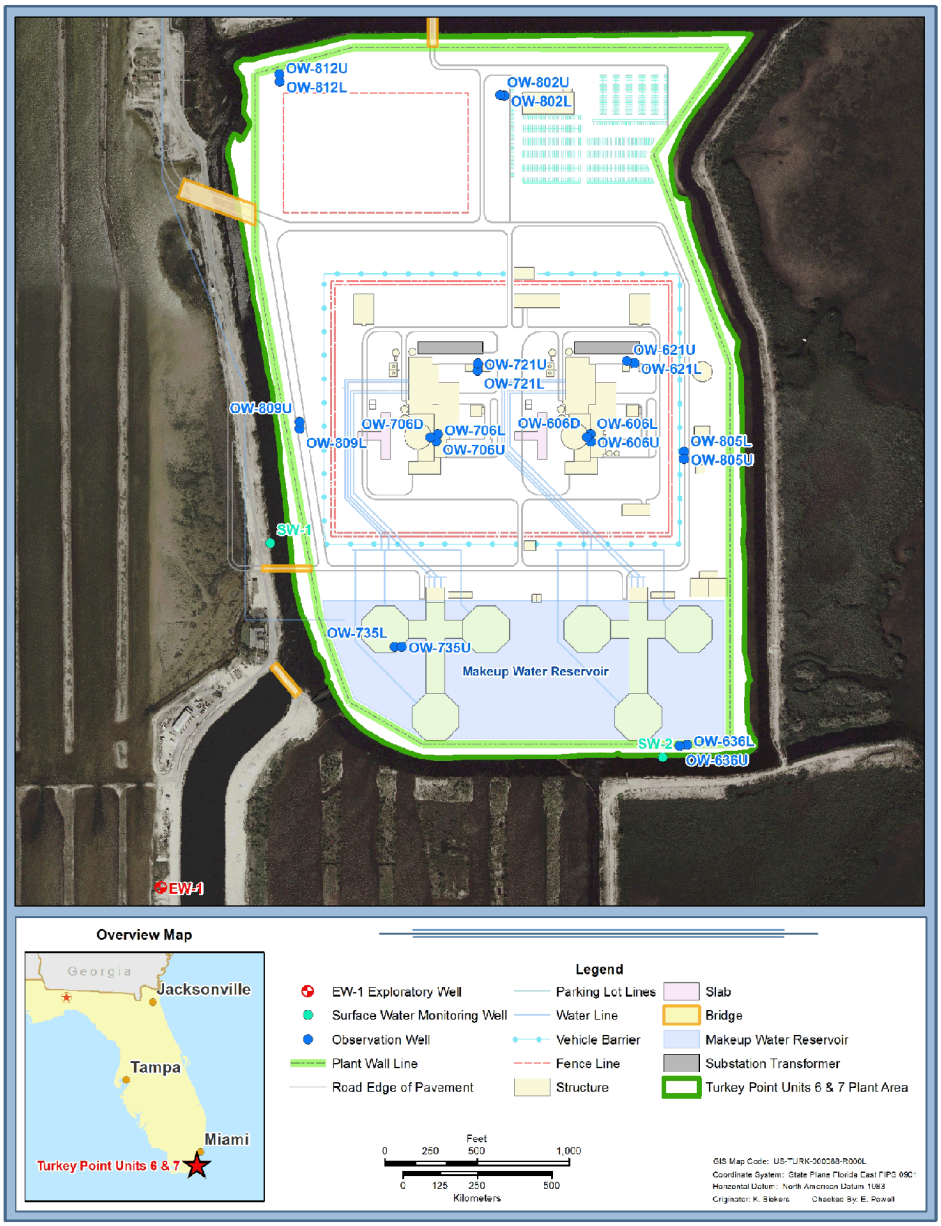

Source: Reference 287

Figure 2.5.4-243 EW-1 Profiles of V_S, Average V_S, Standard Deviation, +/– Standard Deviation and 2008 Average V_S versus Depth Beneath Finished Site Grade

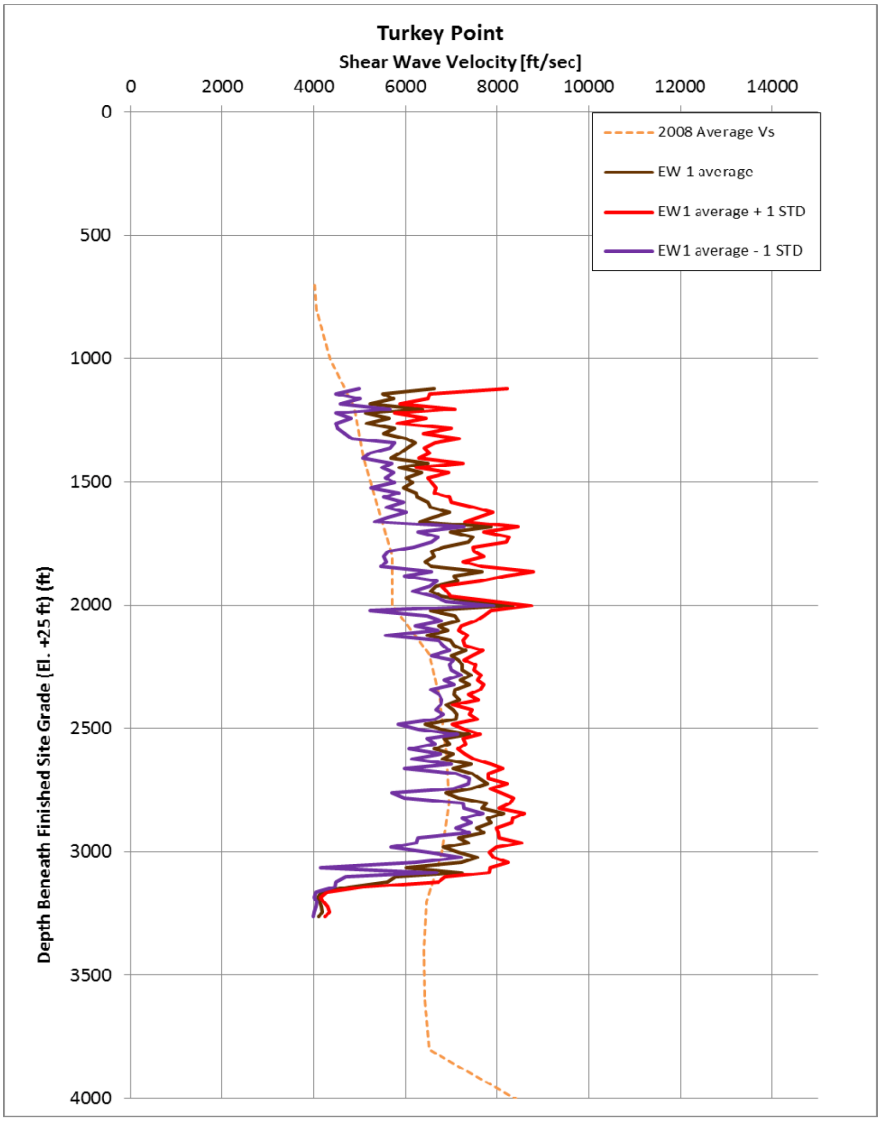

Note: The calculated averages for the "2008 Average V_S" values are computed in 100-foot and 200-foot intervals. The EW-1 calculated average V_S values are in 20-foot intervals.

Source: Reference 287

Figure 2.5.4-244 Initial Shear Modulus Variability from Pressuremeter Tests

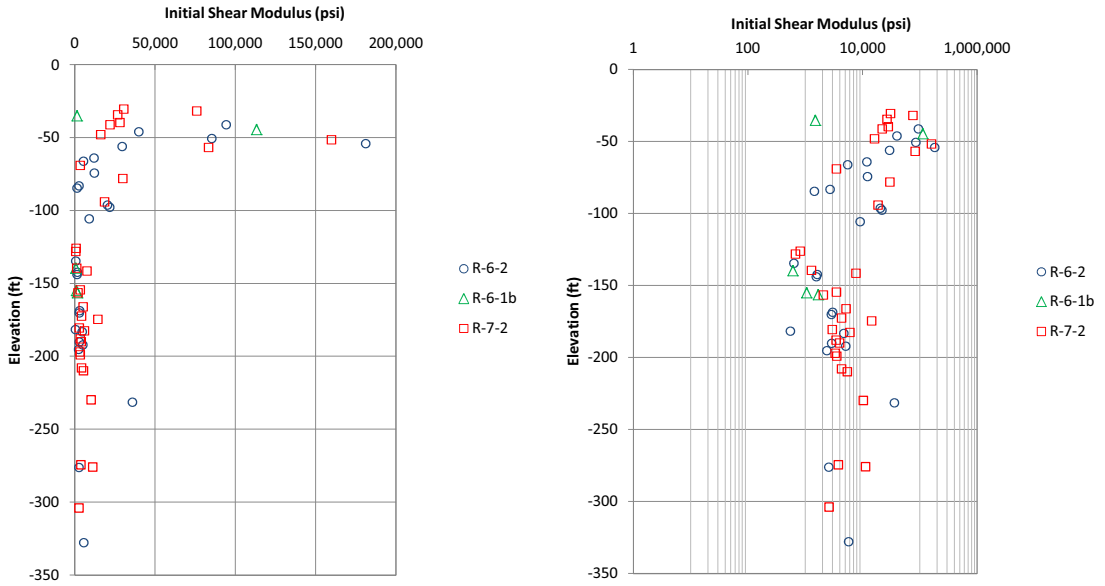

Data from Reference 290.

Figure 2.5.4-245 Unload/Reload Shear Modulus Variability from Pressuremeter Tests

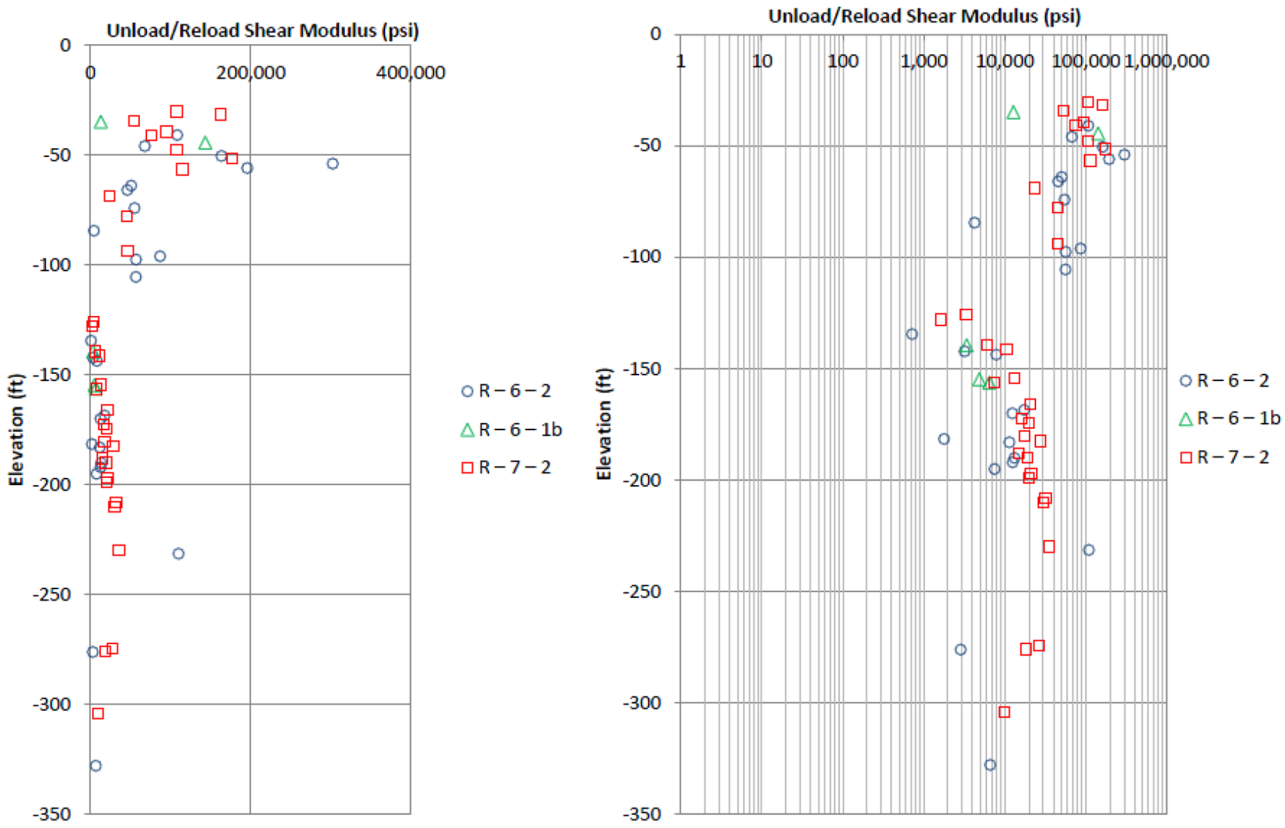

Data from Reference 290.

Figure 2.5.4-246 Shear Modulus Degradation for Fort Thompson Based on RCTS Testing

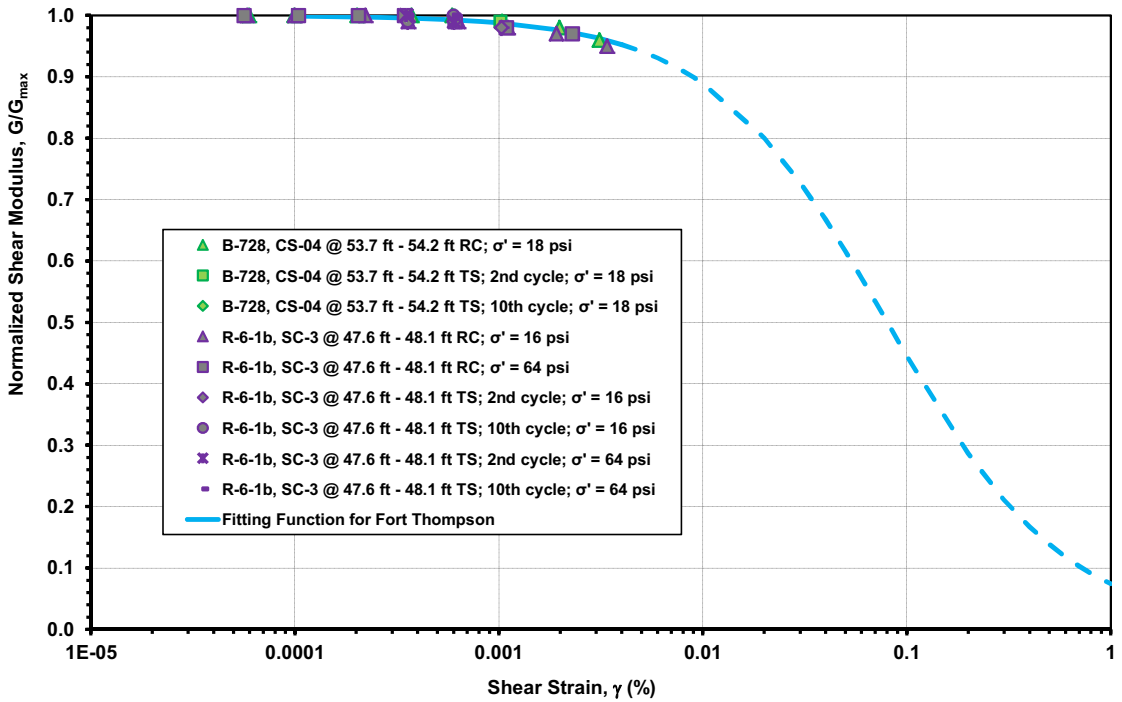

Data from References 257 and 290.

Figure 2.5.4-247 Shear Modulus Degradation for Natural Soil (Depth <150 ft) Based on RCTS Testing

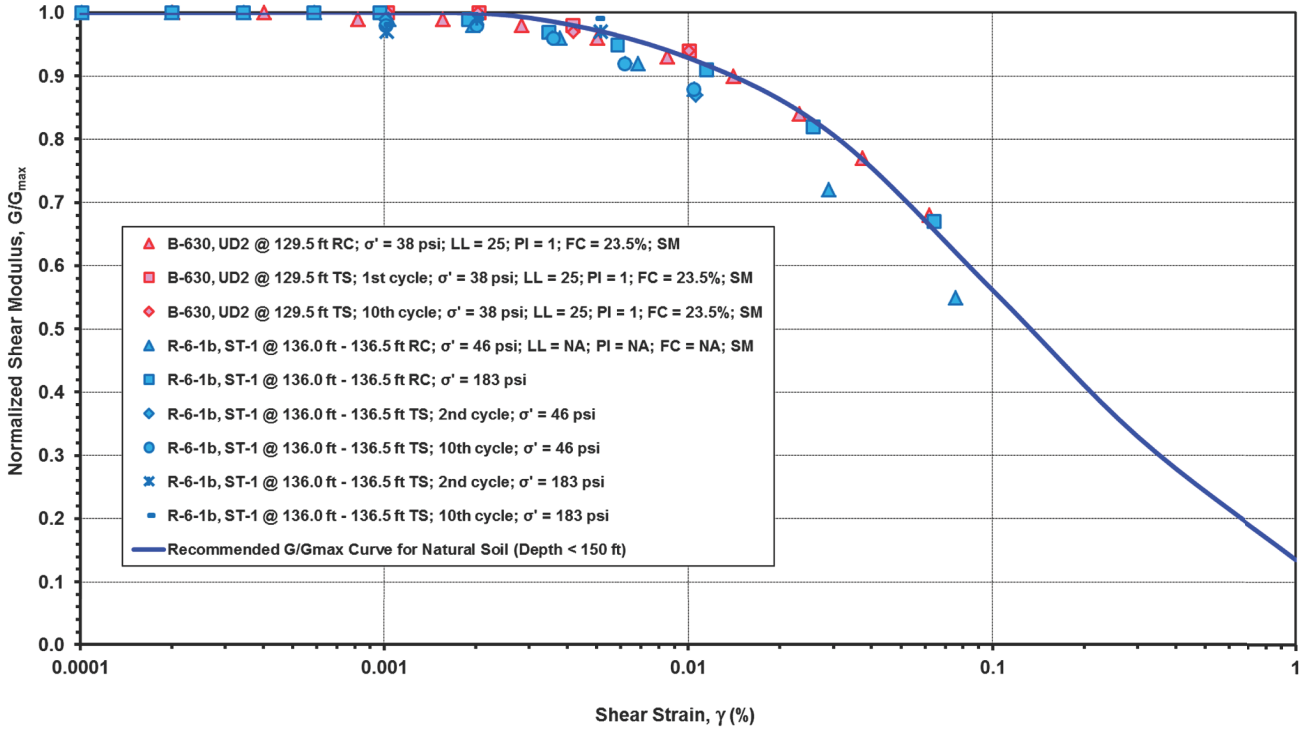

Data from References 257, 258, and 290.

Figure 2.5.4-248 Shear Modulus Degradation for Natural Soil (Depth >150 ft) Based on RCTS Testing

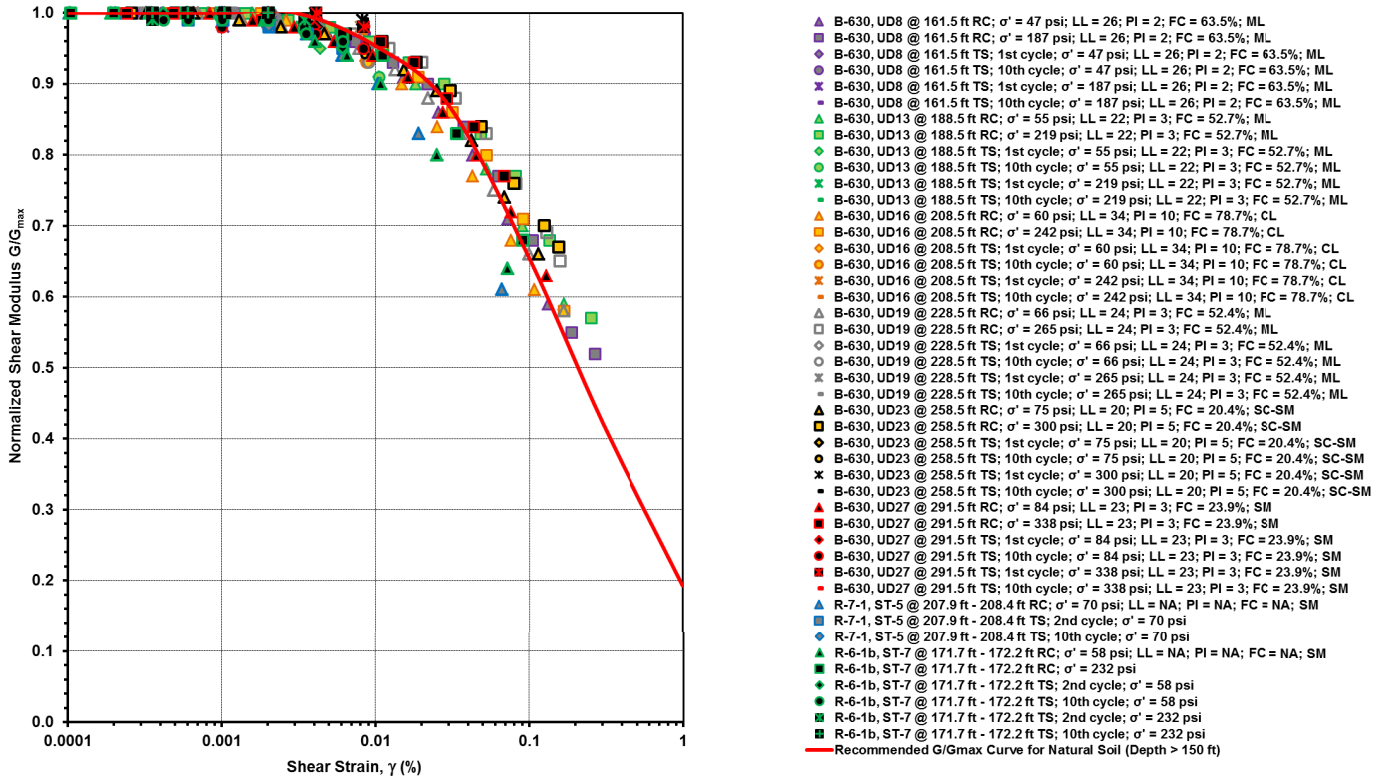

Data from References 257, 258, and 290.

Figure 2.5.4-249 Damping Curve Measurements for Natural Soil Based on RCTS Testing

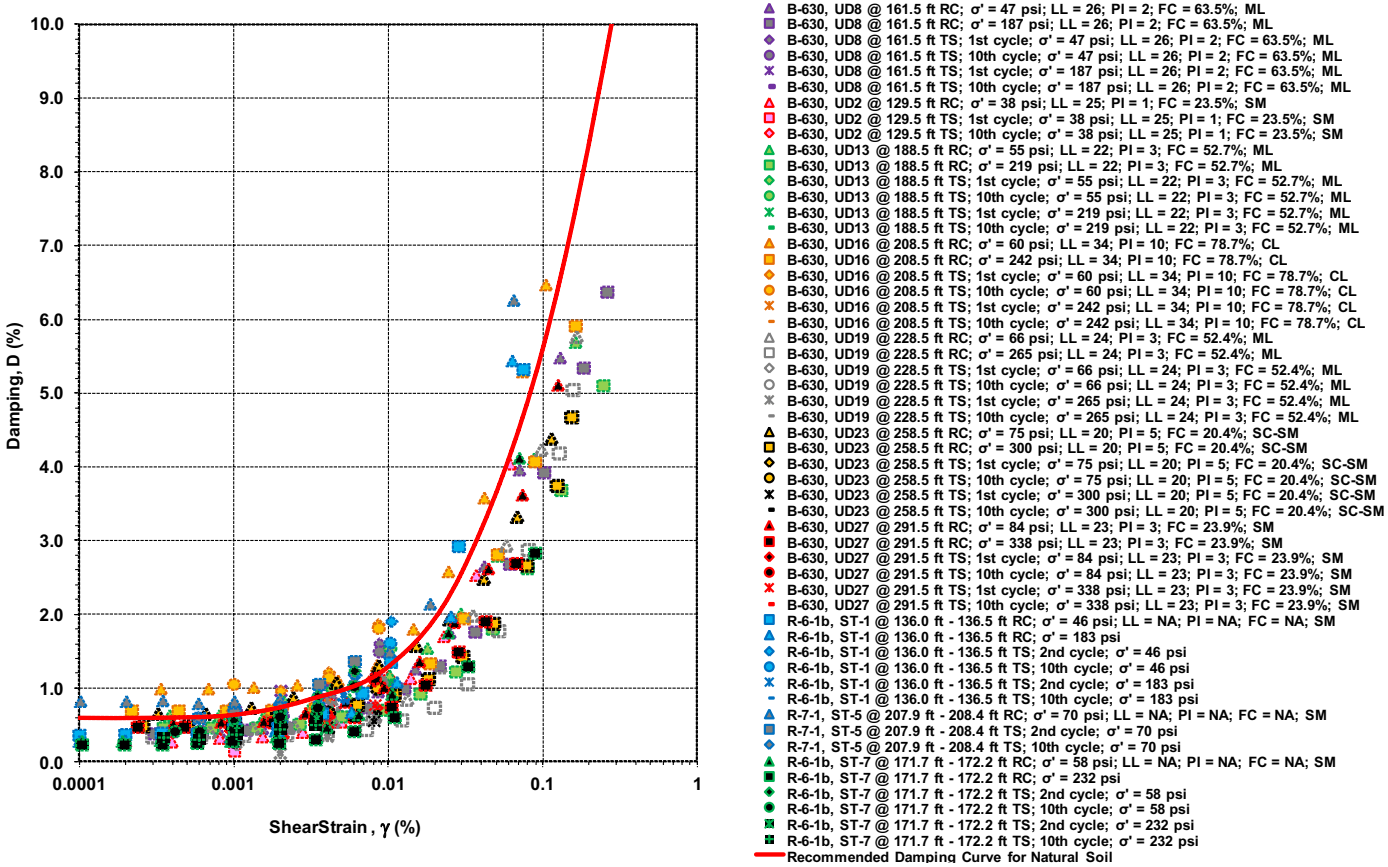

Data from References 257, 258, and 290.

Figure 2.5.4-250 Comparison between Liquefaction Analysis Results using SPT N Values and the Sum of the 3rd and 4th Blow Counts from the Supplemental Investigations

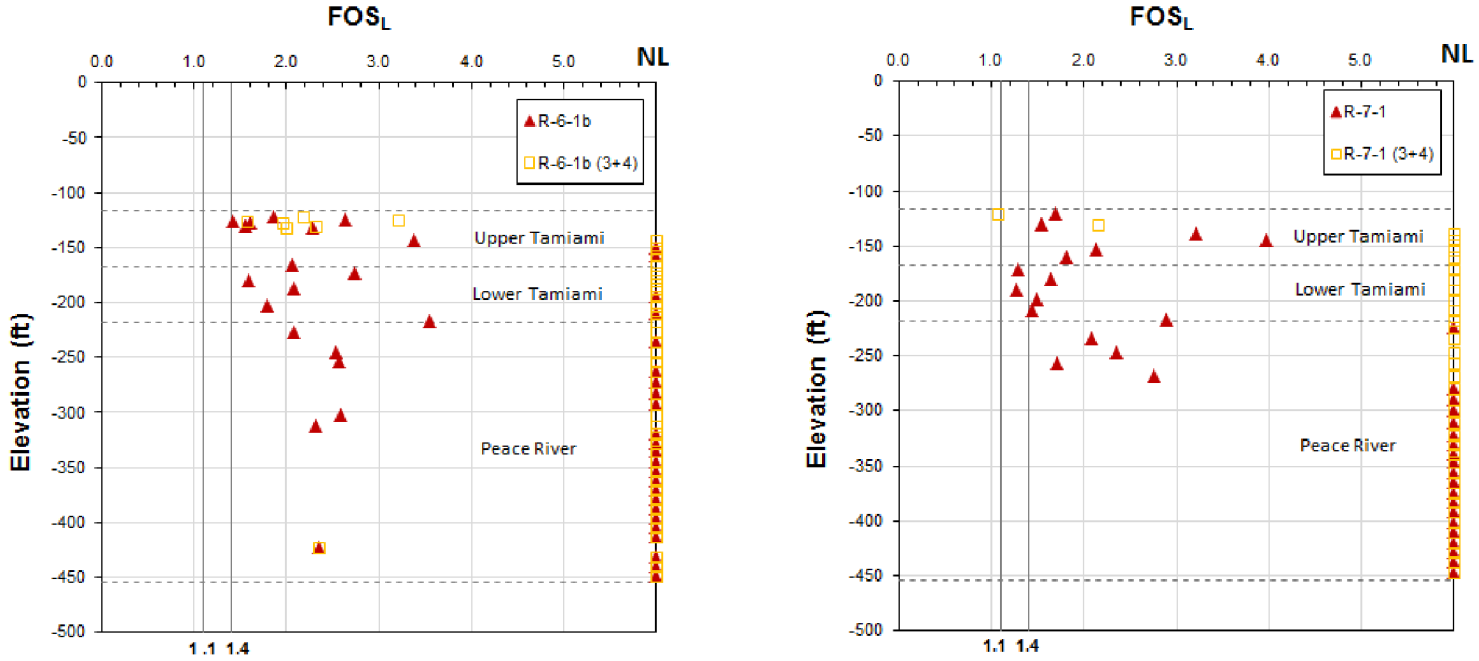

Note: NL corresponds to Non-Liquefiable locations $(N_1)_{60} \geq 30$. No numerical FOS value is obtained.

Figure 2.5.4-251 Factor of Safety against Liquefaction using Shear Wave Velocity

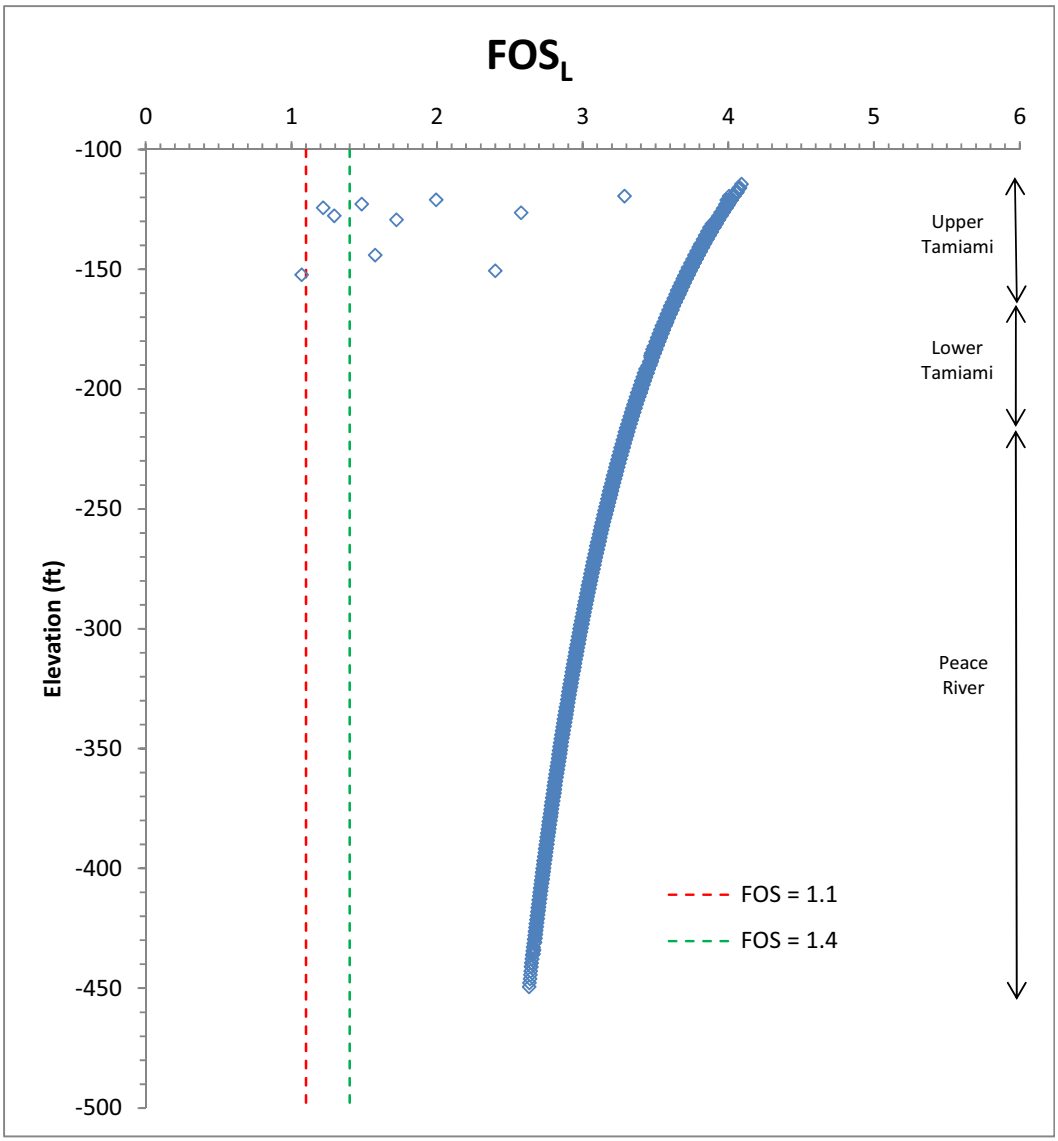

Figure 2.5.4-252 Active Earth Pressure Considering a 4000 psf Surcharge on Fill

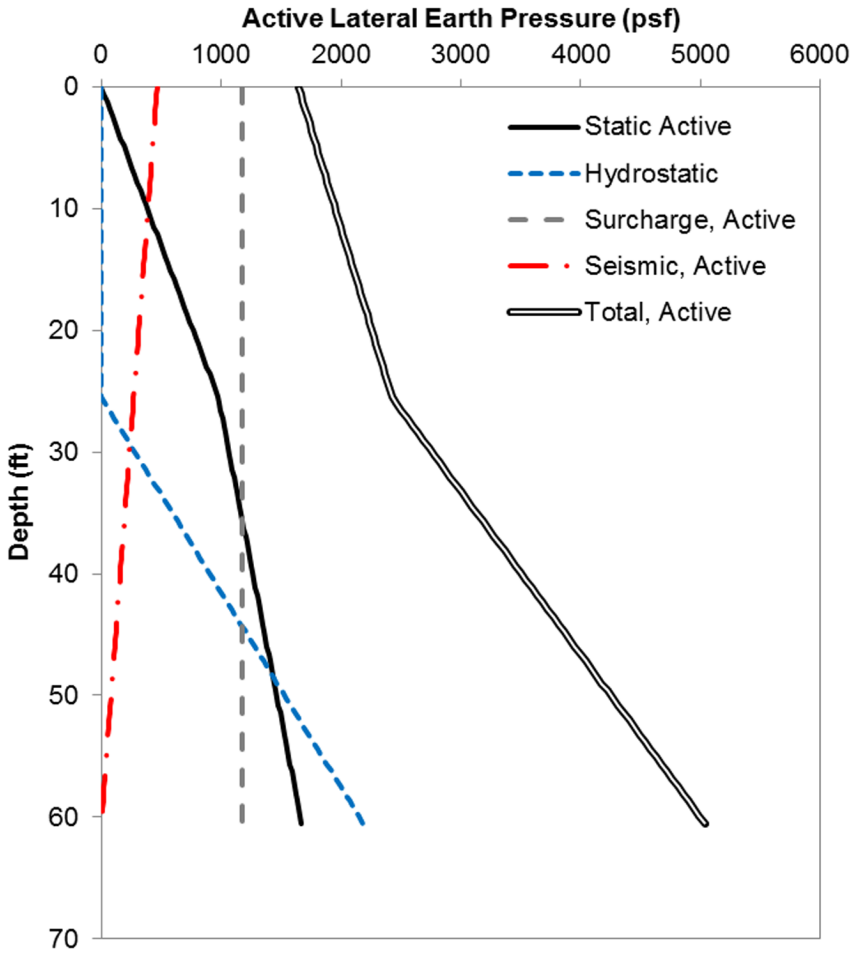

Data from Table 2.5.4-209 for compacted limerock fill.

Figure 2.5.4-253 At-Rest Earth Pressures Considering a 4000 psf Surcharge on Fill

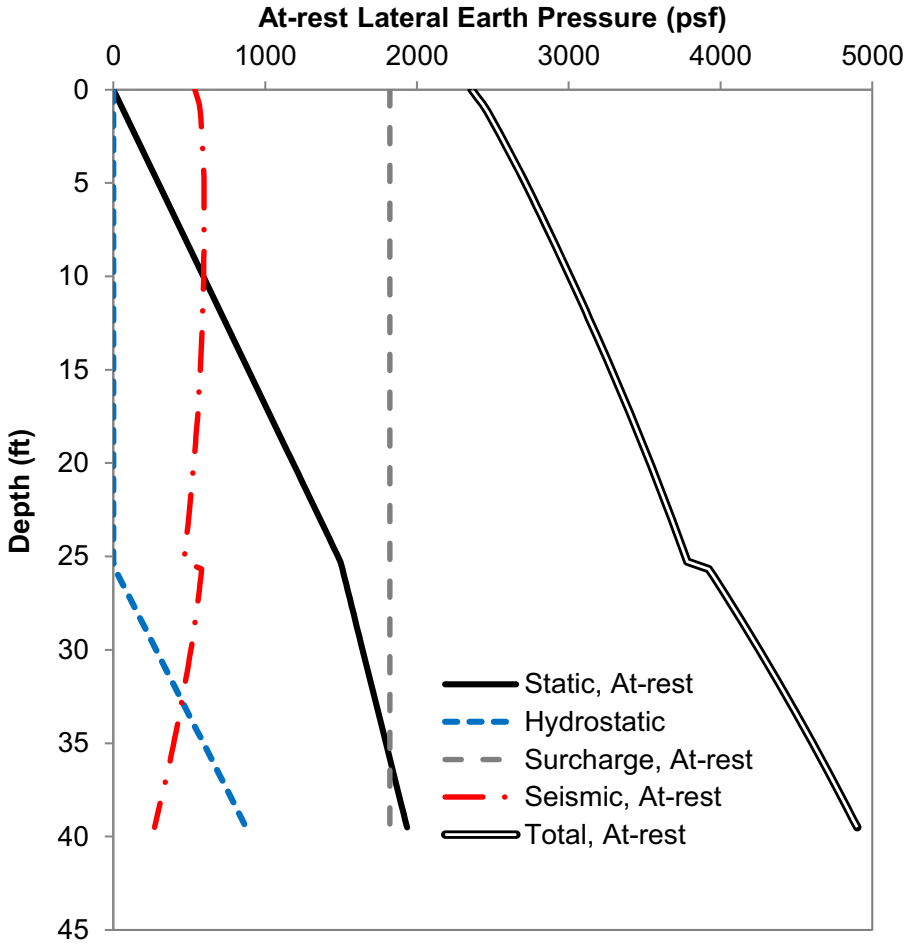

Data from Table 2.5.4-209 for compacted limerock fill.

Figure 2.5.4-254 Estimated Location of Interpreted FD4 (Slightly to Moderately Fractured) Zones

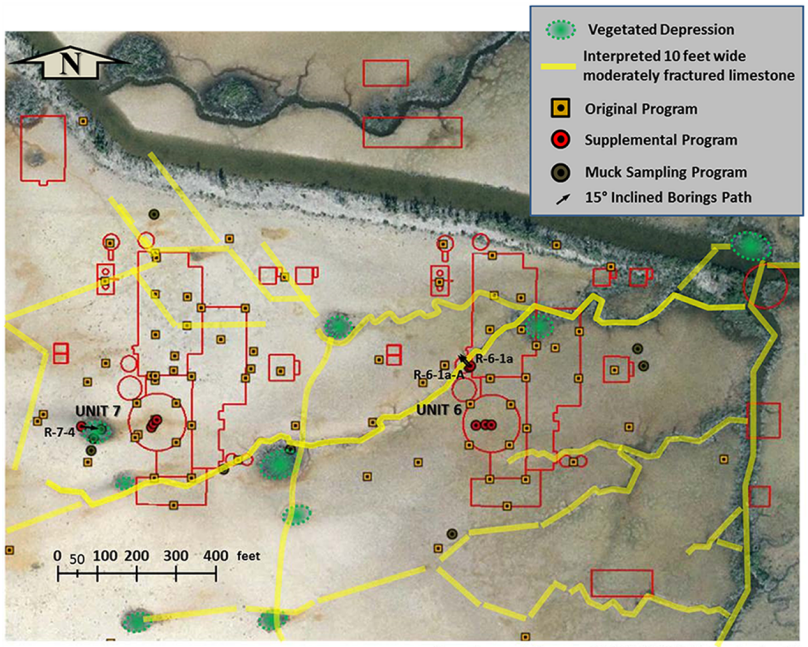

Figure 2.5.4-255 Cross-sections of Inclined Borings Including Notes on Fracture Density (FD)

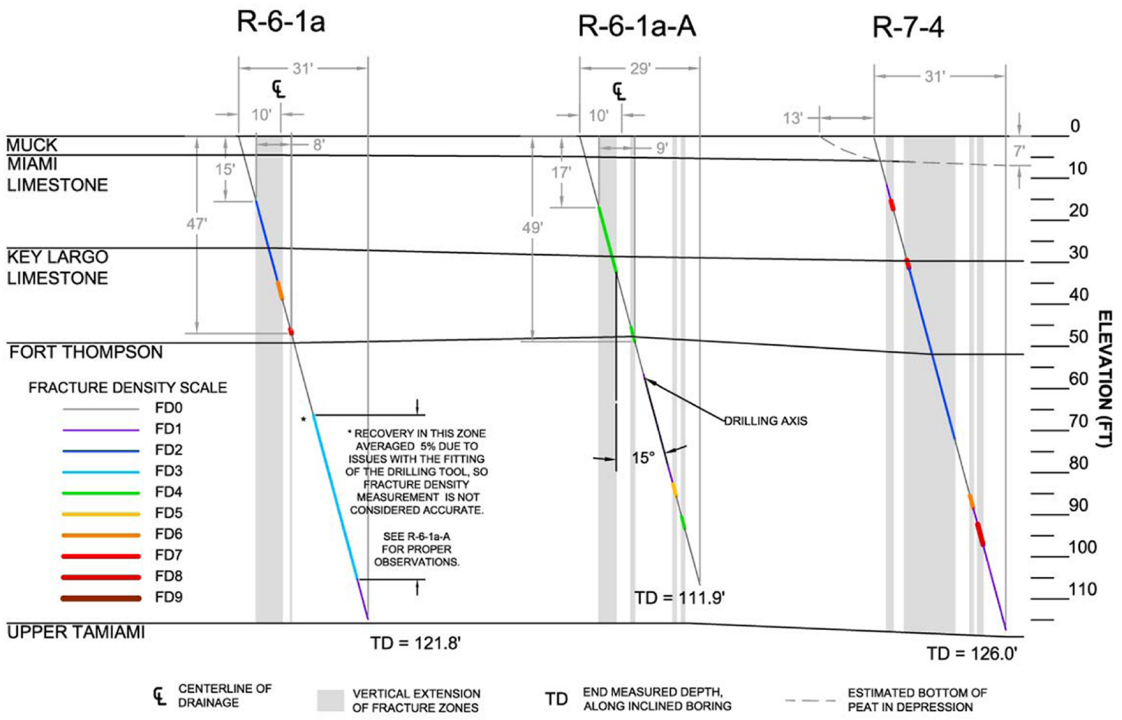

Figure 2.5.4-256 SLOPE/W Analysis of Bearing Capacity, where FOS = 3.0

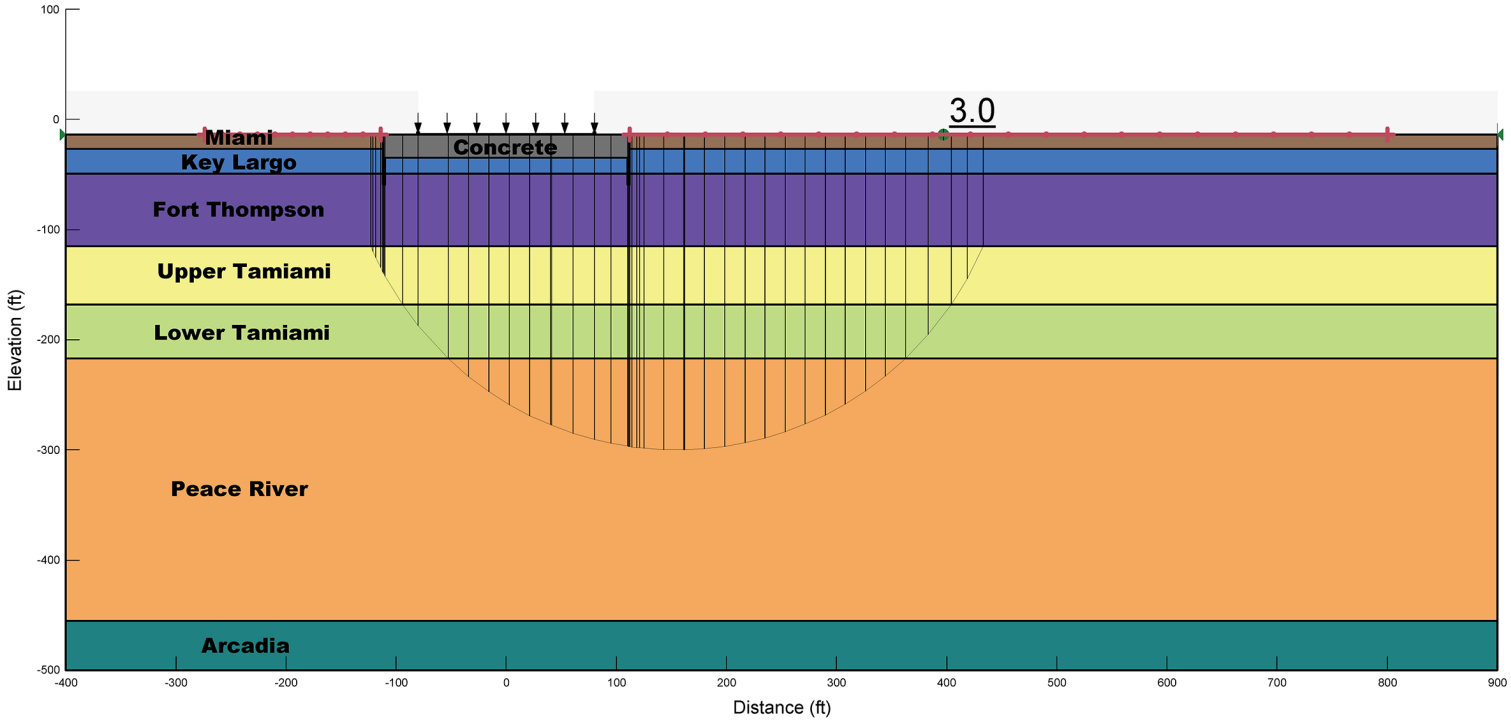

Figure 2.5.4-257 SLOPE/W Analysis of Bearing Capacity, where FOS = 1.0

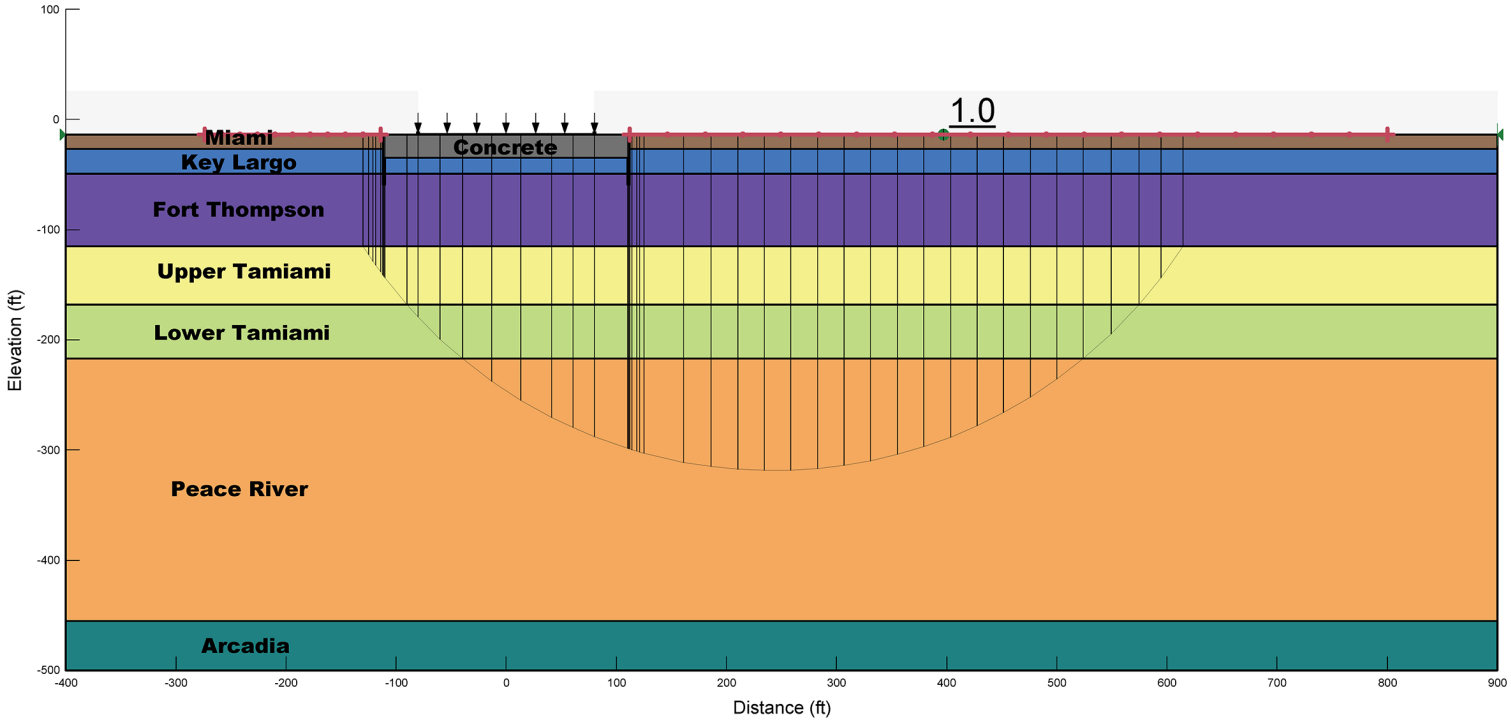

Figure 2.5.4-258 SLOPE/W Analysis, 1x Required Bearing Demand

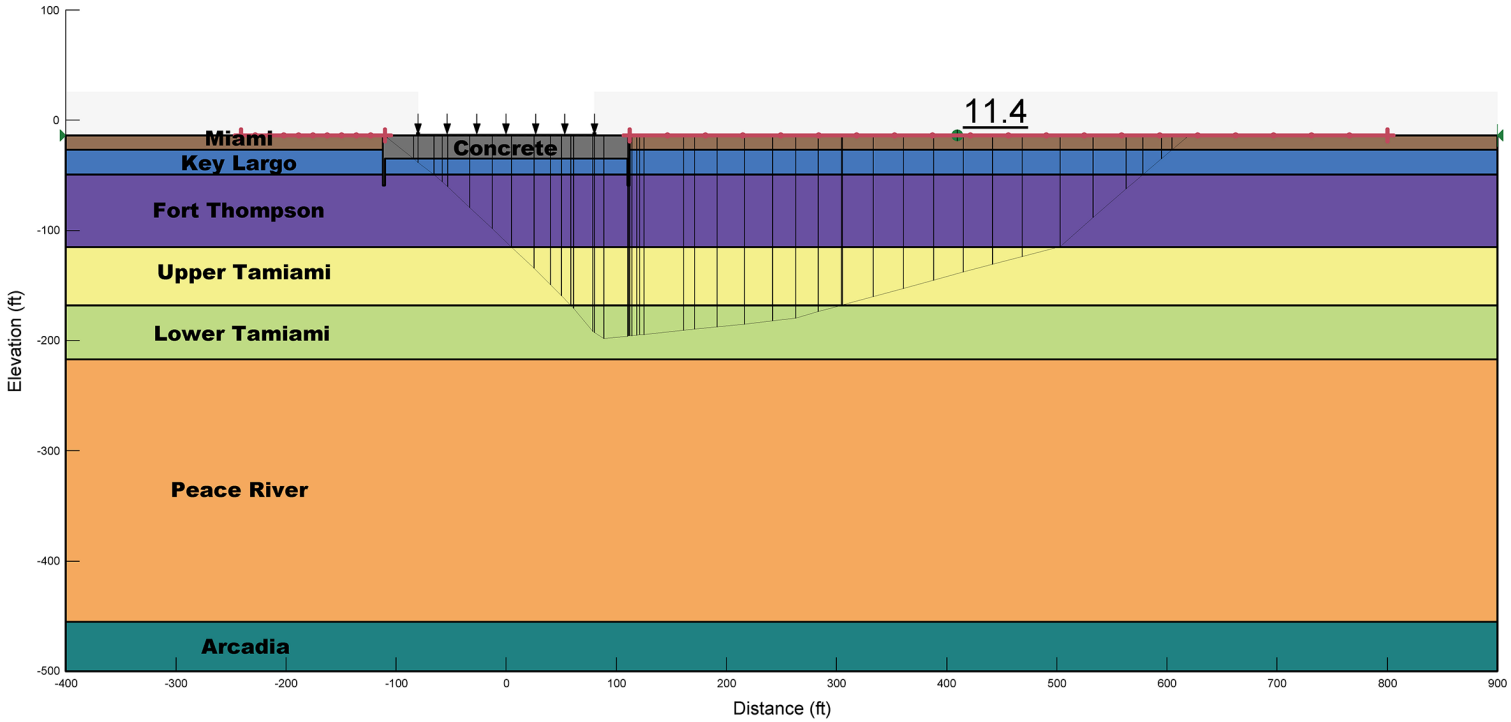

Figure 2.5.4-259 SLOPE/W Analysis with Simulated FD4 Zones, 1x Required Bearing Demand

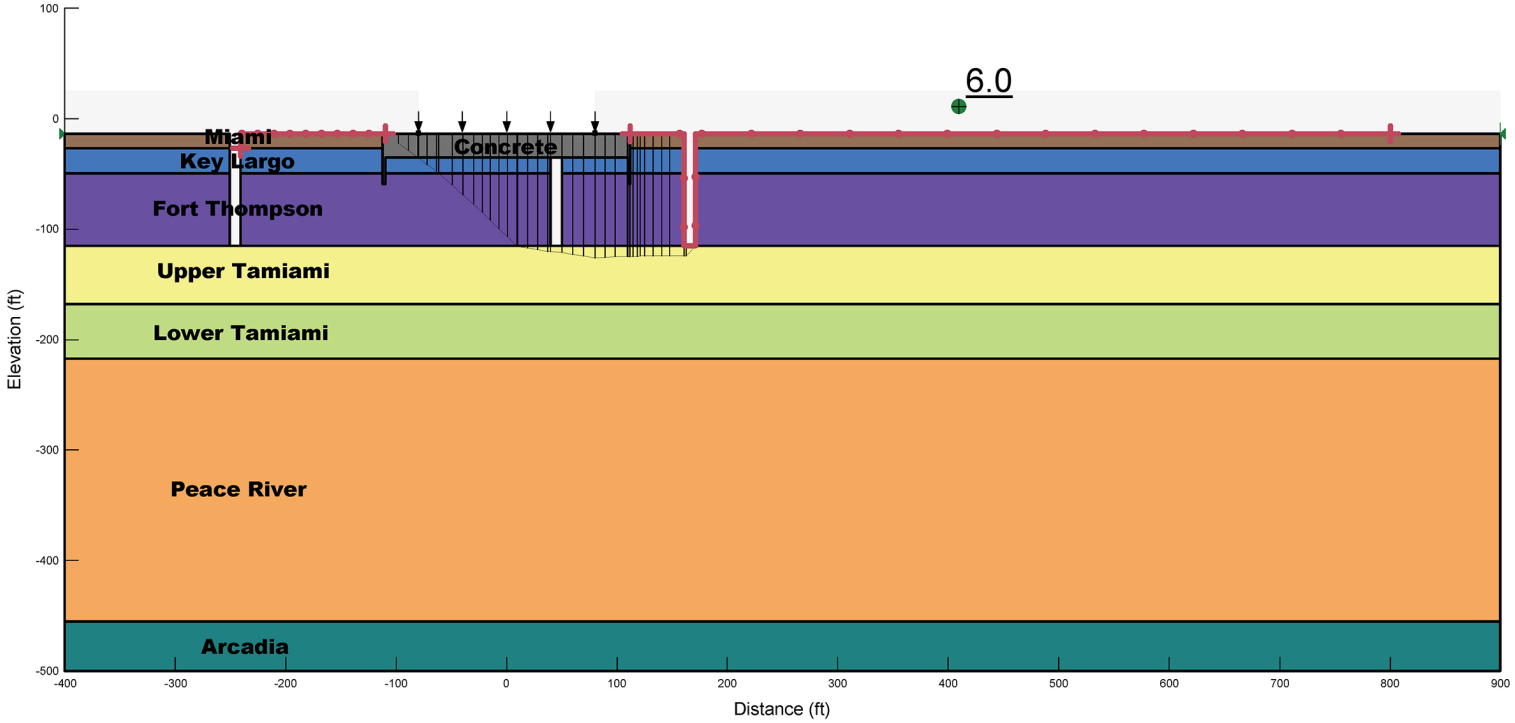

Figure 2.5.4-260 PLAXIS 3D Design Mesh

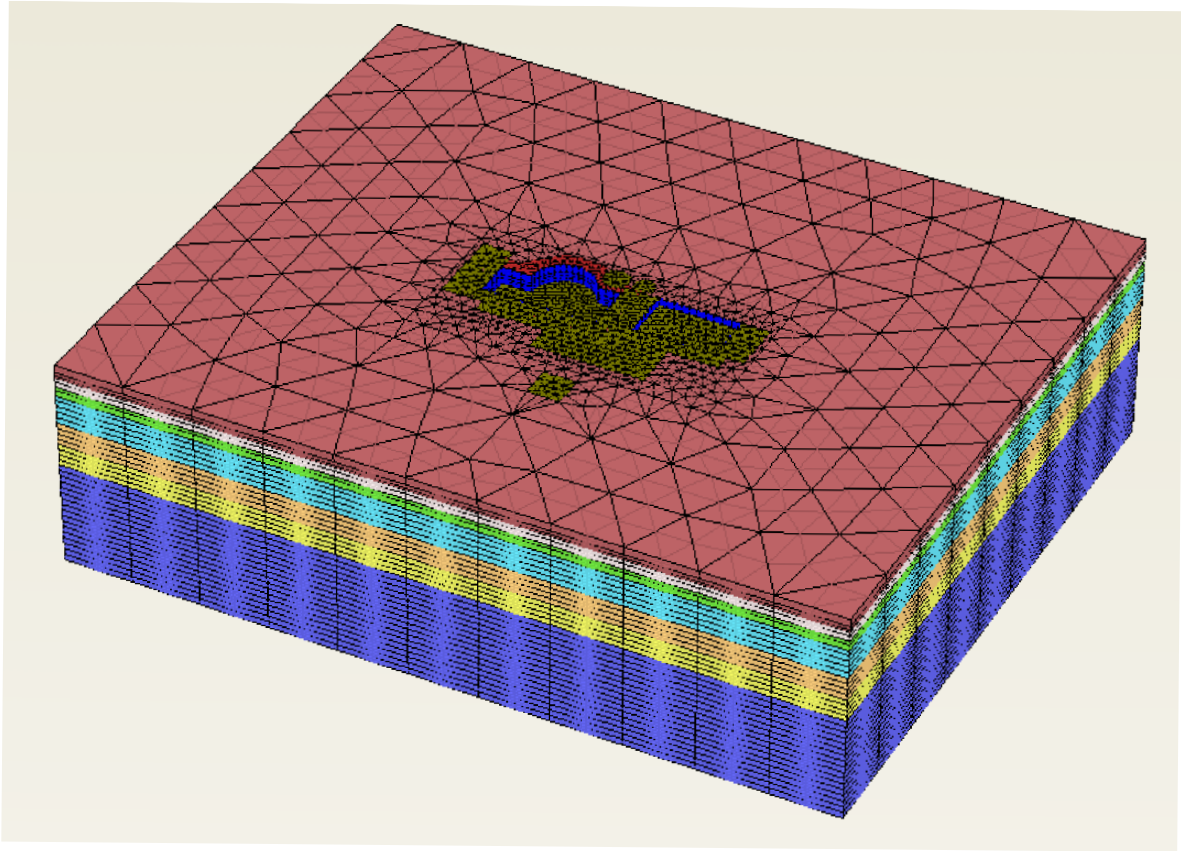

Figure 2.5.4-261 Plot of Soil Hardening Calibration for the Upper Tamiami

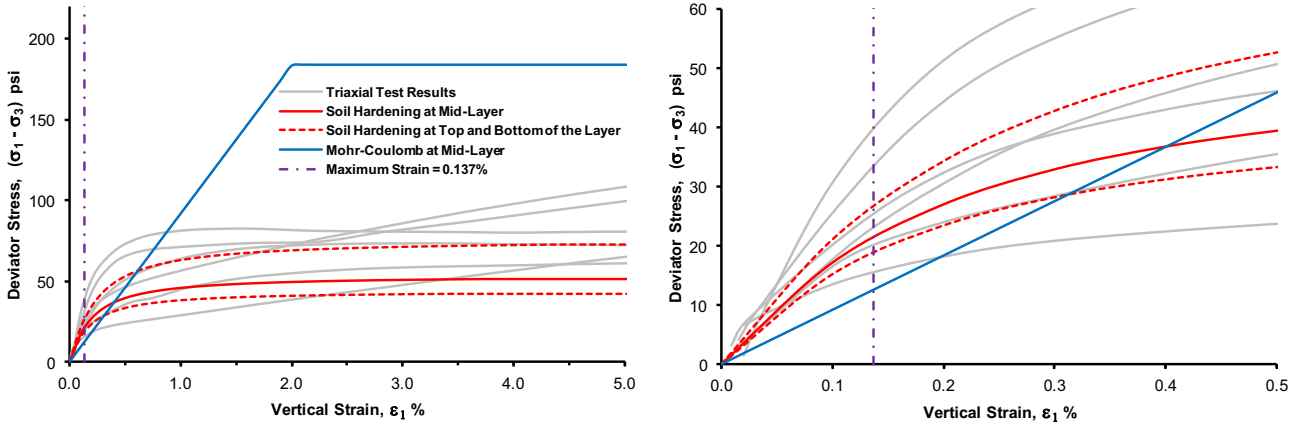

Figure 2.5.4-262 Plot of Soil Hardening Calibration for the Lower Tamiami

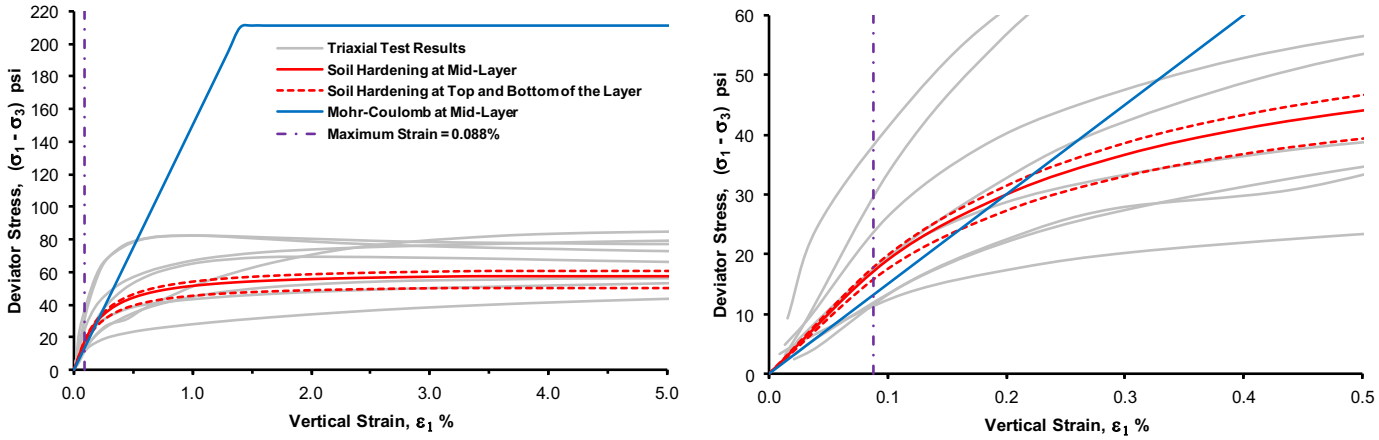

Figure 2.5.4-263 Plot of Soil Hardening Calibration for the Peace River

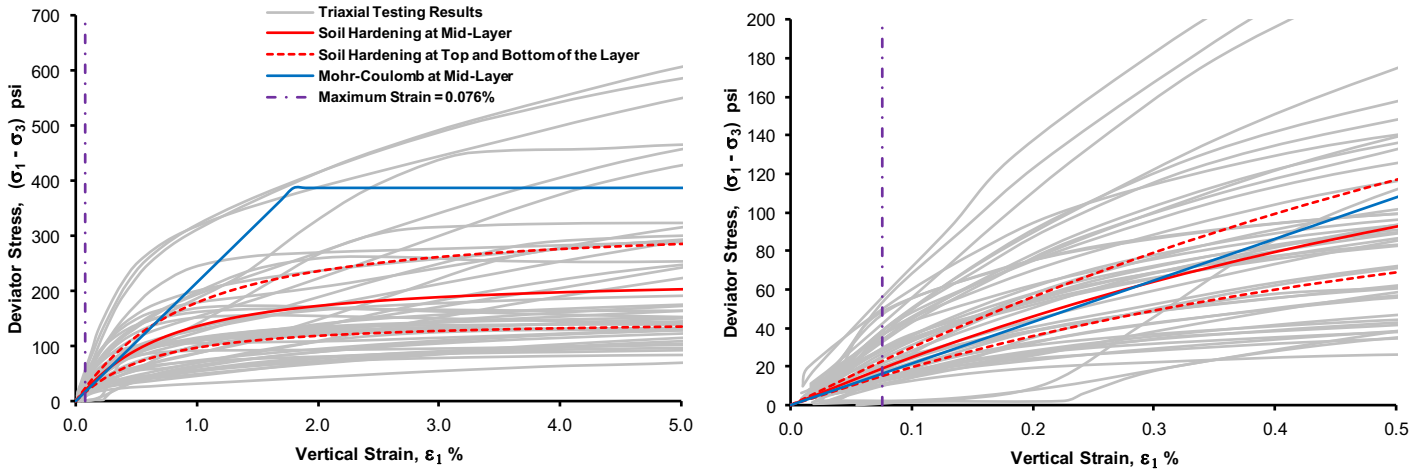

Figure 2.5.4-264 PLAXIS 3D Best Estimate Model Total Settlement After Loading

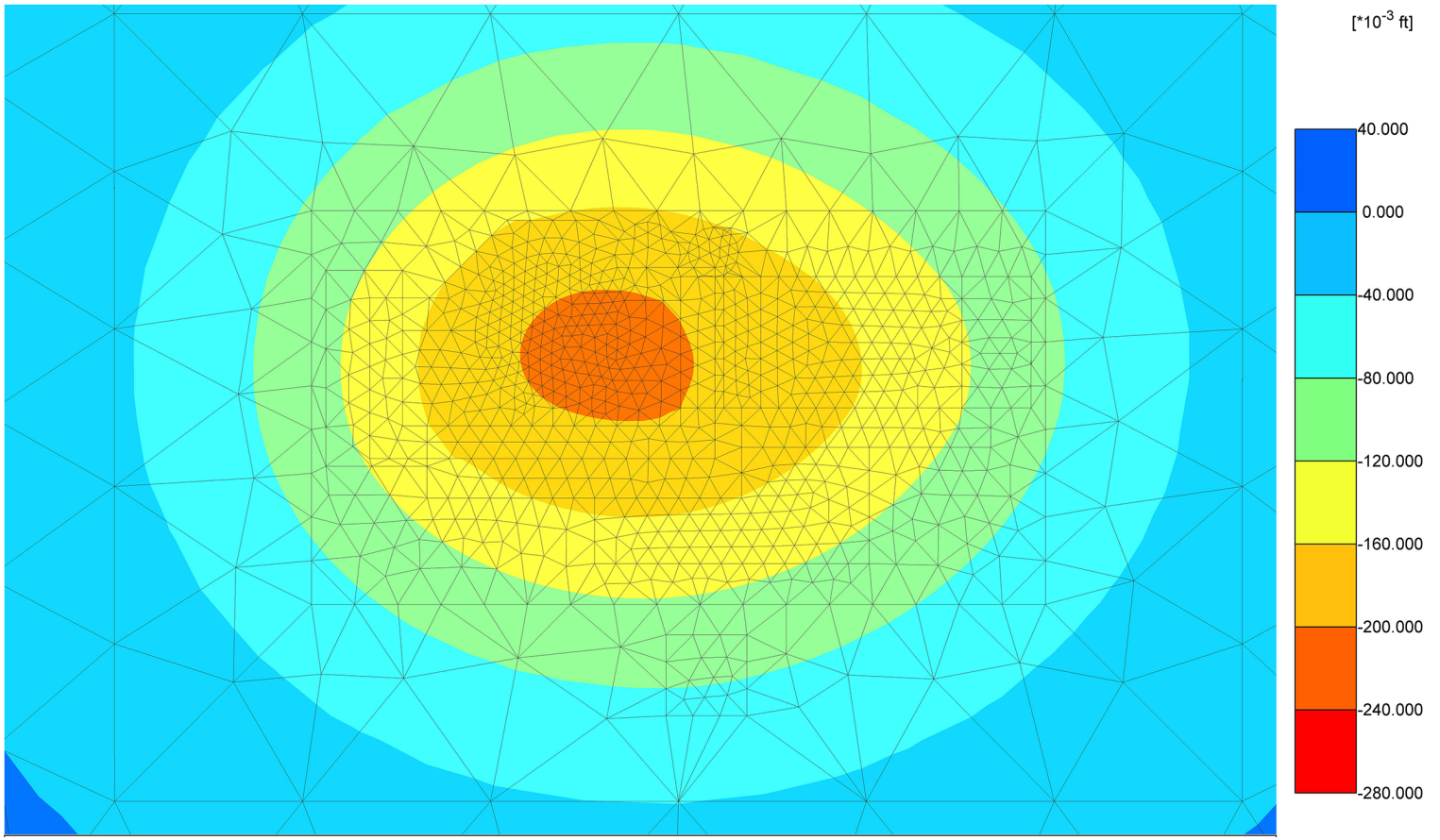

Figure 2.5.4-265 PLAXIS 3D Best Estimate Model Total Settlement After Rewatering

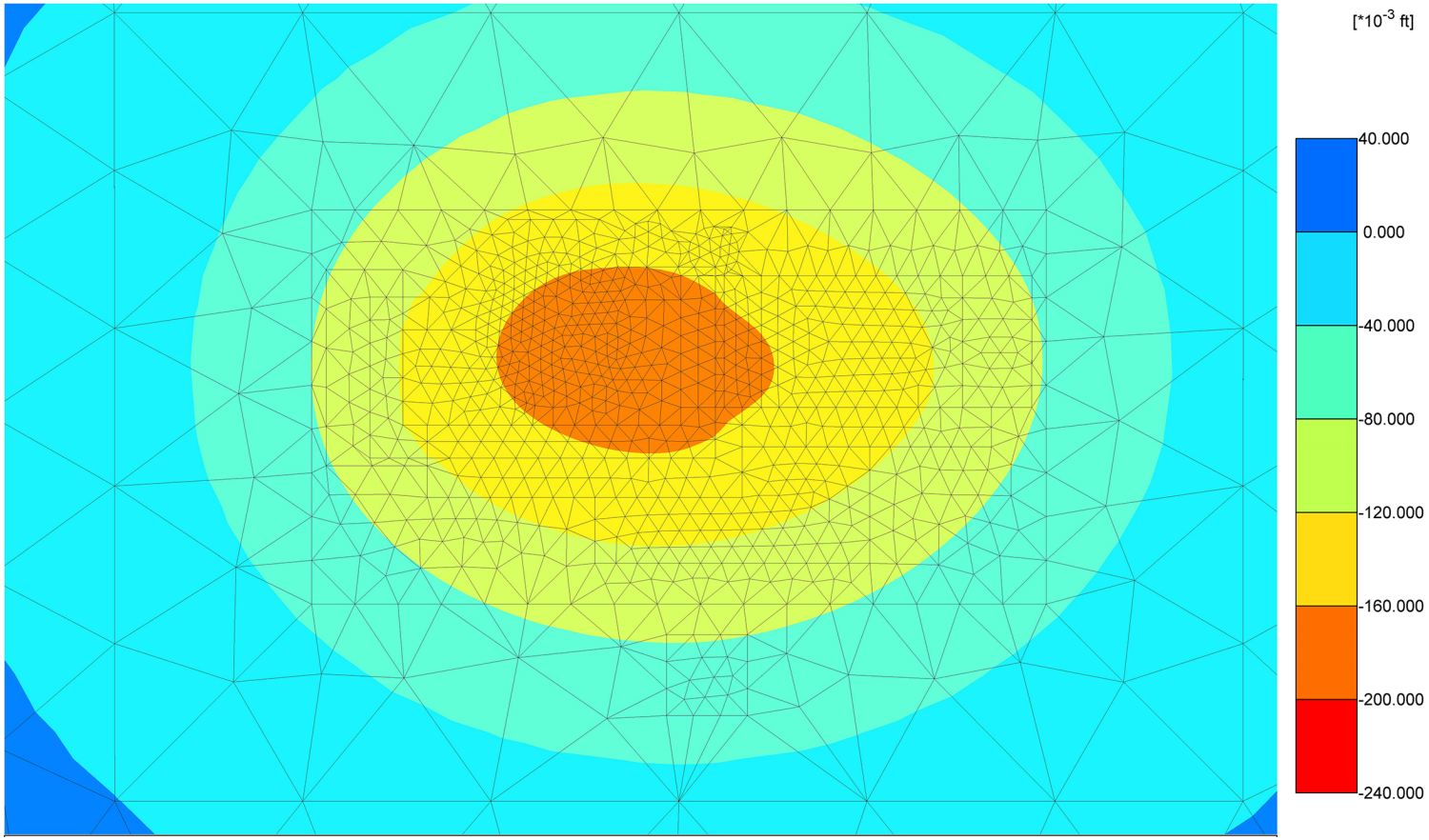

Figure 2.5.4-266 Plastic Deformation from PLAXIS 2D Analysis, 1x Required Bearing Demand

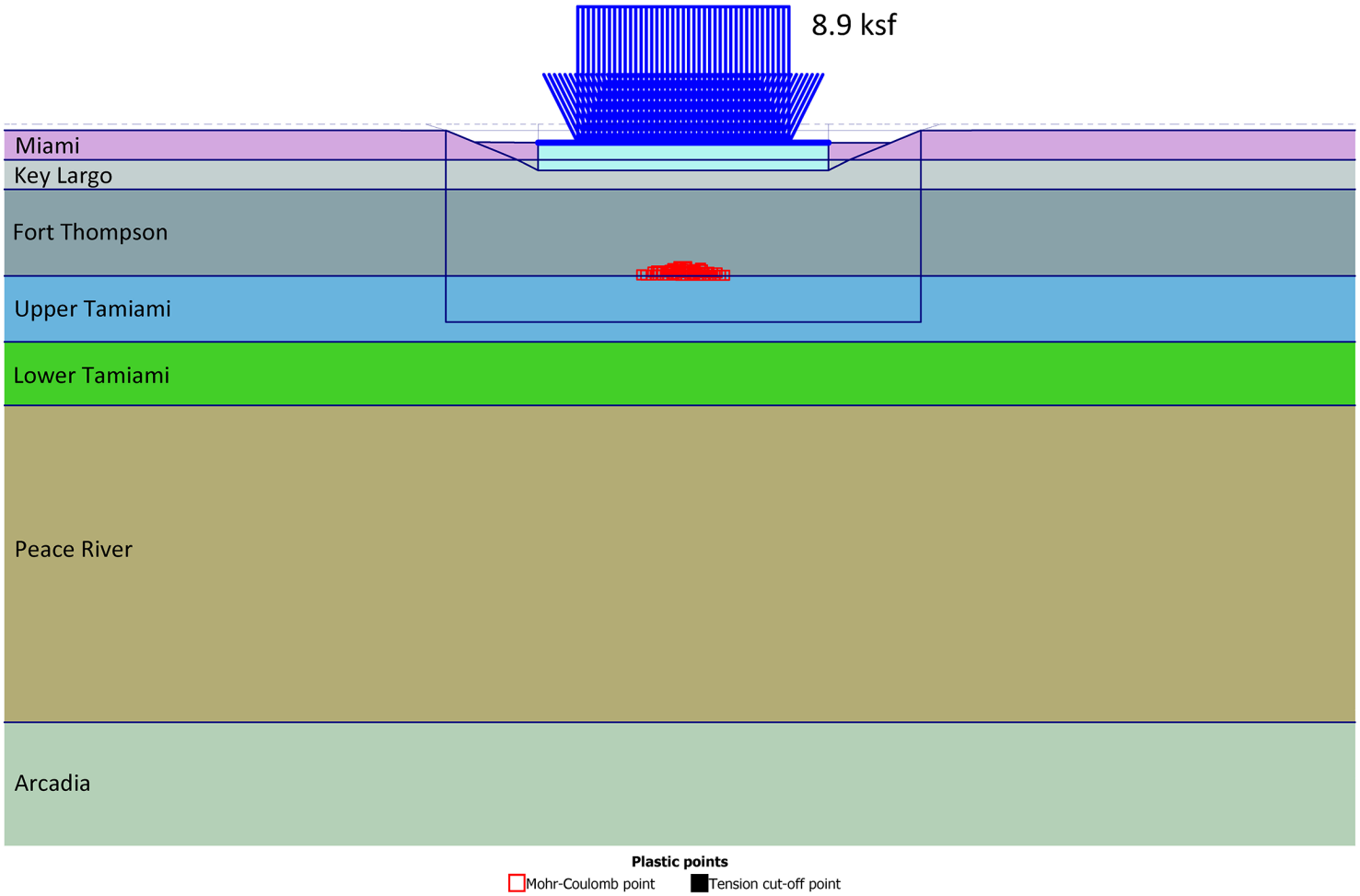

Figure 2.5.4-267 Plastic Deformation from PLAXIS 2D Analysis, 3x Required Bearing Demand

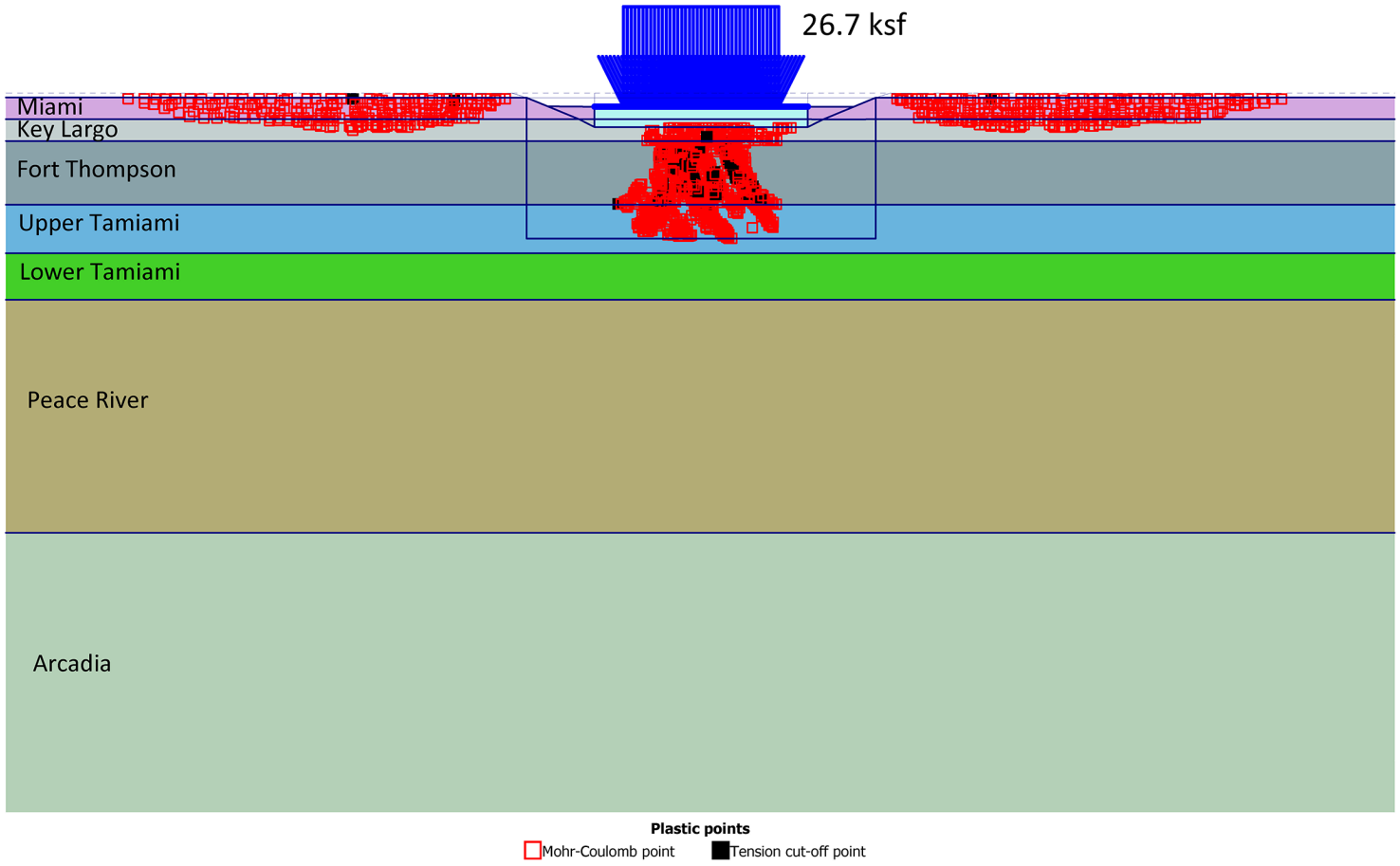

Figure 2.5.4-268 Failure Surface from PLAXIS 2D Analysis

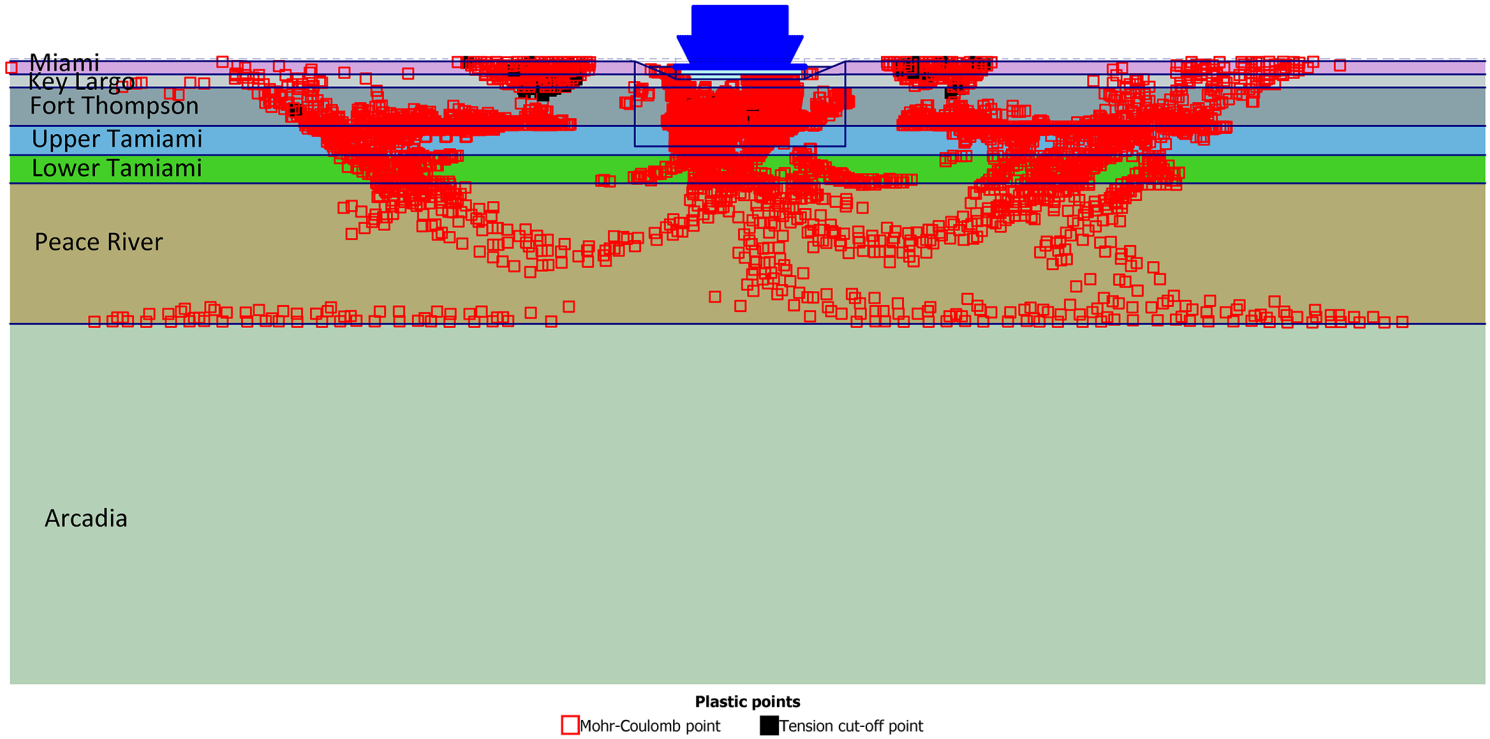

Figure 2.5.4-269 Plot of Uncorrected SPT N Values versus the Summation of 3rd and 4th Blow Counts from the Supplemental Investigation

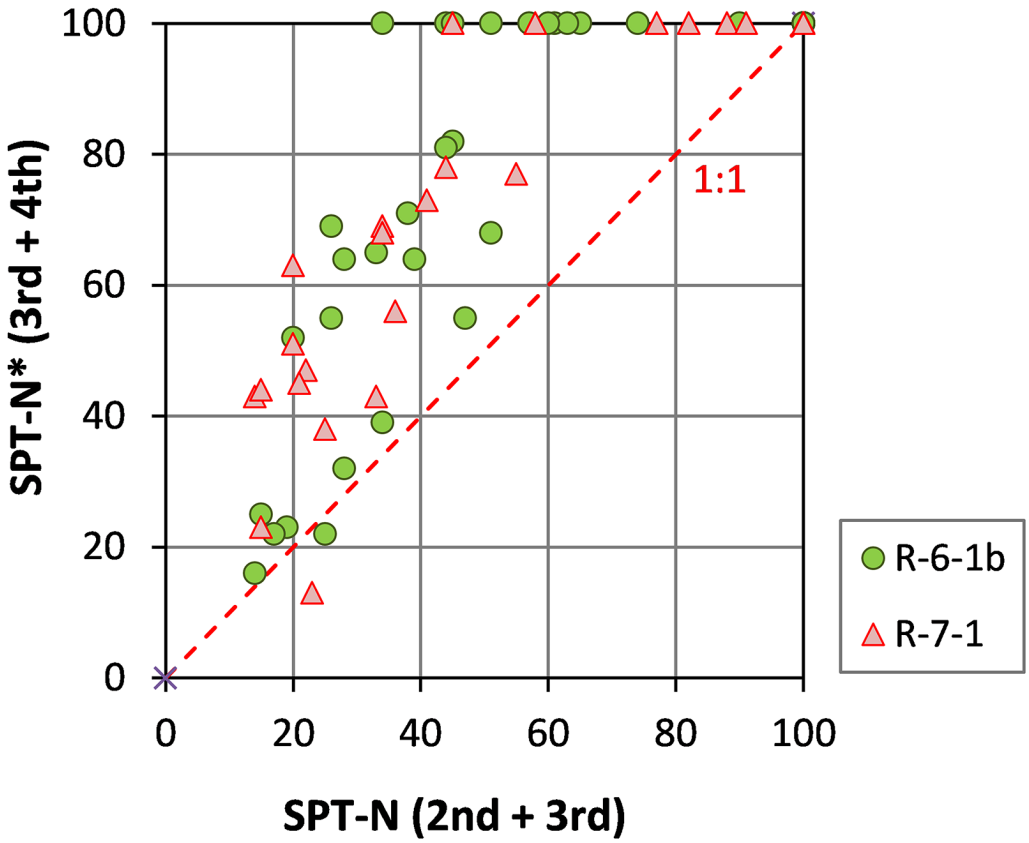

Note:
* Summation of 3rd and 4th blow count intervals

Note: Data from Reference 290.

Figure 2.5.4-270 Plot of Uncorrected SPT N Values for R-6-1b and R-7-1 Vicinity

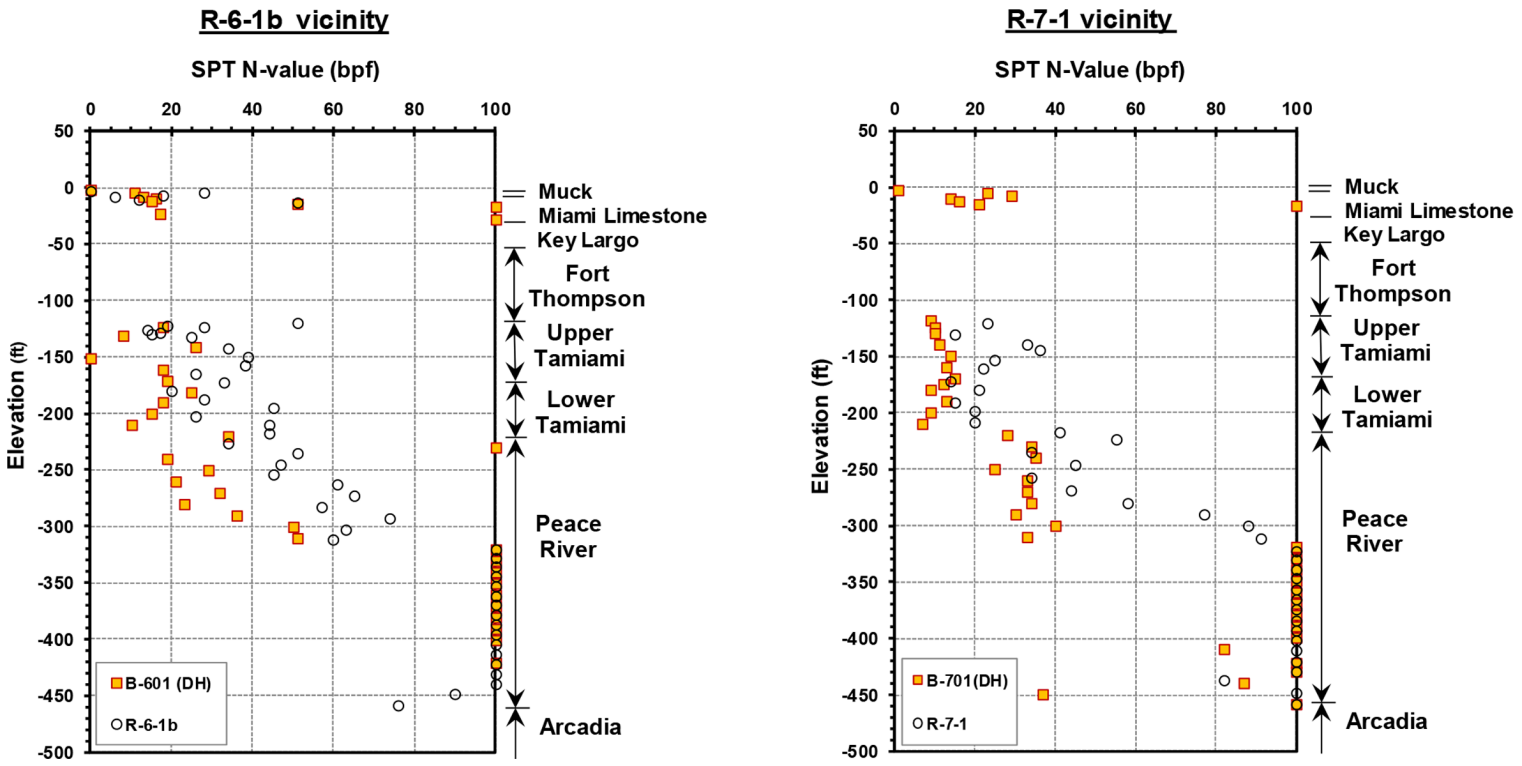

Data from References 257 and 290.
Note: Elevation is NAVD 88.

Figure 2.5.4-271 Continuous and Discontinuous SPT Sampling

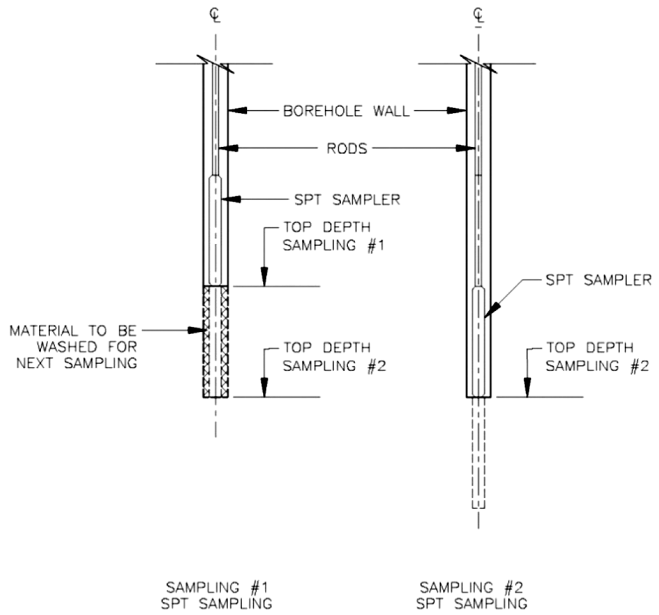

CONTINUOUS SAMPLING CASE
(NOT TO SCALE)

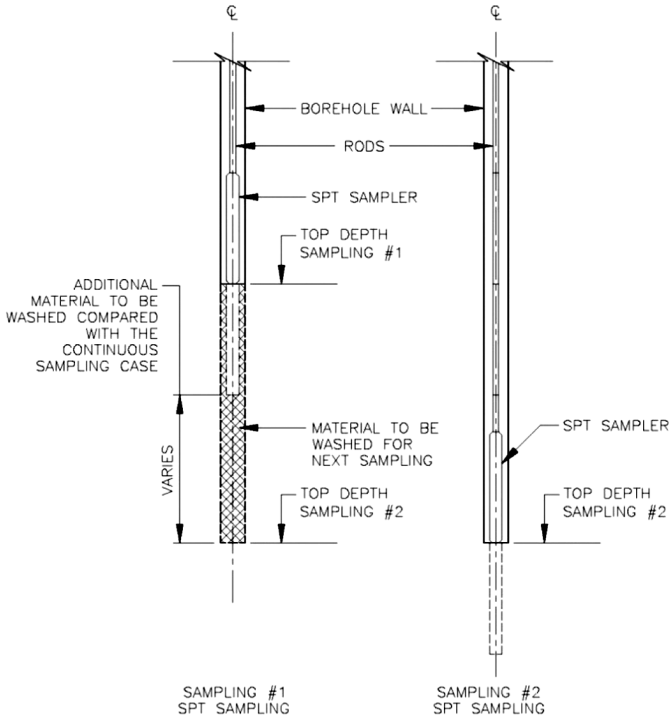

DISCONTINUOUS SAMPLING CASE
(NOT TO SCALE)

Note: General scheme developed as sampling was performed according to References 257 and 290.

Figure 2.5.4-272 Plot of Corrected SPT N_{60} Values for R-6-1b and R-7-1 Vicinity

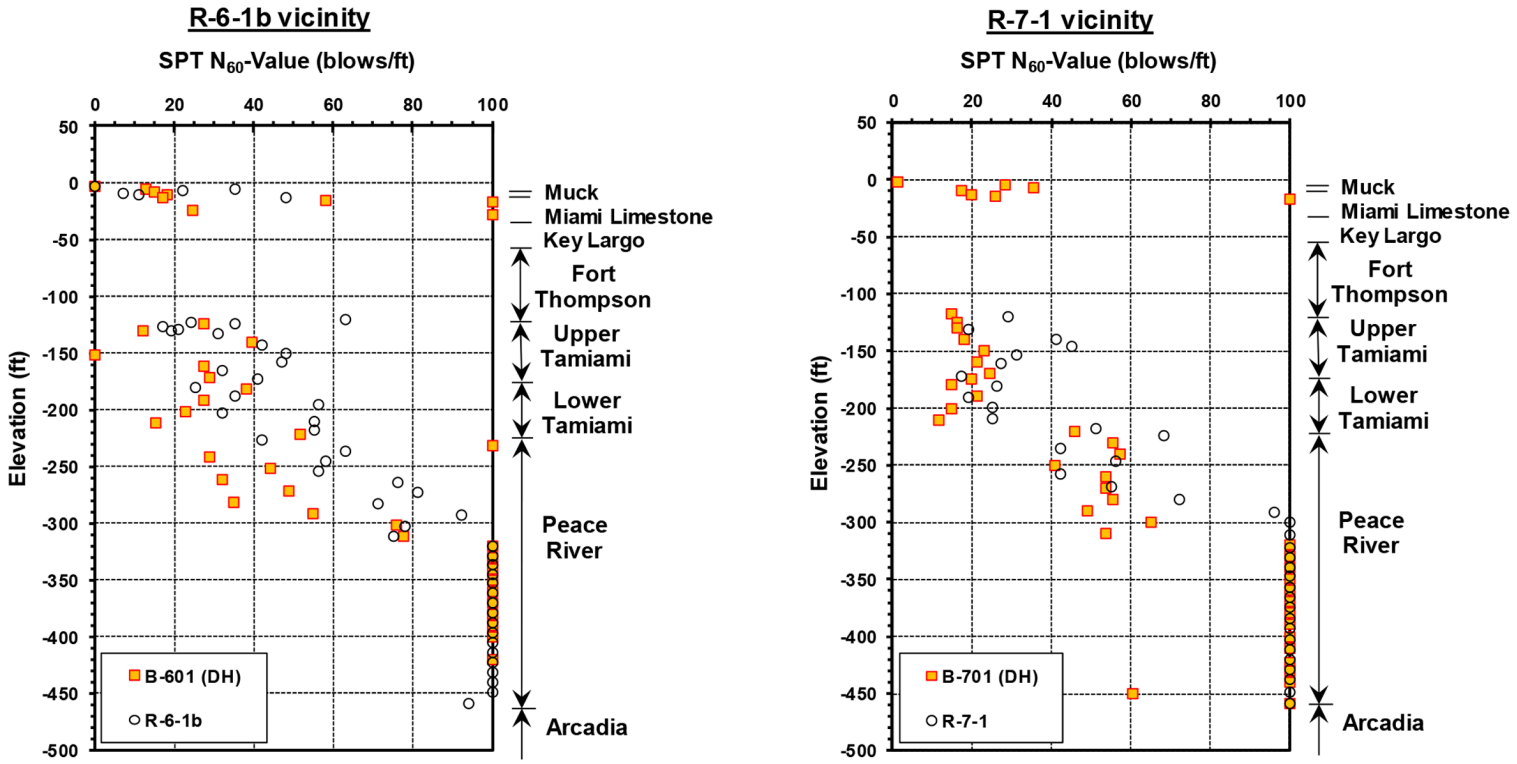

Data from References 257 and 290.
Note: Elevation is NAVD 88.

Figure 2.5.4-273 PLAXIS 3D Sensitivity Model with 20-foot Diameter Cylindrical Void

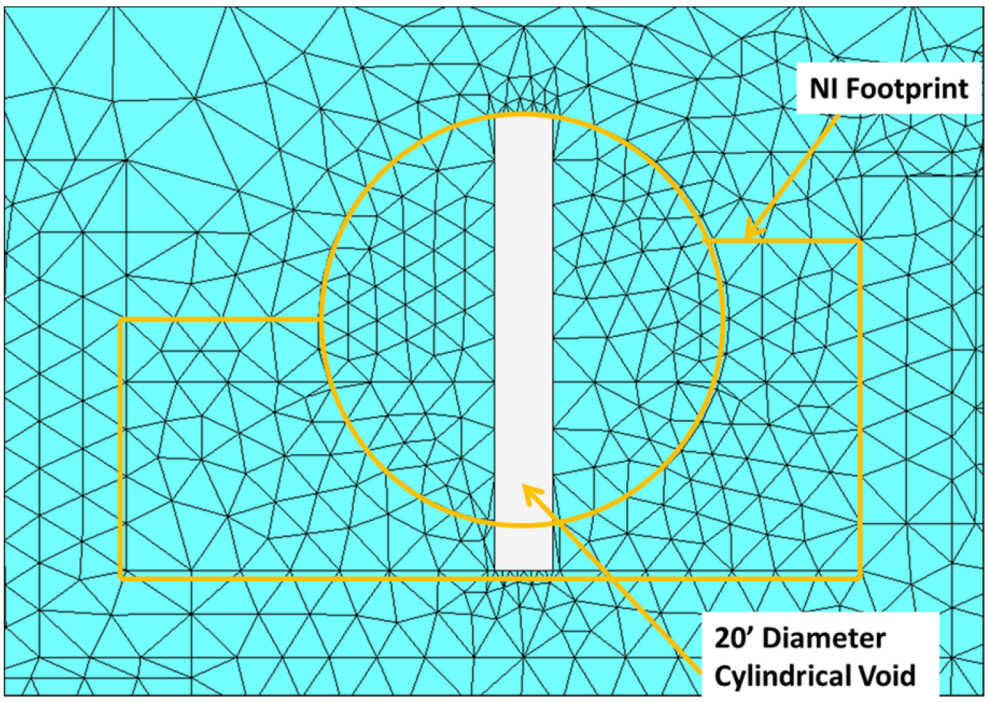

Figure 2.5.4-274 PLAXIS 3D Plastic Points for Sensitivity Model with 20-foot Diameter Cylindrical Void (Static Loading)

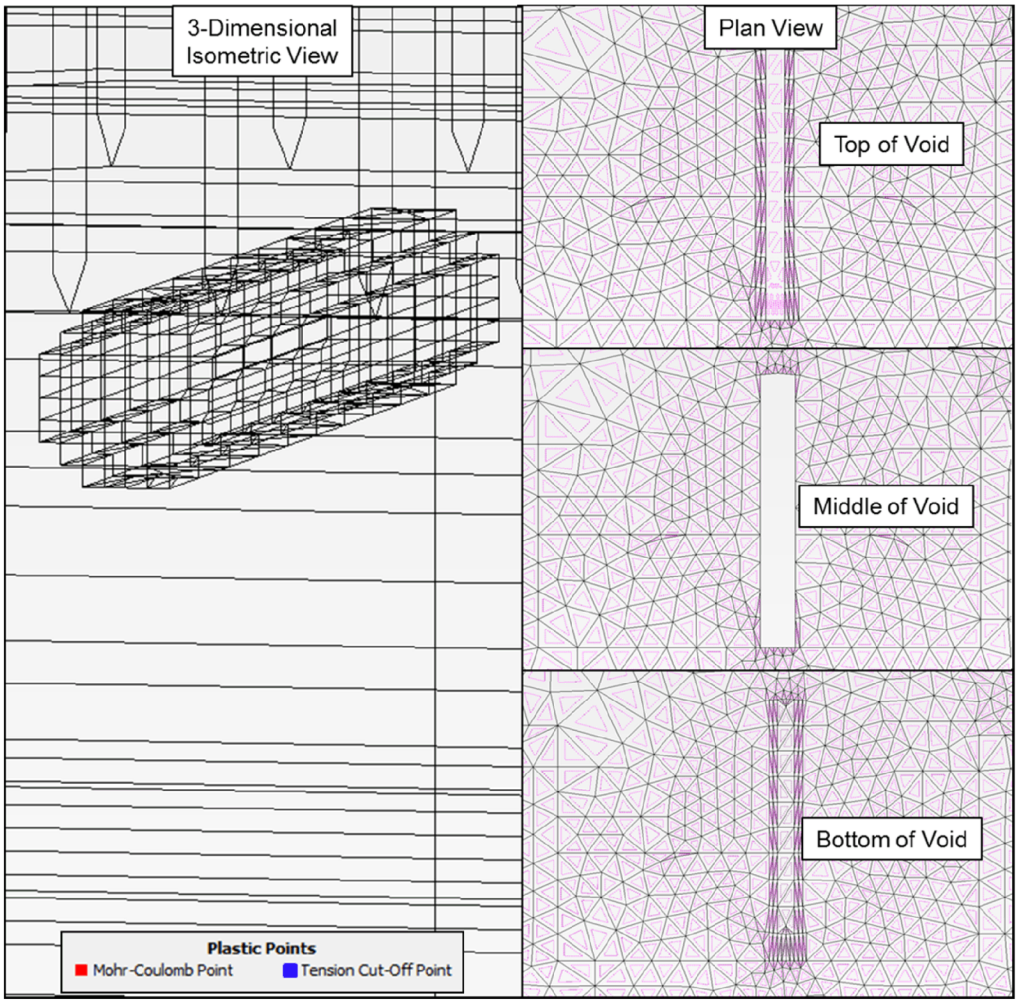

Figure 2.5.4-275 PLAXIS 3D Relative Shear Stresses for Sensitivity Model with 20-Foot Diameter Cylindrical Void (Static Loading)

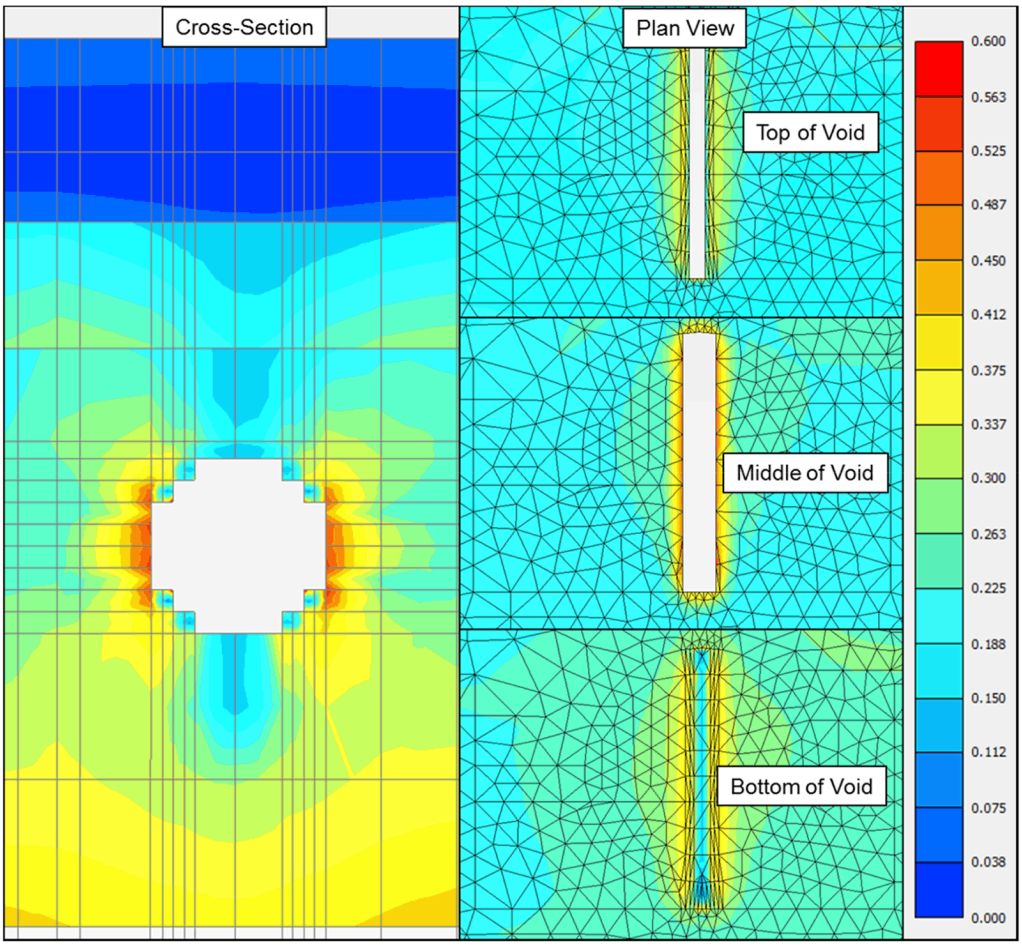

Figure 2.5.4-276 PLAXIS 3D Total Vertical Deformation for Sensitivity Model with 20-Foot Diameter Cylindrical Void (Static Loading)

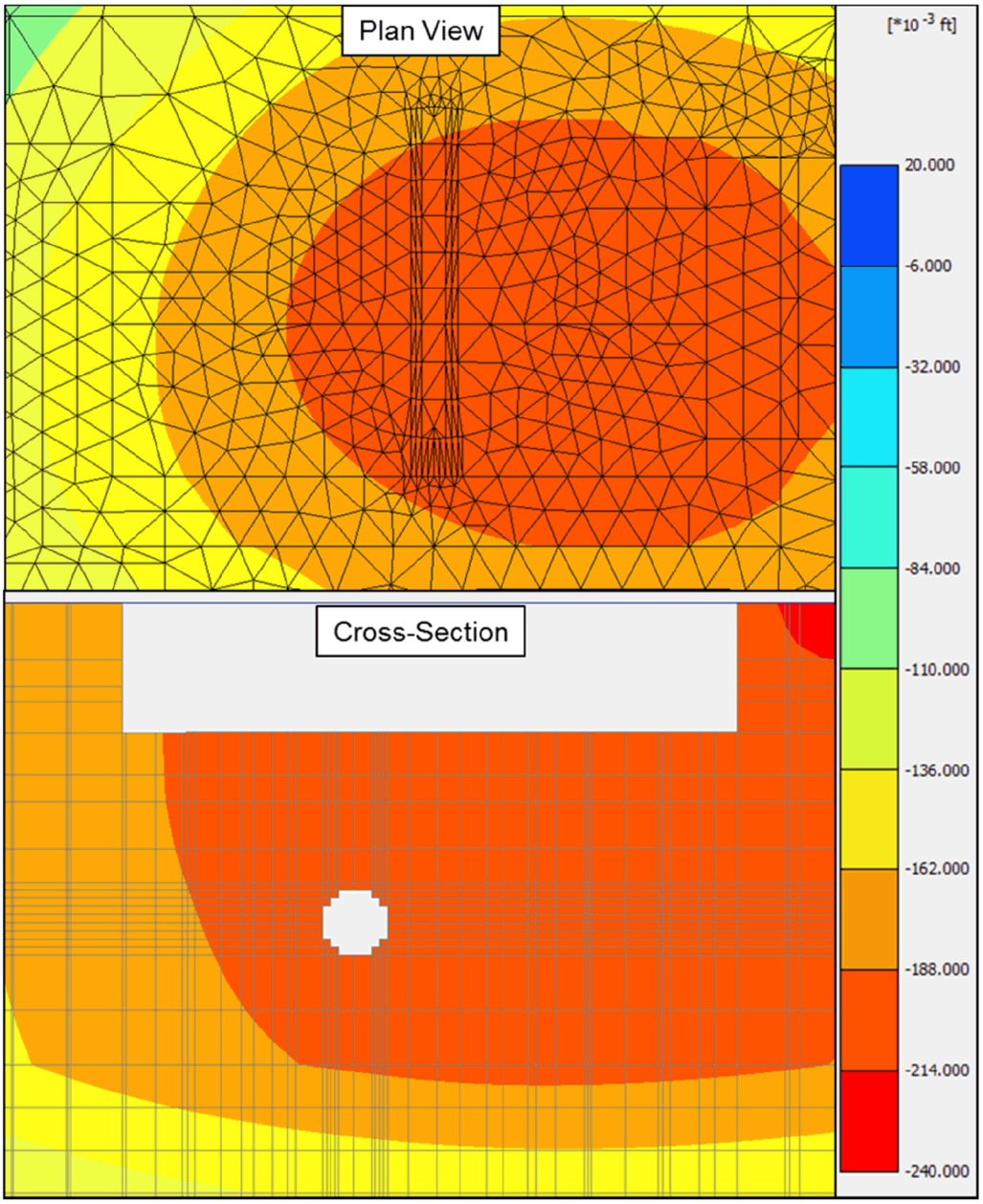

Figure 2.5.4-277 PLAXIS 3D Load Displacement Curve for Sensitivity Model with 20-Foot Diameter Cylindrical Void

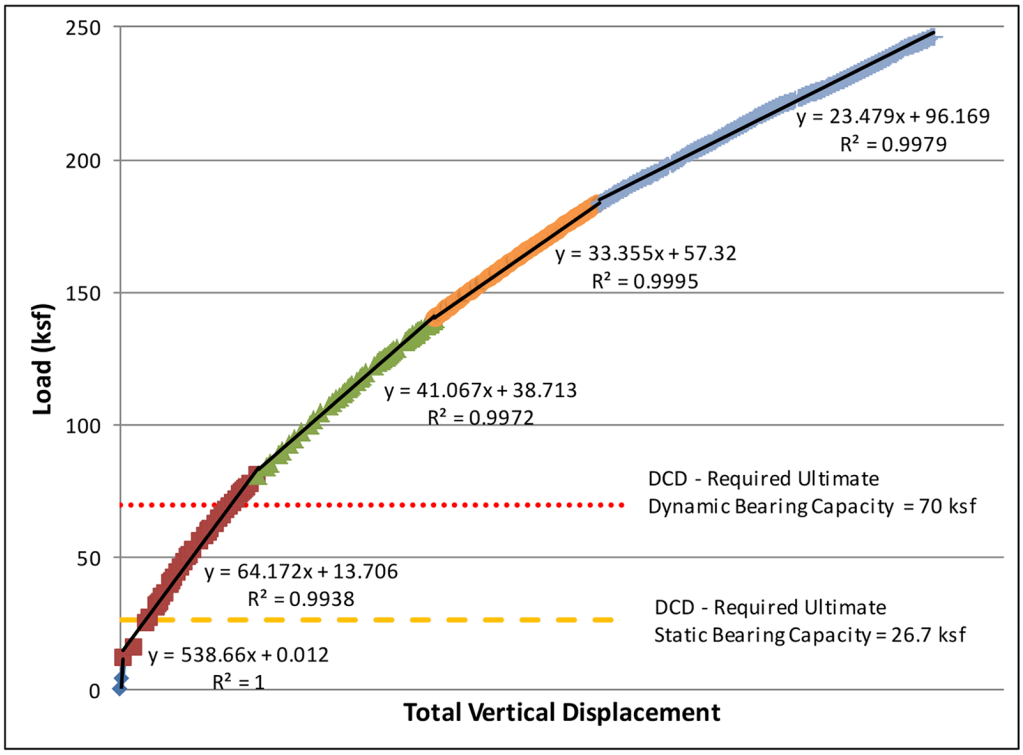

Figure 2.5.4-278 PLAXIS 3D Effective Vertical Stresses on Concrete Fill for Sensitivity Model with 20-Foot Diameter Cylindrical Void and a Multiplier of 1

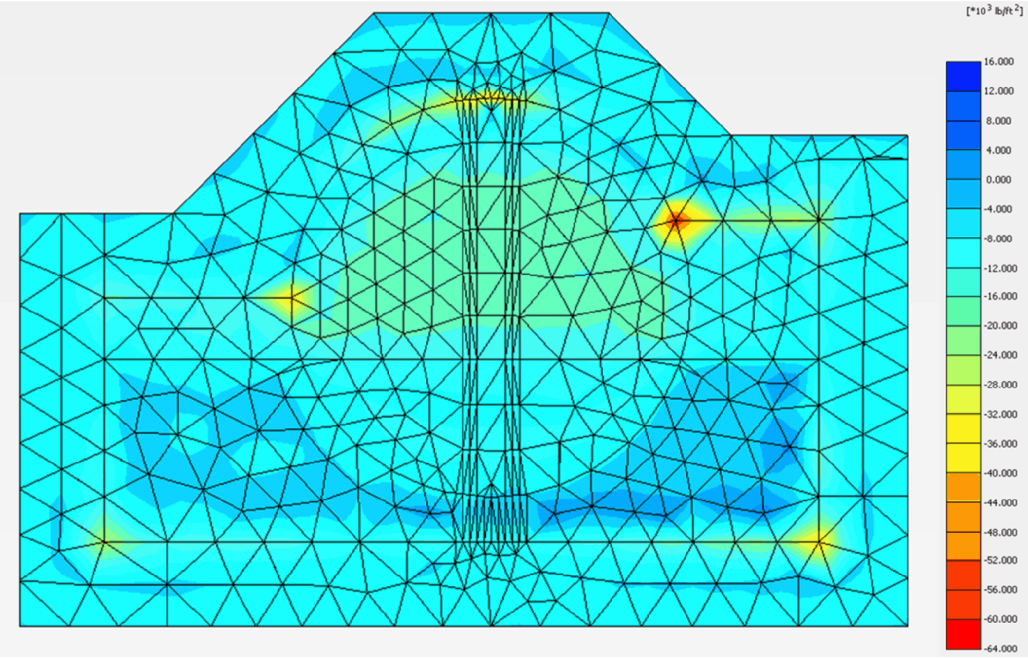

Notes:
1. Total static and pseudo-dynamic loading with a multiplier of 1, as defined in Table 2.5.4-225.
2. Negative effective stresses represent compression, while positive effective stresses represent tension.

Figure 2.5.4-279 PLAXIS 3D Effective Vertical Stresses on Concrete Fill for Sensitivity Model with 20-Foot Diameter Cylindrical Void and a Multiplier of 2

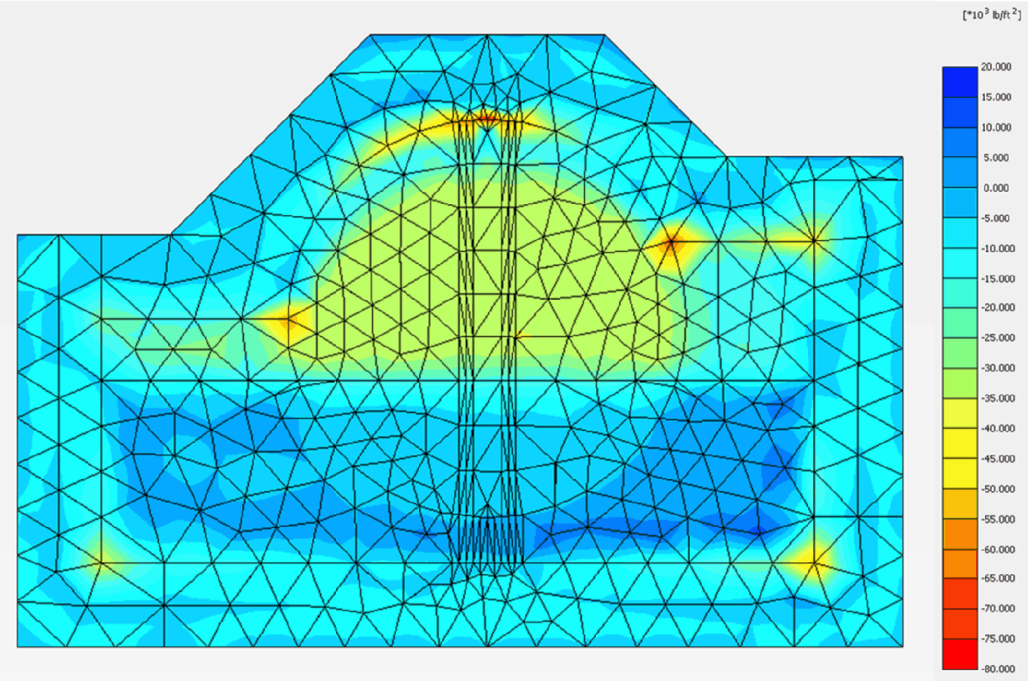

Notes:
1. Total static and pseudo-dynamic loading with a multiplier of 2, as defined in Table 2.5.4-225.
2. Negative effective stresses represent compression, while positive effective stresses represent tension.